Immunotherapy of solid tumors: multimodal imaging strategies for chimeric antigen receptor T cell tracking in the tumor microenvironment

Dissertation

for the award of the degree

"**Doctor rerum naturalium (Dr. rer. nat.)**"

of the Georg-August-Universität Göttingen

within the doctoral program Molecular Medicine

of the Georg-August University School of Science (GAUSS)

submitted by

Janina Henze, M.Sc. Molecular Medicine

Göttingen, 31.05.2021

Thesis Committee

Prof. Dr. Frauke Alves
Translationale Molekulare Bildgebung, Max-Planck-Institut für Experimentelle Medizin
Klinik für Hämatologie und Medizinische Onkologie, Universitätsmedizin Göttingen
Institut für Diagnostische und Interventionelle Radiologie, Universitätsmedizin Göttingen

Prof. Dr. Ralf Dressel
Institut für Zelluläre & Molekulare Immunologie, Universitätsmedizin Göttingen

Prof. Dr. Luis Pardo
Onkophysiologie, Max-Planck-Institut für Experimentelle Medizin Göttingen

Members of the Examination Board

Referee: **Prof. Dr. Frauke Alves**
Translationale Molekulare Bildgebung, Max-Planck-Institut für Experimentelle Medizin
Klinik für Hämatologie und Medizinische Onkologie, Universitätsmedizin Göttingen
Institut für Diagnostische und Interventionelle Radiologie, Universitätsmedizin Göttingen

2nd Referee: **Prof. Dr. Ralf Dressel**
Klinische und Experimentelle Endokrinologie, Universitätsmedizin Göttingen

3rd Referee: **Prof. Dr. Luis Pardo**
Onkophysiologie, Max-Planck-Institut für Experimentelle Medizin Göttingen

Further members of the Examination Board

Prof. Dr. Hubertus Jarry
Klinische und Experimentelle Endokrinologie, Universitätsmedizin Göttingen

Prof. Dr. Dieter Kube
Klinik für Hämatologie und Medizinische Onkologie, Universitätsmedizin Göttingen

Prof. Dr. Lutz Walter
Deutsches Primatenzentrum, Göttingen

Date of oral examination: 13.07.2021

CONTENT

LIST OF FIGURES **5**

LIST OF TABLES **5**

LIST OF ABBREVIATIONS **6**

PUBLICATIONS AND PRESENTATIONS **8**

ABSTRACT **10**

INDIVIDUAL CONTRIBUTIONS TO THE MANUSCRIPTS **12**

REVIEW: ENHANCING THE EFFICACY OF CAR T CELLS IN THE TUMOR MICROENVIRONMENT 12

CHAPTER 1 - A NOVEL SIGLEC-4 DERIVED SPACER IMPROVES THE FUNCTIONALITY OF CAR T CELLS AGAINST MEMBRANE-PROXIMAL EPITOPES 12

CHAPTER 2 – MULTIMODAL IMAGING OF CAR T CELLS USING BIOLUMINESCENCE TOMOGRAPHY AND LIGHT-SHEET MICROSCOPY REVEALS NEGATIVE EFFECTS OF LOCAL INTERLEUKIN-2 13

1 INTRODUCTION **14**

1.1 Cancer Therapy 14

1.1.1 Cancer 14

1.1.2 Tumor Development 14

1.1.3 Cancer Treatment Options 17

1.1.4 Immunotherapy 18

1.1.5 CAR T Cell Therapy 21

1.1.6 CAR T cell therapy of PDAC 26

1.2 Imaging in Preclinical Cancer Research 27

1.2.1 Mouse Models for Preclinical Research 27

1.2.2 Small Animal In Vivo Imaging Modalities 27

1.2.3 Computed Tomography 29

1.2.4 Molecular Bioluminescence Imaging 29

SUMMARY REVIEW 32

1.3 REVIEW: ENHANCING THE EFFICACY OF CAR T CELLS IN THE TUMOR MICROENVIRONMENT OF PANCREATIC CANCER 33

Abstract…. 34

1.Introduction 34

2. CAR T Cells and the Tumor Microenvironment of Pancreatic Cancer 39

3. Conclusions 53

References 55

1.4 Aims of the Study 66

1.4.1 Assessment of the Influence of CAR Composition on In Vivo Functionality 66

1.4.2 Evaluation of an In Vivo and Ex Vivo CAR T cell Tracking Strategy 67
1.4.3 Analysis of IL-2 as a Support for CAR T cells in TME of PDAC 67
SUMMARY CHAPTER 1 68
CHAPTER 1 - A NOVEL SIGLEC-4 DERIVED SPACER IMPROVES THE FUNCTIONALITY OF CAR T CELLS AGAINST MEMBRANE-PROXIMAL EPITOPES 69
Abstract 70
Introduction 71
Materials and Methods 73
Results 78
Discussion 90
Supplementary Material 98
References 101
SUMMARY CHAPTER 2 108
CHAPTER 2 – MULTIMODAL IMAGING OF CAR T CELLS USING BIOLUMINESCENCE TOMOGRAPHY AND LIGHT-SHEET MICROSCOPY REVEALS NEGATIVE EFFECTS OF LOCAL INTERLEUKIN-2 109
Abstract 110
Introduction 110
Material and Methods 112
Results 117
Discussion 129
Supplementary Materials 134
References 135
2 DISCUSSION 142
2.1 Assessment of the Influence of CAR Composition on In Vivo Functionality 142
2.1.1 Impact of CAR components on in vitro and in vivo performance 142
2.1.2 Development of a Novel Spacer Class Derived from the Siglec family 147
2.2 Imaging of CAR T cell therapy 150
2.2.1 In Vivo Tracking of CAR T cells by 2D BLI and 3D BLT Imaging 150
2.2.2 Ex Vivo Tracking of CAR T cells by LSFM and Cyclic Immunofluorescence 155
2.3 Supporting CAR T cells in TME of PDAC 158
2.4 Conclusion and Outlook 160
3 REFERENCES 163
ACKNOWLEDGEMENTS 192
CURRICULUM VITAE ..... Fehler! Textmarke nicht definiert.

LIST OF FIGURES

Figure 1: Central steps during the proposed initiation and progression of pancreatic ductal adenocarcinoma (PDAC). 16
Figure 2: Overview of Immunotherapy Categories. 20
Figure 3: Evolution of chimeric antigen receptors. 23
Figure 4: In vivo Bioluminescence Imaging in Small Animals. 30

LIST OF TABLES

Table 1: Overview of preclinical in vivo imaging techniques. 28

LIST OF ABBREVIATIONS

2D	Two dimensional
3D	Three dimensional
AA	Amino acid
ACE	Angiotensin-converting enzyme
AICD	Activation induced cell death
AT-1	Angiotensin II type 1
ATRA	All-trans retinoic acid
BDCA-2	Blood dendritic cell antigen 2
BLI	2D Bioluminescence
BLT	3D Bioluminescence tomography
BMSC	Bone marrow stromal cells
CAF	Cancer-associated fibroblast
CAR	Chimeric antigen receptor
CBR2opt	Click beetle red luciferase
CCD	Charge-coupled devices
CD	Cluster of differentiation
CEA	Carcinoembryonic antigen
CNS	Central nervous system
CRS	Cytokine release syndrome
CS	Costimulatory domains
CT	Computed tomography
DNA	Deoxyribonucleic acid
ECM	Extracellular matrix
EGFR	Epidermal growth factor
EMA	European medicines agency
EpCAM	Epithelial cell adhesion molecule
Fc	Crystallizable fragments
FcR	Fc receptor
FDA	Food and Drug Administration
FLI	Fluorescence reflectance imaging
FMT	Fluorescence mediated tomography
GFP	Green fluorescent protein
GM-CSF	Granulocyte-macrophage colony-stimulating factor
GvHD	Graft-versus-host disease
HA	Hyaluronic acid
HEK293T	Human Embryonic Kidney 293T
HER2	Human epidermal growth factor receptor 2
HIF-1	Hypoxia-inducible factor 1 alpha
HPV	Human papillomavirus
Ig	Immunoglobulin
IL	Interleukin
IF	Immunofluorescence
IFP	Intestinal fluid pressure
LNGFR	Low-affinity nerve growth factor receptor
LSFM	Light sheet fluorescence microscopy
MAG	Myelin-associated glycoprotein
µCT	Micro–computed tomography
MDSC	Myeloid-derived suppressor cell
MMP	Matrix metalloproteinase

MSC	Bone marrow-derived mesenchymal stem cell
MRI	Magnetic resonance imaging
NK	Natural killer cells
NSG	NOD SCID gamma
PBMC	Peripheral blood mononuclear cell
pDC	Plasmacytoid dendritic cell
PDAC	Pancreatic ductal adenocarcinoma
PDGFR	Platelet-derived growth factor receptor
PET	Positron emission tomography
PNI	Perineural invasion
PNS	Peripheral nervous system
PSC	Pancreatic stellate cell
PSCA	Prostate stem cell antigen
PSM	Pairwise significance matrix
RNA	Ribonucleic acid
ROI	Region of interest
RTK	Receptor tyrosine kinase
scFv	Single-chain variable fragment
Siglec	Sialic acid-binding immunoglobulin-type lectin
SHH	Sonic hedgehog
SPECT	Single photon emission computed tomography
synNotch	Synthetic Notch receptors
TAA	Tumor-associated antigens
TAM	Tumor-associated macrophage
T_{CM}	Central memory T cell
TCR	T cell receptor
TCT	T cell transduction
T_{EM}	Effector memory T cell
TGF	Transforming growth factor
TME	Tumor microenvironment
T_{Naive}	Naïve T cell
TNF	Tumor necrosis factor
T_{reg}	Regulatory T cell
TRUCK	T cell redirected for universal cytokine-mediated killing
TSA	Tumor-specific antigens
T_{SCM}	Stem cell–like memory T cell
TSP-1	Thrombospondin 1
TSPAN8	Tetraspanin-8
VEGF	Vascular endothelial growth factor
V_h	Variable chain heavy
V_l	Variable chain light
VSV-G	Vesicular stomatitis virus glycoprotein G

PUBLICATIONS AND PRESENTATIONS

Publications

Peer reviewed

Henze, J.; Tacke, F.; Hardt, O.; Alves, F.; Al Rawashdeh, W. Enhancing the Efficacy of CAR T Cells in the Tumor Microenvironment of Pancreatic Cancer. Cancers 2020, 12, 1389. doi: 10.3390/cancers12061389

Schäfer, D.; **Henze, J.**; Pfeifer, R.; Schleicher, A.; Brauner, J.; Mockel-Tenbrinck, N.; Barth, C.; Gudert, D.; Al Rawashdeh, W.; Johnston, I.C.D. and Hardt, O. A Novel Siglec-4 Derived Spacer Improves the Functionality of CAR T Cells Against Membrane-Proximal Epitopes. Frontiers in Immunology 2020, 11, 1704. doi: 10.3389/fimmu.2020.01704.

Schäfer, D.; Tomiuk, S.; Küster, L.N., Al Rawashdeh, W.; **Henze, J.**; Tischler-Höhle, G.; Agorku, D.J.; Brauner, J.; Linnartz, C.; Lock, D.; Kaiser, A.; Herbel, C.; Eckardt, D.; Schüler, J.; Ströbel, P.; Missbach-Güntner, J.; Alves, F.; Bosio, A. and Hardt, O. Identification of CD318, TSPAN8 and CD66c as target candidates for CAR T cell based immunotherapy of pancreatic adenocarcinoma. Nat. Commun. 2021, 12, 1453, doi:10.1038/s41467-021-21774-4.

Finalized for submission

Henze, J.; Pfeifer, R.; Wittich, K.; Linnartz, C., Bigott, K.; Jungblut, M.; Hardt, O.; Alves, F.; and Al Rawashdeh, W. Multi-modal imaging of CAR T cells using bioluminescence tomography and light-sheet microscopy reveals negative effects of local interleukin-2.

Contributions at Scientific Meetings

Poster Presentation

Henze, J.; Brauner, J.; Linnartz, C.; Hardt, O.; Alves, F.; Al Rawashdeh, W. Towards clinically-relevant preclinical CAR T cell therapy study models. (2019) European In Vivo Optical Imaging User Group Meeting 2019, Barcelona, Spain – **1st poster prize**

Henze, J.; Hardt, O. and Al Rawashdeh, W. Normalizing the tumor microenvironment for enhanced CAR T cell efficacy in solid tumors. (2019) 3rd GyMIC Molecular Imaging Symposium MoBi 2019, Münster, Germany

Continued on next page

Brauner, J.; Linnartz, C.; **Henze, J**.; Schäfer, D.; Deppenmaier, M.; Schröer, U.; Bosio, A.; Hardt, O.; and Al Rawashdeh, W. In Vivo Labeling for Ex Vivo 3D Tracking of CAR T cells (2019) 3rd GyMIC Molecular Imaging Symposium MoBi 2019, Münster, Germany

Oral Presentation

Henze, J.; Towards clinically-relevant preclinical CAR T cell therapy study models. (2019) 2nd GyMIC Molecular Imaging Symposium MoBi 2018, Göttingen, Germany

Henze, J.; Case Report - Diffuse large B-cell lymphoma (DLBCL). (2019) Kick-off Meeting 1st Consortium Meeting Winter School, EC Innovative Training Network MATURE-NK - ETN-765104, Bergisch Gladbach, Germany

ABSTRACT

Immunotherapy is an emerging building block of modern oncology, after chimeric antigen receptor (CAR) T cells demonstrated groundbreaking survival rates in hematological malignancies. However, therapy success in more common solid tumors has not been achieved yet, due to a variety of obstacles, such as a limited availability of suitable targets and decreased CAR T cells trafficking to the tumor. One of these barriers is the tumor microenvironment (TME), which is most pronounced in pancreatic ductal adenocarcinoma (PDAC). Combinatorial 2D and 3D preclinical multimodal imaging and cell tracking strategies can help to understand the mechanism that play a role in the solid tumor-specific barriers for CAR T cell migration. To this end, three non-solid CARs were characterized in vitro for killing and cytokine expression as well as for in vivo efficacy and tumor control. While in vitro results showed a potent killing and cytokine profile for all three CARs, in vivo analysis revealed a diminished killing potential of one CAR carrying an unspecifically bound IgG1-based spacer. This demonstrates the importance of imaging techniques to identify the most promising CARs for clinical transfer, to depict problematic CAR components and to unravel the underlying mechanisms. Furthermore, in vivo imaging identified the relevance of the CAR spacer domain, which is normally neglected. Favorable targeting of membrane-proximal epitopes with spacer, structural comparable to IgG1, encouraged the development of a novel spacer class, derived from sialic acid-binding immunoglobulin-type lectin (Siglec). Next, CAR T cells, incorporating the new spacers, were evaluated in vitro and ex vivo in solid and hematological malignancies. The functionality of the novel Siglec-4 derived spacer was superior to the established IgG4 and CD8α spacers in terms of the cytotoxic potential and a more potent anti-tumor marker and cytokine expression profile in comparison to IgG1-based spacers, supportive for future clinical trials. These results displayed the general functionality of CAR T cells against PDAC under the optimal conditions, in terms of target specificity, CAR composition and cell number and emphasize the implication of advanced imaging strategies for preclinical CAR T cell research. Thus, a rational multimodal imaging workflow was established and evaluated in a xenograft PDAC mouse model. First, optical 3D in vivo tracking of modified luciferase-expressing CAR T cells was applied. 3D Bioluminescence tomography (BLT) enabled the analysis of whole-body CAR T cells biodistribution and detection of pronounced CAR T cell accumulation in tumor and spleen in PDAC bearing mice. Subsequent combination with ex vivo light-sheet fluorescence microscopy (LSFM) of xenografts facilitated the generation of data visualizing whole-body and intratumoral T cell distribution of two different CARs. The addition of cyclic immunofluorescence staining (IF) provided an in-depth characterization of tumor-infiltrating

CAR T cells and surrounding tumor cells, revealing strong activation and proliferation of target-specific CAR T cells. The multi-modal imaging strategy enabled the evaluation of locally applied interleukin-2 (IL-2) as a support for CAR T cells in the immunosuppressive TME of PDAC. IL-2, repeatedly injected at the tumor site was shown to negatively impact intratumoral T cell distribution and phenotype. IL-2 co-treated CAR T cells infiltrated the tumor tissue less deep and showed a more overstimulated phenotype. These cells were no longer able to perform sufficient tumor eradication and local IL-2 did not translate into an enhanced anti-tumor efficacy. Taken together, this project established optical 3D CAR T cell tracking as part of a combined in vivo and ex vivo workflow for solid tumor cell therapy, TME-redirected treatment protocols and safety-orientated research. This preclinical imaging strategy enables the in-depth characterization of combinatorial CAR T cell approaches against solid tumors and TME in a mouse model of PDAC.

INDIVIDUAL CONTRIBUTIONS TO THE MANUSCRIPTS

REVIEW: ENHANCING THE EFFICACY OF CAR T CELLS IN THE TUMOR MICROENVIRONMENT

Writing

The manuscript was written by me with support from Dr. Wa'el Al Rawashdeh and Prof. Dr. Frauke Alves and input from all co-authors.

Figures and Tables

All figures and tables were created by me based on referenced literature. The staining in figure 2 was performed by Jeannine Missbach-Güntner.

CHAPTER 1 - A NOVEL SIGLEC-4 DERIVED SPACER IMPROVES THE FUNCTIONALITY OF CAR T CELLS AGAINST MEMBRANE-PROXIMAL EPITOPES

Writing and Intellectual

The manuscript was written by me and the shared first authors Dr. Daniel Schäfer and Dr. Rita Pfeifer with input from all co-authors. The initial concept of the manuscript was created by me and Dr. Daniel Schäfer and the study was further refined in collaboration with Dr. Rita Pfeifer, Dr. Olaf Hardt, Dr. Wa'el Al Rawashdeh, and Dr. Ian C. D. Johnston. The Siglec spacers were designed and drafted for a patent application by Dr. Rita Pfeifer.

Figures and Tables

All main and supplementary figures were created by me with support from Dr. Daniel Schäfer. I conducted experimental work regarding Figure 1 and 2 as well as Supplementary Figure 2 and 3 and supported the experimental work in Figure 6. Dr. Rita Pfeifer conducted the experiments depicted in Figure 4, while Dr. Daniel Schäfer conducted the experiments depicted in Figure 5 and 6. Resulting data was analyzed by me and my shared first authors Dr. Daniel Schäfer and Dr. Rita Pfeifer.

CHAPTER 2 – MULTIMODAL IMAGING OF CAR T CELLS USING BIOLUMINESCENCE TOMOGRAPHY AND LIGHT-SHEET MICROSCOPY REVEALS NEGATIVE EFFECTS OF LOCAL INTERLEUKIN-2

Writing and Intellectual

The manuscript was written by myself with support from Dr. Rita Pfeifer and input from all co-authors. The study and the manuscript were conceptualized by me and refined in collaboration with Dr. Rita Pfeifer and Dr. Wa'el Al Rawashdeh.

Figures and Tables

All main and supplementary figures were created by me. I conducted all experiments shown in the figures or analyzed the raw data resulting in the depicted figures.

1 INTRODUCTION

1.1 Cancer Therapy

1.1.1 Cancer

Despite the ongoing pandemic, cancer is still one of the most common causes of death worldwide after cardiovascular diseases and an important hindrance for increasing life expectancy (Ahmad and Anderson 2021). In the group of adolescents and young adults (age 15 – 39 years) in developed countries, cancer is the most common cause of death, which is not self-inflicted (Armenian et al. 2020). This age group has a high five-year relative survival rate ranging between 83 – 86%, as for all groups depending on the type of cancer age, sex, and economic developmental stage of the country (Siegel and Miller 2019). Research gaps for the adolescent age cohort and low alertness among patients and clinicians, result in these mortality rates and raise the risk of long-term and late effects in comparison to older cancer patients (Siegel and Miller 2019). The number of cases is rapidly rising in all age cohorts, which is influenced by many factors, such as aging, lifestyle, pollution, urbanization, and genetic predisposition (You and Henneberg 2018). Recent global cancer statistics expose the serious situation (Sung et al. 2021): 19.3 million patients were newly diagnosed with cancer and 10.0 million died from cancer in 2020. Yet solid tumors, including lung (11.4% of all new cases), breast (11.7%), and pancreatic cancer (2.6%), demonstrate higher incidences than hematological malignancies, such as leukemia (2.5%) and lymphomas (3.2%) and have in turn a high medical need. For new cases, prognosis depends hardly on the tumor classification and the progression of the disease. Some lymphomas have sufficient and multi-layered treatment options resulting in 5 years survival rates of over 80%, while other solid malignancies, especially pancreatic cancer has five-year survival rates between 1 – 5 % and a median survival rate of only a few months (Huang et al. 2018; Liu and Barta 2019). Furthermore, the total number of cancer cases are expected to rise by 47% to 28.4 million in 2040, conjoint by an increasing death toll. Thus, cancer is a rising health problem.

1.1.2 Tumor Development

Further research is necessary to treat the growing number of cancer patients and to reduce the death toll. In this way, it is of high interest to analyze the molecular differences between healthy and tumor cells. Hanahan and Weinberg famously summarized these characteristics, essential for cancer development, termed hallmarks of cancer (Hanahan and Weinberg 2011). In cancer cells, the deregulated proliferation, caused by mutations in tumor suppressor or activator genes, e.g. DNA repair mechanism, is crucial and can contribute to decreasing genetic stability

(Alhmoud et al. 2020). However, this may also occur in benign neoplasms, which can be distinguished from malignant tumor cells by the invasive and metastatic behavior of the latter (Brosseau and Le 2019). The accelerated proliferation of neoplastic cells needs to be sustained by an increase of nutrients, growth factors, and cytokine supply and utilization (De Berardinis and Chandel 2016; Li et al. 2018). Lastly, cell death by internal and external processes needs to be prevented (Sharma, Boise, and Shanmugam 2019). Hence, multiple genetic and transcriptional changes have to accumulate for tumor initiation and progression.

The development of pancreatic ductal adenocarcinoma (PDAC), the most common type of pancreatic cancer accounting for more than 90% of all cases, is well characterized and the aggressiveness rising cascade follows the principles of the hallmarks (Hezel et al. 2006). The evolution of PDAC is often initiated by the activating mutation of the GTPase KRAS in the following healing processes after inflammation or lesions (Figure 1). This results in ductal reprogramming and the formation of acinar-to-ductal metaplasia (ADM) (Schmid 2002). On-going de-differentiation, accompanied by increasingly deregulated β-catenin signaling and overexpression of Hedgehog (Hh) ligands induces progression from ADMs via pancreatic epithelial neoplasia (PanIN) and finally to PDAC establishment (Morris, Wang, and Hebrok 2010). However, for the establishment of PanIN status, β-catenin signaling has to be maintained at a low level before upregulation (Heiser et al. 2008). Subsequently to PanIN development, reactivated β-catenin and Hh expression rise continuously (Sano et al. 2016). The progression process is accompanied by an increasing desmoplastic reaction, a crucial feature for the successful treatment of PDAC (Erkan et al. 2012). Other typical mutations detected in PDAC and associated with malignancies include genetic and expressional alliteration in CDKN2A, SMAD4, and TP53 genes, usually detected during or after PanIN state (Oshima et al. 2013). Each of these mutations and KRAS impact another aspect of the hallmarks and the surrounding tumor stroma, resulting in various PDAC subtypes (Bailey et al. 2016). KRAS is responsible for the regulation of cell growth and proliferation, while the gene TP53 encodes the tumor suppressor protein p53, a common mutation in several types of solid tumor and hematological malignancies (Kandoth et al. 2013; Wood and Hruban 2012). CDKN2A is an important cell cycle regulator and loss of function promotes genetic instability, in contrast to SMAD4, where cells with mutations in this gene lose the ability to respond to growth-inhibitory factors (Lecanda et al. 2009; Moustakas and Heldin 2005; Tang et al. 2015). Combinations of the well-established mutations with further recurrent somatic mutations lead to a multitude of individual subtypes with varying stroma classes (Pompella et al. 2020; Raphael et al. 2017). Circumventing the barriers created by this alternated stroma is essential for PDAC therapy, due

to its pronounced and dense phenotype and the signaling cross-talk between tumor and stroma cells (Sperb, Tsesmelis, and Wirth 2020; Yao, Maitra, and Ying 2020).

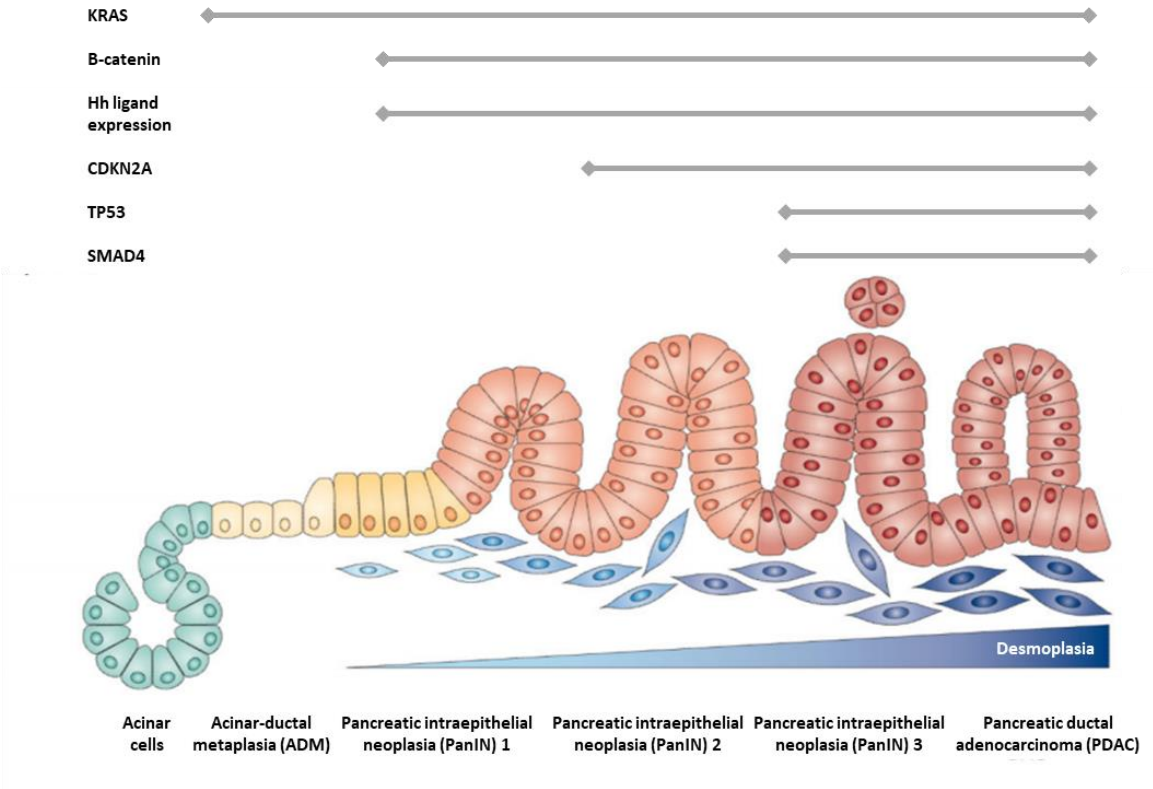

Figure 1: Central steps during the proposed initiation and progression of pancreatic ductal adenocarcinoma (PDAC).

At the beginning of PDCA initiation, acinar or ductal cells undergo a ductal reprogramming resulting in acinar-to-ductal metaplasia (ADM) formation. Highly prevalent KRAS mutation induces the establishment of pancreatic intraepithelial neoplasia (PanIN). Over time genetic instability by acquired mutations, in TP53 or SMAD4 leads together with deregulated β-catenin signaling and Hedgehog (Hh) expression to PDAC establishment, with increasing desmoplasia. Modified from (Morris et al. 2010).

In contrast to pancreatic cancer, there is no dominating lymphoma subtype but development occurs over various individual premalignant states. Multiple lymphoma subtypes have been identified in any organ of the body largely influenced by the differentiation state of the origin B, T, or NK cell, albeit B-cell lymphomas display the highest incidences (Shankland, Armitage, and Hancock 2012). Lymphomas are usually divided into Hodgkin's lymphoma (HL) and Non-Hodgkin lymphomas (NHL), which make up to 90% of all lymphoma cases (Sung et al. 2021). For some subtypes of NHL, typical pathogenic contributors have been identified arising from recurrent mutations, transcriptional regulation, structural rearrangements or deregulated antigen receptor signaling (Elenitoba-Johnson and Lim 2018). Diffuse large B cell lymphoma (DLBCL) is the most common NHL, accounting for more than 30% of all newly diagnosed NHL cases (Campo et al. 2011). DLBCL can be further subdivided into three different subclasses based on

molecular subtypes, such as activated B cell-like (ABC), germinal center B cell-like (GCB), and primary mediastinal large B cell lymphoma (PMBCL) (Alizadeh et al. 2000; Rosenwald et al. 2003). As in PDAC, each of these subtypes is characterized by an identifying group of distinguishing set of mutations and translational changes, verified by gene expression profiling. For example, the ABC type is characterized by constitutive nuclear factor κB (NF-κB) activity due to aberrant B cell receptor signaling, ultimately preventing apoptosis, accompanied by additionally acquired mutations (Eric Davis et al. 2001). Taken together, each cancerous malignancy, independent of the origin, had to go through various steps to develop into a fully established invasive tumor. They can be identified by the site and cell type of origin and by a set of specific genetic and transcriptional changes leading to mutations. These specificities could help to treat patients depending on the molecular expression profile.

1.1.3 Cancer Treatment Options

For solid tumor treatments, surgical removal is often combined with radiation therapy and chemotherapy also termed as the three pillars of cancer therapy (Siamof, Goel, and Cai 2020). Stage and localization of the solid tumor progression, as accessed by imaging and histology, determine the treatment regiment, such as neoadjuvant versus adjuvant therapy, e.g. in the most common subtype of pancreatic cancer (Motoi and Unno 2021).

Despite the overall dismal prognosis of pancreatic ductal adenocarcinoma (PDAC), patients diagnosed with a localized stage I or II diseases can be cured by partial pancreaticoduodenectomy followed by adjuvant chemotherapy with FOLFERINOX regiments (Conroy et al. 2018). FOLFIRINOX scheme, a combination of chemotherapeutics fluorouracil, leucovorin, irinotecan, and oxaliplatin, resulted in an overall survival of 54.4 months in comparison to the 35.0 months of gemcitabine monotherapy, the former standard of care. Notably, grade 3 or 4 adverse events were significantly higher in the FOLFERINOX group, potentially caused by the higher cytotoxic potential of the combinatorial regiment.

However, up to 40% of PDAC patients are diagnosed with a locally advanced disease, which is borderline resectable due to the involvement of the surrounding tissue (Lekka et al. 2019). Different treatment protocols with radiation therapy and chemotherapy were tested as neoadjuvant therapy, to induce tumor shrinkage before surgery and reduce micro-metastases (Heinrich et al. 2011; Versteijne et al. 2016). However, until today there is no standard protocol for neoadjuvant therapy in PDAC due to missing clinical data, comparing the proposed protocols. The establishment of FOLFIRINOX as standard adjuvant therapy would advise

against chemotherapy protocols with one of the components of the FOLFERINOX scheme to avoid potential escape mutations (Bukowski, Kciuk, and Kontek 2020). Many PDAC tumors tend to become resistant to chemotherapy, probably due to genetic instability e.g. induced by KRAS mutation an important factor in PDAC development (Jinesh et al. 2018; Zeng et al. 2019).

The third group of PDAC patients presents with an unresectable local advanced disease and metastasis formation (Soloff et al. 2018). The only options for these and the high number of relapsing patients are often mono- or dual chemotherapy schemes as respective first or second treatment lines with low median survival times between 6 to 11 months (Neoptolemos et al. 2018).

This emphasizes the high research demand for new therapeutic approaches in solid tumors, but especially in PDAC. Chemotherapy resistance and severe side effects of broad and untargeted chemo- or radiotherapy raised the interest in targeted therapies, which have a lower impact on healthy cells, even further. Chemotherapy resistance is also a problem for blood cancers, including lymphomas. However, there are further treatment options available contributing to the higher overall survival rates. Unlike solid tumors, surgery is not a curative option for blood cancers, due to the systematic nature of the disease (Abramson and Zelenetz 2013). But the systemic nature enables the treatment of hematological malignancies by allogeneic or autologous stem cell transplantations, in case of a relapsed or refractory disease after standard chemo- or radiotherapy (Schmitz et al. 2002). Another well-established therapy option for certain subtypes of hematological malignancies is targeted immunotherapy, using specific expression patterns on the malignant cells e.g. immuno-stimulating antibody treatments (Walewski et al. 2001). Nevertheless, targeted therapy can also be applied to deliver chemotherapeutics specifically to the solid tumor or to enhance the anti-tumor efficacy of chemotherapeutics, but neither targeted therapy nor immunotherapy early clinical trials were able to demonstrate extended survival times in pancreatic cancer (Lee et al. 2021; Pérez-Herrero and Fernández-Medarde 2015; Sarantis et al. 2020).

1.1.4 Immunotherapy

Immunotherapy, another form of targeted therapy, has become the fourth and newest pillar of cancer therapy over the last decade, which was rewarded with the Nobel Prize in Physiology or Medicine in 2018 (Guo 2018; Siamof et al. 2020). Despite, this promising and rising reputation of immunotherapy, the concept has already been used by Egyptians in 2600 BC, who applied a microorganism-containing poultice to an incision close to the tumor to induce local

inflammation, leading to the regression of the tumor (Kucerova and Cervinkova 2016). Cancer cells can be suppressed or actively killed by the innate immune cells, composed of eosinophils, basophils, natural killer (NK) cells, and phagocytic cells, such as neutrophils, monocytes, macrophages, dendritic cells (DC) (Corrales et al. 2017; Demaria et al. 2019). Adaptive immune cells complete the tumor immune response. B cells can induce a humoral immune response against malignant cells and T cells can contribute to the active killing of the tumor cells (Gonzalez, Hagerling, and Werb 2018). However, tumor cells establish numerous strategies to escape from the immunosurveillance (Beatty and Gladney 2015). Modern immunotherapy has developed methods to reverse the tumor immune escape, which can be sorted into five categories (Figure 2) (Zhang and Zhang 2020).

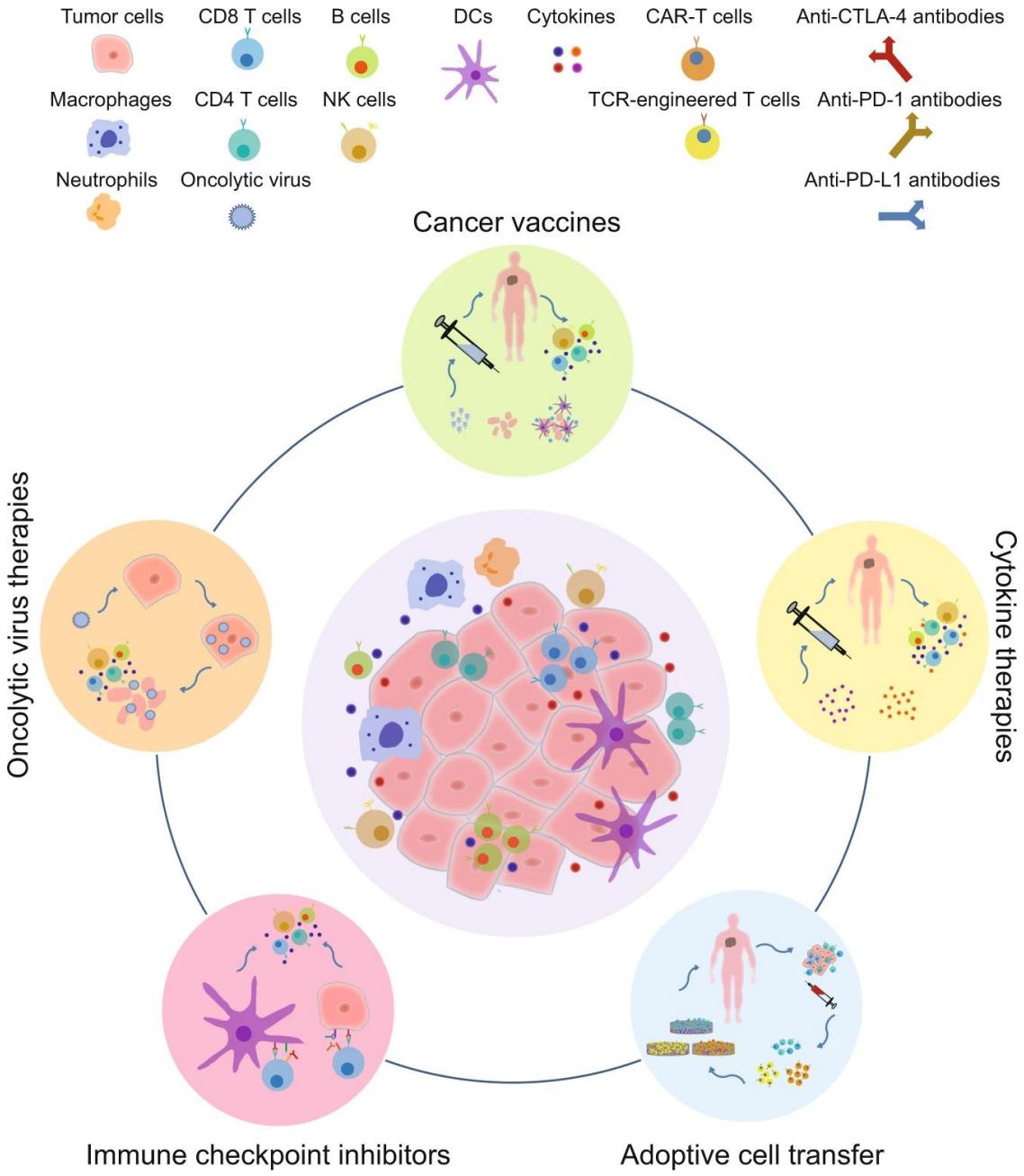

Figure 2: Overview of immunotherapy categories.

Immune checkpoint inhibitors, oncolytic virus therapies, cytokine therapies, cancer vaccines, and adoptive cell transfer represent the five categories. All strategies have been tested in clinical studies and the underlying principles of each technique are depicted in the figure. T-cell receptor (TCR), chimeric antigen receptor (CAR) T cells. Modified from (Zhang and Zhang 2020).

Oncolytic virus builds upon the ancient approaches of the Egyptians, but state-of-the-art genetic and protein engineering provides much safer utilization and direct stimulation of tumor-specific T and B cells (Fukuhara, Ino, and Todo 2016). Impressive clinical success was demonstrated talimogene laherparepvec (T-Vec), also known as Imlygic in patients with advanced melanoma, subsequently leading to FDA approval (Andtbacka et al. 2015). The second category includes cancer vaccines, which are subdivided depending on the target in cellular, peptide, DC, DNA,

and RNA vaccines and are redirected against tumor-associated antigens (TAAs) and tumor-specific antigens (TSAs) (Hollingsworth and Jansen 2019). While preventive vaccines were successful against human papillomavirus (HPV) induced cervical cancer, vaccines targeting established neoplasm yielded only disappointing results despite of advantageous induction of long-term immune memory (Athanasiou et al. 2020; Gillison, Chaturvedi, and Lowy 2008). This applies also to clinical trials evaluating GVAX in PDAC, which were not able to extend the overall survival (Wu et al. 2020). Cytokines mediate cell-to-cell communication between the wide range of innate and adaptive immune cells, leading to the early approval of recombinant interferon-alpha (IFN-α) and interleukin-2 (IL-2) for the treatment of several malignancies (Berraondo et al. 2019). These early approvals paved the way for other immunotherapy strategies, but monotherapies provoked severe toxicities and stopped further clinical development except in combination with other treatment regimens (Wrangle et al. 2018). Clinical trials in melanoma patients analyzed combination with Nobel price-winning checkpoint inhibitors (Rafei-Shamsabadi et al. 2019). Checkpoint inhibitors monoclonal antibodies, which are designed to reverse tumor immune escape by blocking the interaction of inhibitory ligands expressed on cancer cells and inhibitory signaling receptors on immune cells, e.g. T cells (Hodi et al. 2010). Despite the respectable success in immunogenic tumors, many solid tumors, such as PDAC, are poorly infiltrated by immune cells, so the amount of tumor recognizing cytotoxic immune cells has to be increased at the tumor side (Bian and Almhanna 2021; Heinhuis et al. 2019). One option is the adoptive transfer of genetically modified chimeric antigen receptor (CAR) or T-cell receptor (TCR)-engineered T cells since both approaches have already achieved promising clinical outcomes (Zhang and Zhang 2020).

1.1.5 CAR T Cell Therapy

Adoptive cell transfer is another option for the immunotherapy of tumors. It originally started with the development of lymphokine-activated killer cells (LAK) cells, which are generated from ex vivo IL-2 stimulated autologous peripheral blood mononuclear cells and the final cell product contained more NK cells than T cells (Grimm et al. 1982). Whereas in vitro tests were quite promising, LAK cells were not able to recapitulate these results in vivo and failed in clinical trials (Lotze and Rosenberg 1986). The addition of further cytokines for ex vivo stimulation IFN-γ, IL-1, and anti-CD3 monoclonal antibody to cultures, later termed as Cytokine-induced killer cells (CIK), resulting in more efficient anti-tumor cell products (Schmidt-Wolf et al. 1991). Despite this increasing progress, the high interest in these cell products was quickly shifted to engineered and chimeric antigen receptor (CAR) T cells. The concept of implementing an antibody-derived specificity in T cells was first verified by Kuwana

et al. when they modified an immunoglobulin-derived variable region onto a T-cell receptor constant region (Kuwana et al. 1987). Gross et al. evolved this concept to double chain chimeric receptors by the fusion of antibody-derived binding domains to the constant TCR domain but inefficient cloning, complex formation, and surface expression halted further preclinical development (Gross, Waks, and Eshhar 1989). Finally, Eshhar et al. successfully combined the antigen recognizing domains derived from antibodies with the intracellular T cell signaling domains and enabled sufficient in vitro killing and pro-inflammatory cytokine expression of the first CAR (Figure 3) (Eshhar et al. 1993).

In a single-chain CAR, antigen recognition is executed by an antigen-binding single-chain variable fragment (scFv) domain, consisting of the variable heavy (V_h) and variable light (V_l) chains of an antibody, fused to a spacer and transmembrane domain, while signal transduction is performed by the connected TCR-derived CD3ζ signaling chain, carrying immune receptor-tyrosine-based-activation-motifs [ITAMs] (Abate-Daga and Davila 2016; Sadelain, Rivière, and Brentjens 2003). This combination enables the activation of the T cell-independent of the natural TCR antigen processing and presentation, with a higher affinity and specificity to an antigen of choice, such as proteins, carbohydrates, or glycolipid molecules (Irving and Weiss 1991; Stone and Kranz 2013). Of note, scFv affinity can steer density-dependent CAR T cells activation, in case of high-density target expression on tumor cells and low-density target expression on healthy tissue, but high affinities may even lead to overstimulation and activation-induced cell death (AICD) (Watanabe et al. 2016; Weijtens, Hart, and Bolhuis 2000). Since CARs are independent of the natural TCR, they also harbor greater targeting potential than adoptive cell therapy with ex vivo stimulated tumor-infiltrating lymphocytes (TILs), especially for tumors with the low infiltration rate of T cells including PDAC (Carstens et al. 2017; Hall et al. 2016; Orhan et al. 2020).

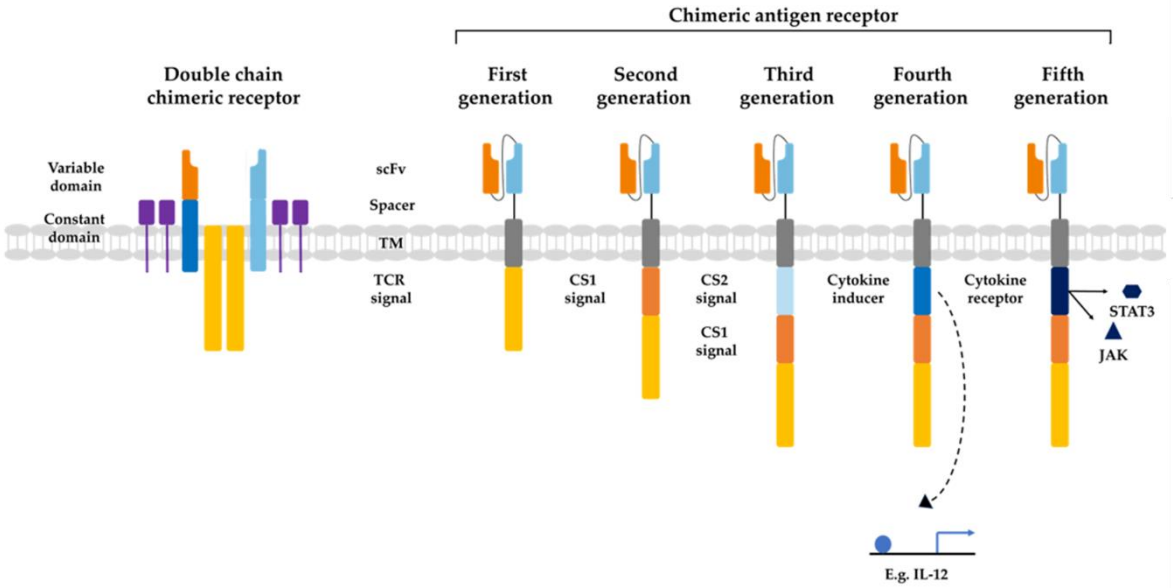

Figure 3: Evolution of chimeric antigen receptors.

The development of single-chain CARs started with double chain chimeric receptors. V_h and V_l chains derived from antibodies (orange and bright blue boxes) were engineered to the constant regions of the TCR α- and β-chains (green and blue boxes). These customized variable T cell receptor (TCR) domain resemble the TCR appearance and functionality. Activation of TCR and double chimeric receptors requires the assembly with intracellular CD3γ, CD3δ, CD3ε (purple boxes) and CD3ζ chains (yellow boxes). First generation CARs consists of an antigen-recognizing scFv, which is fused to the CD3ζ-signalling domain via transmembrane and spacer domains. CAR potential and abilities, including cytokine secretion, cytotoxicity, persistance and proliferation of CARs, were extended and elevated in second- and third-generation CARs by the inclusion e.g. CD27, CD28, or 4-1BB as costimulatory domains (CS1 and CS2). Fourth- and fifth-generation CAR T cells are based on second-generation CARs and increased the application options and the flexibility for various challenges. Fourth-generation CARs, alternatively termed T cell redirected for universal cytokine-mediated killing (TRUCKs), can express cytokines locally constitutively or after CAR activation. Fifth-generation CARs incorporate the intracellular domains of cytokine receptors (dark blue box) e.g., IL-2Rβ. Target recognition of the CAR leads additionally to signal transduction in the STAT3/5 pathway. Modified from (Henze et al. 2020).

However, CAR T cells containing only a CD3ζ signaling domain were not yet clinically effective due to limited anti-tumor efficacy and in vivo persistence (Kershaw et al. 2006). This proved the requirement for further co-stimulatory domains, next to the phosphorylation of the three CD3ζ ITAM motifs after antigen-binding, for enhanced in vivo potency. Interestingly, it was already proposed in 1975 that a full T cell activation might rely on a second costimulatory signal (Figure 3) (Lafferty and Cunningham 1975). The hypothesis was confirmed with antibodies blocking the interaction between CD80 and CD86, expressed on antigen-presenting cells (APCs), and CD28, expressed on T cells (Dilek et al. 2013; Esensten et al. 2016). Hence, CD28 was the first candidate for the co-stimulatory domain. Intensive testing revealed that the incorporation of CD28 before the CD3ζ domain resulted in the strongest impact on in vivo T cell cytokine production and proliferation (Kowolik et al. 2006; Maher et al. 2002). The success

of CD28 encouraged the evaluation of further costimulatory domains expressed by T and NK cells, defining the second-generation of CAR T cells, such as ICOS, CD27, 4-1BB, OX40, and CD40L in contrast to the only CD3ζ containing first-generation CARs. How each co-stimulatory domain may influence in vitro and in vivo CAR T cell efficacy, metabolism, cytokine production, and T cell phenotype is still under investigation (Rafiq, Hackett, and Brentjens 2020; Sadelain, Brentjens, and Rivière 2013). Although the amount of available costimulatory domains has further grown over the years, the majority of clinical trials are performed with 4-1BB or CD28 second-generation CAR T cells (Weinkove et al. 2019). Eventually leading to the FDA approval of up-to-date four CAR T cell therapies for the treatment of hematological malignancies after the tremendous success in clinical trials, with overall remission rates of over 80% (Mullard 2021).

The clinical success of second-generation CAR T cells raised the question if the addition of a second costimulatory domain could further enhance CAR T cell activity. Thus endless combinations and conformations of these third-generation CAR T cells were evaluated in vitro and in vivo (Figure 3). Combination of CD28 and 4-1BB costimulatory demonstrated that third-generation CARs can extend CAR T cell potential, as in this case, where generated CAR T cells were able to persistent in vivo as long as 4-1BB second-generation CARs and elicit similar tumoricidal capacity of CD28-based CARs (Zhao et al. 2015). Unfortunately, the higher degree of the activation did not only resulted in a stronger proliferative capacity and improved efficacy of third-generation CARs in clinical trials but also increased risk for toxicities and faster exhaustion (Cheng et al. 2018; Lee et al. 2019; Ramos et al. 2018). Research to overcome these limitations is still ongoing.

Further challenges and applications for CAR T cells motivated the development of the fourth- and fifth-generation (Figure 3). Both are based on second-generation CARs and ensure co-expression of cytokines (fourth) or extended cytokine signaling (fifth) (Tokarew et al. 2019). The fourth generation is also termed as T cells redirected for universal cytokine-mediated killing (TRUCKs) and co-expression of cytokines, such as IL-12 or IL-15, of fourth-generation CARs can be constitutive or inducible by CAR activation (Chmielewski, Hombach, and Abken 2014). A broadened cytokine expression profile of TRUCKs expressing IL-12 facilitated the eradication of antigen-loss cancer cells in tumors and induced activated macrophage accumulation (Chmielewski et al. 2011). Novel fifth-generation CAR T cells can promote cytokine signaling via JAK–STAT3/5 pathways for synergistic three-way signaling next to TCR (via CD3ζ) and CD28-dependent T cell activation for superior in vivo antitumor effects

(Kagoya et al. 2018). Beyond the five generations of CAR T cells, dual and split CARs have been invented to improve safety in case of critical target expression patterns (Lim and June 2017). Nevertheless, clinical research is needed to verify the beneficial profile of fourth and fifth-generation or duals CARs in patients.

Research is also ongoing to improve and reveal the functions of the further compartments of the CAR, the spacer, and transmembrane domains, but the dimensions are limited in comparison to target-binding and signaling domains (Fujiwara et al. 2020). The transmembrane domain connects the antigen-binding domain and spacer domain with the signaling domain and anchors the CAR in the cell membrane. Its influence on CAR functionality by surface stabilization and CD3ζ dimerization for activation was neglected for a long-time (Bridgeman et al. 2010; Romeo, Amiot, and Seed 1992). Thus, natural transmembrane domains of CD3ζ and CD28 and signaling domains were often used, but further research is necessary. The same holds for the second often neglected CAR domain, the spacer or hinge domain. Initially, the spacer domain was just depicted as a structural but functionally inert element in the CAR composition. Hence, sequences derived from various molecules, including IgG1 and IgG4, IgD, CD28, NKG2D, CD8α, were used as CAR spacer domains (Almåsbak et al. 2015; Barber et al. 2008; Hombach, Hombach, and Abken 2010; Sharifzadeh et al. 2013; Wilkie et al. 2008). Over time it became apparent that the spacer domain has to provide an optimal distance between the scFv and the cell surface to mimic a MHC:TCR-like immunological synapse (Guest et al. 2005; Haso et al. 2013; Hudecek et al. 2013). Thus, CAR redirected to membrane-proximal or membrane-distal targets require different spacer lengths for optimal T cell efficacy (James et al. 2008; Krenciute et al. 2016). Moreover, the spacer domain can contribute to CAR surface stability, T cell expansion, and cytotoxicity (Guedan et al. 2019; Qin et al. 2017). Although the influence of the spacer domain on CAR functionality is known, side-by-side comparisons of spacers are missing, especially since some Ig-derived spacers might interfere with in vitro and in vivo functionality (Almåsbak et al. 2015; Hombach et al. 2010; Hudecek et al. 2015; Jonnalagadda et al. 2015).

Nevertheless, extensive in vitro and in vivo testing is of high importance due to the persistent nature of the transgenic cells and the multiple ways to construct them. Each building block of a chimeric antigen receptor, antigen-binding, spacer, transmembrane, and signaling domains can originate from various immune or even non-immune cells (Fesnak, June, and Levine 2016). Thus, the activation and cytotoxicity of T cells generated by two different CARs might differ greatly, even if they are similar in the majority of building blocks. Additionally, transgenic cells in contrast to other cancer treatment strategies may circulate and persist in the human body for

a long time of up to months, increasing the risk for unfavorable interactions with healthy cells and tissues, highlighting the need for preclinical in vivo analyses (Guedan et al. 2020).

1.1.6 CAR T cell therapy of PDAC

Despite the tremendous success and research of CAR T cell against hematological malignancies, resulting in the FDA approval of up-to-date four CAR therapies, translation to solid tumors, including PDAC, faces some hurdles (Mullard 2021). Several reasons hinder the generation of effective CAR T cells for solid tumors. First of all, there are no safe targets known, which are exclusively expressed on PDAC. CD19 and CD20 classical targets for B-cell redirected immunotherapy, are solely expressed on B cells and patients can handle temporally loss of B-cells as a consequence of the therapy (Salles et al. 2017). Identification of safe targets, such as mesothelin and CD133, for PDAC, requires an in-depth characterization of target expression patterns across the whole-body and many tumor samples (Schäfer et al. 2021). However, a cohesive characterization was not performed for the majority of CAR targets analyzed in preclinical and clinical studies in PDAC, such as carcinoembryonic antigen (CEA), epithelial cell adhesion molecule (EpCAM), mesothelin, and prostate stem cell antigen (PSCA) (Akce et al. 2018). Heterogenic target expression makes the target selection process even more complicated and might encourage the ongoing development of combinatorial CAR approaches (Bailey et al. 2016). Nevertheless, two clinical trials (NCT01355965, NCT02541370) using mesothelin-specific respectively CD133-specific CAR T cells verified the efficacy, feasibility, and safety of CAR T cell therapy in PDCA (Beatty and Gladney 2015; Wang et al. 2018).

A second factor reducing CAR T cell efficacy in PDAC is the limited interaction between CAR T cells and pancreatic cancer cells. Contact of CAR T cells and tumor cells is less likely in PDAC, whereas bone marrow and blood are well accessible for CAR T cells (Tokarew et al. 2019). Additionally, PDAC tumors are characterized by a dense tumor stroma and an immunosuppressive tumor microenvironment (TME), creating physical and environmental barriers for T cells, reducing the amount and potential of infiltration CAR T cells (Allen and Louise Jones 2011; Maria Michela D'Aloia et al. 2018). Various approaches are under investigation to increase the infiltration capacity of CAR T cells, enhance the metabolic profile, or reduce the number of stroma cells (Le Bourgeois et al. 2018; Caruana et al. 2015; Lo et al. 2015). Further research and research strategies are necessary to enhance CAR T cells' abilities in solid tumors.

1.2 Imaging in Preclinical Cancer Research

1.2.1 Mouse Models for Preclinical Research

Preclinical cancer research demands suitable in vivo mouse models to analyze treatment options. Three general types of tumor models exist in mice. One option is the engraftment of human cancer cell lines, engineered tumor cells, or patients samples as a xenograft, which can be performed by subcutaneous, intravenous, or orthotopic transplantation of tumor cells (Day, Merlino, and Van Dyke 2015). Although orthoptic tumor models are of high interest for TME related questions, the volume of the methods varies in their advantages and disadvantages (Erstad et al. 2018). In the case of leukemias, orthotopic tumor implantation can be easily achieved by intravenous injection, whereas some solid tumors such as PDAC models require a complex surgical procedure to transplant the tumor cells into pancreatic tissue with an extended healing period (Bibby 2004). The second option is the application of syngeneic tumor models, where the subcutaneously or orthotopically transferred tumor cells have a similar genetic background as the used mouse model (Narayanan et al. 2018). The benefits of this model include the presence of an intact immune system. The third option is the utilization of spontaneous or induced tumor models (Onaciu et al. 2020).

Other areas, such as immunological or imaging-related research have other requirements. In this way, optical imaging methods are sensitive to light scattering by darker skin and dark fur. Hence, nude mice without any fur and bright skin are often used for optical imaging strategies (Kaijzel, Van Der Pluijm, and Löwik 2007). Evaluation of human CAR for clinical transfer requires the use of human T cells and tumor cells, so immunodeficient mouse models, such as NOD SCID gamma (NSG) mice are often used in preclinical CAR evaluation (Agarwal et al. 2019; Chu et al. 2015; Wen et al. 2019). However, the unavailability of immune cells hinders immunological TME studies and increases the risk for infections after complicated surgical procedures, as in the case of orthotopic tumor implementation. Humanization of NSG mice with $CD34^+$ human hemopoietic stem cells (HSC) is an option to provide a fully-humanized immune system but recovery until full immunological reconstitution takes 4-6 weeks (Wen et al. 2019; Wu and Yu 2019).

1.2.2 Small Animal In Vivo Imaging Modalities

Clinical imaging techniques are applied for the determination of disease progression and treatment decisions, still, it is an advantageous tool for preclinical research. Various two- (2D) and three-dimensional (3D) methods are available with individual advantages and limitations, to monitor cancer development, progression, or treatment (Table 1).

Technology	Means of detection	Resolution	Depth	Agents	Target	Relative cost
Computed tomography (CT)	Ionizing radiation (γ-rays)	50 μm	No limit	Iodinated molecules	Anatomical, physiological	€€
Positron emission tomography (PET)	Ionizing radiation (γ-rays)	1 – 2 mm	No limit	^{19}F-, ^{64}Cu-, ^{68}Ga-, or ^{11}C-labelled compounds	Physiological, molecular	€€
Single photon emission computed tomography (SPECT)	Ionizing radiation (γ-rays)	0.3 – 1 mm	No limit	^{99m}Tc-, ^{111}In-, ^{67}Ga-labelled compounds	Physiological, molecular	€€
Magnetic resonance imaging (MRI)	Electromagnetism	10 – 100 μm	No limit	Paramagnetic and magnetic compounds (iron oxide; chelated Gd^{3+})	Anatomical, physiological	€€€
Ultrasound	Acoustic waves	50 μm	3 cm	Microbubbles	Anatomical	€
Bio-luminescence (BLI)	Bioluminescent light	1–5mm	up to <5cm	Luciferin	Molecular	€
Bio-luminescence tomography (BLT)	Bioluminescent light	2–6mm	up to <5cm	Luciferin	Physiological; molecular	€€
Fluorescence reflectance imaging (FLI)	Fluorescent light	2–3mm	up to <1cm	Fluorochromes; fluorescent proteins	Physiological; molecular	€
Fluorescence mediated Tomography (FMT)	Fluorescent light	1–2mm	up to <5cm	Near-infrared fluorochromes	Physiological; molecular	€€
Intravital microscopy	Fluorescent light	200nm	up to <1mm	Fluorochromes; fluorescent proteins	Anatomical; physiological; molecular	€€

Table 1: Overview of preclinical in vivo imaging techniques.

Each modality differs in cost, detection, resolution, depth, and target. € represents €100,000–€200,000, €€ represents €200,000–€400,000 and €€€ represents >€400,000. Modified from (Chehade, Srivastava, and Bulte 2016; De Jong, Essers, and Van Weerden 2014).

Each scientific question requires the careful selection of an appropriate imaging modality depending on required spatial resolution, imaging depth, and the respective target. Anatomical questions imply the application of CT, MRI, or Ultrasound imaging, which can be used without additional agents. Whereas PET and SPECT offer high resolution of molecular and physiological details, but nuclear agents and radiotracers require special permits, raising the technical barriers for these techniques. Computed tomography (CT), positron emission tomography (PET), single photon emission computed tomography (SPECT), and magnetic

resonance imaging (MRI), ultrasound, imaging are also important tools in clinical imaging, so the transferability of preclinical imaging results is strongly pronounced (reviewed by (De Jong, Essers, and Van Weerden 2014)). In contrast to that, clinical transfer of optical imaging modalities, including FLI, FMT, BLI, and newly established BLT, is prevented by low penetration depths of light, the light absorption of hemoglobin, and attenuation by melanin and hair, but technical improvements are currently under investigation for improved clinical transfer (Pirovano et al. 2020). Thus, optical imaging techniques are currently limited to preclinical research.

1.2.3 Computed Tomography

To date, CT is the gold standard for anatomical imaging questions in clinical and preclinical diagnostic and research. The advantages include the speed, high resolution, with unlimited depth at a comparatively low cost. The CT data is generated by the reconstruction of thousands of X-ray scans of a γ-ray source from different angles around the sample (typically 180° or 360°). The reconstructed data can be analyzed in all different planes, coronal, sagittal, and axial, like a slice or 3D projection of the greyscale image. Thresholding of the greyscale values in a region of interest (ROI) allows the separation of different organs by segmentation and further analysis of certain tissue parameters, such as size, volume, or vascular network (reviewed by (Rawson et al. 2020)). The applied energy has to be adjusted, based on prior evaluation of the ROI, to achieve high-resolution images of individual structures. (Pawałowski et al. 2019). Some structures might even require contrast agents for sufficient differentiation of soft tissues. However, an increase of energy or multiple repeated scans with several energy intensities raise the overall organ dose, which is considerably higher than in comparison to conventional radiography and might even induce cancer in the long term (Brenner and Hall 2007).

1.2.4 Molecular Bioluminescence Imaging

2D BLI imaging is a rapid, cost-effective, non-radioactive, and accessible method for sensitive and quantitative high-throughput imaging in multiple small animals, representing an ideal tool for preclinical cancer research (Rehemtulla et al. 2000). 2D BLI has been applied to study drug development, monitoring of genes, tumor development, metastasis, and protein interaction in various xenograft and orthotopic tumor mouse models (Alsawaftah et al. 2021). Over the last decades, the toolbox has expanded, but the basic principle is still composed of the combination of a luciferase gene expressed under a constant or inducible promotor by a biological organism, such as bacteria, viruses, fungi, or cells, and the respective substrate, e.g. D-Luciferin (Xu et al. 2016). Combination of both in small animals results in an intramolecular electron transfer, via

an oxidation decarboxylation reaction in presence of oxygen, ATP, and MG^{2+}, which is responsible for light emission during return and enables detection with super-cooled (-90°C) back-illuminated charge-coupled devices (CCD) between 400 and 700 nm (Fraga et al. 2006). This results in a light emission proportional to higher amounts of luciferase enzymes, expressed by e.g. proliferating cells. The substrate is often intraperitoneally injected and low-light sensitive CCD image acquisition is performed 10 - 15 minutes after injection at the maximum intensity of light emission before the slow clearance of signal, albeit other injection routes result in other kinetics (Figure 4) (Inoue et al. 2009).

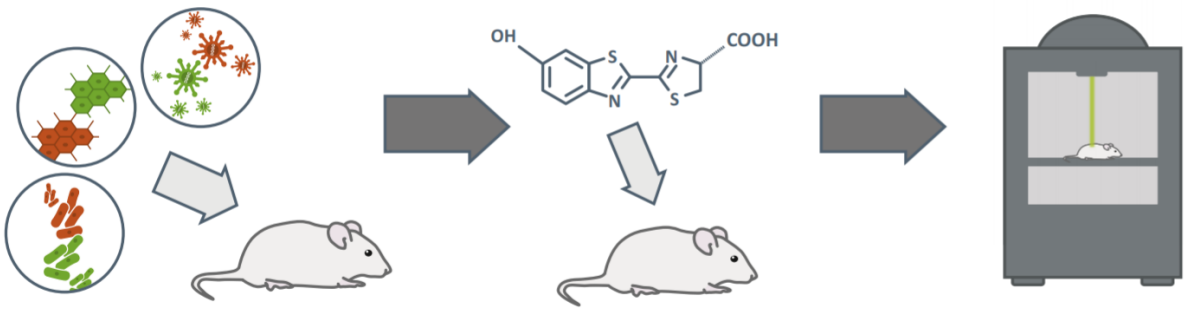

Figure 4: In vivo bioluminescence imaging in small animals.

Bioluminescence imaging requires three different steps. First, animals are injected with genetically modified cells, bacteria, or viruses, expressing a bioluminescent reporter gene. In a second step, animals are injected with the bioluminescent substrate, e.g. D-Luciferin. Subsequently, animals are transferred into an in vivo imaging device for the acquisitions of signals and data processing. For 3D BLT imaging, mice are transferred either horizontally or vertically, depending on the device provider, to an integrated or separated µCT with an γ-ray tube for reconstructed hybrid BLT/CT scans. Modified from (Mezzanotte et al. 2017).

The most widely used combination of luciferase gene and substrate is firefly (ff) luciferase from Photinus pyralis with D-Luciferin, with an emission peak at 600 nm (Zhao et al. 2005). Codon optimization improved the thermostability and its expression in mammalian cells, including human cancer cell lines (Branchini et al. 2007). However, there are other available options from various organisms, including beetle, bacterial, marine, and fungal luciferases with their respective substrates, covering a wide range of emission wavelengths (Zambito, Chawda, and Mezzanotte 2021). Each combination has individual strengths and weaknesses facilitating different applications, supporting the chances, and overcoming some do the drawbacks of BLI imaging.

2D BLI imaging allows low threshold, longitudinal, and non-radioactive imaging of multiple animals at low costs. The continuously growing amount of modified luciferases and improved substrates enable a combination of multiple red- or green- luciferases and spectral unmixing of signals for dual imaging with one or more substrates (Daniel et al. 2015). Fusion of luciferases

achieved intramolecular bioluminescence resonance energy transfer (BRET) and improved the number of photons at high wavelengths for imaging of blood-rich or deep tissues (Taylor et al. 2018; Yeh et al. 2017). This compensated partially the unfavorable emission peak of the ff luciferase at 600 nm outside of the optical window between 700 – 900 nm, where high amounts of the emitted light are absorbed by water and hemoglobin (Sakudo 2016). Despite the high sensitivity of BLI, caused by the low background signal, detection of smaller metastatic tumors close to the primary and brighter tumors is limited (O'Neill et al. 2010). Another drawback is the requirement of ATP and oxygen in living cells for the oxidation decarboxylation reaction since intratumoral areas are often hypoxic with low ATP amounts (Eales, Hollinshead, and Tennant 2016). This reduces the high sensitivity of 2D BLI in larger tumors, whereas small tumors are detectable at an early time-point and low cell numbers of $1x10^4$ (O'Neill et al. 2010). This drawback also prevents ex vivo analysis, due to the unavailability of suitable detection methods.

Beyond 2D BLI imaging, 3D BLT is an emerging optical molecular imaging technology. This modality connects bioluminescence imaging with micro-computed tomography (µCT), by spatial reconstruction of the electrons captured by a CCD to the scanned object (Gu et al. 2004; Rice, Cable, and Nelson 2001). BLT imaging allows the quantitative and localized analysis of the bioluminescent source and distribution in vivo, in contrast to planar 2D imaging (Han and Wang 2008). BLT accuracy is strongly influenced by the reconstruction algorithm and the amount of emitted light, so further progress is needed to improve accuracy by advanced reconstruction algorithm and high emitting luciferase/luciferin systems (Mezzanotte et al. 2017). Nevertheless, BLT imaging represents an attractive tool for biological and medical research in preclinical imaging.

SUMMARY REVIEW

ENHANCING THE EFFICACY OF CAR T CELLS IN THE TUMOR MICROENVIRONMENT OF PANCREATIC CANCER

The manuscript reviews how current strategies of stromal tumor microenvironment (TME) targeting could be connected with cell-based immunotherapy approaches, such as chimeric antigen receptor (CAR) T cells. First of all, the enormous barriers, created by the TME of PDAC for cancer therapy including CAR T cells, were described and depicted in a figure. The next part gives a short overview of the developmental history of transgenic T cells up to the most recent innovations. One major hindrance for CAR T cells in PDAC, next to the TME and the pronounced desmoplastic reaction, is the unavailability of suitable targets with a safe expression profile. Thus, the current progress of clinical CAR T cell targets in pancreatic cancer was summarized, resulting in the implication to use cell-based approaches requiring more than one target for full T cell signaling.

Furthermore, the contribution and potential of stromal TME players were reviewed, in combination with the present-day clinical status of potential therapies utilizing the presence of these players in the TME. Cancer-Associated Fibroblasts (CAFs) are of great significance in PDAC due to their proportion and impact on the TME subtype, which could be indicative for further patient stratification. In the following section the components of the extracellular matrix (ECM), expressed by CAFs, were investigated for their combinatorial potential with cell-based immunotherapies. This was further complemented by the analysis of selected growth factors, which could be an interesting option in combination with CAR T cells. For all parts we describe the clinical progression of the possible combinatorial approach in PDAC.

The conclusive section emphasizes the most advanced and promising approaches, highlights the crucial impact of the stromal TME on T cell-based immunotherapies and stresses the significance of imaging techniques in this context.

1.3 REVIEW: ENHANCING THE EFFICACY OF CAR T CELLS IN THE TUMOR MICROENVIRONMENT OF PANCREATIC CANCER

Published in Cancers: **Henze, J.**; Tacke, F.; Hardt, O.; Alves, F.; Al Rawashdeh, W. Enhancing the Efficacy of CAR T Cells in the Tumor Microenvironment of Pancreatic Cancer. Cancers 2020, 12, 1389. https://doi.org/10.3390/cancers12061389

Authors:

Janina Henze[1,2], Frank Tacke[3], Olaf Hardt[2], Frauke Alves[1,4] and Wa'el Al Rawashdeh[2,*]

Affiliations:

[1]*University Medical Center Göttingen, Translational Molecular Imaging, Institute for Diagnostic and Interventional Radiology & Clinic for Hematology and Medical Oncology, Göttingen, Lower Saxony, Germany; janina.henze@stud.uni-goettingen.de*

[2]*Miltenyi Biotec B.V. & Co. KG, R&D Reagents, Bergisch Gladbach, North Rhine-Westphalia, Germany; (O.H.) Olaf@miltenyibiotec.de, (W.A.R.) wael.alrawashdeh@miltenyibiotec.de*

[3]*Dept of Hepatology & Gastroenterology, Charité University Medicine Berlin, Berlin, Germany; frank.tacke@charite.de*

[4]*Max-Planck-Institute for Experimental Medicine, Translational Molecular Imaging, Göttingen, Lower Saxony, Germany; falves@gwdg.de*

[*] Corresponding author

Received: 24 April 2020; Accepted: 26 May 2020; Published: 28 May 2020

Abstract

Pancreatic cancer has the worst prognosis and lowest survival rate among all types of cancers and thus, there exists a strong need for novel therapeutic strategies. Chimeric antigen receptor (CAR)-modified T cells present a new potential option after successful FDA-approval in hematologic malignancies, however, current CAR T cell clinical trials in pancreatic cancer failed to improve survival and were unable to demonstrate any significant response. The physical and environmental barriers created by the distinct tumor microenvironment (TME) as a result of the desmoplastic reaction in pancreatic cancer present major hurdles for CAR T cells as a viable therapeutic option in this tumor entity. Cancer cells and cancer-associated fibroblasts express extracellular matrix molecules, enzymes, and growth factors, which can attenuate CAR T cell infiltration and efficacy. Recent efforts demonstrate a niche shift where targeting the TME along CAR T cell therapy is believed or hoped to provide a substantial clinical added value to improve overall survival. This review summarizes therapeutic approaches targeting the TME and their effect on CAR T cells as well as their outcome in preclinical and clinical trials in pancreatic cancer.

Keywords: tumor microenvironment; pancreatic cancer; immunotherapy; CAR T cell therapy; extracellular matrix; cancer-associated fibroblasts

1. Introduction

Pancreatic cancer, i.e., pancreatic ductal adenocarcinoma (PDAC), is a fatal disease with five-year overall survival rates of 1% to 5% and median survival duration of fewer than six months [1]. The poor prognosis has not substantially changed during the past decades, establishing pancreatic cancer as the fourth leading cause of cancer-related deaths in Western countries [2,3,4]. Therapeutic progress in other types of cancer will lead to its ascension in second place among all cancers within the next decade [5]. Surgery remains the only potentially curative treatment, but only a minority of patients show a resectable disease stage at diagnosis, due to invasion to the surrounding vasculature and due to lack of symptoms at an early stage [6]. Nonetheless, the median overall survival is still only 24 months for patients with resectable disease [7].

Therapeutic failures of chemotherapy, targeted therapy, and immunotherapy of PDAC can be largely attributed to the special features of this cancer, which exhibits highly nutrient-poor, immunosuppressive, hypoxic and desmoplastic characteristics leading to rapid cancer progression [8]. The tumor is composed of only a minor number of malignant cells within a microenvironment of dense extracellular matrix (ECM), a barrier that prevents adequate drug

delivery and might serve as a prognostic factor (Figure 1 and Figure 2) [8]. Responsible for the stromal reaction are mainly cancer-associated fibroblasts (CAFs) that develop from bone marrow-derived mesenchymal stem cells (MSCs), pancreatic stellate cells (PSCs), and quiescent resident fibroblasts through multiple pathways of activation [9]. The complex tumor vasculature in PDAC is characterized by a lack of blood vessels, leading to high levels of hypoxia in the tumor interior [10]. Furthermore, the capillaries and lymphatic vessels that are present tend to be collapsed due to high interstitial pressure, either from excess fluid or from solid stress [11]. Other non-neoplastic cancer-associated cells consist of immune-suppressor cells such as regulatory T cells (T_{reg}), myeloid-derived suppressor cells (MDSC), and tumor-associated macrophages (TAM) that can inhibit $CD8^+$ T cells, which play a key role in the antitumor immune response, and thereby establish an immunosuppressive tumor microenvironment [12]. Neural remodeling and perineural invasion (PNI), the neoplastic invasion of tumor cells into nerves, are further unfavorable histological features, and are considered as one of the main routes for cancer recurrence and metastasis after surgery [13]. Conventional therapies such as chemotherapy and radiation have focused on effective therapy of the malignant cell population. Thus, a concordant combination of various treatments targeting additional key cellular features of PDAC such as stroma, reversing suppressive immune reactions and enhancing antitumor reactivity may lead to more successful treatment strategies [14]. Thus, there is a clinically unmet need for new therapeutic options.

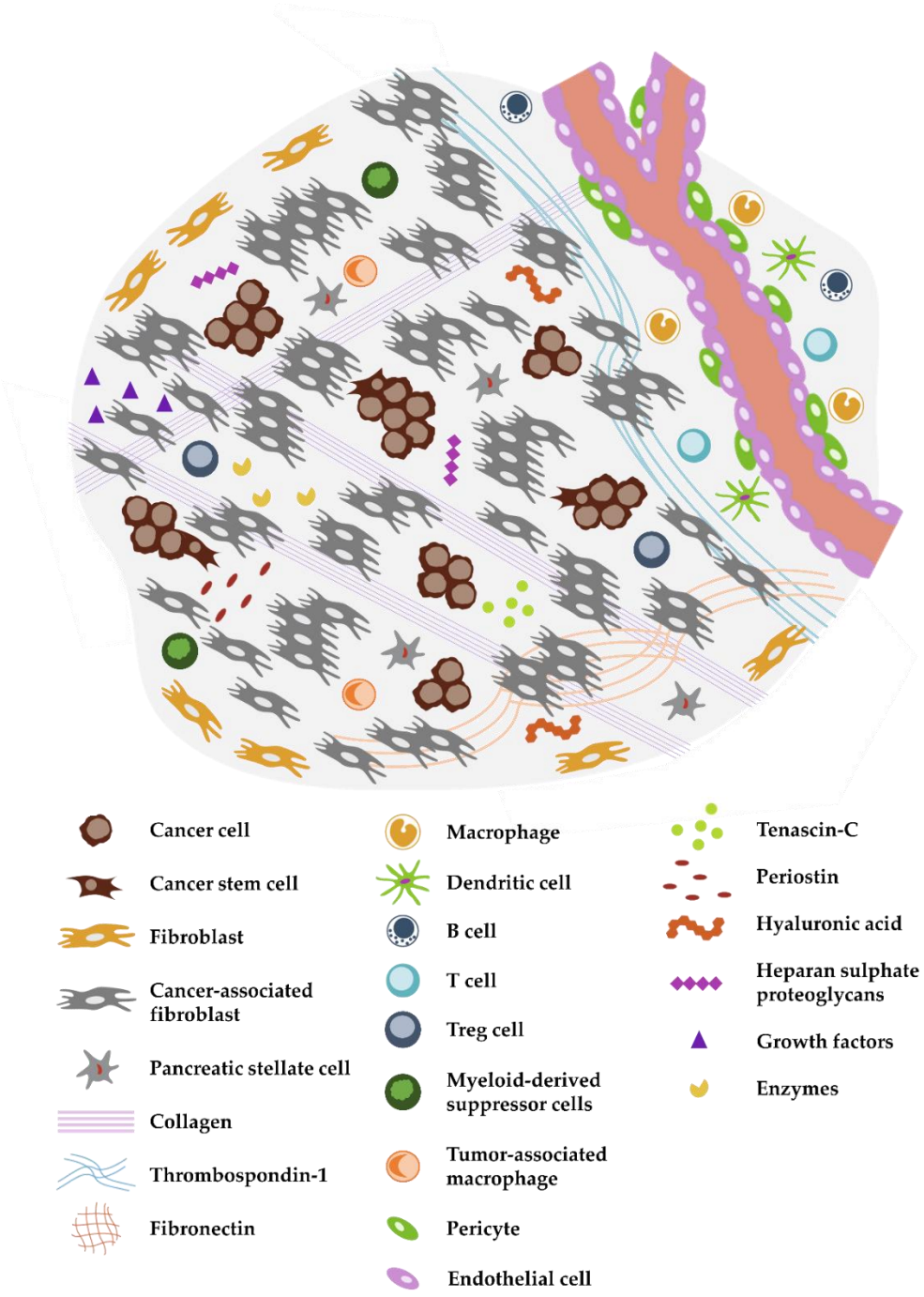

Figure 1. Complex tumor microenvironment (TME) of pancreatic cancer. The pancreatic ductal adenocarcinoma (PDAC) microenvironment is characterized by a dense desmoplastic stroma, with cancer-associated fibroblasts (CAFs) presenting the majority of the cell population (in grey). Tumor cells (round and brown) in aggressive PDACs can occur in tumor buds, small groups of cells, especially in the invasive front. A high abundance of extracellular matrix (ECM) molecules, enzymes, and growth factors is another important feature. Immune cells are often excluded from the TME or exhibit an immunosuppressive phenotype. The distribution of pro- and anti-inflammatory immune cells as well as the exact composition of the tumor stroma is dependent on the subtype of pancreatic cancer as discussed by Bailey et al. or by Karamitopoulou [12,15].

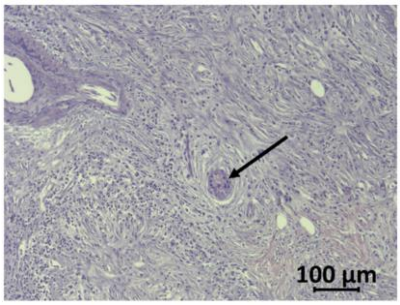

Figure 2. Hematoxylin/eosin-stained human PDAC sample. Tumor cells (arrow) are surrounded by the desmoplastic reaction of stromal cells and few immune cells.

Immunotherapy is a rapidly developing field within oncological research, especially since the development of chimeric antigen receptor (CAR) T cells, which are genetically engineered to express receptors targeting cancer cells for immunotherapy. CAR technology has made leaps of development since its conception in 1993, combining antigen recognizing regions from antibodies with intracellular T cell signaling domains (Figure 3) [16]. In this way, potential demasking of tumor cells by major histocompatibility complex (MHC) class I downregulation, can be overcome [17]. At first, double chimeric receptors were developed by engineering the VH and VL chains of immunoglobulins to the constant regions of the T cell receptor (TCR) [18]. Over time, CARs were modified into a single chain approach coupling a single chain variable fragment (scFv) derived from an antibody via a spacer and transmembrane domain to the CD3ζ signaling domain of the TCR [16]. The addition of costimulatory domains from CD28 or 4-1BB generated a stronger activating signal, circumventing the intracellular activation by TCR-domains, defining the second CAR generation [19]. Second-generation CARs targeting CD19 are the first CAR success-story wherein phase II study 81% of the B cell acute lymphoblastic leukemia patients demonstrated complete remission 28 days after infusion [20]. Their tremendous success in the treatment of leukemia and lymphoma patients led to the FDA approval of the first CAR T cell therapy as a second-line treatment in 2017 [21]. The incorporation of further costimulatory domains derived from CD27 or CD40 as well as the introduction of additional cytokine expression or induction of other signaling pathways established the third, fourth, and fifth generations of CAR T cells, increasing cytokine production, cell survival, and persistence [22]. In recent years, advanced CAR concepts, such as Tandem or Universal CAR approaches have been developed and enabled the targeting of challenging antigen expression profiles on cancer cells [23]. Other advanced CAR technologies explore mechanisms to switch on and off CAR expression on T cells to control possible toxic side effects [24]. Another upcoming class of engineered receptors is synthetic Notch (synNotch)

receptors, which can induce transcriptional activation after target recognition [25]. Ultimately, all developmental generations of CARs offer various opportunities and challenges for prospective cell-based approaches as reviewed before [22,24,26].

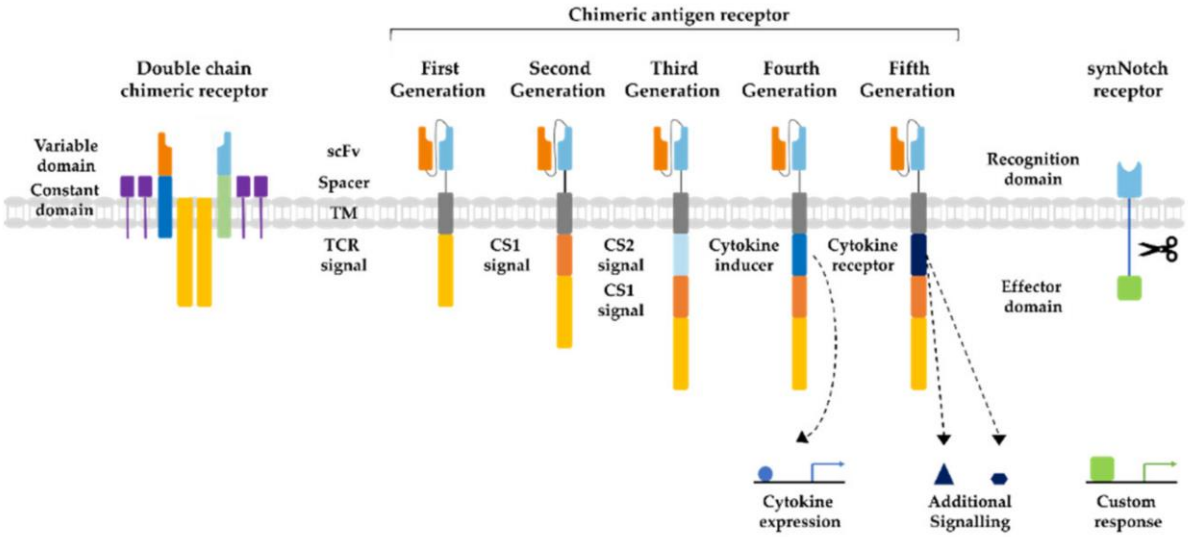

	Double chain chimeric receptor	First Gen. CAR	Second Gen. CAR	Third Gen. CAR	Fourth Gen. CAR	Fifth Gen. CAR	synNotch receptor
Cytotoxicity	Not compared	+	++	+++	+++	Dependent on signalling	Dependent on custom response
Proliferation	Not compared	+	++	+++	+++	Dependent on signalling	Dependent on custom response
Cytokine secretion	Not compared	+	++	+++	++++	Dependent on signalling	Dependent on custom response
Persistence	Not compared	+	++	+++	Dependent on cytokine profile	Dependent on signalling	Dependent on custom response
Flexibility	-	-	+	++	+++	+++	++++

Figure 3. Developmental stages of chimeric antigen receptors. The first double chain chimeric receptors were engineered to customize the variable T cell receptor (TCR) domain by using V_H and V_L chains of antibodies (orange and bright blue boxes) fused to the constant regions of the TCR α- and β-chains (green and blue boxes). They mimicked the TCR in appearance and functionality. Activation relies on association with intracellular CD3ζ (yellow boxes), CD3γ, CD3δ, and CD3ε chains (purple boxes). The first generation of CARs combined the antigen recognizing scFv directly with the CD3ζ-signalling domain in one construct overcoming expression difficulties by the tremendous construct length of double chain chimeric receptors. Cytotoxicity, proliferation, cytokine secretion, and persistence of CARs were increased in second and third generation CARs by the addition of further costimulatory domains (CS1 and CS2) such as CD27, CD28, CD134, or 4-1BB. Introduction of T cell redirected for universal cytokine-mediated killing (TRUCKs) or fourth generation CARs increased the flexibility in CAR design for specific challenges even further, enabling local expression of cytokines such as IL-12, which are toxic in high concentrations. Fifth generation CARs, as fourth generation CARs, are based on second generation CARs. The individual antigen response is complemented by activation of intracellular domains of cytokines (dark blue box) e.g., IL-2Rβ, which induced signal transduction in the STAT3/5 pathway. Another group of artificial antigen receptors, gaining increased interest in recent years, are synNotch receptors. These receptors use the cleavage process after Delta-Notch binding and enable an unlimited variety of responses (green box) after target recognition such as cell fate determination with transcription factors and expression of selected cytokines or therapeutic antibodies. In this way, they bring the potential of immune cells as “living drugs” a big step forward.

Unfortunately, fewer exciting outcomes were achieved in initial clinical trials with CAR T cells targeting solid tumors, including PDAC. Successful CAR therapy for carcinomas needs to overcome the physical and environmental barriers in the tumor microenvironment (TME) [27]. The TME consists, next to tumor cells, of endothelial, immune, and inflammatory cells, stromal cells, the extracellular matrix and a broad spectrum of enzymes, cytokines, and growth factors [28]. This creates a strong physical barrier for $CD8^+$ T cells, while their immune response is further diminished by the high amount of immunosuppressive immune cells present in the TME of PDAC [12,29]. These aspects must be considered and addressed in the field of cell-based immunotherapy against solid cancers. Here we review different strategies to overcome these hurdles for successful CAR T cell therapy in pancreatic cancer.

2. CAR T Cells and the Tumor Microenvironment of Pancreatic Cancer

2.1. CAR Targets for Pancreatic Cancer

The first obstacle for effective CAR T-cell therapy for carcinomas is the lack of suitable targets on carcinoma cells. CAR T therapy induces an ablation of all cells with a certain degree of antigen expression leading to potentially fatal side effects such as "on target/off tumor" toxicities [30]. Unfortunately, this is also the case for most of the PDAC targets tested in preclinical and clinical trials such as carcinoembryonic antigen (CEA), CD133, CD70, Claudin 18.2, epithelial cell adhesion molecule (EpCAM), receptor tyrosine-protein kinase erbB-2 (HER2), mesothelin, and prostate stem cell antigen (PSCA) (Table 1) [31].

Table 2: Therapeutic options for combinatorial stromal and immunotherapy.

Therapeutic	Proposed effect	Clinical trials	References
2.1. CAR T cell therapy for pancreatic cancer			
Carcinoembryonic antigen (CEA)	CAR Target	Pancreatic cancer: NCT03818165, NCT04037241, NCT02850536, NCT02349724, NCT03682744, NCT03267173, NCT02416466, NCT02959151	[31]
CD133	CAR Target	Pancreatic cancer: NCT02541370	[31,32]
CD70	CAR Target	Pancreatic cancer: NCT02830724	[31]
Claudin 18.2	CAR Target	Pancreatic cancer: NCT03890198, NCT03302403	[31]

Epithelial cell adhesion molecule (EpCAM)	CAR Target	Pancreatic cancer: NCT03013712	[31]
HER2	CAR Target	Pancreatic cancer: NCT02713984, NCT03267173	[31]
Mesothelin	CAR Target	Pancreatic cancer: NCT02706782, NCT03267173, NCT03497819, NCT03638193, NCT01897415, NCT01583686, NCT02465983, NCT03323944, NCT02959151, NCT02580747	[31,33]
Prostate stem cell antigen (PSCA)	CAR Target	Pancreatic cancer: NCT03267173, NCT02744287	[31]
2.2.1. Cancer-Associated Fibroblasts			
Fibroblast activation protein (FAP)-CAR T cells	CAF depletion	Solid tumors: NCT03932565, NCT01722149, NCT03050268	[34,35,36,37,38]
Vismodegib	CAF depletion	Pancreatic cancer: NCT01195415, NCT01064622, NCT01537107, NCT01088815, NCT00878163, NCT01713218, NCT02465060	[39]
CAF vaccine	CAF depletion	N/A	[40]
All-trans retinoic acid (ATRA)	CAF remodeling	Pancreatic cancer: NCT03307148, NCT03878524	[41,42]
JQ1	CAF remodeling	N/A	[43,44]
Calpeptin	CAF remodeling	N/A	[45]
2.2.2. Components of Extracellular Matrix in Pancreatic Cancer			
Heparanase-expressing CAR T cells	Heparan sulphate proteoglycans degradation	N/A	[46]
Collagen binding domain (CBD)-immune checkpoint inhibitors (CPI)/CBD-IL-2	Collagen redirected delivery	N/A	[47]
BC-1	Fibronectin redirected delivery	N/A	[48]
DARLEUKIN	Fibronectin redirected delivery	Pancreatic cancer: NCT01198522 Solid tumors:	[49,50,51]

		NCT01058538, NCT02086721, NCT02735850, NCT03705403	
TELEUKIN	Tenascin-C redirected delivery	Solid tumors: NCT01131364, NCT01134250	[52,53]
PEGPH20	Hyaluronic acid degradation	Pancreatic cancer: NCT03481920, NCT01453153, NCT01839487, NCT04058964, NCT03634332, NCT02241187, NCT02921022, NCT02910882, NCT01959139, NCT04134468, NCT03193190, NCT02715804	[54,55,56,57]
ABT-510	Thrombospondin 1 inhibition	Pancreatic cancer: NCT00586092 Solid tumors: NCT00113334, NCT00073125, NCT00061646	[58,59,60,61]
CVX-045	Thrombospondin 1 inhibition	Solid tumors: NCT00879554	[62,63]
Trabectedin	Thrombospondin 1 inhibition	Pancreatic cancer: NCT01339754 Solid tumors: NCT00002904, NCT00786838, NCT03127215, NCT01273480, NCT01267084	[62,63,64]
MZ-1	Periostin inhibition	N/A	[65]
2.2.3. Growth Factors in Pancreatic Cancer			
Bevacizumab	Vascular endothelial growth factor (VEGF) inhibition	Pancreatic cancer: NCT00614653, NCT00365144, NCT00088894., NCT00112528, NCT00366457, etc.	[66,67,68]
BGB324	AXL RTK inhibition	Pancreatic cancer: NCT03649321	[69]
TP-0903	AXL RTK inhibition	N/A	[70]

Abbreviations: CEA, carcinoembryonic antigen; EpCAM, epithelial cell adhesion molecule; HER-2, receptor tyrosine-protein kinase erbB-2; PSCA, prostate stem cell antigen; FAP, fibroblasts activation protein; CAR, chimeric antigen receptor; CAF, cancer-associated fibroblasts; ATRA, all-trans retinoic acid; N/A, not applicable; CBD, collagen binding domain; CPI, immune checkpoint inhibitors; PEGPH20, PEGylated recombinant human hyaluronidase; VEGF, vascular endothelial growth factor; RTK, receptor tyrosine kinase.

The most advanced targets for clinical consideration are CEA and mesothelin, with up to five clinical trials completed, active, or recruiting (CEA: NCT03818165, NCT02850536, NCT02416466, NCT04037241, NCT03682744; mesothelin: NCT03323944, NCT03497819, NCT03638193, NCT01897415). In contrast, the only published results from clinical trials of CAR T cells in PDAC originate from mesothelin and CD133. The mesothelin-specific CAR trial resulted in two patients with a progression-free survival of four to five months and another patient showed a reduction of liver lesions, but not of the primary tumor (NCT01355965) [33]. The CD133 CAR trial also demonstrated a partial remission in two PDAC patients with Grade II toxicity, potentially due to the expression pattern of CD133 in hemopoietic stem cells (NCT02541370) [32]. Both studies verified the feasibility, safety, and principal efficacy of CAR T cell therapy for pancreatic cancer. Nevertheless, several problems prevented the induction of full remission and improvement of survival by immunotherapy despite its efficacy against metastases, often the discriminating factor for successful cancer therapy [71]. Two of the problems that must be solved for effective CAR T cell treatment are (i) emerging exhaustion and (ii) missing persistence of CAR T cells [32,33]. Co-treatment with PD-1/PD-L1 interfering checkpoint inhibitors or multiple infusions of CAR T cells might overcome these problems [72]. This aims to precondition chemotherapy and CAR constructs modifications, e.g., different costimulatory domains for $CD4^+$ and $CD8^+$ CAR T cells as well as transgenic cytokine expression, might overcome these problems [72]. However expression levels of cytokines need to be steered carefully, e.g., with conditional induction, to limit the risk for toxic cytokine release syndrome (CRS) [73].

The heterogeneity underlying PDAC makes therapeutic options based on one-size-fits-all approaches ineffective. Among others, Bailey et al. [15] defined for example four subtypes of PDAC, based on genomic analysis correlating with histopathological characteristics. These various PDAC types and their distinct stroma subtypes imply a specific stratification of the patients due to different behavior under the same treatment [74]. The complexity is further increased by another hurdle, which remains unchallenged: advanced targets in pancreatic cancer are usually heterogeneously expressed and are sometimes just present on 20% of the tumor cells, leading to progression of the diseases by the target-negative cells in the clinical trials [31,32,33]. Therefore, classifying patients in subtypes that could benefit from cell therapy would help improve outcomes and quality of life as well as avoid ineffective or even risky therapy approaches. These complex circumstances require the identification of new CAR targets as well as sophisticated Tandem, Universal CAR, and adapter-CAR approaches. In this way,

unintentional “on target/off tumor” toxicities can be prevented for a safe and balanced application of CAR T cells in pancreatic cancer [75].

2.2. Targeting the Tumor Microenvironment in Pancreatic Cancer

A second major hindrance for cell therapy is the complex TME of solid tumors, representing an exceptional challenge in comparison to other tumor types. However, the histological key feature of PDAC is the occurrence of a unique desmoplastic reaction, comprising over two-thirds of the total tumor volume and destructing the architecture of normal pancreatic tissue [76]. Desmoplasia is marked by a dramatic increase in the proliferation of alpha-smooth muscle actin-positive fibroblasts and is also accompanied by the increased deposition of extracellular matrix molecules [77]. This has a strong impact on treatment outcomes since cytotoxic therapy can not only increase the amount of active CAFs but also increase their treatment resistance and tumor aggressiveness [78]. Another aspect of the dense tumor stroma is the limited availability of nutrients and oxygen [12]. The consequences of this deprivation for immune cells, including CAR T cells, in the stroma of solid tumors as well as major changes in the metabolic processes of the TME, have been extensively reviewed elsewhere [79,80,81] and will not be addressed in this review.

2.2.1. Cancer-Associated Fibroblasts

Under normal conditions, stromal fibroblast cells communicate and interact with the surrounding ECM. They secrete and synthesize new ECM molecules as well as growth factors and enzymes, e.g., upon stimulation by tissue injury [82]. Under pathological conditions in the context of cancer however, the complexity of fibroblasts’ roles increases. In an early tumor stage, fibroblasts have been demonstrated to prevent tumor growth by remodeling the ECM and inducing an anti-tumor immune response [83]. Whereas at later stages with an established tumor, fibroblasts transform into activated CAFs, where they become tumorigenic and enhance metastasis-potential and chemoresistance [84]. ECM molecule expression and release of tumor-promoting cytokines can also be increased in activated CAFs, but stimuli and time point of phenotype switch are still under investigation [85]. CAFs can originate from various cell types, such as resident fibroblasts, chondrocytes, adipocytes, mesenchymal stem cells, pericytes, and mesenchymal transitioned endothelial and epithelial cells, including cancer cells and cancer stem cells [86]. In PDAC, CAFs can additionally be derived from PSCs, quiescent under normal conditions but transitioned into a myofibroblast-like phenotype under pathophysiological conditions in the pancreas [87]. Regardless of CAF origin, this cell type can constitute up to

90% of the tumor mass in PDAC, representing an inevitable hurdle for expedient treatment strategies [88].

Accordingly, numerous efforts have tried to dispose of CAFs or reprogram them within the TME [89]. In the context of CARs, several groups have generated fibroblast activation protein (FAP)-redirected CAR T cells to erase FAP-expressing CAFs, resulting in a reduction of ECM molecules and tumor growth, also in a syngeneic murine pancreatic cancer model [34,35,36]. FAP is a serine protease capable of local ECM modification by changing fibronectin orientation [90]. All studies emphasized the value of co-targeting CAFs and tumor cells simultaneously for solid tumors. Nevertheless, a debate is on-going regarding the safety of FAP as a CAR target, after the demonstration of hematopoietic side effects due to FAP^+ bone marrow stromal cells (BMSCs) in mice [37,38]. Other possible extracellular markers expressed on CAFs, e.g., platelet-derived growth factor receptor (PDGFR) α and β, exhibit inappropriate expression patterns [86,91]. Therefore, more convenient and safe targets or target combinations need to be evaluated for successful CAF-redirected CAR establishment.

Next to cell-based CAF depletion, drug-based therapeutic options have also been proposed. Nab-paclitaxel has been shown to decrease CAFs numbers in PDAC in a clinical trial in combination with gemcitabine (NCT00398086) [92]. Small molecules inhibiting the sonic hedgehog (SHH) pathway have demonstrated promising preclinical results but failed to recapitulate these outcomes in clinical trials [93,94]. A phase II clinical trial (NCT01130142, NCT01064622) with a combination of vismodegib (GDC-0449) and gemcitabine revealed no survival benefit [39]. One possible explanation supported by the results of Özdemir et al. [95] is that the depletion of myofibroblasts in pancreatic cancer may also accelerate cancer growth and reduce survival. While the myofibroblast-depleted tumors did not respond to gemcitabine, anti-CTLA4 immunotherapy inverted the outcome and resulted in prolonged animal survival. Although FAP^+ cell-depletion upon adenoviral vaccination demonstrated an improvement of $CD8^+$ T cell function [40], remodeling of CAF expression pattern instead of CAF depletion might be a better-suited strategy for combinatorial approaches with immunotherapy in PDAC. The clinically most advanced substance to alter CAF expression phenotype is all-trans retinoic acid (ATRA), currently used as the standard treatment of acute promyelocytic leukemia but also tested in PDAC [96]. It reduces ECM and cytokine secretion by inhibiting FAP, ACTA2 and transforming growth factor β receptor (TGF-βR) expression on CAFs [41]. Suitability of ATRA for stromal remodeling in pancreatic cancer is currently under clinical investigation (NCT03307148, NCT03878524) [42]. Another preclinical substance reducing CAF activation

and expression in PDAC is JQ1; an inhibitor of the BET family of bromodomain chromatin-modulating proteins [43]. JQ1 has been demonstrated to control MYC silencing [97]. Since MYC-activated cells secrete factors, which can induce an MYC-dependent metabolic program in CAFs, JQ1 might be able to interfere with the tumor cell-CAF crosstalk [44]. Furthermore, the PDAC-specific CAF precursor cells, PSCs, can be remodeled to decrease the desmoplastic reaction. Calpeptin, a calpain inhibitor, was also able to decrease fibrosis in a subcutaneous xenografts mouse model using co-implantations of PSCs and pancreatic cancer cells [45]. A combination of metformin and gemcitabine resulted in significantly lower tumor size and reduced collagen amounts in an orthotopic mouse model [98]. Unfortunately, most of the approaches are not protein or nucleic acid-based and cannot be produced by CAR effector cells. Therefore, FAP-depleting or remodeling molecules could be applied as a pharmacological pre-treatment to reshape the therapy-inhibiting expression pattern of CAFs. Alternatively, FAP-redirected CAR T cells could be used to deliver CAF remodeling factors or antibodies to inhibit the crucial expression profile of CAFs and their autocrine feedback loops (Figure 4) [99]. Tandem chimeric antigen or synNotch receptor approaches could be applied simultaneously or in a time-shifted manner.

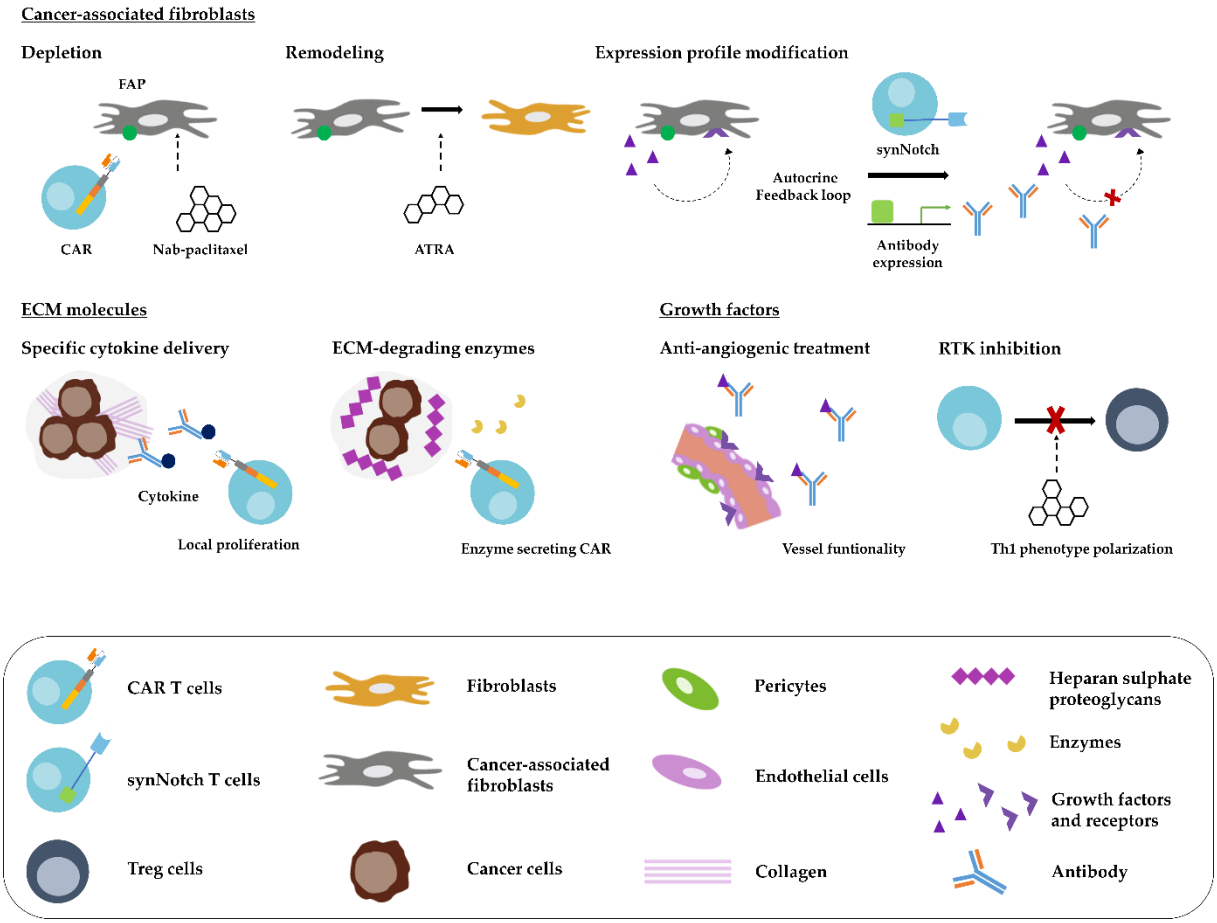

Figure 4. Strategies for CAR T cells to overcome or use the TME for successful immunotherapy. CAR T cells face major hinderances created by the distinctive TME of pancreatic cancer. Some of the hinderances might be surmounted or turned into a specific targeting strategy. CAFs may represent up to two thirds of the pancreatic tumor mass. However, CAF-depletion or remodeling approaches using CAR T cells or pharmacological substances such as ATRA or nab-paclitaxel might be able to break their crucial influence in the TME. Another strategy, potentially breaking the crucial influence of CAF expression profile in the TME, could be the application of FAP-redirected synNotch CAR T cells to deliver specific antibodies for inhibition of excess growth factors. Collagen is a key molecule in the creation of the dense ECM of PDAC, while its presence could be used for specific delivery of cytokines, required to boost CAR T cell efficacy and persistence. Moreover, it has already been demonstrated that CARs, re-equipped with ECM-degrading enzymes, such as heparanase, had higher infiltration compared to the control CARs. Multiple TME components have a high potential of influencing vessels development and growth. These components need to be targeted and modified, e.g., by inhibitory antibodies to improve vessel functionality and ensure directed CAR T cell transport to the pancreatic tumor. Use of broad RTK inhibition needs to be balanced after careful consideration of their influence on different TME players. In this way, polarization of pro-inflammatory cells into anti-inflammatory cells can be prevented.

2.2.2. Components of Extracellular Matrix in Pancreatic Cancer

One of the key features of activated fibroblasts is their distinct ECM production, especially crucial in PDAC with its pronounced desmoplasia [86]. Whatcott et al. [100] observed a strong negative correlation between patient survival and high levels of ECM deposition, also a solid tumor-specific hurdle for immunotherapy [101]. Thus, the composition of the ECM in

combination with the capability of CAR T cells to degrade extracellular matrix proteins can have a major influence on T cell tumor-trafficking and infiltration. A major challenge, however, is the fact that ECM proteins are not necessarily tumor-specific, but exert important physiological functions in organ development, tissue integrity, and wound healing [102].

Caruana et al. [46] demonstrated that ex vivo manipulated CAR T cells may downregulate ECM-degrading enzymes and overexpression heparanase improved CAR T cell infiltration and anti-tumor activity in vivo. However, heparan sulphate proteoglycans are not the only obstacle in the ECM of PDAC [103]. It is composed of collagens, non-collagen glycoproteins, glycosaminoglycans, growth factors, and proteoglycans as well as modulators of the cell-matrix interaction. Overexpressed ECM molecules, including thrombospondin, periostin, hyaluronic acid (HA), tenascin-C, vitronectin, collagens, and fibronectin increase pancreatic cancer cell migration and invasion [104]. Some of these molecules have already been exploited for possible effects on immunotherapy approaches.

Structural protein

Collagen is the most frequent molecule in the ECM of PDAC and a major component of the desmoplastic reaction [105]. Furthermore, a collagen-derived proline can compensate as an alternative nutrient source in the resource-deprived TME [106]. However, collagen also regulates the activity, phenotype ratio and the amount of tumor-infiltrating T cells due to its dense network [107]. In this way, mammary tumors with a high collagen-density, correlated with a worse prognosis, contained a higher ratio of $CD4^+$ to $CD8^+$ T cells and an overall reduced amount of infiltrating $CD8^+$ T cells. In PDAC, it was demonstrated that excessive collagen amounts abrogated tumor cell-directed movement of T cells by chemokines, but favored T cell movement to the stroma cells in a contact guidance dependent manner [108]. These findings imply the relevance of the ECM composition for cell-based immunotherapy in solid tumors. Despite the severe impairment created by the collagen network, Ishihara et al. [47] managed to turn the presence of collagen into an advantage by increasing the delivery of cytokines with a short half-life, such as IL-2, and checkpoint inhibitors specifically and doseable to the TME through coupling to a collagen-binding domain. This enables a safe approach to shift the balance of pro- and anti-tumorigenic cytokines and stimulate the immune cells in the TME. Consequently, collagen-redirected IL-2 reduced common side effects such as vascular leak syndrome and increased tumor-infiltrating $CD8^+$ T cells in an orthotopic breast cancer mouse model [47].

Glycoproteins

Fibronectin, another common molecule in the ECM of pancreatic cancer, but not in healthy tissues, is considered to be a significant hallmark of epithelial-to-mesenchymal transition (EMT) occurring in advanced tumors [109]. Fibronectin interacts with many ECM and surface molecules, creating an active interaction platform. This stimulates the EMT and multiple aggressiveness- and resistance-related signalling pathways, which in turn upregulate fibronectin expression, resulting in a strong feedback loop in the TME [110]. As in the case of collagen, intratumoural regions with low fibronectin amounts displayed high leukocyte infiltration [111]. The important role of fibronectin led to the creation of several approaches inhibiting its functions or using its presence in the TME for imaging, drug delivery, and therapy [112,113]. BC-1 coupled to IL-12 was used for TME-targeted cytokine delivery in clinical studies and resulted in stable disease in 46% of melanoma or renal cell carcinoma patients [48]. However, the single-chain variable fragment (scFv) L19-based cytokine delivery is more clinically advanced than the BC-1 based IL-2 delivery [49]. L19-IL2 (DARLEUKIN®) is already in clinical trials against various solid tumor types (NCT01058538, NCT02086721, NCT02735850, NCT03705403). Despite the promising preclinical results, a clinical trial of L19-IL2 with gemcitabine in patients with advanced pancreatic cancer had to be terminated due to lack of recruitment (NCT01198522). Nevertheless, phase II trials in melanoma patients resulted in reduced metastasis and increased survival demonstrating the potential of fibronectin-redirected IL-2 [50,51]. Besides IL-2, L19 was also coupled to IL-12 and tumor necrosis factor (TNF) α, revealing equally promising results in solid metastatic cancers [58,114], in particular for L19-TNF in combination with L19-IL2 [115]. In this way, targeting fibronectin enabled TME-specific cytokine delivery to outbalance immunosuppressive cytokines. This can be exploited as a combinatorial therapeutic strategy together with CAR T cells or as a pre-treatment.

Similar to fibronectin, tenascin-C is mostly present in the pathophysiological conditions of adults, building up a provisional matrix in the scar formation process [59]. It is upregulated in the ECM of solid tumors, including PDAC [60]. While the exact role of tenascin-C remains undefined, it is widely known for its modulation capacity on cell adhesion to fibronectin and its promotion of EMT, enhancing cancer cell growth and motility [116,117]. It has also been shown to interact with multiple ECM molecules and to facilitate the angiogenic switch by representing an important factor of the AngioMatrix (ECM and related protein involved in the angiogenic switch) inducing resistance to chemo- and anti-angiogenic therapy in PDAC [118].

Nevertheless, no correlation between high tenascin-C expression and survival has been determined. However, overexpression of tenascin-C together with other ECM-related factors has been shown to correlate with poor prognosis for patients of pancreatic cancer [119]. Tenascin-C pronounced importance in the context of solid tumors led to multiple approaches to modify tenascin-C in the ECM or to make use of its presence. Inhibition of tenascin-C expression is possible by blocking its natural activation pathways such as transforming growth factor β (TGF-β), but also by RNA interference resulting in only short survival prolongation [120]. Tenascin-C expression and signalling have been demonstrated to be prevented by angiotensin II type 1 receptor (AT-1) and angiotensin-converting enzyme (ACE) inhibitors, which has not yet been assessed in the clinic [120]. Another possibility would be to erase tenascin-C, as previously described for heparan sulphate proteoglycans, from the ECM of solid carcinomas, a process occurring after wound healing. Unfortunately, this mechanism has not yet been identified (reviewed by Spenle et al. [120]). Therefore, as in the case of fibronectin, multiple antibodies have been generated redirecting radionuclides and cytokines to the tenascin-C-rich ECM. F16-IL2 (TELEUKIN®), an IL-2 coupled antibody-cytokine fusion protein is the most advanced candidate with two clinical trials in solid tumors, such as breast and lung cancer (NCT01131364, NCT01134250). This recombinant protein demonstrated its ability to increase survival as well as the number of macrophages and NK cells in the tumor stroma in a BALB/c nude mice breast cancer model [52]. F16-IL2 clinical potency has also been analyzed in a clinical setting in solid tumors including pancreatic tumors, demonstrating an anti-cancer activity in combination with doxorubicin [53].

Thrombospondin 1 (TSP-1) is a strong inhibitor of angiogenesis, promotes inflammatory ('M1-type') macrophage recruitment and prevents stemness of cancer cells. Via its crosslinking-interaction with the "don't eat me"-signal CD47 it can directly induce tumor cell death [121,122]. However, it also releases the active form of TGF-β from its latent form, promotes T_{reg} formation and inhibits T cell proliferation [123,124]. Several inhibitors for TSP-1 are available with the most advanced being ABT-510, CVX-045, and Trabectedin [62,63]. While ABT-510 showed a limited increase of cytotoxic T cell frequency, it did not demonstrate efficacy in various solid tumors as a monotherapy leading to its suspension from clinical development (NCT00586092) [62,125,126]. Trabectedin, approved for the treatment of sarcoma and ovarian cancer, indicated a tremendous effect on favorable cytokines/chemokine expression level, although there was no efficacy as a single agent in stage II clinical trial for salvage therapy in metastatic pancreatic cancer (NCT01339754) [64]. Nevertheless, based on the findings of Weng et al. [127] TSP-1-targeted therapy in combination with cell therapy may

deserve a second chance as a more nuanced treatment. Here it was shown that downregulation of TSP-1 solely in dendritic cells increased the amount of tumor-infiltrating $CD4^+$ and $CD8^+$ T cells [127].

Glycosaminoglycan

Next to heparan sulphate proteoglycans, hyaluronic acid (HA) is another glycosaminoglycan, overexpressed in the ECM of PDAC [104]. HA is widely expressed in all tissues and plays an important role in multiple biological processes, e.g., cell proliferation, inflammation, and angiogenesis [128]. Nevertheless, it exerts its most important biological functions by regulating cell motility via CD44, the tissue hydration influencing the intestinal fluid pressure (IFP), tissue permeability, and drug delivery potential [100,129]. Consequently, high amounts of high molecular weight HA contribute to a stiff tumor matrix increasing the IFP and reducing the ability of chemo-, nanomedicine, and cell-based therapies to penetrate stroma-rich tumors [130]. Accordingly, HA accumulation in the ECM of pancreatic cancer patients correlates with poor survival [131]. Unlike tenascin-C, there is a specific way to remove excess high molecular weight HA from the ECM. HA disruption with the PEGylated human recombinant PH20 hyaluronidase (PEGPH20) indicated improved drug delivery and response in a mouse model of pancreatic cancer and increased $CD8^+$ T cell infiltration and better checkpoint inhibitor efficacy in a syngeneic breast cancer mouse model [54,55]. PEGPH20 treatment also resulted in a remodeling of the TME by decreasing other ECM molecules, such as collagen and tenascin-C. The promising preclinical success was also transferred to the clinic (NCT03481920, NCT01453153, NCT01839487, NCT04058964, NCT03634332, NCT02241187, NCT02921022, NCT02910882, NCT01959139, NCT04134468, NCT03193190, NCT02715804) and was in stage III of clinical development for pancreatic cancer [56]. Unfortunately, the phase III study was not able to meet the endpoint criteria, halting further development [57]. Nevertheless, especially for cell-based therapy approaches, which are limited by larger diameters (hydrodynamic size) than chemotherapeutics, depletion of HA may have a potential of exerting a significant impact on therapy delivery.

Altogether, these findings imply the importance of the ECM for the outcome of cancer therapy including immunotherapy. The impact of the ECM on the therapeutic outcome is further strengthened by the wide range of cytokines, which are bound and released by various ECM molecules after expression by CAFs and tumor cells, as recently reviewed by Tzanakakis et al. [132] for the group of the proteoglycans. Furthermore, options that failed before as monotherapies or in combination with chemotherapeutics deserve a second consideration for

suitability in combination with immunotherapy. In the long-term, the latest CAR technologies could be utilized to secrete engineered proteins to increase tumoricidal immune response and CAR T cell infiltration, overcoming the complex barriers created by the ECM.

Growth Factors in Pancreatic Cancer

The majority of the growth factors, expressed by cancer cells or CAFs in the TME, increase cell survival, proliferation, migration, and metastasis in an autocrine feedback loop or in a paracrine manner, via their associated receptors [99]. They can also be bound by ECM molecules and be released by enzymes, such as matrix metalloproteinases (MMPs) [86,133]. Aside from the close cancer cell and fibroblast communication network, some of these factors are also released by other immune cells in the TME, such as tumor-favoring M2 macrophages or neutrophils [134,135].

A thoroughly investigated factor is the vascular endothelial growth factor A (VEGF-A), and its receptor (VEGFR2), which regulates the process of angiogenesis [28]. Unlike most hematologic malignancies, solid tumors heavily depend on the formation of new vessels for sufficient blood supply. Hypoxia in all tissues, including cells present in the intertumoral regions of PDAC, induces the expression of VEGF after hypoxia-inducible factor 1 alpha (HIF-1) translocation to the nucleus in a gradient manner, which in turn initiates the growth of new blood vessels into hypoxic regions [136,137]. Nevertheless, the relationship between angiogenesis and PDAC is far more complex. On the one hand, PSCs and CAFs secrete VEGF, which leads to increased, disorganized vascular growth and formation with enhanced IFP [11]. While on the other hand, the dense desmoplastic reaction around pancreatic tumors leads to vascular disruption, which further increases hypoxia and reduces drug administration [10]. This leads to insufficient therapeutic-dose delivery that might, to some extent, explain the low survival rates in patients with pancreatic cancer [61,138]. Cell therapy also relies on functioning vessels [79]. Fortunately, vessel function can be restored by using anti-angiogenic treatments, such as bevacizumab, to normalize vessel organization and IFP [139]. Co-treatment of angiogenesis inhibitor bevacizumab together with GD2-redirected CAR T cells increased tumor infiltration and antitumor activity in a preclinical neuroblastoma model [66]. Bevacizumab was already tested in pancreatic cancer patients in combination with gemcitabine. Despite the promising objective response rate of 21%, there was no difference in the overall survival time between the bevacizumab and the placebo group (NCT00088894) [67]. This undesirable outcome may be attributed to the ability of tumors to acquire resistance to VEGF inhibition, e.g., by the release of more proangiogenic factors, such as angiopoietin 1 (ANGPT1), resulting

in increased amounts of vascular progenitor cells [140]. Recently, another mechanism dependent on the ECM molecule periostin, present in ECM of PDAC, has been revealed and induced revascularization and macrophage recruitment [65]. The second effect was reversible by the addition of an anti-colony stimulating factor 1 receptor (CSFR1) antibody, blocking macrophage infiltration [65]. This highlights the importance of understanding the individual TME composition of each patient in order to match the most suitable anti-angiogenic treatment, because many of the early mentioned ECM molecules have been shown to modify angiogenesis in different ways, e.g., by VEGF interaction [129]. Modification of other TME molecules, such as thrombospondin-1, together with anti-angiogenic treatment has already been evaluated in the clinic by the co-treatment of advanced solid tumors with bevacizumab and ABT-510, resulting in partial response for one patient and stable disease for more than a year in five patients [68]. Hence, combining multiple anti-angiogenic approaches with cell therapy might be necessary for a successful cell-based immunotherapy of PDAC. These findings stress the importance of moving away from the current one-size-fits-all therapy approaches to more personalized combinatorial therapies, simulating personalized nanomedicine approaches [141].

Tumor cells in hypoxic areas often express other growth factors next to VEGF. Their interactions with their defined receptors lead to receptor tyrosine kinase (RTK) induction, which can be antagonized by the blockage of downstream signalling pathways with RTK inhibitors [142]. RTKs are a group of cell surface receptors involved in multiple key pathways of cell proliferation, differentiation, survival, and migration. The inhibition of the RTK, Axl, attracted attention for its influence on immune cells and not on tumor cells. Axl has been associated with the traditional RTK pathways in cancer cells and with the regulation of innate immune response and a more aggressive and resistant phenotype [143,144]. These findings motivated the preclinical evaluation of the Axl receptor as a target for monoclonal antibody immunotherapy in pancreatic cancer [145]. Small molecule inhibition by BGB324 of Axl decreased immune suppression and increased chemotherapy potency in pancreatic cancer and synergized with CAR T cell therapy in B cell malignancies [69,70]. This in vivo demonstrated synergy was dependent on T helper cell type 1 phenotype polarization, expressing an anti-tumorigenic cytokine profile, induced by Axl inhibition. Given the great influence on vessel functionality and further, on immune cells, growth factor modification might have a significant influence on the improvement of immunotherapy in solid tumors. These findings encourage the application of already clinically approved drugs as supporting combinatorial approaches with immunotherapy. Upon favorable outcomes from clinical trials, biological inhibitors such as bevacizumab, could even be secreted by the CAR T cells, creating a living drug.

3. Conclusions

Pancreatic cancer represents an exceptional challenge for successful cancer therapy. CAR T cells are no exception, instead, they face great obstacles but also have the capacity to offer valuable chances. Cell-based immunotherapy has shown pronounced clinical success in hematologic malignancies and its feasibility has been demonstrated in pancreatic cancer, but it needs to overcome certain barriers, such as infiltration, persistence, and exhaustion. However, the first major hurdle is the heterogeneity of pancreatic cancers in terms of proposed subtypes and varying target expression. This requires advanced CAR technology to ensure the successful targeting of all cancer cells. The complex and heterogenous TME is the second major hurdle specifically for CAR T cells against pancreatic cancer. All parts of the TME require individual strategies. Reprogramming of CAFs might be more favorable than CAFs depletion without directly powering up the therapy intensity. The presence of tumor-specific ECM molecules, as described in this review, would enable a specific delivery of cytokines, using agents such as F19-IL-2 [53]. In this way, both approaches could be combined strategically to first loosen the dense stroma, before boosting up CAR T cells. This represents an option to increase the temperature of immunological "cold" tumors, similar to PDACs [146]. However, tremendous tumor growth in areas that are no longer suppressed needs to be vigorously prevented. The same holds true for situations, where CAR T cells are equipped with ECM-degrading enzymes, such as overexpressed heparanase, or tumors are pre-treated with IFP decreasing molecules such as PEGPH20 [55,56]. Restored baseline IFP and vessel function is of major importance for successful CAR T cell delivery to the tumor, even if they are provided with infiltration-increasing mechanisms, such as heparanase [46]. IFP and enhanced permeability and retention (EPR) effect in cancer nanomedicine are closely related. Hence, high-resolution 3D imaging techniques, used in nanotherapy, could be applied for translational approaches in terms of vessel functionality in vivo and later patient stratification for combinatorial cell-based therapies [147].

A high need for vessel functionality assessment is also present for the analysis of the interplay of all the ECM molecules and growth factors in the TME, which can influence vessel growth and development [11,68]. Tumors undergoing anti-angiogenic treatment strategies, such as bevacizumab, may develop resistance mechanisms. Those mechanisms can be dependent on the ECM composition, but might also be overcome by modifications of the present molecules. The availability of vessel-independent growth factors, secreted by the various players in the TME indicates a medical need for in-depth patient-stratifications based on the presence of key different TME molecules, especially when it comes to the application broad range RTK

inhibitors. This research requires technically advanced organoid or tissue printing methods, combined with established immunological assays.

Taken together, there is an overall need for the development of new in vivo and in vitro assays in combination with imaging strategies to facilitate combinatorial research and improve preclinical translation potential. Agents, which might have failed as monotherapies, might deserve a second look in the context of combinatorial approaches with immunotherapy, due to their characteristics as a "living drug". Research on different TME subtypes needs to be intensified and these parameters, in addition to molecular markers, need to be taken into account to define clear subgroups of PDAC. The acquired knowledge should assist in identifying only the PDAC patient, who will benefit from a particular personalized medicine concepts (Figure 5). Therefore, sub classifying patients would help to improve outcomes and quality of life, as well as avoid ineffective therapy and reduce financial and organizational burdens on the health systems, healthcare providers, and the patients. These efforts will hopefully utilize existing and developing pharmacological therapies, regardless of their stand-alone therapeutic success, in combination with CAR T cells to create highly improved multifactorial therapeutic strategies, that can overcome the current hurdles faced by the challenging TME in pancreatic cancer.

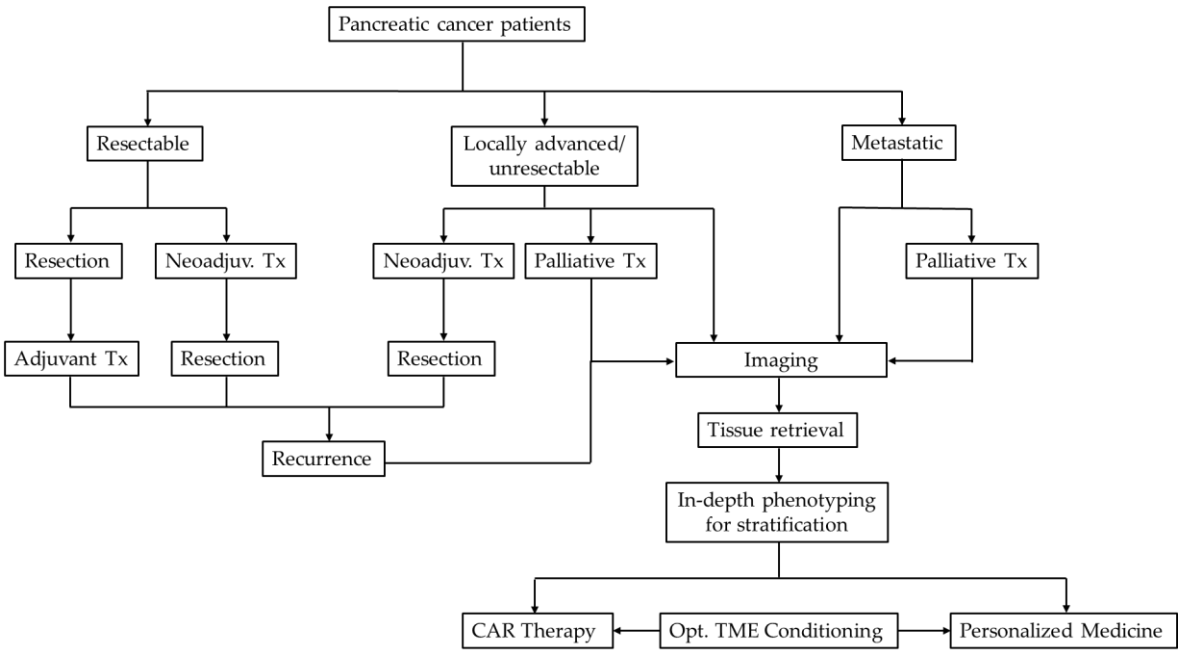

Figure 5. Strategy flow chart for PDAC therapy. Pancreatic cancer patients are classified into one of three categories upon diagnosis. Therapy (Tx) is chosen on the basis of this classification. In case of later stage PDAC or recurrent tumor, personalized medicine approaches could be of use. Imaging of patients would be followed by tissue retrieval to perform in-depth phenotyping of the tumor and its stroma. This could be performed by the application of up and coming technologies such as patient-derived organoids analysis, RNA-Seq or multiplex immunofluorescence staining. All in all, such refined selection criteria enable the balanced and careful stratification of patients into further effective and safe

therapy paths, including personalized therapy approaches, such as CAR T cell therapy, with or without conditioning of the tumor microenvironment.

Funding

This research received no external funding.

Acknowledgments

The authors would like to thank Rita Pfeifer for the scientific advice and helpful discussion and Jeannine Mißbach-Güntner for providing the hematoxylin/eosin-stained PDAC sample.

Conflicts of Interest

J.H., O.H. and W.A. are employees of Miltenyi Biotec B.V. & Co. KG. All other authors declare no competing interests.

References

1. Huang, L.; Jansen, L.; Balavarca, Y.; Babaei, M.; van der Geest, L.; Lemmens, V.; Van Eycken, L.; De Schutter, H.; Johannesen, T.B.; Primic-Žakelj, M.; et al. Stratified survival of resected and overall pancreatic cancer patients in Europe and the USA in the early twenty-first century: A large, international population-based study. BMC Med. 2018, 16, 125. [Google Scholar] [CrossRef]
2. Siegel, R.L.; Miller, K.D. Cancer statistics, 2019. CA Cancer J. Clin. 2019, 69, 7–34. [Google Scholar] [CrossRef]
3. Bray, F.; Ferlay, J.; Soerjomataram, I.; Siegel, R.L.; Torre, L.A.; Jemal, A. Global cancer statistics 2018: GLOBOCAN estimates of incidence and mortality worldwide for 36 cancers in 185 countries. CA Cancer J. Clin. 2018, 68, 394–424. [Google Scholar] [CrossRef]
4. Ercan, G.; Karlitepe, A.; Ozpolat, B. Pancreatic Cancer Stem Cells and Therapeutic Approaches. Anticancer Res. 2017, 37, 2761–2775. [Google Scholar] [CrossRef]
5. Rahib, L.; Smith, B.D.; Aizenberg, R.; Rosenzweig, A.B.; Fleshman, J.M.; Matrisian, L.M. Projecting cancer incidence and deaths to 2030: The unexpected burden of thyroid, liver, and pancreas cancers in the United States. Cancer Res. 2014, 74, 2913–2921. [Google Scholar] [CrossRef]
6. Kleeff, J.; Korc, M.; Apte, M.; La Vecchia, C.; Johnson, C.D.; Biankin, A.V.; Neale, R.E.; Tempero, M.; Tuveson, D.A.; Hruban, R.H.; et al. Pancreatic cancer. Nat. Rev. Dis. Prim. 2016, 2, 16022. [Google Scholar] [CrossRef]
7. Clancy, T.E. Surgery for Pancreatic Cancer. Hematol. Oncol. Clin. North Am. 2015, 29, 701–716. [Google Scholar] [CrossRef]
8. Wu, J.; Liang, C.; Chen, M.; Su, W. Association between tumor-stroma ratio and prognosis in solid tumor patients: A systematic review and meta-analysis. Oncotarget 2016, 7, 68954–68965. [Google Scholar] [CrossRef]
9. Yao, W.; Maitra, A.; Ying, H. Recent insights into the biology of pancreatic cancer. EBioMedicine 2020, 53, 53. [Google Scholar] [CrossRef]
10. Spivak-Kroizman, T.R.; Hostetter, G.; Posner, R.; Aziz, M.; Hu, C.; Demeure, M.J.; Von Hoff, D.; Hingorani, S.R.; Palculict, T.B.; Izzo, J.; et al. Hypoxia triggers hedgehog-mediated tumor-

stromal interactions in pancreatic cancer. Cancer Res. 2013, 73, 3235–3247. [Google Scholar] [CrossRef]

11. Fu, Y.; Liu, S.; Zeng, S.; Shen, H. The critical roles of activated stellate cells-mediated paracrine signaling, metabolism and onco-immunology in pancreatic ductal adenocarcinoma. Mol. Cancer 2018, 17, 1–14. [Google Scholar] [CrossRef]

12. Karamitopoulou, E. Tumour microenvironment of pancreatic cancer: Immune landscape is dictated by molecular and histopathological features. Br. J. Cancer 2019, 121, 5–14. [Google Scholar] [CrossRef]

13. Jurcak, N.; Zheng, L. Signaling in the microenvironment of pancreatic cancer: Transmitting along the nerve. Pharmacol. Ther. 2019, 200, 126–134. [Google Scholar] [CrossRef]

14. Ho, W.J.; Jaffee, E.M.; Zheng, L. The tumour microenvironment in pancreatic cancer—Clinical challenges and opportunities. Nat. Rev. Clin. Oncol. 2020, 1–14. [Google Scholar] [CrossRef]

15. Bailey, P.; Chang, D.K.; Nones, K.; Johns, A.L.; Patch, A.-M.; Gingras, M.-C.; Miller, D.K.; Christ, A.N.; Bruxner, T.J.C.; Quinn, M.C.; et al. Genomic analyses identify molecular subtypes of pancreatic cancer. Nature 2016, 531, 47–52. [Google Scholar] [CrossRef]

16. Eshhar, Z.; Waks, T.; Gross, G.; Schindler, D.G. Specific activation and targeting of cytotoxic lymphocytes through chimeric single chains consisting of antibody-binding domains and the gamma or zeta subunits of the immunoglobulin and T-cell receptors. Proc. Natl. Acad. Sci. USA 1993, 90, 720–724. [Google Scholar] [CrossRef]

17. Garrido, F.; Aptsiauri, N.; Doorduijn, E.M.; Garcia Lora, A.M.; van Hall, T. The urgent need to recover MHC class I in cancers for effective immunotherapy. Curr. Opin. Immunol. 2016, 39, 44–51. [Google Scholar] [CrossRef]

18. Goverman, J.; Gomez, S.M.; Segesman, K.D.; Hunkapiller, T.; Laug, W.E.; Hood, L. Chimeric immunoglobulin-T cell receptor proteins form functional receptors: Implications for T cell receptor complex formation and activation. Cell 1990, 60, 929–939. [Google Scholar] [CrossRef]

19. Sadelain, M.; Brentjens, R.; Riviere, I. The basic principles of chimeric antigen receptor design. Cancer Discov. 2013, 3, 388–398. [Google Scholar] [CrossRef]

20. Maude, S.L.; Laetsch, T.W.; Buechner, J.; Rives, S.; Boyer, M.; Bittencourt, H.; Bader, P.; Verneris, M.R.; Stefanski, H.E.; Myers, G.D.; et al. Tisagenlecleucel in Children and Young Adults with B-Cell Lymphoblastic Leukemia. New Engl. J. Med. 2018, 378, 439–448. [Google Scholar] [CrossRef]

21. Arabi, F.; Torabi-Rahvar, M.; Shariati, A.; Ahmadbeigi, N.; Naderi, M. Antigenic targets of CAR T Cell Therapy. A retrospective view on clinical trials. Exp. Cell Res. 2018, 369, 1–10. [Google Scholar] [CrossRef]

22. Tokarew, N.; Ogonek, J.; Endres, S.; von Bergwelt-Baildon, M.; Kobold, S. Teaching an old dog new tricks: Next-generation CAR T cells. Br. J. Cancer 2019, 120, 26–37. [Google Scholar] [CrossRef]

23. Ma, S.; Li, X.; Wang, X.; Cheng, L.; Li, Z.; Zhang, C.; Ye, Z.; Qian, Q. Current Progress in CAR-T Cell Therapy for Solid Tumors. Int. J. Biol. Sci. 2019, 15, 2548–2560. [Google Scholar] [CrossRef]

24. Fesnak, A.D.; June, C.H.; Levine, B.L. Engineered T cells: The promise and challenges of cancer immunotherapy. Nat. Rev. Cancer 2016, 16, 566–581. [Google Scholar] [CrossRef]

25. Roybal, K.T.; Williams, J.Z.; Morsut, L.; Rupp, L.J.; Kolinko, I.; Choe, J.H.; Walker, W.J.; McNally, K.A.; Lim, W.A. Engineering T Cells with Customized Therapeutic Response

Programs Using Synthetic Notch Receptors. Cell 2016, 167, 419–432.e16. [Google Scholar] [CrossRef]

26. Bansal, R.; Reshef, R. Revving the CAR—Combination strategies to enhance CAR T cell effectiveness. Blood Rev. 2020, 100695. [Google Scholar] [CrossRef]

27. D'Aloia, M.M.; Zizzari, I.G.; Sacchetti, B.; Pierelli, L.; Alimandi, M. CAR-T cells: The long and winding road to solid tumors. Cell Death Dis. 2018, 9, 282. [Google Scholar] [CrossRef]

28. Allen, M.; Louise Jones, J. Jekyll and Hyde: The role of the microenvironment on the progression of cancer. J. Pathol. 2011, 223, 162–176. [Google Scholar] [CrossRef]

29. Ene-Obong, A.; Clear, A.J.; Watt, J.; Wang, J.; Fatah, R.; Riches, J.C.; Marshall, J.F.; Chin-Aleong, J.; Chelala, C.; Gribben, J.G.; et al. Activated pancreatic stellate cells sequester CD8+ T cells to reduce their infiltration of the juxtatumoral compartment of pancreatic ductal adenocarcinoma. Gastroenterology 2013, 145, 1121–1132. [Google Scholar] [CrossRef]

30. Morgan, R.A.; Yang, J.C.; Kitano, M.; Dudley, M.E.; Laurencot, C.M.; Rosenberg, S.A. Case report of a serious adverse event following the administration of T cells transduced with a chimeric antigen receptor recognizing ERBB2. Mol. Ther. 2010, 18, 843–851. [Google Scholar] [CrossRef]

31. Akce, M.; Zaidi, M.Y.; Waller, E.K.; El-Rayes, B.F.; Lesinski, G.B. The Potential of CAR T Cell Therapy in Pancreatic Cancer. Front. Immunol. 2018, 9, 2166. [Google Scholar] [CrossRef] [PubMed]

32. Wang, Y.; Chen, M.; Wu, Z.; Tong, C.; Dai, H.; Guo, Y.; Liu, Y.; Huang, J.; Lv, H.; Luo, C.; et al. CD133-directed CAR T cells for advanced metastasis malignancies: A phase I trial. Oncoimmunology 2018, 7, e1440169. [Google Scholar] [CrossRef] [PubMed]

33. Beatty, G.L.; Haas, A.R.; Maus, M.V.; Torigian, D.A.; Soulen, M.C.; Plesa, G.; Chew, A.; Zhao, Y.; Levine, B.L.; Albelda, S.M.; et al. Mesothelin-specific chimeric antigen receptor mRNA-engineered T cells induce anti-tumor activity in solid malignancies. Cancer Immunol. Res. 2014, 2, 112–120. [Google Scholar] [CrossRef] [PubMed]

34. Lo, A.; Wang, L.S.; Scholler, J.; Monslow, J.; Avery, D.; Newick, K.; O'Brien, S.; Evans, R.A.; Bajor, D.J.; Clendenin, C.; et al. Tumor-Promoting Desmoplasia Is Disrupted by Depleting FAP-Expressing Stromal Cells. Cancer Res. 2015, 75, 2800–2810. [Google Scholar] [CrossRef]

35. Kakarla, S.; Chow, K.K.; Mata, M.; Shaffer, D.R.; Song, X.T.; Wu, M.F.; Liu, H.; Wang, L.L.; Rowley, D.R.; Pfizenmaier, K.; et al. Antitumor effects of chimeric receptor engineered human T cells directed to tumor stroma. Mol. Ther. 2013, 21, 1611–1620. [Google Scholar] [CrossRef]

36. Schuberth, P.C.; Hagedorn, C.; Jensen, S.M.; Gulati, P.; van den Broek, M.; Mischo, A.; Soltermann, A.; Jungel, A.; Marroquin Belaunzaran, O.; Stahel, R.; et al. Treatment of malignant pleural mesothelioma by fibroblast activation protein-specific re-directed T cells. J. Transl. Med. 2013, 11, 187. [Google Scholar] [CrossRef]

37. Roberts, E.W.; Deonarine, A.; Jones, J.O.; Denton, A.E.; Feig, C.; Lyons, S.K.; Espeli, M.; Kraman, M.; McKenna, B.; Wells, R.J.; et al. Depletion of stromal cells expressing fibroblast activation protein-alpha from skeletal muscle and bone marrow results in cachexia and anemia. J. Exp. Med. 2013, 210, 1137–1151. [Google Scholar] [CrossRef]

38. Tran, E.; Chinnasamy, D.; Yu, Z.; Morgan, R.A.; Lee, C.C.; Restifo, N.P.; Rosenberg, S.A. Immune targeting of fibroblast activation protein triggers recognition of multipotent bone marrow stromal cells and cachexia. J. Exp. Med. 2013, 210, 1125–1135. [Google Scholar] [CrossRef]

39. Catenacci, D.V.; Junttila, M.R.; Karrison, T.; Bahary, N.; Horiba, M.N.; Nattam, S.R.; Marsh, R.; Wallace, J.; Kozloff, M.; Rajdev, L.; et al. Randomized Phase Ib/II Study of Gemcitabine

Plus Placebo or Vismodegib, a Hedgehog Pathway Inhibitor, in Patients with Metastatic Pancreatic Cancer. J. Clin. Oncol. 2015, 33, 4284–4292. [Google Scholar] [CrossRef]

40. Zhang, Y.; Ertl, H.C. Depletion of FAP+ cells reduces immunosuppressive cells and improves metabolism and functions CD8+ T cells within tumors. Oncotarget 2016, 7, 23282–23299. [Google Scholar] [CrossRef]

41. Chronopoulos, A.; Robinson, B.; Sarper, M.; Cortes, E.; Auernheimer, V.; Lachowski, D.; Attwood, S.; García, R.; Ghassemi, S.; Fabry, B.; et al. ATRA mechanically reprograms pancreatic stellate cells to suppress matrix remodelling and inhibit cancer cell invasion. Nat. Commun. 2016, 7, 12630. [Google Scholar] [CrossRef]

42. North, B.; Kocher, H.M.; Sasieni, P. A new pragmatic design for dose escalation in phase 1 clinical trials using an adaptive continual reassessment method. BMC Cancer 2019, 19. [Google Scholar] [CrossRef]

43. Yamamoto, K.; Tateishi, K.; Kudo, Y.; Hoshikawa, M.; Tanaka, M.; Nakatsuka, T.; Fujiwara, H.; Miyabayashi, K.; Takahashi, R.; Tanaka, Y.; et al. Stromal remodeling by the BET bromodomain inhibitor JQ1 suppresses the progression of human pancreatic cancer. Oncotarget 2016, 7, 61469–61484. [Google Scholar] [CrossRef]

44. Coller, H.A. MYC sets a tumour-stroma metabolic loop. Nat. Cell Biol. 2018, 20, 506–507. [Google Scholar] [CrossRef]

45. Yoshida, M.; Miyasaka, Y.; Ohuchida, K.; Okumura, T.; Zheng, B.; Torata, N.; Fujita, H.; Nabae, T.; Manabe, T.; Shimamoto, M.; et al. Calpain inhibitor calpeptin suppresses pancreatic cancer by disrupting cancer-stromal interactions in a mouse xenograft model. Cancer Sci. 2016, 107, 1443–1452. [Google Scholar] [CrossRef]

46. Caruana, I.; Savoldo, B.; Hoyos, V.; Weber, G.; Liu, H.; Kim, E.S.; Ittmann, M.M.; Marchetti, D.; Dotti, G. Heparanase promotes tumor infiltration and antitumor activity of CAR-redirected T lymphocytes. Nat. Med. 2015, 21, 524–529. [Google Scholar] [CrossRef]

47. Ishihara, J.; Ishihara, A. Targeted antibody and cytokine cancer immunotherapies through collagen affinity. Sci. Transl. Med. 2019, 11. [Google Scholar] [CrossRef]

48. Rudman, S.M.; Jameson, M.B.; McKeage, M.J.; Savage, P.; Jodrell, D.I.; Harries, M.; Acton, G.; Erlandsson, F.; Spicer, J.F. A phase 1 study of AS1409, a novel antibody-cytokine fusion protein, in patients with malignant melanoma or renal cell carcinoma. Clin. Cancer Res. 2011, 17, 1998–2005. [Google Scholar] [CrossRef]

49. Schliemann, C.; Palumbo, A.; Zuberbuhler, K.; Villa, A.; Kaspar, M.; Trachsel, E.; Klapper, W.; Menssen, H.D.; Neri, D. Complete eradication of human B-cell lymphoma xenografts using rituximab in combination with the immunocytokine L19-IL2. Blood 2009, 113, 2275–2283. [Google Scholar] [CrossRef]

50. Weide, B.; Eigentler, T.K.; Pflugfelder, A.; Zelba, H.; Martens, A.; Pawelec, G.; Giovannoni, L.; Ruffini, P.A.; Elia, G.; Neri, D.; et al. Intralesional treatment of stage III metastatic melanoma patients with L19-IL2 results in sustained clinical and systemic immunologic responses. Cancer Immunol. Res. 2014, 2, 668–678. [Google Scholar] [CrossRef]

51. Eigentler, T.K.; Weide, B.; de Braud, F.; Spitaleri, G.; Romanini, A.; Pflugfelder, A.; Gonzalez-Iglesias, R.; Tasciotti, A.; Giovannoni, L.; Schwager, K.; et al. A dose-escalation and signal-generating study of the immunocytokine L19-IL2 in combination with dacarbazine for the therapy of patients with metastatic melanoma. Clin. Cancer Res. 2011, 17, 7732–7742. [Google Scholar] [CrossRef] [PubMed]

52. Marlind, J.; Kaspar, M.; Trachsel, E.; Sommavilla, R.; Hindle, S.; Bacci, C.; Giovannoni, L.; Neri, D. Antibody-mediated delivery of interleukin-2 to the stroma of breast cancer strongly

enhances the potency of chemotherapy. Clin. Cancer Res. 2008, 14, 6515–6524. [Google Scholar] [CrossRef] [PubMed]

53. Catania, C.; Maur, M.; Berardi, R.; Rocca, A.; Di Giacomo, A.M.; Spitaleri, G.; Masini, C.; Pierantoni, C.; González-Iglesias, R.; Zigon, G.; et al. The tumor-targeting immunocytokine F16-IL2 in combination with doxorubicin: Dose escalation in patients with advanced solid tumors and expansion into patients with metastatic breast cancer. Cell Adhes. Migr. 2015, 9, 14–21. [Google Scholar] [CrossRef] [PubMed]

54. Jacobetz, M.A.; Chan, D.S.; Neesse, A.; Bapiro, T.E.; Cook, N.; Frese, K.K.; Feig, C.; Nakagawa, T.; Caldwell, M.E.; Zecchini, H.I.; et al. Hyaluronan impairs vascular function and drug delivery in a mouse model of pancreatic cancer. Gut 2013, 62, 112–120. [Google Scholar] [CrossRef] [PubMed]

55. Clift, R.; Lee, J.; Thompson, C.B.; Huang, Y. Abstract 641: PEGylated recombinant hyaluronidase PH20 (PEGPH20) enhances tumor infiltrating CD8+ T cell accumulation and improves checkpoint inhibitor efficacy in murine syngeneic breast cancer models. Cancer Res. 2017, 77, 641. [Google Scholar] [CrossRef]

56. Doherty, G.J.; Tempero, M.; Corrie, P.G. HALO-109-301: A Phase III trial of PEGPH20 (with gemcitabine and nab-paclitaxel) in hyaluronic acid-high stage IV pancreatic cancer. Futur. Oncol. 2018, 14, 13–22. [Google Scholar] [CrossRef]

57. Hakim, N.; Patel, R.; Devoe, C.; Saif, M.W. Why HALO 301 Failed and Implications for Treatment of Pancreatic Cancer. Pancreas 2019, 3, e1–e4. [Google Scholar] [CrossRef]

58. Spitaleri, G.; Berardi, R.; Pierantoni, C.; De Pas, T.; Noberasco, C.; Libbra, C.; Gonzalez-Iglesias, R.; Giovannoni, L.; Tasciotti, A.; Neri, D.; et al. Phase I/II study of the tumour-targeting human monoclonal antibody-cytokine fusion protein L19-TNF in patients with advanced solid tumours. J. Cancer Res. Clin. Oncol. 2013, 139, 447–455. [Google Scholar] [CrossRef]

59. Midwood, K.S.; Hussenet, T.; Langlois, B.; Orend, G. Advances in tenascin-C biology. Cell Mol. Life Sci. 2011, 68, 3175–3199. [Google Scholar] [CrossRef]

60. Juuti, A.; Nordling, S.; Louhimo, J.; Lundin, J.; Haglund, C. Tenascin C expression is upregulated in pancreatic cancer and correlates with differentiation. J. Clin. Pathol. 2004, 57, 1151–1155. [Google Scholar] [CrossRef]

61. Jain, R.K. Normalizing tumor microenvironment to treat cancer: Bench to bedside to biomarkers. J. Clin. Oncol. 2013, 31, 2205–2218. [Google Scholar] [CrossRef] [PubMed]

62. Huang, T.; Sun, L.; Yuan, X.; Qiu, H. Thrombospondin-1 is a multifaceted player in tumor progression. Oncotarget 2017, 8, 84546–84558. [Google Scholar] [CrossRef] [PubMed]

63. Jeanne, A.; Schneider, C.; Martiny, L.; Dedieu, S. Original insights on thrombospondin-1-related antireceptor strategies in cancer. Front. Pharmacol. 2015, 6, 252. [Google Scholar] [CrossRef]

64. Belli, C.; Piemonti, L.; D'Incalci, M.; Zucchetti, M.; Porcu, L.; Cappio, S.; Doglioni, C.; Allavena, P.; Ceraulo, D.; Maggiora, P.; et al. Phase II trial of salvage therapy with trabectedin in metastatic pancreatic adenocarcinoma. Cancer Chemother. Pharmacol. 2016, 77, 477–484. [Google Scholar] [CrossRef] [PubMed]

65. Keklikoglou, I.; Kadioglu, E.; Bissinger, S.; Langlois, B.; Bellotti, A.; Orend, G.; Ries, C.H.; De Palma, M. Periostin Limits Tumor Response to VEGFA Inhibition. Cell Rep. 2018, 22, 2530–2540. [Google Scholar] [CrossRef] [PubMed]

66. Bocca, P.; Di Carlo, E.; Caruana, I.; Emionite, L.; Cilli, M.; De Angelis, B.; Quintarelli, C.; Pezzolo, A.; Raffaghello, L.; Morandi, F.; et al. Bevacizumab-mediated tumor vasculature remodelling improves tumor infiltration and antitumor efficacy of GD2-CAR T cells in a human

neuroblastoma preclinical model. Oncoimmunology 2017, 7, e1378843. [Google Scholar] [CrossRef]

67. Kindler, H.L.; Niedzwiecki, D.; Hollis, D.; Sutherland, S.; Schrag, D.; Hurwitz, H.; Innocenti, F.; Mulcahy, M.F.; O'Reilly, E.; Wozniak, T.F.; et al. Gemcitabine plus bevacizumab compared with gemcitabine plus placebo in patients with advanced pancreatic cancer: Phase III trial of the Cancer and Leukemia Group B (CALGB 80303). J. Clin. Oncol. 2010, 28, 3617–3622. [Google Scholar] [CrossRef]

68. Uronis, H.E.; Cushman, S.M.; Bendell, J.C.; Blobe, G.C.; Morse, M.A.; Nixon, A.B.; Dellinger, A.; Starr, M.D.; Li, H.; Meadows, K.; et al. A phase I study of ABT-510 plus bevacizumab in advanced solid tumors. Cancer Med. 2013, 2, 316–324. [Google Scholar] [CrossRef]

69. Ludwig, K.F.; Du, W.; Sorrelle, N.B.; Wnuk-Lipinska, K.; Topalovski, M.; Toombs, J.E.; Cruz, V.H.; Yabuuchi, S.; Rajeshkumar, N.V.; Maitra, A.; et al. Small-Molecule Inhibition of Axl Targets Tumor Immune Suppression and Enhances Chemotherapy in Pancreatic Cancer. Cancer Res. 2018, 78, 246–255. [Google Scholar] [CrossRef]

70. Sakemura, R.; Yang, N.; Cox, M.J.; Sinha, S.; Hefazi, M.; Hansen, M.J.; Schick, K.J.; Boysen, J.C.; Tschumper, R.C.; Mouritsen, L.; et al. Axl-RTK Inhibition Modulates T Cell Functions and Synergizes with Chimeric Antigen Receptor T Cell Therapy in B Cell Malignancies. Biol. Blood Marrow Transplant. 2019, 25, S165. [Google Scholar] [CrossRef]

71. Zaorsky, N.G.; Churilla, T.M.; Egleston, B.L.; Fisher, S.G.; Ridge, J.A.; Horwitz, E.M.; Meyer, J.E. Causes of death among cancer patients. Ann. Oncol. 2017, 28, 400–407. [Google Scholar] [CrossRef] [PubMed]

72. DeRenzo, C.; Gottschalk, S. Genetic Modification Strategies to Enhance CAR T Cell Persistence for Patients With Solid Tumors. Front. Immunol. 2019, 10, 218. [Google Scholar] [CrossRef] [PubMed]

73. Brandt, L.J.B.; Barnkob, M.B.; Michaels, Y.S.; Heiselberg, J.; Barington, T. Emerging Approaches for Regulation and Control of CAR T Cells: A Mini Review. Front. Immunol. 2020, 11, 326. [Google Scholar] [CrossRef] [PubMed]

74. Puleo, F.; Nicolle, R.; Blum, Y.; Cros, J.; Marisa, L.; Demetter, P.; Quertinmont, E.; Svrcek, M.; Elarouci, N.; Iovanna, J.; et al. Stratification of Pancreatic Ductal Adenocarcinomas Based on Tumor and Microenvironment Features. Gastroenterology 2018, 155, 1999–2013.e3. [Google Scholar] [CrossRef]

75. Bonifant, C.L.; Jackson, H.J.; Brentjens, R.J.; Curran, K.J. Toxicity and management in CAR T-cell therapy. Mol. Ther. Oncolytics 2016, 3, 16011. [Google Scholar] [CrossRef]

76. Apte, M.; Park, S.; Phillips, P.; Santucci, N.; Goldstein, D.; Kumar, R.K.; Ramm, G.A.; Buchler, M.; Friess, H.; McCarroll, J.; et al. Desmoplastic Reaction in Pancreatic Cancer: Role of Pancreatic Stellate Cells. Pancreas 2004, 29, 179–187. [Google Scholar] [CrossRef]

77. Thomas, D.; Radhakrishnan, P. Tumor-stromal crosstalk in pancreatic cancer and tissue fibrosis. Mol. Cancer 2019, 18, 14. [Google Scholar] [CrossRef]

78. Chan, T.-S.; Shaked, Y.; Tsai, K.K. Targeting the Interplay Between Cancer Fibroblasts, Mesenchymal Stem Cells, and Cancer Stem Cells in Desmoplastic Cancers. Front. Oncol. 2019, 9, 688. [Google Scholar] [CrossRef]

79. Martinez, M.; Moon, E.K. CAR T Cells for Solid Tumors: New Strategies for Finding, Infiltrating, and Surviving in the Tumor Microenvironment. Front. Immunol. 2019, 10, 128. [Google Scholar] [CrossRef]

80. Knochelmann, H.M.; Smith, A.S.; Dwyer, C.J.; Wyatt, M.M.; Mehrotra, S.; Paulos, C.M. CAR T Cells in Solid Tumors: Blueprints for Building Effective Therapies. Front. Immunol. 2018, 9, 1740. [Google Scholar] [CrossRef]

81. Le Bourgeois, T.; Strauss, L.; Aksoylar, H.-I.; Daneshmandi, S.; Seth, P.; Patsoukis, N.; Boussiotis, V.A. Targeting T Cell Metabolism for Improvement of Cancer Immunotherapy. Front. Oncol. 2018, 8, 237. [Google Scholar] [CrossRef]

82. Alkasalias, T.; Moyano-Galceran, L.; Arsenian-Henriksson, M.; Lehti, K. Fibroblasts in the Tumor Microenvironment: Shield or Spear? Int. J. Mol. Sci. 2018, 19, 1532. [Google Scholar] [CrossRef] [PubMed]

83. Liu, T.; Zhou, L.; Li, D.; Andl, T.; Zhang, Y. Cancer-Associated Fibroblasts Build and Secure the Tumor Microenvironment. Front. Cell Dev. Biol. 2019, 7. [Google Scholar] [CrossRef] [PubMed]

84. Chandler, C.; Liu, T.; Buckanovich, R.; Coffman, L.G. The double edge sword of fibrosis in cancer. Transl. Res. 2019, 209, 55–67. [Google Scholar] [CrossRef] [PubMed]

85. LeBleu, V.S.; Kalluri, R. A peek into cancer-associated fibroblasts: Origins, functions and translational impact. Dis. Model. Mech. 2018, 11. [Google Scholar] [CrossRef] [PubMed]

86. Kalluri, R. The biology and function of fibroblasts in cancer. Nat. Rev. Cancer 2016, 16, 582–598. [Google Scholar] [CrossRef] [PubMed]

87. Ferdek, P.E.; Jakubowska, M.A. Biology of pancreatic stellate cells-more than just pancreatic cancer. Pflug. Arch. 2017, 469, 1039–1050. [Google Scholar] [CrossRef]

88. Neesse, A.; Algul, H.; Tuveson, D.A.; Gress, T.M. Stromal biology and therapy in pancreatic cancer: A changing paradigm. Gut 2015, 64, 1476–1484. [Google Scholar] [CrossRef]

89. Fiori, M.E.; Di Franco, S.; Villanova, L.; Bianca, P.; Stassi, G.; De Maria, R. Cancer-associated fibroblasts as abettors of tumor progression at the crossroads of EMT and therapy resistance. Mol. Cancer 2019, 18, 70. [Google Scholar] [CrossRef]

90. Lee, H.O.; Mullins, S.R.; Franco-Barraza, J.; Valianou, M.; Cukierman, E.; Cheng, J.D. FAP-overexpressing fibroblasts produce an extracellular matrix that enhances invasive velocity and directionality of pancreatic cancer cells. BMC Cancer 2011, 11, 245. [Google Scholar] [CrossRef]

91. Andrae, J.; Gallini, R.; Betsholtz, C. Role of platelet-derived growth factors in physiology and medicine. Genes Dev. 2008, 22, 1276–1312. [Google Scholar] [CrossRef] [PubMed]

92. Alvarez, R.; Musteanu, M.; Garcia-Garcia, E.; Lopez-Casas, P.P.; Megias, D.; Guerra, C.; Munoz, M.; Quijano, Y.; Cubillo, A.; Rodriguez-Pascual, J.; et al. Stromal disrupting effects of nab-paclitaxel in pancreatic cancer. Br. J. Cancer 2013, 109, 926–933. [Google Scholar] [CrossRef] [PubMed]

93. Roy Chaudhuri, T.; Straubinger, N.L.; Pitoniak, R.F.; Hylander, B.L.; Repasky, E.A.; Ma, W.W.; Straubinger, R.M. Tumor-Priming Smoothened Inhibitor Enhances Deposition and Efficacy of Cytotoxic Nanoparticles in a Pancreatic Cancer Model. Mol. Cancer Ther. 2016, 15, 84–93. [Google Scholar] [CrossRef] [PubMed]

94. Olive, K.P.; Jacobetz, M.A.; Davidson, C.J.; Gopinathan, A.; McIntyre, D.; Honess, D.; Madhu, B.; Goldgraben, M.A.; Caldwell, M.E.; Allard, D.; et al. Inhibition of Hedgehog signaling enhances delivery of chemotherapy in a mouse model of pancreatic cancer. Science 2009, 324, 1457–1461. [Google Scholar] [CrossRef] [PubMed]

95. Ozdemir, B.C.; Pentcheva-Hoang, T.; Carstens, J.L.; Zheng, X.; Wu, C.C.; Simpson, T.R.; Laklai, H.; Sugimoto, H.; Kahlert, C.; Novitskiy, S.V.; et al. Depletion of carcinoma-associated fibroblasts and fibrosis induces immunosuppression and accelerates pancreas cancer with reduced survival. Cancer Cell 2014, 25, 719–734. [Google Scholar] [CrossRef]

96. Noguera, N.I.; Catalano, G.; Banella, C.; Divona, M.; Faraoni, I.; Ottone, T.; Arcese, W.; Voso, M.T. Acute promyelocytic Leukemia: Update on the mechanisms of leukemogenesis, resistance

and on innovative treatment strategies. Cancers 2019, 11, 1591. [Google Scholar] [CrossRef] [PubMed]

97. Mertz, J.A.; Conery, A.R.; Bryant, B.M.; Sandy, P.; Balasubramanian, S.; Mele, D.A.; Bergeron, L.; Sims, R.J., 3rd. Targeting MYC dependence in cancer by inhibiting BET bromodomains. Proc. Natl. Acad. Sci. USA 2011, 108, 16669–16674. [Google Scholar] [CrossRef]

98. Duan, W.; Chen, K.; Jiang, Z.; Chen, X.; Sun, L.; Li, J.; Lei, J.; Xu, Q.; Ma, J.; Li, X.; et al. Desmoplasia suppression by metformin-mediated AMPK activation inhibits pancreatic cancer progression. Cancer Lett. 2017, 385, 225–233. [Google Scholar] [CrossRef]

99. Sun, Q.; Zhang, B.; Hu, Q.; Qin, Y.; Xu, W.; Liu, W.; Yu, X.; Xu, J. The impact of cancer-associated fibroblasts on major hallmarks of pancreatic cancer. Theranostics 2018, 8, 5072–5087. [Google Scholar] [CrossRef]

100. Whatcott, C.J.; Diep, C.H.; Jiang, P.; Watanabe, A.; LoBello, J.; Sima, C.; Hostetter, G.; Shepard, H.M.; Von Hoff, D.D.; Han, H. Desmoplasia in Primary Tumors and Metastatic Lesions of Pancreatic Cancer. Clin. Cancer Res. 2015, 21, 3561–3568. [Google Scholar] [CrossRef]

101. Lu, P.; Weaver, V.M.; Werb, Z. The extracellular matrix: A dynamic niche in cancer progression. J. Cell Biol. 2012, 196, 395–406. [Google Scholar] [CrossRef] [PubMed]

102. Weiskirchen, R.; Weiskirchen, S.; Tacke, F. Organ and tissue fibrosis: Molecular signals, cellular mechanisms and translational implications. Mol. Asp. Med. 2019, 65, 2–15. [Google Scholar] [CrossRef] [PubMed]

103. Gress, T.M.; Muller-Pillasch, F.; Lerch, M.M.; Friess, H.; Buchler, M.; Adler, G. Expression and in-situ localization of genes coding for extracellular matrix proteins and extracellular matrix degrading proteases in pancreatic cancer. Int. J. Cancer 1995, 62, 407–413. [Google Scholar] [CrossRef]

104. Lunardi, S.; Muschel, R.J.; Brunner, T.B. The stromal compartments in pancreatic cancer: Are there any therapeutic targets? Cancer Lett 2014, 343, 147–155. [Google Scholar] [CrossRef] [PubMed]

105. Weniger, M.; Honselmann, K.C.; Liss, A.S. The Extracellular Matrix and Pancreatic Cancer: A Complex Relationship. Cancers 2018, 10, 316. [Google Scholar] [CrossRef]

106. Olivares, O.; Mayers, J.R.; Gouirand, V.; Torrence, M.E.; Gicquel, T.; Borge, L.; Lac, S.; Roques, J.; Lavaut, M.N.; Berthezene, P.; et al. Collagen-derived proline promotes pancreatic ductal adenocarcinoma cell survival under nutrient limited conditions. Nat. Commun. 2017, 8, 16031. [Google Scholar] [CrossRef]

107. Kuczek, D.E.; Larsen, A.M.H.; Thorseth, M.-L.; Carretta, M.; Kalvisa, A.; Siersbæk, M.S.; Simões, A.M.C.; Roslind, A.; Engelholm, L.H.; Noessner, E.; et al. Collagen density regulates the activity of tumor-infiltrating T cells. J. Immunother. Cancer 2019, 7, 68. [Google Scholar] [CrossRef]

108. Hartmann, N.; Giese, N.A.; Giese, T.; Poschke, I.; Offringa, R.; Werner, J.; Ryschich, E. Prevailing Role of Contact Guidance in Intrastromal T-cell Trapping in Human Pancreatic Cancer. Clin. Cancer Res. 2014, 20, 3422–3433. [Google Scholar] [CrossRef]

109. Mani, S.A.; Guo, W.; Liao, M.J.; Eaton, E.N.; Ayyanan, A.; Zhou, A.Y.; Brooks, M.; Reinhard, F.; Zhang, C.C.; Shipitsin, M.; et al. The epithelial-mesenchymal transition generates cells with properties of stem cells. Cell 2008, 133, 704–715. [Google Scholar] [CrossRef]

110. Han, Z.; Lu, Z.R. Targeting Fibronectin for Cancer Imaging and Therapy. J. Mater. Chem. B 2017, 5, 639–654. [Google Scholar] [CrossRef]

111. Valkenburg, K.C.; de Groot, A.E.; Pienta, K.J. Targeting the tumour stroma to improve cancer therapy. Nat. Rev. Clin. Oncol. 2018, 15, 366–381. [Google Scholar] [CrossRef] [PubMed]

112. Gu, G.; Hu, Q.; Feng, X.; Gao, X.; Menglin, J.; Kang, T.; Jiang, D.; Song, Q.; Chen, H.; Chen, J. PEG-PLA nanoparticles modified with APTEDB peptide for enhanced anti-angiogenic and anti-glioma therapy. Biomaterials 2014, 35, 8215–8226. [Google Scholar] [CrossRef] [PubMed]

113. Hemmerle, T.; Neri, D. The antibody-based targeted delivery of interleukin-4 and 12 to the tumor neovasculature eradicates tumors in three mouse models of cancer. Int. J. Cancer 2014, 134, 467–477. [Google Scholar] [CrossRef] [PubMed]

114. Halin, C.; Rondini, S.; Nilsson, F.; Berndt, A.; Kosmehl, H.; Zardi, L.; Neri, D. Enhancement of the antitumor activity of interleukin-12 by targeted delivery to neovasculature. Nat. Biotechnol. 2002, 20, 264–269. [Google Scholar] [CrossRef]

115. Danielli, R.; Patuzzo, R.; Di Giacomo, A.M.; Gallino, G.; Maurichi, A.; Di Florio, A.; Cutaia, O.; Lazzeri, A.; Fazio, C.; Miracco, C.; et al. Intralesional administration of L19-IL2/L19-TNF in stage III or stage IVM1a melanoma patients: Results of a phase II study. Cancer Immunol. Immunother. 2015, 64, 999–1009. [Google Scholar] [CrossRef] [PubMed]

116. Paron, I.; Berchtold, S.; Voros, J.; Shamarla, M.; Erkan, M.; Hofler, H.; Esposito, I. Tenascin-C enhances pancreatic cancer cell growth and motility and affects cell adhesion through activation of the integrin pathway. PLoS ONE 2011, 6, e21684. [Google Scholar] [CrossRef]

117. Chiquet-Ehrismann, R.; Orend, G.; Chiquet, M.; Tucker, R.P.; Midwood, K.S. Tenascins in stem cell niches. Matrix Biol. 2014, 37, 112–123. [Google Scholar] [CrossRef] [PubMed]

118. Langlois, B.; Saupe, F.; Rupp, T.; Arnold, C.; van der Heyden, M.; Orend, G.; Hussenet, T. AngioMatrix, a signature of the tumor angiogenic switch-specific matrisome, correlates with poor prognosis for glioma and colorectal cancer patients. Oncotarget 2014, 5, 10529–10545. [Google Scholar] [CrossRef] [PubMed]

119. Xu, Y.; Li, Z.; Jiang, P.; Wu, G.; Chen, K.; Zhang, X.; Li, X. The co-expression of MMP-9 and Tenascin-C is significantly associated with the progression and prognosis of pancreatic cancer. Diagn. Pathol. 2015, 10, 211. [Google Scholar] [CrossRef] [PubMed]

120. Spenlé, C.; Saupe, F.; Midwood, K.; Burckel, H.; Noel, G.; Orend, G. Tenascin-C: Exploitation and collateral damage in cancer management. Cell Adhes. Migr. 2015, 9, 141–153. [Google Scholar] [CrossRef]

121. Martin-Manso, G.; Galli, S.; Ridnour, L.A.; Tsokos, M.; Wink, D.A.; Roberts, D.D. Thrombospondin 1 promotes tumor macrophage recruitment and enhances tumor cell cytotoxicity of differentiated U937 cells. Cancer Res. 2008, 68, 7090–7099. [Google Scholar] [CrossRef] [PubMed]

122. Zheng, Y.; Zou, F.; Wang, J.; Yin, G.; Le, V.; Fei, Z.; Liu, J. Photodynamic therapy-mediated cancer vaccination enhances stem-like phenotype and immune escape, which can be blocked by thrombospondin-1 signaling through CD47 receptor protein. J. Biol. Chem. 2015, 290, 8975–8986. [Google Scholar] [CrossRef] [PubMed]

123. Murphy-Ullrich, J.E.; Poczatek, M. Activation of latent TGF-beta by thrombospondin-1: Mechanisms and physiology. Cytokine Growth Factor Rev. 2000, 11, 59–69. [Google Scholar] [CrossRef]

124. Grimbert, P.; Bouguermouh, S.; Baba, N.; Nakajima, T.; Allakhverdi, Z.; Braun, D.; Saito, H.; Rubio, M.; Delespesse, G.; Sarfati, M. Thrombospondin/CD47 interaction: A pathway to generate regulatory T cells from human CD4+ CD25- T cells in response to inflammation. J. Immunol. 2006, 177, 3534–3541. [Google Scholar] [CrossRef] [PubMed]

125. Markovic, S.N.; Suman, V.J.; Rao, R.A.; Ingle, J.N.; Kaur, J.S.; Erickson, L.A.; Pitot, H.C.; Croghan, G.A.; McWilliams, R.R.; Merchan, J.; et al. A phase II study of ABT-510

(thrombospondin-1 analog) for the treatment of metastatic melanoma. Am. J. Clin. Oncol. 2007, 30, 303–309. [Google Scholar] [CrossRef]

126. Ebbinghaus, S.; Hussain, M.; Tannir, N.; Gordon, M.; Desai, A.A.; Knight, R.A.; Humerickhouse, R.A.; Qian, J.; Gordon, G.B.; Figlin, R. Phase 2 Study of ABT-510 in Patients with Previously Untreated Advanced Renal Cell Carcinoma. Clin. Cancer Res. 2007, 13, 6689–6695. [Google Scholar] [CrossRef]

127. Weng, T.Y.; Huang, S.S.; Yen, M.C.; Lin, C.C.; Chen, Y.L.; Lin, C.M.; Chen, W.C.; Wang, C.Y.; Chang, J.Y.; Lai, M.D. A novel cancer therapeutic using thrombospondin 1 in dendritic cells. Mol. Ther. 2014, 22, 292–302. [Google Scholar] [CrossRef]

128. Pardue, E.L.; Ibrahim, S.; Ramamurthi, A. Role of hyaluronan in angiogenesis and its utility to angiogenic tissue engineering. Organogenesis 2008, 4, 203–214. [Google Scholar] [CrossRef]

129. Kultti, A.; Li, X.; Jiang, P.; Thompson, C.B.; Frost, G.I.; Shepard, H.M. Therapeutic targeting of hyaluronan in the tumor stroma. Cancers 2012, 4, 873–903. [Google Scholar] [CrossRef]

130. Provenzano, P.P.; Hingorani, S.R. Hyaluronan, fluid pressure, and stromal resistance in pancreas cancer. Br. J. Cancer 2013, 108, 1–8. [Google Scholar] [CrossRef]

131. Sato, N.; Kohi, S.; Hirata, K.; Goggins, M. Role of hyaluronan in pancreatic cancer biology and therapy: Once again in the spotlight. Cancer Sci. 2016, 107, 569–575. [Google Scholar] [CrossRef]

132. Tzanakakis, G.; Neagu, M.; Tsatsakis, A.; Nikitovic, D. Proteoglycans and Immunobiology of Cancer-Therapeutic Implications. Front. Immunol. 2019, 10, 875. [Google Scholar] [CrossRef]

133. Mueller, M.M.; Fusenig, N.E. Friends or foes—Bipolar effects of the tumour stroma in cancer. Nat. Rev. Cancer 2004, 4, 839–849. [Google Scholar] [CrossRef]

134. Jetten, N.; Verbruggen, S.; Gijbels, M.J.; Post, M.J.; De Winther, M.P.; Donners, M.M. Anti-inflammatory M2, but not pro-inflammatory M1 macrophages promote angiogenesis in vivo. Angiogenesis 2014, 17, 109–118. [Google Scholar] [CrossRef]

135. Tazzyman, S.; Lewis, C.E.; Murdoch, C. Neutrophils: Key mediators of tumour angiogenesis. Int. J. Exp. Pathol. 2009, 90, 222–231. [Google Scholar] [CrossRef]

136. Dor, Y.; Porat, R.; Keshet, E. Vascular endothelial growth factor and vascular adjustments to perturbations in oxygen homeostasis. Am. J. Physiol. Cell Physiol. 2001, 280, C1367–C1374. [Google Scholar] [CrossRef]

137. Itakura, J.; Ishiwata, T.; Friess, H.; Fujii, H.; Matsumoto, Y.; Buchler, M.W.; Korc, M. Enhanced expression of vascular endothelial growth factor in human pancreatic cancer correlates with local disease progression. Clin. Cancer Res. 1997, 3, 1309–1316. [Google Scholar]

138. Longo, V.; Brunetti, O.; Gnoni, A.; Cascinu, S.; Gasparini, G.; Lorusso, V.; Ribatti, D.; Silvestris, N. Angiogenesis in pancreatic ductal adenocarcinoma: A controversial issue. Oncotarget 2016, 7, 58649–58658. [Google Scholar] [CrossRef]

139. Carmeliet, P.; Jain, R.K. Principles and mechanisms of vessel normalization for cancer and other angiogenic diseases. Nat. Rev. Drug Discov. 2011, 10, 417–427. [Google Scholar] [CrossRef]

140. Zarrin, B.; Zarifi, F.; Vaseghi, G.; Javanmard, S.H. Acquired tumor resistance to antiangiogenic therapy: Mechanisms at a glance. J. Res. Med. Sci. 2017, 22, 117. [Google Scholar] [CrossRef]

141. Lammers, T.; Rizzo, L.; Storm, G.; Kiessling, F. Personalized Nanomedicine. Clin. Cancer Res. 2012, 18, 4889–4894. [Google Scholar] [CrossRef]

142. Takeuchi, K.; Ito, F. Receptor tyrosine kinases and targeted cancer therapeutics. Biol. Pharm. Bull. 2011, 34, 1774–1780. [Google Scholar] [CrossRef]

143. Lemke, G.; Rothlin, C. V Immunobiology of the TAM receptors. Nat. Rev. Immunol. 2008, 8, 327–336. [Google Scholar] [CrossRef]

144. Wu, F.; Li, J.; Jang, C.; Wang, J.; Xiong, J. The role of Axl in drug resistance and epithelial-to-mesenchymal transition of non-small cell lung carcinoma. Int. J. Clin. Exp. Pathol. 2014, 7, 6653–6661. [Google Scholar]

145. Leconet, W.; Larbouret, C.; Chardes, T.; Thomas, G.; Neiveyans, M.; Busson, M.; Jarlier, M.; Radosevic-Robin, N.; Pugniere, M.; Bernex, F.; et al. Preclinical validation of AXL receptor as a target for antibody-based pancreatic cancer immunotherapy. Oncogene 2014, 33, 5405–5414. [Google Scholar] [CrossRef]

146. Bonaventura, P.; Shekarian, T.; Alcazer, V.; Valladeau-Guilemond, J.; Valsesia-Wittmann, S.; Amigorena, S.; Caux, C.; Depil, S. Cold Tumors: A Therapeutic Challenge for Immunotherapy. Front. Immunol. 2019, 10, 168. [Google Scholar] [CrossRef]

147. Dasgupta, A.; Biancacci, I.; Kiessling, F.; Lammers, T. Imaging-assisted anticancer nanotherapy. Theranostics 2020, 10, 956–967. [Google Scholar] [CrossRef]

1.4 Aims of the Study

Treatment of solid tumors and in particular of PDAC represent an enormous challenge, due to the pronounced TME. Immunotherapy is an emerging field of oncology after the sensational success of CAR T cells against hematological malignancies. These accomplishments suggest cell-based therapies as an option for solid tumors, including pancreatic cancer. However, CAR T cells face several hindrances in vivo, such as immunosuppressive stromal and immune cells, limited CAR T cell trafficking, and physical barriers created by the extracellular matrix (ECM), which need to be overcome. Thus, treatment strategies including adjusted CARs and cytokine application have to be evaluated to increase the efficacy of CAR T cells in solid tumors. In addition, there is a high need to implement 2D and emerging 3D bioluminescence imaging of tumor and CAR T cells as decisive tools for preclinical research. These tools combined with ex vivo imaging methods can provide insights into immunotherapy functionality aspects. This study aimed to modulate CAR T cells by cytokine supplementation and CAR composition adjustments and to monitor the infiltration of CAR T cells and their anti-tumor efficacy into solid tumors by the application of multimodal imaging methods. Therefore, in this study, the following specific aims were addressed.

1.4.1 Assessment of the Influence of CAR Composition on In Vivo Functionality

All structural parts of a CAR can impact the cytotoxic potential of CAR T cells. However, the spacer region is merely depicted as inert and just a few groups performed comparative studies of different spacers. Thus, the first aim of this study was to perform side-by-side comparisons of multiple spacers to identify the impact of the spacer domain on in vitro and in vivo CAR T cell behavior. This was achieved by in vitro and in vivo characterization of CARs, with CD8α- and IgG1-derived spacers, in the most established model for CAR T cell research, a CD20-expressing lymphoma model. Here, a modified IgG1 based spacer demonstrated opposing in vitro and in vivo anti-tumor efficacy. To provide a structural alternative for impaired IgG1-based spacers, a novel class of spacers, with Ig-like structures, was developed in the well-established lymphoma model with the aim to test this construct in a PDAC xenograft model. In vitro and in vivo testing of the newly established spacer class is described in the first chapter: “A Novel Siglec-4 Derived Spacer Improves the Functionality of CAR T Cells Against Membrane-Proximal Epitopes”.

1.4.2 Evaluation of an In Vivo and Ex Vivo CAR T cell Tracking Strategy

Under certain circumstances, CAR T cells can execute their cytotoxic potential towards PDAC xenografts. Although, they face a tremendous hurdle with the distinct TME in the clinical setting. Data generated with in vivo and ex vivo imaging tools are crucial to analyze the ideal working condition for CAR T cells and to validate combinatorial approaches for the TME in PDAC. Hence, the second aim of this study was the development and establishment of an in vivo and ex vivo imaging approach for tracking and monitoring of EGFR and BDCA-2 CAR T cell localization, distribution and status. To accomplish the following, a workflow of in vivo bioluminescence imaging and ex vivo microscopy techniques was applied to a PDAC xenograft mouse model. 2D BLI and 3D BLT in vivo imaging of EGFR and BDCA-2 CAR T cells was performed for direct cell tracking using a modified click beetle luciferase. Light-sheet fluorescence microscopy and cyclic immunofluorescence stainings facilitated spatial resolution and characterization of tumor-infiltrating CAR T cells by indirect ex vivo cell labeling. This part of the study is investigated in the second chapter: “Multimodal imaging of CAR T cells using bioluminescence tomography and light-sheet microscopy reveals negative effects of local interleukin-2.”

1.4.3 Analysis of IL-2 as a Support for CAR T cells in TME of PDAC

IL-2 is a well-established cytokine and a crucial factor for B and T cell proliferation. This major role as a determining growth factor for T cells resulted in one of the first approvals in the field of immunotherapy. However, patients experienced severe and partially lethal side effects after systemic IL-2 cancer treatment. Despite these drawbacks, localized IL-2 could assist CAR T cells in the hostile TME with its immunosuppressive milieu. Therefore, the third aim of this study was to evaluate local IL-2 as support for EGFR CAR T cell efficacy in solid tumors. Tumor killing and infiltration were analyzed by repeated subcutaneous injection of IL-2 at the tumor site of previously PDAC engrafted mice, treated with target-specific and unspecific CAR T cells. In vivo and ex vivo tracking of CAR T cells was performed to analyze the influence of local IL-2 on whole-body and intratumoral T cell distribution and phenotype. Local IL-2 in combination with CAR T cell therapy was addressed in the second chapter: “Multimodal imaging of CAR T cells using bioluminescence tomography and light-sheet microscopy reveals negative effects of local interleukin-2.”

SUMMARY CHAPTER 1

A NOVEL SIGLEC-4 DERIVED SPACER IMPROVES THE FUNCTIONALITY OF CAR T CELLS AGAINST MEMBRANE-PROXIMAL EPITOPES

In this manuscript, we evaluated the in vitro and in vivo functionality of three different CD20 redirected chimeric antigen receptor (CAR) constructs, with varying spacer regions and single-chain variable fragments (scFv). All second-generation CAR constructs demonstrated comparable cytotoxicity of transduced T cells against a lymphoma cell line in vitro. However, one of the constructs, incorporating a modified CH2-CH3 domain of IgG1 as a spacer domain, failed to exert any anti-tumor efficacy in vivo, in contrast to CARs with a shorter but less structured CD8α spacer.

The lack of available long and structured spacers with a beneficial functionality profile but without the risk of unspecific binding, resulted in the evaluation of a new spacer class derived from sialic acid-binding immunoglobulin-type lectins (Siglecs). Five different spacers were designed and tested in vitro in a CD20 specific CAR setting. One of the spacers, based on Siglec-4, demonstrated a high cytotoxicity comparable to the well-established CD8α spacer.

The new Siglec-4 derived spacer was combined with scFvs redirected against a membrane-proximal TSPAN8 epitope or a membrane-distal CD66c epitope. In vitro testing in a PDAC setting, demonstrated a favorable cytotoxic profile of TSPAN8-Siglec-4 CAR, while T cells transduced with a CD66c-Siglec-4 CAR were not activated. The transfer into a xenograft in vivo model confirmed the effective functionality profile of the TSPAN8-Siglec-4 CAR T cells, which outperformed an IgG4 spacer in terms of efficacy and a CD8α spacer, in terms of cytokine expression profile and T cell phenotype. This manuscript established a new class of spacers and demonstrated the functionality of CAR T cells in PDAC dependent on the target and the CAR design.

CHAPTER 1 - A NOVEL SIGLEC-4 DERIVED SPACER IMPROVES THE FUNCTIONALITY OF CAR T CELLS AGAINST MEMBRANE-PROXIMAL EPITOPES

Published in Frontiers in Immunology: Schäfer D, **Henze J**, Pfeifer R, Schleicher A, Brauner J, Mockel-Tenbrinck N, Barth C, Gudert D, Al Rawashdeh W, Johnston ICD and Hardt O (2020) A Novel Siglec-4 Derived Spacer Improves the Functionality of CAR T Cells Against Membrane-Proximal Epitopes. Front. Immunol. 11:1704. doi: 10.3389/fimmu.2020.01704

Authors:

Daniel Schäfer[1,3†], **Janina Henze**[1,2†], Rita Pfeifer[2†], Anna Schleicher[3], Janina Brauner[2], Nadine Mockel-Tenbrinck[2], Carola Barth[2], Daniela Gudert[2], Wa'el Al Rawashdeh[2], Ian C. D. Johnston[2‡], Olaf Hardt[2‡*]

Affiliations:

[1]*Translational Molecular Imaging, Institute for Diagnostic and Interventional Radiology & Clinic for Hematology and Medical Oncology, University Medical Center Göttingen, Göttingen, Germany*

[2]*R&D Reagents, Miltenyi Biotec B.V. & Co. KG, Bergisch Gladbach, Germany*

[3]*Chemical Biology, Faculty of Chemistry and Biosciences, Karlsruher Institute of Technology, Germany*

† Shared first authorship

‡ Shared last authorship

***Correspondence:**

Wa'el Al Rawashdeh, wael.alrawashdeh@miltenyibiotec.de; Ian C. D. Johnston, ian.johnston@miltenyibiotec.de; Olaf Hardt, olaf.hardt@miltenyibiotec.de

Received: 03 March 2020; Accepted: 25 June 2020; Published: 07 August 2020.

Abstract

A domain that is often neglected in the assessment of chimeric antigen receptor (CAR) functionality is the extracellular spacer module. However, several studies have elucidated that membrane proximal epitopes are best targeted through CARs comprising long spacers, while short spacer CARs exhibit highest activity on distal epitopes. This finding can be explained by the requirement to have an optimal distance between the effector T cell and target cell. Commonly used long spacer domains are the CH2-CH3 domains of IgG molecules. However, CARs containing these spacers generally show inferior in vivo efficacy in mouse models compared to their observed in vitro activity, which is linked to unspecific Fcγ-Receptor binding and can be abolished by mutating the respective regions. Here, we first assessed a CAR therapy targeting membrane proximal CD20 using such a modified long IgG1 spacer. However, despite these mutations, this construct failed to unfold its observed in vitro cytotoxic potential in an in vivo model, while a shorter but less structured CD8α spacer CAR showed complete tumor clearance. Given the shortage of well-described long spacer domains with a favorable functionality profile, we designed a novel class of CAR spacers with similar attributes to IgG spacers but without unspecific off-target binding, derived from the Sialic acid-binding immunoglobulin-type lectins (Siglecs). Of five constructs tested, a Siglec-4 derived spacer showed highest cytotoxic potential and similar performance to a CD8α spacer in a CD20 specific CAR setting. In a pancreatic ductal adenocarcinoma model, a Siglec-4 spacer CAR targeting a membrane proximal (TSPAN8) epitope was efficiently engaged in vitro, while a membrane distal (CD66c) epitope did not activate the T cell. Transfer of the TSPAN8 specific Siglec-4 spacer CAR to an in vivo setting maintained the excellent tumor killing characteristics being indistinguishable from a TSPAN8 CD8α spacer CAR while outperforming an IgG4 long spacer CAR and, at the same time, showing an advantageous central memory CAR T cell phenotype with lower release of inflammatory cytokines. In summary, we developed a novel spacer that combines cytotoxic potential with an advantageous T cell and cytokine release phenotype, which make this an interesting candidate for future clinical applications.

Keywords: Chimeric antigen receptor, hinge, spacer, Siglec, CH2-CH3, IgG, CAR design

Introduction

The unprecedented therapeutic efficacy of CAR T cells in previously refractory blood cancers is considered to be one of the major breakthroughs in cancer immunotherapy, culminating in the recent market approvals by the Food and Drug Administration (FDA) and the European Medicines Agency (EMA) for two CAR T cell products (1–7). While CAR therapies have now achieved public recognition, their development and the quest for optimal CAR design has been a multistep process stretching over several decades. Ever since their initial description in 1989 by Eshhar et al. (8), the receptors have evolved from a two-chimeric-TCR chain architecture to a one-protein design. This design commonly incorporates a single-chain variable fragment (scFv) of a given antibody as the antigen binding moiety, an extracellular spacer and a transmembrane region as structural features, as well as signal transduction units for T cell activation. Originally, the spacer domain was introduced into the CAR framework as an inert building block to allow the antigen binding moiety to extend beyond the T cell's glycocalyx and improve antigen accessibility (9). Following this assumption, a plethora of spacer regions were designed simultaneously ranging from the immunoglobulin (Ig) domains of the crystallizable fragments (Fc) of antibodies to extracellular domains of CD8α, CD28, the TCRβ chain or NKG2D (10–16) and were applied without comparative analyses. However, already very early on, Patel and colleagues provided the scientific proof that the spacer region can be of paramount importance for the receptor function and affects its expression, surface stability through the turnover rate, and signal transduction (17). More recent accumulating research has further been showing that in addition to the nature of the spacer, effective antigen recognition depends on the functional interplay between the spatial localization of the target epitope and the CAR spacer length (18–20). For instance, membrane-distal epitopes were shown to most efficiently trigger CARs with short spacers, while membrane-proximal epitopes required receptors with extended spacer domains to elicit accurate effector function, in this way emphasizing the biological requirement of optimal T cell-target cell distance (18–22). Thus, the design of CARs against novel antigens needs to consider both the epitope position within the target antigen as well as the nature and length of the spacer region and customize these variables accordingly.

The use of Ig-derived spacers is particularly attractive as it provides the opportunity to modulate the spacer length into long (CH2-CH3 domain), medium (CH3) and short (hinge only) structures, while retaining the nature of the parent protein. However, Ig-derived spacers have faced various complications during their development. In particular, off-target activation, CAR T cell sequestration in the lung, tonic signaling and activation-induced cell death (AICD) have

been described leading to only a limited T cell persistence (23–26). Although these effects could be abrogated by mutating the amino acid sequence essential for FcR binding (23, 25, 27), it needs to be taken into consideration that these experiments were conducted in immunosuppressed NSG mice and whether FcR binding can be entirely eliminated in humans remains unclear. Of note, several clinical studies that used IgG-derived spacers described only limited anti-tumor efficacy and low CAR T cell persistence (28–31) while others are showing some promising clinical responses (32–34). Interestingly, the first commercially available CAR T cell-based therapies use CD28 (Yescarta) and CD8 (Kymriah) derived spacer domains.

Taking into account the shortage of well-described long spacer domains with a favorable functionality profile, we endeavored to develop a novel long spacer for membrane-proximal epitopes, which naturally lacks an FcR binding domain. Based on the postulated spatial requirements between CARs and their target antigens, we anticipated finding a CAR spacer construct whose functionality against membrane-proximal epitopes extends beyond that of a CD8α spacer CAR. Hence, we generated novel CAR spacers and analyzed their efficacy side-by-side to the cognate CD8α spacer counterpart – a comparison that has not been extensively undertaken thus far. The design of the novel spacers was based on the sialic acid binding Ig-like lectin (Siglec) receptor family, whose members are broadly expressed on various immune cells (35, 36). Structurally, each receptor member is composed of an N-terminal Ig-like V-set domain which is involved in sialic acid binding and a defined number of Ig-like C2-set domains that serve as a structural spacer and extend the binding moiety away from the plasma membrane. The selection of the Siglec family was inspired by the hypothesis that the incorporation of naturally occurring spacer domains into the CAR architecture will preserve the biological requirements of a spacer region and minimize unspecific interactions with other cells.

In this study, we confirm this strategy of using naturally occurring spacer domains by first demonstrating, that in a $CD20^+$ lymphoma model a long IgG1 spacer CAR is as functional as the CD8α spacer in vitro, but fails to translate its effectiveness in vivo, despite containing the earlier reported mutations to abrogate FcR binding (23). Subsequently, we evaluate novel spacers derived from the Siglec family of proteins and identify a long alternative spacer derived from Siglec-4 that performs with equal efficiency to the CD8α spacer in vitro. Finally, we demonstrate in a solid tumor model that the novel Siglec-4 spacer CAR does not exceed, but rather matches the CD8α spacer CAR cytotoxic activity in vivo on membrane-proximal targets, while maintaining a favorable cell phenotype profile and cytokine release pattern.

Materials and Methods

CAR Gene Construction

Commercial gene synthesis in combination with an optimization algorithm for codon usage in humans (ATUM) was used to construct the CAR genes of interest. The CD20-specific scFv was derived from the murine monoclonal antibody Leu16 as originally described by Jensen and colleagues (37), while the CD66c- and TSPAN8-targeting scFv sequences were derived from the antibody clones REA414 (CD66c) and REA443 (TSPAN8) (Miltenyi Biotec). All antigen binding domains contained a $(G4S)_3$-linker between the VL and the VH regions. To facilitate receptor trafficking to the plasma membrane, a human CD8α leader signaling peptide was added N-terminally to the respective scFv sequence. The spacer region downstream of the scFv encompassed either the domain for IgG1 hinge-CH2CH3 (234 amino acids), IgG4 hinge-CH2CH3 (228 amino acids), or CD8α hinge (45 amino acids). To abrogate potential interactions of the Fc spacer CARs with FcR-expressing cells, the PELLGG and ISR motives in the IgG1 CH2 domain were replaced by the corresponding IgG2 amino acids (23). In the case of the IgG4 CH2 domain, the APEFLG sequence was replaced by APPVA from IgG2 and an N279Q mutation was introduced to remove glycosylation at this site (25). Spacers derived from the Siglec family were designed based on the protein sequences extracted from UniProt and the plasma membrane-proximal domains were incorporated into the CAR architecture. Thus, the Siglec-3 spacer comprised the amino acids 145–259 of the parent protein with a C169S mutation to abrogate unspecific disulfide-bond formation. The Siglec-4 spacer contained the amino acids 238–519, the Siglec-7.1 spacer the amino acids 150–353, the Siglec-7.2 spacer the amino acids 234–353, and the Siglec-8 spacer the amino acids 241–363 of the respective parent protein. All spacers were linked to the transmembrane domain of human CD8α, the intracellular domain of 4-1BB, and the CD3ζ signaling domain as derived from UniProt. The CAR genes were fused to a Furin-P2A sequence to include co-expression of the truncated low affinity nerve growth factor receptor (ΔLNGFR). Transgene expression was promoted by the PGK promoter located upstream of the CAR gene.

Lentiviral Vector Production

Second generation self-inactivating VSV-G-pseudotyped lentiviral vectors were produced by transient transfection of adherent HEK293T cells. One day before transfection, 1.6×10^7 HEK293T cells were seeded per T175 flask to reach a confluency of 70–90% on the following day. Each T175 flask was then transfected with a total of 35 µg plasmid DNA composed of pMDG2 (encoding VSV-G), pCMVdR8.74 (encoding gag/pol), and the respective transgene-

encoding transfer vector using MACSfectin reagent (Miltenyi Biotec). All transfection reactions were performed with a DNA: MACSfectin ratio of 1:2. Following overnight incubation, sodium butyrate was supplied at a final concentration of 10 mM and at 48 h after transfection the medium was collected, cleared by centrifugation at 300 × g and 4°C for 5 min and filtered through 0.45 μm-pore-size PVDF filters. Concentration of the viral stock was performed by centrifugation at 4°C and 4,000 × g for 24 h. Pellets containing lentiviral vector were air-dried and resuspended at a 100-fold concentration with 4°C cold PBS. Lentiviral vector aliquots were stored at −80°C.

Generation of CAR T Cells

Automated CAR T Cell Generation

The CliniMACS Prodigy® TCT (T cell transduction) application was used for the automated manufacturing of large amounts of gene-modified T cells. Technical features and experimental procedures have previously been described in detail (38, 39). In brief, T cells were obtained from non-mobilized leukapheresis from healthy anonymous donors (University Hospital Cologne or the German Red Cross Ulm) and were typically processed 24–48 h after collection. Transduced and enriched CAR T cells were finally formulated and harvested in Composol® solution (Fresenius Kabi), supplemented with 2.5% human serum albumin (Grifols). For quality assurance, the transduction efficiency and T cell phenotype was determined using a MACSQuant Analyzer 10 (Miltenyi Biotec) after the TCT process. Transduction efficiency were determined by flow cytometry on days 5 and 12 of the TCT process using a flow cytometer.

Manual CAR T Cell Generation

Buffy coats from healthy anonymous donors were obtained from the German Red Cross Dortmund. Peripheral blood mononuclear cells (PBMCs) were then isolated from buffy coats by density gradient centrifugation. T cells were purified from PBMCs applying the Pan T Cell Isolation Kit, human (Miltenyi Biotec) and activated in TexMACS™ Medium (Miltenyi Biotec) supplemented with T Cell TransAct™, human (Miltenyi Biotec) and 100 IU/ml of recombinant Human IL-2 IS, research grade (Miltenyi Biotec). T cells were transduced 24 h after activation using VSV-G pseudotyped lentiviral particles. 3 days post activation, T Cell TransAct™, human and excess viral vector were removed and T cells were cultured in TexMACS™ Medium only supplemented with IL-2. T cells were expanded for 12 days and used directly for in vitro assays or frozen in TexMACS™ Medium containing 10% DMSO for later in vivo use.

Frozen T cells that were used for in vivo testing were thawed 24 h before injection and cultivated at 37°C in TexMACS™ Medium without further supplements.

Target Cell Lines

HEK293T, JeKo-1, Raji and AsPC1 cells were obtained from ATCC and cultured as recommended. Raji cells were transduced with with a ffLuc cassette for in vivo detection and AsPC1 cells were transduced with with a eGFP/ffLuc cassette for in vitro and in vivo detection. To validate authenticity of the cell lines used, we used the Human STR Profiling Cell Authentication Service (ATCC).

Flow Cytometry

Antibodies specific for anti-human CD62L, CD45RO, CD95, CD271 (LNGFR), CD107a, TNF-α, CD223 (LAG3), CD279 (PD1), CD366 (TIM3), CD137 (4-1BB), CD4, CD8, CD3 were monoclonal recombinant antibodies (Miltenyi Biotec). For anti-CD20 CAR detection the CD20 CAR Detection Reagent (Miltenyi Biotec) was used. Staining of Miltenyi Biotec antibodies was performed according to the supplier's instructions. For direct CAR detection of CD66c and TSPAN8 specific CARs a sequential staining was used. First, samples were incubated with polyclonal Fab specific anti-mouse IgG antibodies produced in goat (Merck) at concentrations of 10 µg/ml for 30 min at 4°C. Samples were washed and then incubated with polyclonal anti-goat IgG antibodies produced in chicken (Thermo Fisher) at concentrations of 10 µg/ml for 30 min at 4°C. Stained samples were measured on a MACSQuant® Analyzer 8 or MACSQuant Analyzer 10 (Miltenyi Biotec) and analyzed using the MACSQuantify™ Software.

In vitro Functional Assays

With JeKo-1 Target Cells

1×10^5 JeKo-1 and 1×10^5 CAR T cells were co-cultured in TexMACS™ Medium (Miltenyi Biotec) for 24 h in 96-well round bottom plates. Supernatants were collected at the endpoint and used to detect the cytokines released by anti-CD20 CAR T cells using the MACSPlex Cytokine 12 Kit (Miltenyi Biotec) with the four selected human cytokines IFN-γ, IL-2, TNF-α and GM-CSF, according to the manufacturer's instructions. The cytolytic activity of the engineered T cells was evaluated by using 1×10^4 $CD20^+$ JeKo-1 cells labeled with 1 µM CellTraceTM Violet (Life Technologies), as target cells. Effector and target cells were co-cultured for 24 h at the indicated ratios (E:T) in 96-well round bottom plates. Detection of the

specific lysis was performed by quantitation of Violet dye labeled target cells using a MACSQuant Analyzer 8 (Miltenyi Biotec). Mock-transduced T cells were used as control at the same effector-to-target ratios.

With Raji Cells

2×10^5 CAR T cells were incubated with 2×10^5 $CD20^+$ Raji cells in 200 µl TexMACS™ Medium at 37°C. In addition, the medium was supplemented with 20 µl of a CD107a specific antibody. After 1 h of incubation the protein transport inhibitors Monensin and Brefeldin A (BD Biosiences) were added as recommended for 4 h. After this incubation period, cells were washed and first surface stained with LNGFR specific antibodies to label transduced T cells and subsequently intracellularly stained for TNF-α using the Inside Stain Kit and a TNF-α specific antibody (all Miltenyi Biotec). Cells were then measured by flow cytometry. For TIM3, LAG3 and PD1 detection 1×10^5 CAR T cells were inoculated with 2×10^5 $CD20^+$ Raji cells in 200 µl TexMACS™ Medium at 37°C for 24 h. Subsequently T cells were stained and analyzed by flow cytometry.

For functionality assays in the presence of NSG macrophages, 2×10^5 CAR T cells were incubated in a 1:1:1 ratio with Raji target cells and macrophages derived from a peritoneal lavage. The assay was performed in the presence or absence of murine FcR-blocking reagent. After 24 h of incubation, detection of the specific lysis was performed by quantitation of Violet dye labeled target cells via flow cytometry using a MACSQuant Analyzer 8 (Miltenyi Biotec).

With AsPC1 Cells

GFP^+/Luc^+ AsPC1 target cells were inoculated in 96-well plates at 2.5×10^4 cells per well in TexMACS™ Medium. CAR T cells or untransduced Mock T cells were added with at an E:T ratio of 2:1. The amount of T cells in the Mock control was adjusted to the number of total T cells in the CAR group with the highest total cell count. Cytotoxicity was measurement as the decrease of green surface area as assessed by the IncuCyte® S3 Live-Cell Analysis System (Sartorius). Measured values were normalized to the start of the experiment. After 24 h a supernatant sample was taken for cytokine measurements using the MACSPlex Cytokine 12 Kit. At the end of the experiment expression of LAG3, PD1, and 4-1BB were measured using a MACSQuant Analyzer 8 (Miltenyi Biotec). Specific endpoint killing was calculated from the green surface area values with the following formula:

specific killing [%]= 100−(100 ∗ green area Mockgreen area CAR).

In vivo Assays

Experiments involving animal handling were approved by the Governmental Review Committee on Animal Care in NRW, Germany and performed according to guidelines and regulations (Landesamt für Natur, Umwelt and Verbraucherschutz NRW, Approval number 84-02.04.2015.A168 and Approval number 84-02.04.2017.A021).

Raji lymphoma were established by tail vein injection of 5×10^5 Raji Luc^+ cells. After 7 days, 1×10^6 CAR T cells or Mock GFP-transduced T cells, adjusted to the total amount of T cells according to transduction efficiency of the CARs, were infused intravenously.

For AsPC1 GFP^+/Luc^+ cell line derived tumors 1×10^6 cells were injected subcutaneously in the right flank of NOD SCID gamma (NSG; NOD.Cg-PrkdcscidIl2rgtm1Wjl/SzJ) mice (Jackson Laboratory, provided by Charles River). When tumors reached a size of 25 mm^2, 5×10^6 CAR T cells were injected into the tail vein. The amount of injected untransduced Mock T cells was adjusted to the number of total T cells in the CAR group with the highest total cell count.

Therapeutic response was measured longitudinally using the IVIS Lumina in vivo imaging system (PerkinElmer) after intraperitoneal injection of 100 µL (30 mg/mL) D-Luciferin (for Raji studies: XenoLight Rediject D-Luciferin Ultra (PerkinElmer). For AsPC1 studies: Potassium Salt, LUCK-2G, GoldBio) and additionally by manual caliper measurement for pancreatic tumors. All measures to secure the well-being of mice were executed following the relevant animal use guidelines and ethical regulations. Upon reaching the endpoint (weight loss of >19%, paralysis, stress score of >20 or end-point of the experiment, Day 20 for the lymphoma model and Day 29 for the pancreatic model), animals were euthanized according to guidelines and post-mortem analysis was performed in order to determine tumor burden, persistence and killing of the different CAR T cell constructs. In particular blood, bone marrow and spleen were subjected to flow cytometric analysis. Therefore, spleen was dissociated using the gentleMACS™ Octo Dissociator with Heaters according to the manufacturers protocol (Miltenyi Biotec) and bone marrow was extracted from the femurs and tibias of mice by cutting off the epiphyses of the bones and rinsing the inner fragments. The cell suspensions were filtered through a 70 µm pore size MACS SmartStrainer (Miltenyi Biotec) and following red blood cell lysis on blood, bone marrow and spleen single-cell suspensions using Red Blood Cell Lysis Solution (Miltenyi Biotec), samples were stained and analysis was conducted on a MACSQuant Analyzer 8.

Statistics

Unless otherwise specified, all graphical error bars represent standard error of the mean. Statistical comparisons between more than two groups were conducted by One-way ANOVA with $p < 0.05$ using GraphPad Prism 7. To facilitate the statistical overview of the in vivo experiments, the significance analyses were organized in a pairwise significance matrix (PSM) where each box represents a comparison between two groups, as shown by Al Rawashdeh et al. (40). The order, in which the groups were compared, is illustrated in Figures S1, S4. Significant differences between two comparing groups are defined by a green box, while insignificant differences by a red box.

Results

CD20 Specific CD8α and IgG1 CH2-CH3 Spacer CARs Exhibit Comparable in vitro Activity

During pre-clinical development of a CD20 directed CAR candidate (39) we also evaluated a number of different CAR configurations (Figure 1A). We used an scFv derived from the Leu16 monoclonal antibody (30, 41), binding to the large extracellular loop of CD20 (42). This loop is only 47 amino acids long, which is why we hypothesized it would be more effectively targeted with a flexible CD8α or long IgG spacer. We generated two second generation CAR constructs, that comprised a CD8α transmembrane domain, a 4-1BB co-stimulatory domain and a CD3ζ main activator domain. Both bind CD20 via the Leu16 derived scFv in a VH-VL orientation and only differed in the spacer domain. The CD20_hl_IgG1 CAR comprises an IgG1 CH2-CH3 spacer while the CD20_hl_CD8 CAR possesses a CD8α spacer. The PELLGG and ISR motif of the IgG1 CH2-CH3 spacer were replaced by the corresponding IgG2 amino acids to reduce Fcγ-Receptor binding, as described previously (23). To assess whether the order of binding domains in the scFv also can play a role in CAR function, we constructed a CD8α spacer CAR with swapped scFv orientation (CD20_lh_CD8). We generated CD20 specific CAR T cells by genetically modifying CD3/CD28 polyclonally activated T cells with lentiviral vectors in a fully automated manner in a closed system using the CliniMACS Prodigy® as described previously (39). At the end of the manufacturing on day 12, similar T cell phenotypes were obtained for the samples modified with the different CAR constructs and the untransduced Mock control (Figure 1B). More than 80% of T cells had a memory phenotype (central memory T cell (TCM) and stem cell memory T cell (TSCM) as defined by their phenotypes being $CD62L^+/CD45RO^+/CD95^+$ and $CD62L^+/CD45RO^-/CD95^+$, respectively). Also, the three

constructs demonstrated comparable functionality in terms of cytokine release (Figure 1C) and cytotoxicity (Figure 1D) upon co-culture with CD20$^+$ JeKo-1 target cells.

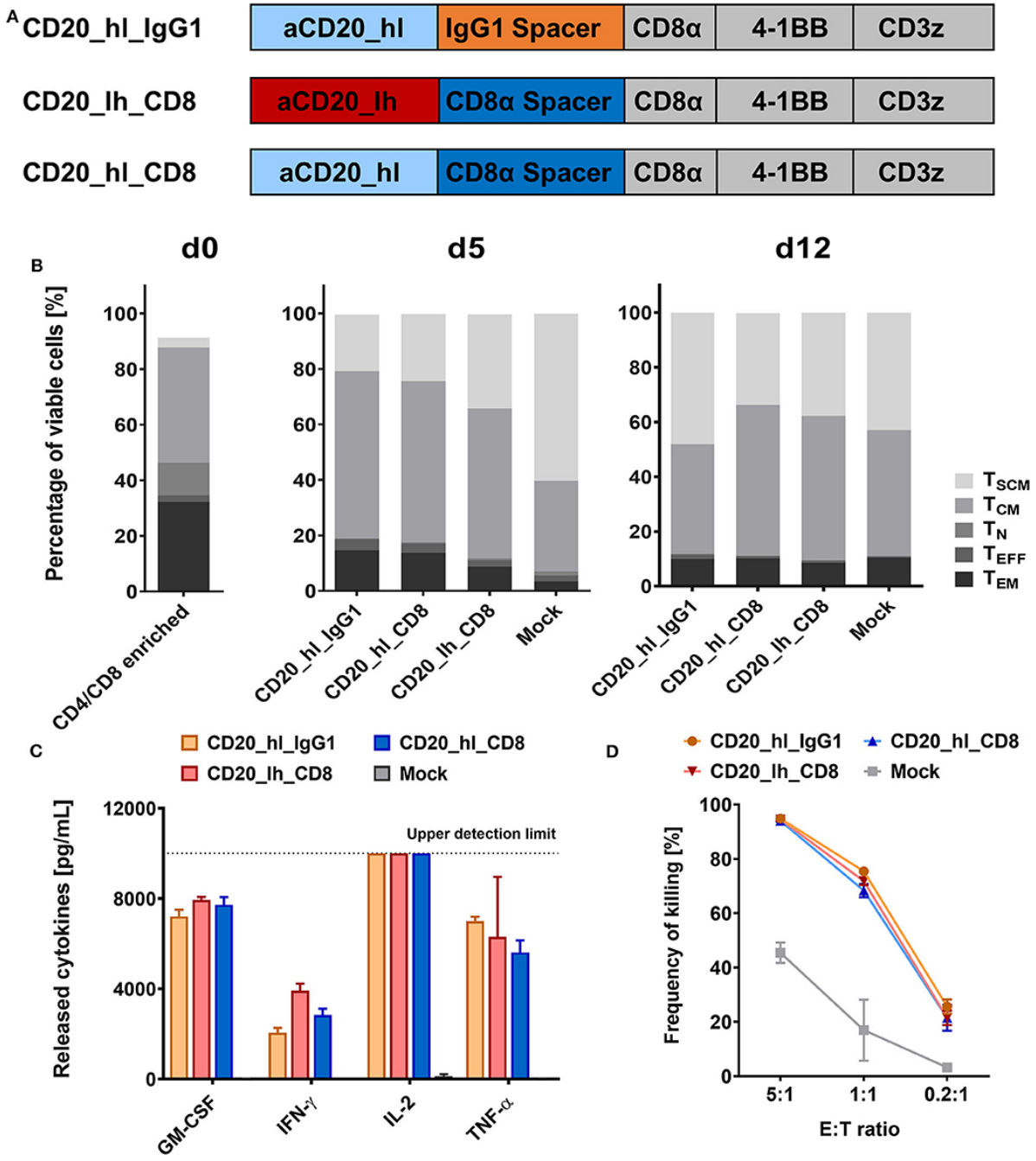

Figure 1. CD20 specific CAR T cells with short CD8α and long IgG1 CH2-CH3 spacers show similar in vitro functionality. (A) Structure of the three CD20 CAR constructs. (B) T cell phenotypes in the CD4/CD8 enriched fraction on d0, d5, and d12 of the automated T cell transduction process by flow cytometry. (C) GM-CSF, IFN-γ, IL-2, IL-6, and TNF-α production after 24 h co-culture of CD20 CAR T cells with CD20$^+$ JeKo-1 target cells at 1:1 effector to target ratio analyzed by flow cytometry. n = 3. (D) Cytolytic activity of the engineered CAR T cells. Effector CAR T cells and target-positive JeKo-1 target cells were co-cultured for 24 h at the indicated ratios (E:T). Detection of the specific lysis was performed by flow cytometry. n = 3.

CD8α and IgG1 CH2-CH3 Spacer CARs Differ in Their in vivo Performance

Having assessed the in vitro activity, we next analyzed the same lentivirally modified T cells in a pre-clinical NSG mouse model. 5×10^5 $CD20^+$ Raji cells, which were modified to constitutively express luciferase, were injected into the tail vein of each mouse. Seven days later, 1×10^6 CD20 specific CAR T cells or GFP transduced Mock T cells (Figure 2A) were also applied intravenously. Tumor burden was monitored longitudinally over 3 weeks by non-invasive bioluminescent imaging (BLI) of tumor cells in vivo. Neither the Mock treated group nor mice treated with the IgG1 spacer CAR showed any control of tumor growth compared to the untreated group, and the animals in these groups were sacrificed according to the ethical code on day 17 and day 15, respectively (Figure 2B). On the other hand, significant therapeutic responses were achieved by the CD20_hl_CD8 and CD20_lh_CD8 CAR T cells (Figures 2B,D). Both groups exhibited a reduced tumor growth 6 days post T cell injection. While the CD20_hl_CD8 CAR T cells reached background fluorescence on day 13, CAR T cells equipped with the same CAR but with the scFv in the converse orientation needed longer to reduce tumor burden and did not reach background levels until the end of the experiment. This difference between the scFv variants could be attributed to a single mouse having remnants of tumor present in the jawbone, which in our experience is difficult to treat and possibly inaccessible to CAR T cells. We verified that the scFv orientation indeed had only a minor influence by repeating the experiment with the CD8α spacer CARs with the different scFv orientations using a different donor (Figures 2C,E). Again, both groups of CAR-modified T cells were effective in rapidly controlling the tumor growth, with no significant difference being observed between the different scFv orientations. Ex vivo analysis of spleen, bone marrow and blood at the end of the study showed no detectable IgG1 spacer CAR T cells in the treated mice while CAR T cells with the CD8α spacer could be readily detected, implying a reduced in vivo persistence or expansion of the T cells modified with the IgG1 spacer CAR (Figure S2).

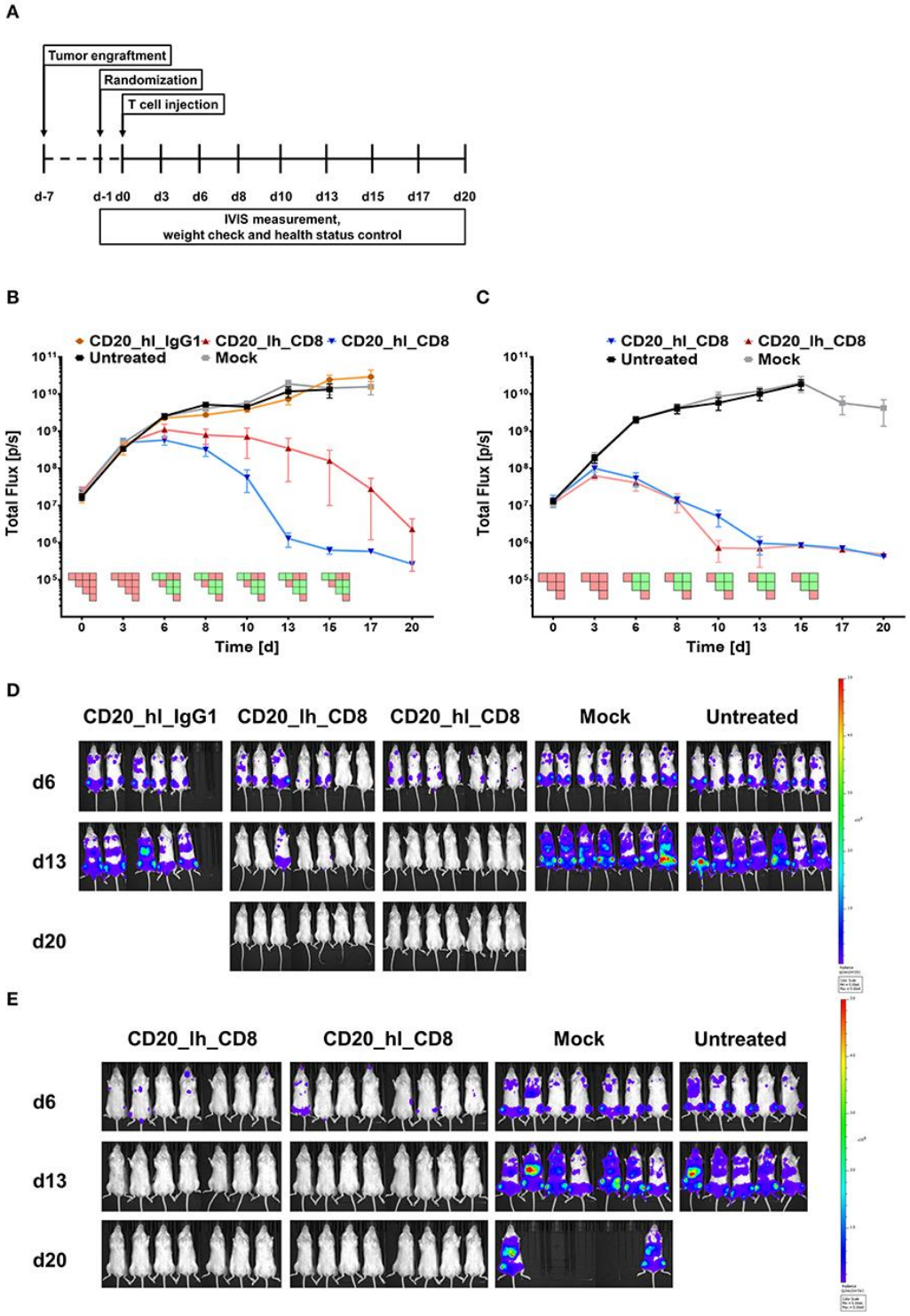

Figure 2. CD20 specific CAR T cells with an IgG1 spacer domain fail to exhibit in vivo efficacy. (A) Overview of the study workflows. (B) Tumor burden change over time in mice treated with anti-CD20 IgG1 CH2-CH3 and CD8α spacer CAR T cells from one donor. n = 5/group. PSM $p < 0.05$ (green) [one-way ANOVA]. (C) Tumor burden change over time in presence of the two different CD8α CAR constructs with T cells from a second donor. n = 6/group. PSM $p < 0.05$ (green) [one-way ANOVA]. (D) Representative in vivo bioluminescence images of tumor bearing mice from (B). Images are arranged according to the treatment group and time after CAR T cell injection. T cells were generated from one donor. Scale factor: min: 5×10^6, max: 5×10^8 p/s. (E) Representative in vivo bioluminescence images of tumor bearing mice from (C). Images are arranged according to the treatment group and time after CAR T cell injection. T cells were generated from a second donor. Scale factor: min: 5×10^6, max: 5×10^8 p/s.

These findings were in line with earlier results of other groups, showing reduced in vivo efficacy of full length IgG family spacers (25, 27). These groups mutated FcR binding sites or developed other solutions in order to decrease off-target binding of the T cell, which we were also able to confirm in an in vitro assay using mouse macrophages (Figure S3), but it is unclear whether all potential off-target binding has been abrogated as binding to other lower affinity FcγRs may be retained (25).

Construction and Characterization of a New Family of CAR Spacers

These findings motivated us to develop a new class of CAR spacer regions that naturally lack FcR binding sites. In this context we identified the Sialic acid-binding immunoglobulin-type lectin (Siglec) family whose members are expressed on various immune cells and incorporate Ig-like domains in their receptor architecture (43, 44). More specifically, while the membrane distal sialic acid binding Ig-like V-set domain is positioned N-terminally, the more C-terminally located Ig-like C2-set domains, which vary in number, serve as spacer regions. Based on previous reports describing that CAR T cell activation can be optimized according to the epitope location and spacer length, we selected one, two or three C2-set domains derived from Siglec-3, -4, -7, or -8 for spacer design (Figure 3).

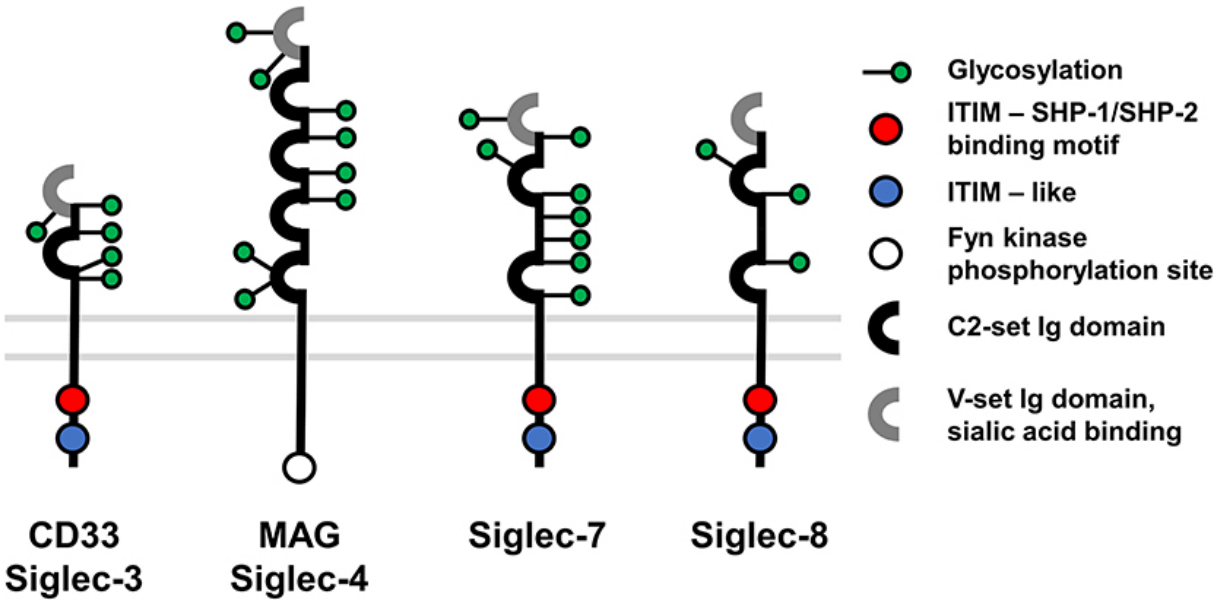

Figure 3. Overview of Siglec membrane proteins used for CAR construction.

To confirm correct translation and surface expression of the constructs, bicistronic lentiviral expression vectors were generated with a downstream ΔLNGFR gene linked to the CAR by a P2A sequence (Figure 4A). After transfection of the DNA constructs into HEK293T cells,

detection of the reporter protein ΔLNGFR confirmed successful transcription and translation of the CAR cassette, while direct staining of the CAR with a CD20 CAR detection reagent (PE) visualized surface expression of the CAR constructs. All constructs showed both ΔLNGFR and CAR expression in >80% of HEK293T cells (Figure 4B). Subsequently, we transduced primary T cells with lentiviral vectors and assessed the CAR expression 6 days post transduction (Figure 4C). The ΔLNGFR reporter protein was expressed in all cases demonstrating effective lentiviral transduction of the T cells and translation of the expression cassette (range 46–75% $LNGFR^+$ T cells). However, while three CAR constructs showed CAR expression levels comparable to the CD8α spacer CAR control, no CD20_hl_Sig7.1 CAR expression was detectable and the CD20_hl_Sig3 CAR was expressed on only 5% of the T cells. Based on these results, we excluded these constructs from further analysis.

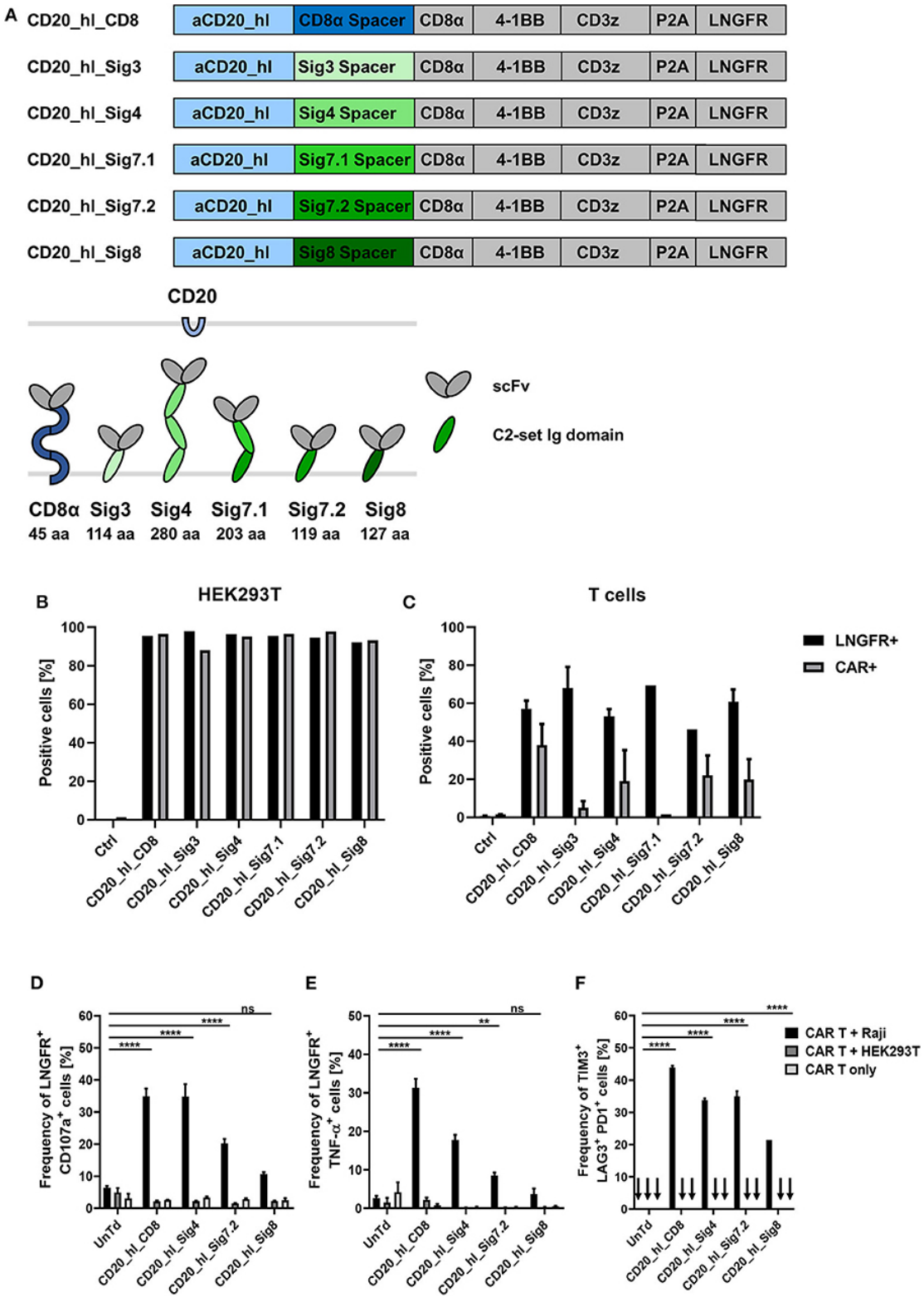

Figure 4. In vitro evaluation of novel CD20 specific Siglec spacer CAR T cells. (A) Modular structure of the CD20 CAR constructs with the Siglec spacers and extracellular domain comparison of the CAR constructs. (B) Expression analysis of the CAR constructs in transiently transfected HEK293T cells 24 h post transfection and (C) in transduced T cells from two donors 6 days post transduction. LNGFR and CAR expression were evaluated by flow cytometry. (D,E) Siglec spacer CAR T cells were cocultured with Raji or HEK293T cells for 5 h at a ratio of 1:1 and T cell expression of CD107a (D) and intracellular TNF-α (E) were analyzed by flow cytometry. (F) The frequency of TIM3, LAG3, and PD1 triple positive CAR T cells was analyzed after 24 h co-culture at a 1:2 ratio of CAR T cells to Raji or

HEK293T cells by flow cytometry. CAR T cells alone were also cultured in order to exclude unspecific activation. n = 3. Error bars, mean ± SD. ns > 0.05, **p < 0.01, and ****p < 0.0001 [one-way ANOVA, CAR T^+ Raji compared to Untreated (UnTd)].

Siglec-4 Spacer Shows Comparable in vitro Functionality To CD8α Spacer in a CD20 CAR Model

Next, we investigated the cytotoxic potential of the novel constructs. We co-cultured CAR T cells for 5 h with $CD20^+$ Raji cells or CD20− HEK293T cells at an E:T ratio of 1:1. Effector function was assessed by determining degranulation and intracellular detection of the cytokine TNF-α in the transduced cells (gated on ΔLNGFR expression). Only CAR T cells co-cultured with $CD20^+$ target cells showed significant degranulation (Figure 4D). Strongest degranulation could be observed for the CD8α and Siglec-4 spacer variants with around 35% of CD107α positive cells. The Siglec-7.2 spacer CAR produced an intermediate amount of CD107α at 20% positive cells and the Siglec-8 variant had the lowest degranulation with only 10% positive cells but still more than the negative controls (Figure 4D). Similar to the degranulation analysis, the proportion of $\Delta LNGFR^+/TNF\text{-}\alpha^+$ cells was also highest in CD8α spacer CAR T cells (Figure 4E; 31%) but the CD20_hl_Sig4 CARs only displayed 18% of TNF-α positive cells, followed by Siglec-7.2 and Siglec-8 spacer CARs. Again, no unspecific activation could be observed in the controls.

We also assessed the activation state of the modified T cells by analyzing TIM3, LAG3, and PD1 surface expression. $CD20^+$ Raji cells were co-cultured with CAR T cells for 24 h at an E:T ratio of 1:2. The CD8α and Siglec-4 spacer CAR modified T cells contained the largest fraction of TIM3/LAG3/PD1 triple positive cells (Figure 4F). As the Siglec-7.2 and Siglec-8 spacer CAR T cells displayed lower degranulation and upregulation of activation markers after antigen engagement throughout these in vitro experiments, we decided to investigate only the Siglec-4 spacer in more detail.

The Siglec-4 Spacer CAR Displays High Functional Potency Against Membrane-Proximal Targets

In our $CD20^+$ Raji lymphoma model the Siglec-4 spacer CAR demonstrated a comparable in vitro functionality to the CD8α spacer CAR. As described above the Leu16 epitope is very proximal to the target cell membrane, making it more susceptible for engagement with long spacer CARs. From the CAR variants that could be efficiently expressed in T cells, the Siglec-

4 spacer was the only spacer with three C2-set Ig domains, agreeing with previous work that long spacers are excellent for targeting "short," membrane-proximal targets. To verify this hypothesis and to prove the robustness of the Siglec-4 spacer functionality, we assessed the Siglec-4 spacer CAR in an additional solid tumor model of pancreatic ductal adenocarcinoma (PDAC). We have recently identified CD66c and TSPAN8 as novel target candidates for cellular treatment of PDAC (Schäfer et al. manuscript under revision). These two target molecules are especially suitable for investigating our novel long spacer, as the scFv binding epitopes differ greatly in terms of membrane proximity.

TSPAN8 has two extracellular loops extending from the membrane that span 24 and 96 amino acids, respectively, the larger having two interconnecting disulfide bonds. Thus, the whole protein is very membrane proximal. On the other hand, CD66c is a glycophosphatidylinositol anchored protein and consists of two C2-set domains and one V-set domain. In consequence it extends further into the extracellular space compared to TSPAN8. In addition, the epitope of the aCD66c scFv is localized on the outer N terminal V-set domain. In summary, TSPAN8 can be considered a membrane proximal target, while CD66c is a membrane distal target.

We exchanged the Leu16 scFv from our CD20_hl_Sig4 CAR with the CD66c and TSPAN8 specific scFvs that were previously identified (Figure 5A) (Schäfer et al. manuscript under revision). Additionally, we incorporated in our experiments CD66c and TSPAN8 specific CD8α spacer CARs and a TSPAN8 specific IgG4 CH2-CH3 spacer CAR, which contained a 4/2 NQ mutation in the CH2 domain as well as a S → P substitution which has been reported to reduce FcR binding also in vivo (25), which was not the case for our IgG1 construct (25).

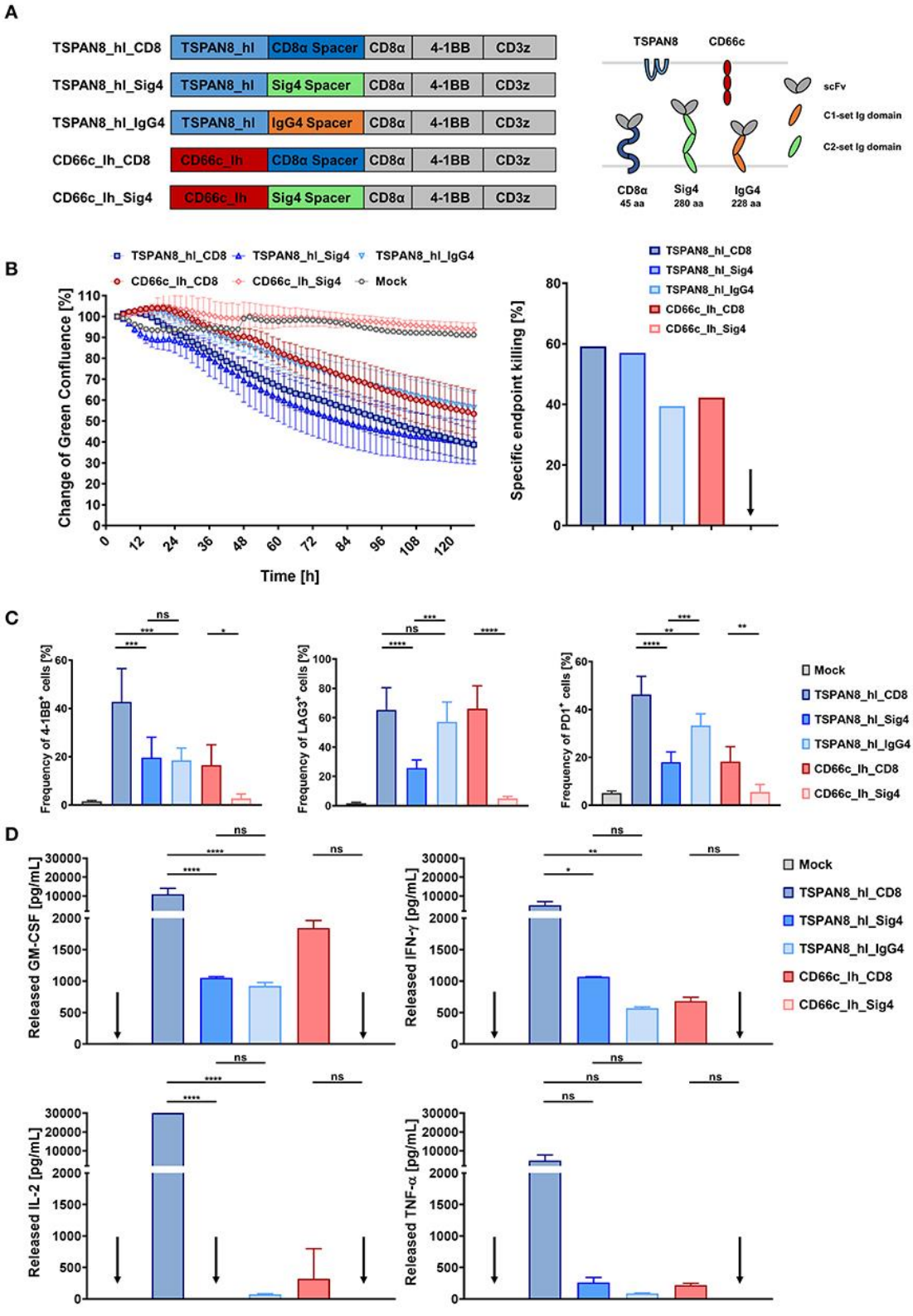

Figure 5. In vitro comparison of T cells transduced with TSPAN8 and CD66c CAR constructs, incorporating different spacer domains. (A) Structure of the TSPAN8 and CD66c CAR constructs with the Siglec spacers and extracellular domain comparison of the CAR constructs and target molecules. (B) Cytolytic kinetics and specific endpoint killing of AsPC1 target cells incubated with CAR T cells and Mock T cells from three different donors in effector to target ratios of 2:1. n = 6. (C) Frequency of 4-1BB, LAG3 and PD1 positive CAR T cells was analyzed at the end of the cytolytic evaluation with AsPC1 cells by flow cytometry. (D) GM-CSF, IFN-γ, IL-2, IL-6, and TNF-α production after 24 h of

co-culture of TSPAN8 or CD66c CAR T cells with AsPC1 cells from one donor assessed by flow cytometry. n = 2. Data from (B–D) were taken from the same experiment. Shown is the mean ± SD. ns > 0.05, *p < 0.05, **p < 0.01, ***p < 0.001, and ****p < 0.0001 [one-way ANOVA, multiple comparisons].

$CD66c^+/TSPAN8^+$ AsPC1 PDAC cells that were additionally modified to express GFP and luciferase were co-cultivated with CAR T cells specific for CD66c and TSPAN8 at an E:T ratio of 2:1 and analyzed using a fluorescent live cell analysis system. We assessed cytotoxicity as a decrease in green fluorescence surface area normalized to 2 h after co-inoculation. After 48 h, a supernatant sample was taken for cytokine quantitation while activation markers were measured at the end of the experiment (132 h).

Both, the CD66c_lh_Siglec-4 CAR T cells, as well as the untransduced control T cells showed no specific killing of target cells, while the CD66c_lh_CD8 CAR showed a specific endpoint killing of 42%, (Figure 5B). On the other hand, when targeting the membrane proximal TSPAN8, the Siglec-4 spacer CAR T cells showed a similar killing to that of the TSPAN8_hl_CD8α CAR T cells approaching 60% endpoint killing. In contrast, CAR T cells modified with a TSPAN8 CAR with the alternative long IgG4 CH2-CH3 spacer exhibited only 40% killing at the end of the experiment, showing the weakest cytotoxicity of all tested TSPAN8 CAR T cells. The CD66c_lh_Sig4 CAR T cells, which showed no cytotoxicity, also expressed no activation markers (Figure 5C). The strongest upregulation of activation markers 4-1BB, LAG3 and PD-1 was observed in TSPAN8_hl_CD8α CAR T cells. Interestingly, the TSPAN8 specific Siglec-4 CAR T cells displayed a lower expression of activation markers, even though the cytotoxicity equalled that of the CD8α spacer CAR T cells. This difference between the CD8α and the Siglec-4 spacer CAR T cells was even more striking at the cytokine level (Figure 5D). The TSPAN8_hl_CD8 CAR T cells released markedly higher levels of cytokines than the other CAR T cells. The TSPAN8_hl_Sig4 CAR T cells secreted cytokines at levels more similar to CD66c_lh_CD8 and TSPAN8_hl_IgG4 CAR T cells, which was very surprising, with regard to the same observed cytotoxicity as the TSPAN8 CD8α CAR T cells.

The Siglec-4 Spacer Is Highly Efficacious in an in vivo PDAC Model

Finally, we investigated the functionality of the three TSPAN8 specific CAR constructs in vivo in a pre-clinical PDAC tumor model. 1×10^6 AsPC1 $eGFP^+/Luc^+$ cells were injected subcutaneously in NSG mice. Tumor growth was measured non-invasively by BLI imaging and furthermore assessed by physical caliper measurement. When the first tumors reached a diameter of 25 mm2, treatment groups were randomized according to the BLI signal and tumor

size, and treatment was started by i.v. injection of 5×10^6 CAR T or untransduced Mock T cells (Figure 6A). Untransduced T cells did not display a therapeutic benefit over the untreated group (Figure 6B). All mice from these two groups had to be sacrificed before the end of the experiment as tumor ulcerations began to become established. The therapeutic effect for the CD8α and Siglec-4 CARs became apparent in BLI measurements from day 6 onwards. The tumor burden within the groups treated with the CD8α and Siglec-4 spacer CARs decreased in a comparable manner and reached baseline by the end of the experiment 29 days after T cell injection. At the same time, tumor growth was controlled by the IgG4 CH2-CH3 spacer group, but there was no tumor clearance as seen with the other groups. Persistence of CAR T cells could be demonstrated in the spleens of all CAR T cell treated groups with the highest amounts found in the CD8α spacer CAR and Siglec-4 spacer CAR groups (Figure 6C). A markedly lower amount of CAR T cells could be recovered from the IgG4 spacer CAR group. Interestingly, when the phenotype of the human T cells was examined the proportion of TCM was twice as high in CD4 and CD8 CAR T cells of the Siglec-4 spacer CAR group as compared to the CD8α spacer CAR T cells (Figure 6D).

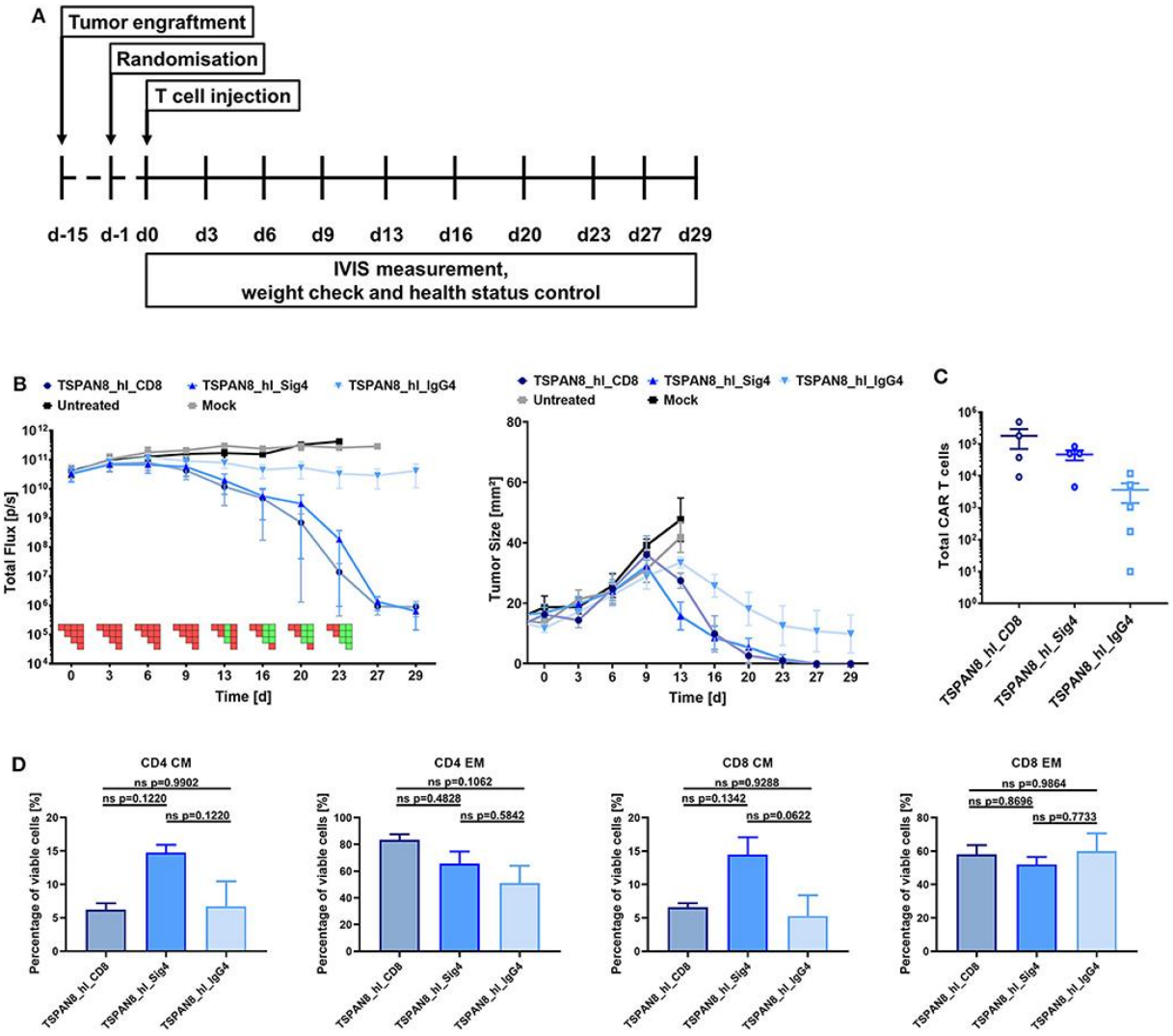

Figure 6. The TSPAN8 specific Siglec-4 spacer CAR T cells exhibit the same anti-tumor efficacy as the CD8α spacer CAR T cells, while retaining a more memory-like phenotype. (A) Overview of the study workflow. (B) Tumor burden and change in tumor size over time after TSPAN8 CAR T cell infusion. Untreated and Mock T cell treated animals served as controls, T cells from one donor were used. IgG4: n = 5; Sig4 and CD8α: n = 4. PSM $p < 0.05$ (green) [one-way ANOVA, multiple comparisons]. (C) Total number of CAR positive T cells recovered from spleens of TSPAN8 CAR-treated animals at the end of the experiment calculated after flow cytometric analysis. IgG4: n = 5; Sig4 and CD8α: n = 4. (D) CD4 and CD8 CAR^+ T cell phenotypes in the spleens of TSPAN8 CAR-treated animals analyzed at the end of the experiment by flow cytometry. n = 4.

Discussion

Despite the largely empirical design of CARs based on the functional principles of an antibody and the T cell receptor (TCR), CAR T cell therapies have demonstrated remarkable efficacy in the hematological tumor setting. Although a direct comparison of results across CAR T cell-based clinical trials is difficult due to the various differences in protocols, target antigens, co-stimulatory signaling, treatment regimen, patient groups and disease burden, the rough trend

can be observed that those receptors that incorporate a CD8α or CD28 spacer region in their architecture display better therapeutical efficacy than those that utilize IgG-based Fc domains (1–7, 28–31). Non-clinical studies investigating this effect suggest that the inferiority of IgG spacers is due to the engagement with FcγR-expressing myeloid cells (23) resulting in off-target activation of both gene-modified T cells and the respective $Fc\gamma R^+$ cells. In parallel, additional work has been demonstrating that the exemplary performance of CD8α or CD28 spacer CARs is partially also attributed to the epitope location on the targeted antigen CD19 and a number of studies have affirmed the postulate that membrane-proximal epitopes are best targeted by long spacer modules while membrane-distal epitopes are effectively recognized by CARs incorporating short spacer elements (18–22, 45).

In light of these developments, we identified a shortage of functional CAR spacer modules for membrane-proximal epitopes. Taking advantage of the well-described CD20 antigen and the membrane-proximal binding epitope of Leu16-derived anti-CD20 scFv (42), we sought to characterize the properties of CD8α- vs. IgG-based spacer CARs against CD20 *in vivo*. To avoid unintended cross-activation of CAR- and FcγR-expressing cells in the context of the IgG spacer, the amino acid sequence for IgG1-FcγR interactions in the IgG1-CH2 extracellular domain of the CAR was replaced by the corresponding IgG2 amino acids as described previously (23). However, contrary to reports describing increased anti-tumor activity and CAR T cell persistence following modifications in the IgG4 spacer to abrogate FcγR-binding in the CAR spacer domain (25, 27), we did not observe any *in vivo* therapeutic efficacy of IgG1 CAR T cells after similar modifications in our study. More specifically, the lack of efficacy was accompanied with an inefficient persistence of the gene-modified T cells. These results were in stark contrast to the functional capacity of the CD8α CAR T cells which – according to current understanding – display a less favorable receptor architecture due to the short spacer region. Although it is reasonable to conclude that the introduced mutations into the IgG spacer domain may not entirely abrogate FcγR binding, it cannot be ruled out that additional mechanisms are in play that sacrifice the therapeutic efficacy. For example, it has already been described that murine scFvs and other non-self gene products can elicit HLA-restricted T cell-mediated immune responses (3, 46, 47). Thus, the possibility exists that the introduced mutations into the Fc region can create immunogenic peptides by the T cell's antigen processing machinery which are then presented on the T cell's HLA and render the gene-modified lymphocytes susceptible to TCR-triggered fratricidal activity. Therefore, it is to be appreciated that the interplay of CAR T cells with their cognate counterparts and the immune system is complex and further work is required to understand the full immunogenic potential of CAR molecules.

To exclude the possibility of potential immunological barriers elicited by the spacer region, we switched our test system to the IgG4 backbone which was previously described to show *in vivo* performance (25, 27) and which has also shown successful translation to the clinic (34). In addition, a new set of spacer domains was designed based on the Siglec family whose members are expressed throughout the immune system and display evolutionary structural similarities to the constant region of immunoglobulins, but lack the inherent ability to interact with FcγRs (36). To determine systematically the optimal spacer length for the membrane-proximal CD20 epitope, five Siglec spacer CAR variants were generated incorporating either one, two or three Ig domains. Of note, different parent proteins were selected, as different Siglec molecules encompass distinct glycosylation patterns which are likely involved in modulating the protein's stability, flexibility, spatial architecture etc. and thus may have different effects on the CAR molecule. Moreover, in an attempt to maintain the original architecture of the molecule, the domains closest to the plasma membrane were selected. Consequently, the Siglec spacer regions within the otherwise identical CAR framework encompassed either a 114 amino acid (aa) Siglec-3, 119 aa Siglec-7, 127 aa Siglec-8, 203 aa Siglec-7, and 280 aa Siglec-4 spacer domain as opposed to the control 45 aa CD8α spacer domain.

Subsequent expression profiling revealed that not all Siglec spacer-based CARs were efficiently expressed on the T cell surface. In particular, Siglec-7.1 and Siglec-3 spacer CARs showed the lowest expression efficiency emphasizing the importance of the spacer region not only on the receptor's functionality but also on its optimal expression. In fact, Patel and colleagues have already described that the CAR spacer domain can affect the receptor's stability and modify its turnover rate (17). It is plausible that the glycosylation patterns present in Siglec-7.1 and Siglec-3 spacer CARs render the receptors less stable, in this way increasing the turnover kinetics and a decreased CAR detectability on the cell surface. Another potential reason for the inefficient expression of the Siglec-3 spacer CAR may lie in the C169S mutation which was introduced in order to abrogate unspecific disulfide bond formation as C169 is involved in an interdomain disulfide bond within the parent protein. Moreover, it is possible that the Siglec-3 C2-set domain *per-se* is instable when isolated from the membrane-distal V-set domain. Although a splice variant of CD33 has been described, which lacks the N-terminal domain ($CD33^{\Delta E2}$), these reports rely on mRNA analyses (48, 49). Protein-based detection using antibodies remains controversial, as it is still not clear whether a clone exists that can specifically recognize the Siglec-3 C2-set domain (49, 50). Importantly, using lentiviral transduction of His-tagged $CD33^{\Delta E2}$, Laszlo and colleagues have shown that the expression of the splice variant is also dependent on the cell type (49). In this context, HEK293T exhibited highest transgene

expression while hematopoietic cells displayed only low level expression of the truncated immune receptor which is in line with our observations on the expression of the Siglec-3 spacer CAR (Figures 4B,C).

In the next series of experiments, the three best expressed Siglec spacer CAR candidates were analyzed for their ability to induce T cell effector function upon antigen engagement. Consistent with previous reports (17–19, 25, 26, 51), our study provides evidence that the CAR spacer region can modulate the effector function of transgenic T cells. Intriguingly, however, we find that depending on the effector function analyzed, the functional hierarchy may vary. In particular with regard to cytotoxicity, no significant differences between the CD8α spacer (45 aa in length, no Ig domain) and Siglec-4 spacer (280 aa in length; three Ig domains) CAR can be observed while in terms of cytokine secretion the CD8α spacer CAR displays a significant dominance over other CAR constructs. Importantly, in addition to the CD20 system, this observation was further confirmed in the setting of another membrane-proximal antigen, TSPAN8, indicating a common functional feature for membrane-adjacent epitopes.

It has already been demonstrated in the TCR-context that distinct thresholds exist for the cytolytic machinery, the proliferative induction as well as the cytokine production system (52–56) and emerging work suggests similar principles for CAR-triggered T cells (26). The current study further supports this finding and the data obtained indicate that the nature of the spacer region can modulate the nature and degree of effector function. An alternative strategy has been described by Liu and colleagues (57) and Caruso and colleagues (58) in two independent studies, in which they demonstrate the ability of effector function fine-tuning through scFv affinity modulation. The clinical impact of such modifications was impressively demonstrated by Ghorashian and colleagues, who reported a better overall therapeutic profile of CD19 CAR T cell therapies in patients who received lower affinity CARs compared to the commonly used FMC63-scFv-based CARs (59). In particular, while the antileukemic activity was retained, the CAR T cells displayed an enhanced proliferative capacity and reduced severity of cytokine release syndrome (CRS). Though this clearly reveals the effectiveness of such an approach, scFv affinity modulation is a laborious undertaking and bears the risk to result in unwanted modifications to the target specificity. Therefore, fine tuning the chimeric receptor's spacer region provides a time-profitable option with a lower risk profile. More importantly, it further allows to create a variety of receptors with a range of signal transduction intensities independent of the binding domain.

Besides, based on the efficacy data obtained with the CD8α spacer (45 aa) vs. Siglec-4 spacer (280 aa) CARs targeting CD20 and TSPAN8, we find that the receptors' cytotoxic efficacy is not dominated by the spatial constraints of the CAR and its target epitope. This is significant as previous studies reporting such a trend were performed primarily in the context of IgG-derived sequences (25, 26, 51) and have not been compared extensively to spacers derived from other parental proteins. Thus, our work demonstrates that not only structural and spatial elements in CAR T cell:target cell interaction influence a receptor's bioactivity, but also additional factors are in play that are not entirely understood or fully considered yet. It is likely that e.g., CAR flexibility/rigidity and surface stability may have a greater relevance than previously assumed. For instance, Patel and colleagues have shown that the spacer domain can diminish a CAR's functionality by increasing its turnover rate (17). Thus, it is important to take into consideration that Ig domains as they are present in IgG and Siglec spacer domains display a distinct structural folding while the CD8α spacer is derived from a stalk connecting an Ig-like domain with the membrane. Attempts to resolve the structure of the CD8α hinge domain were of limited success so far, indicating the relative flexibility of this region (60). The Siglec-4 or the IgG spacers are missing this flexibility and in this way reduce targetable epitopes to the ones located in membrane proximity.

Another important aspect to be taken into consideration is the tendency of the CD8α stalk region to heterodimerize with CD8β, the subunit that contains raft-localizing determinants (61). As lipid rafts contain an accumulation of accessory molecules decisive for signal transduction and the intracellular CD8β domain has been described to promote association with the two crucial players Lck and LAT (62), it is likely that – in the context of cytotoxic T cells – the CD8α spacer region is capable of attenuating the effector function threshold by fostering interaction with downstream signaling molecules. These effects are absent in IgG- and Siglec-based spacers, so that the overall induction of T cell function is likely primarily guided by the number of triggered CAR molecules (Figure S5).

In support of the *in vitro* data, the Siglec-4 spacer CAR displayed a similar anti-tumor efficacy *in vivo* as the cognate CD8α spacer CAR against TSPAN8 and both therapies were superior to the IgG4-based spacer CAR treatment. Taking into account the length of the spacer regions (CD8α: 45aa; Siglec-4: 280 aa; IgG4: 228aa), we could not observe any obvious correlation with CAR potency and rather identified an intrinsic inferiority of the IgG4 spacer *in vivo*. However, in the context of the TSPAN8 targeting, the modified IgG4 spacer CAR showed a much better relative *in vivo* performance to the CD8α spacer compared to the IgG1 spacer

performance in the CD20 study. Indeed, the modified IgG4 spacer (25) has now demonstrated good efficacy in ongoing clinical studies (34) indicating that other factors in CAR design such as the scFv binding domain, transmembrane domain or the drug product formulation may also play a role in *in vivo* function and T cell persistence.

Strikingly, however, while the cytotoxic activity was comparable between the CD8α and Siglec-4 spacer CARs, we observed a reduced secretion of pro-inflammatory cytokines and an attenuated upregulation of activation/exhaustion markers such as 4-1BB, LAG3, and PD1 in the Siglec-4 spacer CAR T cells. Moreover, while the proliferative capacity of Siglec-4 CAR T cells was slightly lower compared to CD8α spacer CAR T cells, the Siglec-4 CAR-treated mice featured a trend toward a higher fraction of T_{CM} phenotype within the CAR T cell cohort which is associated with better overall remission and decreased likelihood of relapse in a clinical context.

It is currently widely established that CAR efficacy correlates closely with the development and severity of CRS in the clinic, an adverse event whose management has proven challenging in the clinical setting. Although tocilizumab and glucocorticoids have been described as effective intervention options, finding the right timing for their application represents a big hurdle (1, 63). In fact, too early intervention may jeopardize the therapeutic efficacy and increase the risk of relapse, while too late intervention bears the risk of CRS-induced multi-organ failure and irreversible neurotoxicities resulting in a patient's death (1, 3, 5, 7, 64–68). Thus, a treatment modality that retains the cytotoxic ability of currently approved CAR T cell therapies but attenuates the levels of secreted cytokines may turn engineered T cells not only into a reliable and effective, but also a safer platform. Moreover, a concomitant increase of the memory phenotype in the CAR T cell cohort of the patient holds promise to further increase the therapeutic efficacy while reducing life-threatening side effects.

Although the phenotype of Siglec-4 CAR modified T cells bodes well for future clinical application, what is the potential toxicity profile of this novel spacer structure? The parent protein Siglec-4, also known as myelin-associated glycoprotein (MAG), has been reported to be exclusively produced by myelinating glial cells such as oligodendrocytes in the central nervous system (CNS; 1% of total protein mass) and Schwann cells in the peripheral nervous system (PNS; 0.1% of total protein mass) (69, 70). Its specific expression on the innermost layer of myelin directly opposite to the axon surface supports its crucial role in the stabilization of axon-myelin interactions, the regulation of myelination, and the inhibition of axon regeneration after injury (71–73). These effects have been first described to be mediated by the

N-terminal V-set domain of the receptor, as determined by ligand specificity analyses, site-directed mutagenesis and analogy to the crystal structure of Siglec-1 (74–77). In our evaluation of homology studies, we found the protein sequence to be the best conserved among the Siglecs and within mammalian species. Indeed, the highest sequence homology was identified to lie within the first two N-terminal domains of Siglec-4 (78). Consequently, in order to abrogate these interactions, both N-terminal domains were excluded from our CAR spacer design.

More recent studies, however, suggest that an alternative binding domain exists that interacts with the Nogo receptor 1 and 2 (NgR1, NgR2), but not NgR3 (79–82). Deletion analysis demonstrated that while the first three Ig-like C2-set domains (amino acids 17-325) of Siglec-4 are involved in these interactions, C2-set domains 3-5 (amino acids 234-506) as they are present in our CAR architecture fail to associate with NgR1 or NgR2 (83) indicating that domains 1 and 2 are the major interaction partners. Interestingly, both a soluble and membrane-bound receptor construct comprising the C2-set domains 3-5 of Siglec-4 (amino acids 234-506) are still able to inhibit neurite outgrowth in the CNS, suggesting the existence of an as of yet unidentified ligand partner (83, 84). This observation may indicate the potential risk of unwanted interactions of the Siglec-4 spacer-based CAR T cells with this unknown binding partner. Although the CNS is an immune-privileged organ an intensive infiltration by CAR T cells has been shown to occur as a result of blood-brain-barrier (BBB) damage due to strong CRS. However, as Siglec-4 spacer CAR T cells appear to produce lower levels of cytokines, BBB disruption is expected to be mitigated, in this way minimizing CNS accessibility for CAR T cells.

In support of this hypothesis, despite the high homology between human and rodent Siglec-4 of 95% at the amino acid level over the entire extracellular domain (85, 86), we did not observe any toxicities in the mouse cohort receiving Siglec-4 spacer CAR therapy in our *in vivo* studies. Nevertheless, since - to the best of our knowledge - human-mouse cross-reactivity of Siglec-4 and its interaction partners has not been determined, these data need to be handled with care and further analysis is required to investigate the extent of potential side-effects of Siglec-4 spacer-based CAR T cells.

In summary, this study introduces the new class of Siglec CAR spacers, which structurally resemble IgG class spacers without their FcγR binding features. The Siglec-4 spacer proved to be as efficient as a conventional CD8α spacer in both *in vitro* and *in vivo* CAR function, but exhibited advantageous traits in terms of the T cell phenotype and CAR T cell cytokine release,

which make it an interesting candidate CAR structure to translate into future clinical applications.

Data Availability Statement

All datasets generated for this study are included in the article/Supplementary Material.

Ethics Statement

The studies involving human participants were reviewed and approved by German Red Cross Dortmund, University Hospital Cologne and German Red Cross Ulm. The patients/participants provided their written informed consent to participate in this study. The animal study was reviewed and approved by Landesamt für Natur, Umwelt, and Verbraucherschutz NRW, Approval numbers 84-02.04.2015.A168 and 84-02.04.2017.A021.

Author Contributions

RP designed the Siglec based spacers. DS and RP designed the Siglec spacer-based CARs. DS, JH, RP, WA, IJ, and OH designed the study. DS, JH, AS, JB, CB, DG, and WA conducted experiments. DS, JH, and RP wrote the manuscript with input from all authors. NM-T, RP, WA, IJ, and OH supervised the project. All authors discussed the data and reviewed the manuscript.

Conflict of Interest

DS, JH, RP, JB, NM-T, CB, DG, WA, IJ, and OH are employees of Miltenyi Biotec B.V. & Co. KG. Patent applications are pending to this work.

The remaining author declares that the research was conducted in the absence of any commercial or financial relationships that could be construed as a potential conflict of interest.

Acknowledgments

We would like to acknowledge Andrew Kaiser and Dina Schneider for helpful discussions, Dina Schneider for providing the CD8 CAR construct, Hinrich Abken for providing the IgG1 CAR construct, and Dominik Lock for the eGFP/ffLuc transfer vector plasmid.

Supplementary Material

The Supplementary Material for this article can be found online at: https://www.frontiersin.org/articles/10.3389/fimmu.2020.01704/full#supplementary-material

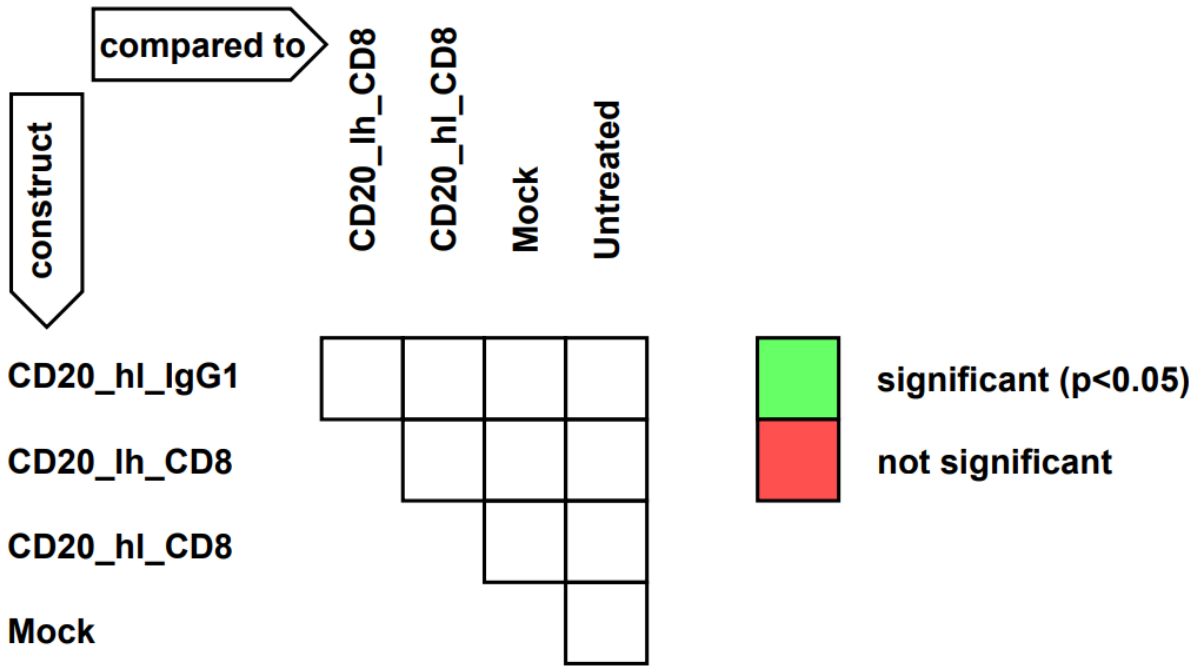

Figure S1: Organization of the pairwise significant matrix for group comparison of in vivo performance of CD20_hl_IgG1, CD20_lh_CD8, CD20_hl_CD8, Untreated and Mock. PSM $p<0.05$ (green) [one-way ANOVA, multiple comparisons].

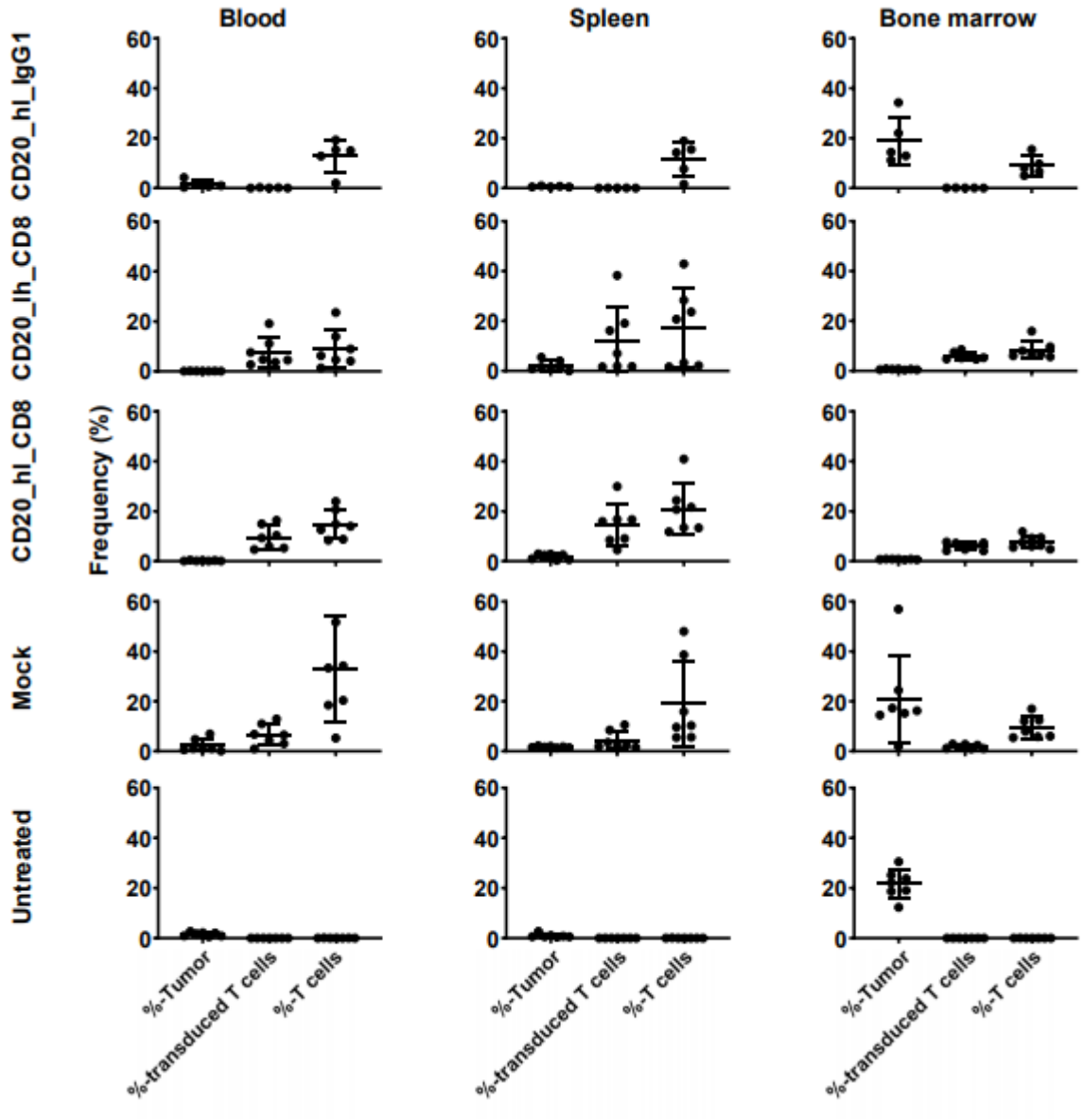

Figure S2: Flow cytometry analysis of tumor and CD20 CAR T cells persistence in blood, spleen and bone marrow. Ex vivo analyses were performed at the endpoint of the study. Percentage of transduced T cells in the Mock group was calculated based on GFP expression. n = 5 – 6.

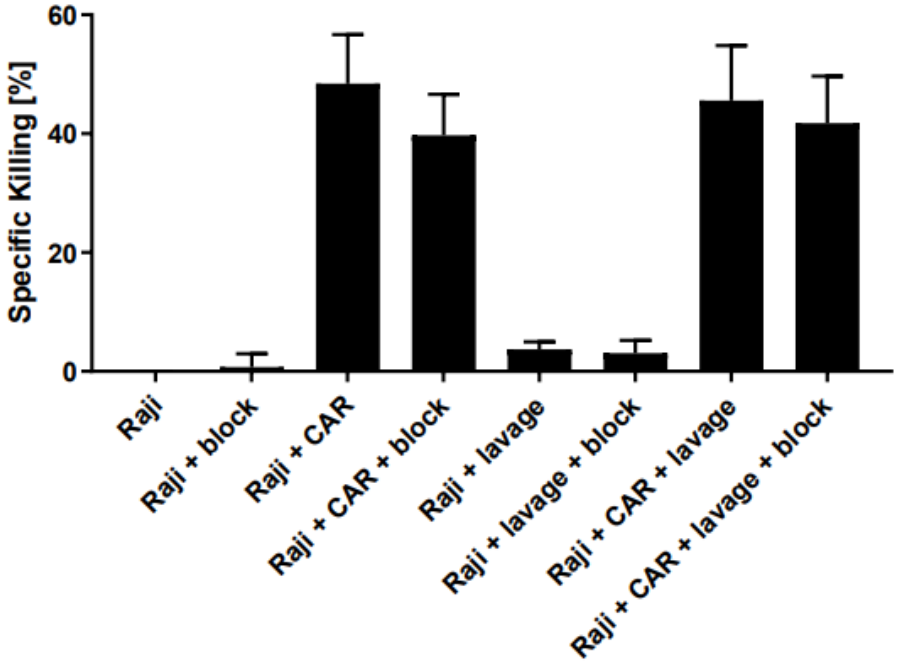

Figure S3: Macrophages do not inhibit the function of CAR T cells containing an IgG1 spacer with mutated Fc-binding sites. CD20_hl_IgG1 CAR T cells were mixed in a 1:1:1 ratio with Raji target cells and NSG macrophages, derived from a peritoneal lavage. Macrophages, tumor and CAR T cells were co-incubated for 24 hours in absence or presence of murine FcR-blocking reagent (block). n = 3.

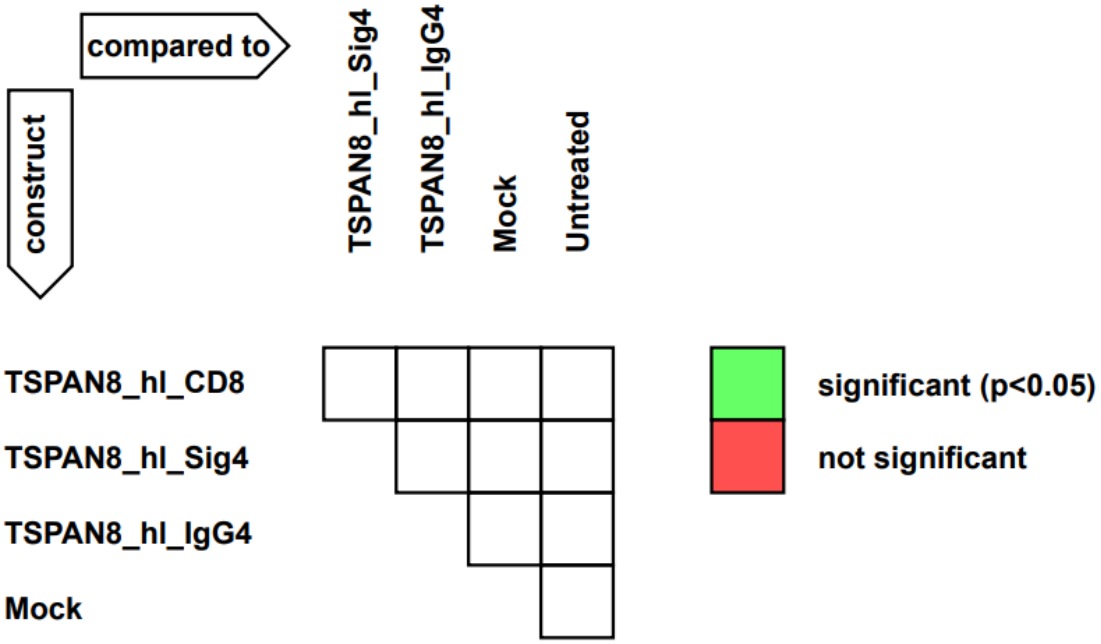

Figure S4: Organization of the pairwise significant matrix for group comparison of in vivo performance of TSPAN8_hl_CD8, TSPAN8_hl_Sig4, TSPAN8_hl_IgG4, Untreated and Mock. PSM p<0.05 (green) [one-way ANOVA, multiple comparisons].

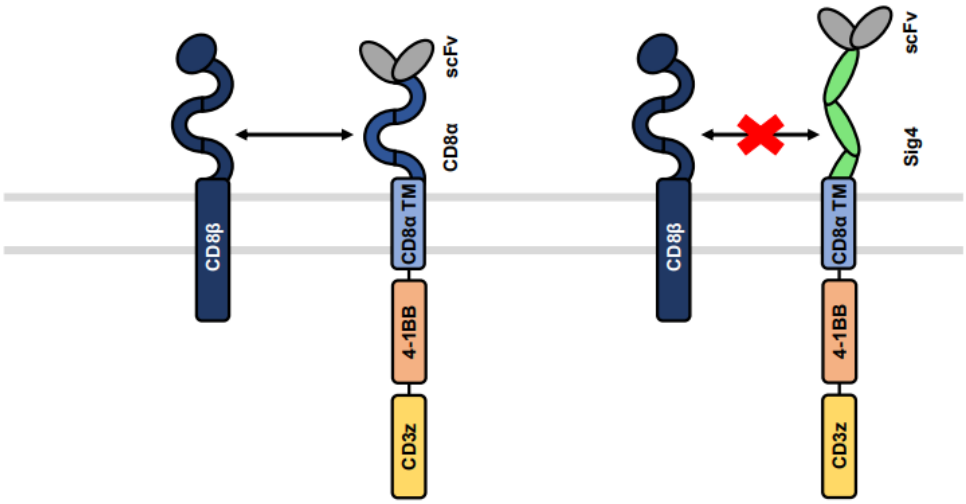

Figure S5: Schematic model of spacer dimerization with natural CD8β leading to increased signaling.

References

1. Lee DW, Kochenderfer JN, Stetler-Stevenson M, Cui YK, Delbrook C, Feldman SA, et al. T cells expressing CD19 chimeric antigen receptors for acute lymphoblastic leukaemia in children and young adults: a phase 1 dose-escalation trial. *Lancet*. (2015) 385:517–28. doi: 10.1016/S0140-6736(14)61403-3

2. Porter DL, Hwang WT, Frey NV, Lacey SF, Shaw PA, Loren AW, et al. Chimeric antigen receptor T cells persist and induce sustained remissions in relapsed refractory chronic lymphocytic leukemia. *Sci Transl Med*. (2015) 7:303ra139. doi: 10.1126/scitranslmed.aac5415

3. Turtle CJ, Hanafi L-A, Berger C, Gooley TA, Cherian S, Hudecek M, et al. CD19 CAR-T cells of defined CD4+:CD8+ composition in adult B cell ALL patients. *J Clin Investig*. (2016) 126:2123–38. doi: 10.1172/JCI85309

4. Neelapu SS, Locke FL, Bartlett NL, Lekakis LJ, Miklos DB, Jacobson CA, et al. Axicabtagene ciloleucel CAR T-cell therapy in refractory large B-cell lymphoma. *N Engl J Med*. (2017) 377:2531–44. doi: 10.1056/NEJMoa1707447

5. Schuster SJ, Svoboda J, Chong EA, Nasta SD, Mato AR, Anak Ö, et al. Chimeric antigen receptor t cells in refractory B-cell lymphomas. *N Engl J Med*. (2017) 377:2545–54. doi: 10.1056/NEJMoa1708566

6. Maude SL, Laetsch TW, Buechner J, Rives S, Boyer M, Bittencourt H, et al. Tisagenlecleucel in children and young adults with B-cell lymphoblastic leukemia. *N Engl J Med*. (2018) 378:439–48. doi: 10.1056/NEJMoa1709866

7. Park JH, Rivière I, Gonen M, Wang X, Sénéchal B, Curran KJ, et al. Long-term follow-up of CD19 CAR therapy in acute lymphoblastic leukemia. *N Engl J Med*. (2018) 378:449–59. doi: 10.1056/NEJMoa1709919

8. Gross G, Waks T, Eshhar Z. Expression of immunoglobulin-T-cell receptor chimeric molecules as functional receptors with antibody-type specificity. *Proc Natl Acad Sci USA*. (1989) 86:10024–8. doi: 10.1073/pnas.86.24.10024

9. Moritz D, Groner B. A spacer region between the single chain antibody- and the CD3 zeta-chain domain of chimeric T cell receptor components is required for efficient ligand binding and signaling activity. *Gene Therap*. (1995) 2:539–46.

10. Darcy PK, Kershaw MH, Trapani JA, Smyth MJ. Expression in cytotoxic T lymphocytes of a single-chain anti-carcinoembryonic antigen antibody. Redirected Fas ligand-mediated lysis of colon carcinoma. *Euro J Immunol*. (1998) 28:1663–72. doi: 10.1002/sici1521-414119980528:051663::aid-immu16633.0.co;2-l

11. Eshhar Z, Waks T, Bendavid A, Schindler DG. Functional expression of chimeric receptor genes in human T cells. *J Immunol Methods*. (2001) 248:67–76. doi: 10.1016/s0022-17590000343-4

12. Niederman TMJ, Ghogawala Z, Carter BS, Tompkins HS, Russell MM, Mulligan RC. Antitumor activity of cytotoxic T lymphocytes engineered to target vascular endothelial growth factor receptors. *Proc Natl Acad Sci*. (2002) 99:7009–14. doi: 10.1073/pnas.092562399

13. Zhang L, Lizzio EF, Chen T, Kozlowski S. Peptide immunization excludes antigen-specific T cells from splenic lymphoid compartments. *Euro J Immunol*. (2005) 35:776–85. doi: 10.1002/eji.200425479

14. Morgenroth A, Cartellieri M, Schmitz M, Günes S, Weigle B, Bachmann M, et al. Targeting of tumor cells expressing the prostate stem cell antigen. (PSCA) using genetically engineered T-cells. *Prostate*. (2007) 67:1121–31. doi: 10.1002/pros.20608

15. Zhang H, Snyder KM, Suhoski MM, Maus MV, Kapoor V, June CH, et al. 4-1BB is superior to CD28 costimulation for generating $CD8^+$ cytotoxic lymphocytes for adoptive immunotherapy. *J Immunol*. (2007) 179:4910–8. doi: 10.4049/jimmunol.179.7.4910

16. Barber A, Zhang T, Megli CJ, Wu J, Meehan KR, Sentman CL. Chimeric NKG2D receptor-expressing T cells as an immunotherapy for multiple myeloma. *Exp Hematol*. (2008) 36:1318–28. doi: 10.1016/j.exphem.2008.04.010

17. Patel SD, Moskalenko M, Smith D, Maske B, Finer MH, McArthur JG. Impact of chimeric immune receptor extracellular protein domains on T cell function. *Gene Therap*. (1999) 6:412–9. doi: 10.1038/sj.gt.3300831

18. Guest RD, Hawkins RE, Kirillova N, Cheadle EJ, Arnold J, O'Neill A, et al. The role of extracellular spacer regions in the optimal design of chimeric immune receptors: evaluation of four different scfvs and antigens. *J Immunother*. (2005) 28:203–11. doi: 10.1097/01.cji.0000161397.96582.59

19. Haso W, Lee DW, Shah NN, Stetler-Stevenson M, Yuan CM, Pastan IH, et al. Anti-CD22-chimeric antigen receptors targeting B-cell precursor acute lymphoblastic leukemia. *Blood*. (2013) 121:1165–74. doi: 10.1182/blood-2012-06-438002

20. Hudecek M, Lupo-Stanghellini M-T, Kosasih PL, Sommermeyer D, Jensen MC, Rader C, et al. Receptor affinity and extracellular domain modifications affect tumor recognition by ROR1-specific chimeric antigen receptor T cells. *Clin Cancer Res*. (2013) 19:3153–64. doi: 10.1158/1078-0432.CCR-13-0330

21. James SE, Greenberg PD, Jensen MC, Lin Y, Wang J, Till BG, et al. Antigen sensitivity of CD22-specific chimeric TCR is modulated by target epitope distance from the cell membrane. *J Immunol*. (2008) 180:7028–38. doi: 10.4049/jimmunol.180.10.7028

22. Krenciute G, Krebs S, Torres D, Wu M-F, Liu H, Dotti G, et al. Characterization and functional analysis of scFv-based chimeric antigen receptors to redirect T cells to IL13Rα2-positive glioma. *Mol Thera*. (2016) 24:354–63. doi: 10.1038/mt.2015.199

23. Hombach A, Hombach AA, Abken H. Adoptive immunotherapy with genetically engineered T cells: modification of the IgG1 Fc 'spacer' domain in the extracellular moiety of chimeric antigen receptors avoids 'off-target' activation and unintended initiation of an innate immune response. *Gene Thera*. (2010) 17:1206–13. doi: 10.1038/gt.2010.91

24. Almåsbak H, Walseng E, Kristian A, Myhre MR, Suso EM, Munthe LA, et al. Inclusion of an IgG1-Fc spacer abrogates efficacy of CD19 CAR T cells in a xenograft mouse model. *Gene Thera*. (2015) 22:391–403. doi: 10.1038/gt.2015.4

25. Hudecek M, Sommermeyer D, Kosasih PL, Silva-Benedict A, Liu L, Rader C, et al. The nonsignaling extracellular spacer domain of chimeric antigen receptors is decisive for *in vivo* antitumor activity. *Cancer Immunol Res*. (2015) 3:125–35. doi: 10.1158/2326-6066.CIR-14-0127

26. Watanabe N, Bajgain P, Sukumaran S, Ansari S, Heslop HE, Rooney CM, et al. Fine-tuning the CAR spacer improves T-cell potency. *Oncoimmunology*. (2016) 5:e1253656. doi: 10.1080/2162402X.2016.1253656

27. Jonnalagadda M, Mardiros A, Urak R, Wang X, Hoffman LJ, Bernanke A, et al. Chimeric antigen receptors with mutated IgG4 Fc spacer avoid fc receptor binding and improve T cell persistence and antitumor efficacy. *Mol Thera*. (2015) 23:757–68. doi: 10.1038/mt.2014.208

28. Jensen MC, Popplewell L, Cooper LJ, DiGiusto D, Kalos M, Ostberg JR, et al. Antitransgene rejection responses contribute to attenuated persistence of adoptively transferred CD20/CD19-specific chimeric antigen receptor redirected T cells in humans. *Biol Blood Marrow Transplant*. (2010) 16:1245–56. doi: 10.1016/j.bbmt.2010.03.014

29. Savoldo B, Ramos CA, Liu E, Mims MP, Keating MJ, Carrum G, et al. CD28 costimulation improves expansion and persistence of chimeric antigen receptor-modified T cells in lymphoma patients. *J Clin Investig*. (2011) 121:1822–6. doi: 10.1172/JCI46110

30. Till BG, Jensen MC, Wang J, Qian X, Gopal AK, Maloney DG, et al. CD20-specific adoptive immunotherapy for lymphoma using a chimeric antigen receptor with both CD28 and 4-1BB domains: pilot clinical trial results. *Blood*. (2012) 119:3940–50. doi: 10.1182/blood-2011-10-387969

31. Gargett T, Yu W, Dotti G, Yvon ES, Christo SN, Hayball JD, et al. GD2-specific CAR T cells undergo potent activation and deletion following antigen encounter but can be protected from activation-induced cell death by PD-1 blockade. *Mol Therap*. (2016) 24:1135–49. doi: 10.1038/mt.2016.63

32. Brown CE, Alizadeh D, Starr R, Weng L, Wagner JR, Naranjo A, et al. Regression of glioblastoma after chimeric antigen receptor T-cell therapy. *N Engl J Med*. (2016) 375:2561–9. doi: 10.1056/NEJMoa1610497

33. Wang X, Popplewell LL, Wagner JR, Naranjo A, Blanchard MS, Mott MR, et al. Phase 1 studies of central memory–derived CD19 CAR T–cell therapy following autologous HSCT in patients with B-cell NHL. *Blood*. (2016) 127:2980–90. doi: 10.1182/blood-2015-12-686725

34. Abramson JS, Palomba ML, Gordon LI, Lunning MA, Wang ML, Arnason JE, et al. Pivotal safety and efficacy results from transcend NHL 001, a multicenter phase 1 study of lisocabtagene maraleucel (liso-cel) in relapsed/refractory (R/R) large B cell lymphomas. *Blood.* (2019) 134(Suppl.1):241. doi: 10.1182/blood-2019-127508

35. Crocker PR, Varki A. Siglecs, sialic acids and innate immunity. *Trends Immunol*. (2001) 22:337–42. doi: 10.1016/s1471-4906(01)01930-5

36. Crocker PR, Paulson JC, Varki A. Siglecs and their roles in the immune system. *Nat Rev Immunol*. (2007) 7:255–66. doi: 10.1038/nri2056

37. Jensen M, Tan G, Forman S, Wu AM, Raubitschek A. CD20 is a molecular target for scFvFc:zeta receptor redirected T cells: implications for cellular immunotherapy of CD20+ malignancy. *Biol Blood Marrow Transplant*. (1998) 4:75–83. doi: 10.1053/bbmt.1998.v4.pm9763110

38. Apel M, Brüning M, Granzin M, Essl M, Stuth J, Blaschke J, et al. Integrated clinical scale manufacturing system for cellular products derived by magnetic cell separation, centrifugation and cell culture. *Chem Ingen Tech.* (2013) 85:103–10. doi: 10.1002/cite.201200175

39. Lock D, Mockel-Tenbrinck N, Drechsel K, Barth C, Mauer D, Schaser T, et al. Automated manufacturing of potent CD20-directed chimeric antigen receptor t cells for clinical use. *Hum Gene Ther*. (2017) 28:914–25. doi: 10.1089/hum.2017.111

40. Al Rawashdeh W, Zuo S, Melle A, Appold L, Koletnik S, Tsvetkova Y, et al. Noninvasive assessment of elimination and retention using CT-FMT and kinetic whole-body modeling. *Theranostics.* (2017) 7:1499–510. doi: 10.7150/thno.17263

41. Till BG, Jensen MC, Wang J, Chen EY, Wood BL, Greisman HA, et al. Adoptive immunotherapy for indolent non-hodgkin lymphoma and mantle cell lymphoma using genetically modified autologous CD20-specific T cells. *Blood*. (2008) 112:2261–71. doi: 10.1182/blood-2007-12-128843

42. Polyak MJ, Deans JP. Alanine-170 and proline-172 are critical determinants for extracellular CD20 epitopes; heterogeneity in the fine specificity of CD20 monoclonal antibodies is defined by additional requirements imposed by both amino acid sequence and quaternary structure. *Blood*. (2002) 99:3256–62. doi: 10.1182/blood.v99.9.3256

43. Macauley MS, Crocker PR, Paulson JC. Siglec-mediated regulation of immune cell function in disease. *Nat Rev Immunol*. (2014) 14:653–66. doi: 10.1038/nri3737

44. Bornhöfft KF, Goldammer T, Rebl A, Galuska SP. Siglecs: a journey through the evolution of sialic acid-binding immunoglobulin-type lectins. *Dev Comparat Immunol*. (2018) 86:219–31. doi: 10.1016/j.dci.2018.05.008

45. Srivastava S, Riddell SR. Engineering CAR-T cells: design concepts. *Trends Immunol*. (2015) 36:494–502. doi: 10.1016/j.it.2015.06.004

46. Riddell SR, Elliott M, Lewinsohn DA, Gilbert MJ, Wilson L, Manley SA, et al. T-cell mediated rejection of gene-modified HIV-specific cytotoxic T lymphocytes in HIV-infected patients. *Nat Med*. (1996) 2:216–23. doi: 10.1038/nm0296-216

47. Berger C, Flowers ME, Warren EH, Riddell SR. Analysis of transgene-specific immune responses that limit the *in vivo* persistence of adoptively transferred HSV-TK-modified donor T cells after allogeneic hematopoietic cell transplantation. *Blood*. (2006) 107:2294–302. doi: 10.1182/blood-2005-08-3503

48. Hernández-Caselles T, Martínez-Esparza M, Pérez-Oliva AB, Quintanilla-Cecconi AM, García-Alonso A, Alvarez-López DMR, et al. A study of CD33. (SIGLEC-3) antigen expression and function on activated human T and NK cells: two isoforms of CD33 are generated by alternative splicing. *J Leukocyte Biol*. (2006) 79:46–58. doi: 10.1189/jlb.0205096

49. Laszlo GS, Harrington KH, Gudgeon CJ, Beddoe ME, Fitzgibbon MP, Ries RE, et al. Expression and functional characterization of CD33 transcript variants in human acute myeloid leukemia. *Oncotarget*. (2016) 7:43281–94. doi: 10.18632/oncotarget.9674

50. Pérez-Oliva AB, Martínez-Esparza M, Vicente-Fernández JJ, Corral-San Miguel R, García-Peñarrubia P, Hernández-Caselles T. Epitope mapping, expression and post-translational modifications of two isoforms of CD33 (CD33M and CD33m) on lymphoid and myeloid human cells. *Glycobiology.* (2011) 21:757–70. doi: 10.1093/glycob/cwq220

51. Künkele A, Johnson AJ, Rolczynski LS, Chang CA, Hoglund V, Kelly-Spratt KS, et al. Functional tuning of CARs reveals signaling threshold above which CD8+ CTL antitumor potency is attenuated due to cell Fas-FasL-dependent AICD. *Cancer Immunol Res*. (2015) 3:368–79. doi: 10.1158/2326-6066.CIR-14-0200

52. Valitutti S, Müller S, Dessing M, Lanzavecchia A. Signal extinction and T cell repolarization in T helper cell-antigen-presenting cell conjugates. *Euro J Immunol*. (1996) 26:2012–6. doi: 10.1002/eji.1830260907

53. Itoh Y, Germain RN. Single cell analysis reveals regulated hierarchical T cell antigen receptor signaling thresholds and intraclonal heterogeneity for individual cytokine responses of CD4+ T cells. *J Exp Med*. (1997) 186:757–66. doi: 10.1084/jem.186.5.757

54. Hemmer B, Vergelli M, Gran B, Ling N, Conlon P, Pinilla C, et al. Predictable TCR antigen recognition based on peptide scans leads to the identification of agonist ligands with no sequence homology. *J Immunol*. (1998) 160:3631–6

55. Auphan-Anezin N, Verdeil G, Schmitt-Verhulst A-M. Distinct thresholds for CD8 T cell activation lead to functional heterogeneity: CD8 T cell priming can occur independently of cell division. *J Immunol.* (2003) 170:2442–8. doi: 10.4049/jimmunol.170.5.2442

56. Faroudi M, Zaru R, Paulet P, Müller S, Valitutti S. Cutting edge: T lymphocyte activation by repeated immunological synapse formation and intermittent signaling. *J Immunol.* (2003) 171:1128–32. doi: 10.4049/jimmunol.171.3.1128

57. Liu Z, Gerner MY, Van Panhuys N, Levine AG, Rudensky AY, Germain RN. Immune homeostasis enforced by co-localized effector and regulatory T cells. *Nature*. (2015) 528:225–30. doi: 10.1038/nature16169

58. Caruso HG, Hurton LV, Najjar A, Rushworth D, Ang S, Olivares S, et al. Tuning sensitivity of CAR to EGFR density limits recognition of normal tissue while maintaining potent antitumor activity. *Cancer Res*. (2015) 75:3505–18. doi: 10.1158/0008-5472.can-15-0139

59. Ghorashian S, Kramer AM, Onuoha S, Wright G, Bartram J, Richardson R, et al. Enhanced CAR T cell expansion and prolonged persistence in pediatric patients with ALL treated with a low-affinity CD19 CAR. *Nat Med*. (2019) 25:1408–14. doi: 10.1038/s41591-019-0549-5

60. Leahy DJ, Axel R, Hendrickson WA. Crystal structure of a soluble form of the human T cell coreceptor CD8 at 2.6 a resolution. *Cell.* (1992) 68:1145–62. doi: 10.1016/0092-8674(92)90085-q

61. Pang S, Zhang L, Wang H, Yi Z, Li L, Gao L, et al. CD8(+) T cells specific for beta cells encounter their cognate antigens in the islets of NOD mice. *Euro J Immunol*. (2009) 39:2716–24. doi: 10.1002/eji.200939408

62. Bosselut R, Kubo S, Guinter T, Kopacz JL, Altman JD, Feigenbaum L, et al. Role of CD8β domains in CD8 coreceptor function: importance for MHC I binding, signaling, and positive selection of CD8+ T cells in the thymus. *Immunity*. (2000) 12:409–18. doi: 10.1016/S1074-7613(00)80193-4

63. Brudno JN, Kochenderfer JN. Toxicities of chimeric antigen receptor T cells: recognition and management. *Blood*. (2016) 127:3321–30. doi: 10.1182/blood-2016-04-703751

64. Brentjens RJ, Davila ML, Riviere I, Park J, Wang X, Cowell LG, et al. CD19-targeted T cells rapidly induce molecular remissions in adults with chemotherapy-refractory acute lymphoblastic leukemia. *Sci Transl Med.* (2013) 5:177ra138. doi: 10.1126/scitranslmed.3005930

65. Grupp SA, Kalos M, Barrett D, Aplenc R, Porter DL, Rheingold SR, et al. Chimeric antigen receptor-modified T cells for acute lymphoid leukemia. *N Engl J Med*. (2013) 368:1509–18. doi: 10.1056/NEJMoa1215134

66. Maude SL, Barrett D, Teachey DT, Grupp SA. Managing cytokine release syndrome associated with novel T cell-engaging therapies. *Cancer J.* (2014) 20:119–22. doi: 10.1097/PPO.0000000000000035

67. Kochenderfer JN, Dudley ME, Kassim SH, Somerville RP, Carpenter RO, Stetler-Stevenson M, et al. Chemotherapy-refractory diffuse large B-cell lymphoma and indolent B-cell malignancies can be effectively treated with autologous T cells expressing an anti-CD19 chimeric antigen receptor. *J Clin Oncol*. (2015) 33:540–9. doi: 10.1200/jco.2014.56.2025

68. Hay KA, Hanafi L-A, Li D, Gust J, Liles WC, Wurfel MM, et al. Kinetics and biomarkers of severe cytokine release syndrome after CD19 chimeric antigen receptor-modified T-cell therapy. *Blood*. (2017) 130:2295–306. doi: 10.1182/blood-2017-06-793141

69. Bartsch U, Kirchhoff F, Schachner M. Immunohistological localization of the adhesion molecules L1, N-CAM, and MAG in the developing and adult optic nerve of mice. *J Comparat Neurol*. (1989) 284:451–62. doi: 10.1002/cne.902840310

70. Trapp BD, Andrews SB, Cootauco C, Quarles R. The myelin-associated glycoprotein is enriched in multivesicular bodies and periaxonal membranes of actively myelinating oligodendrocytes. *J Cell Biol*. (1989) 109:2417–26. doi: 10.1083/jcb.109.5.2417

71. McKerracher L, David S, Jackson DL, Kottis V, Dunn RJ, Braun PE. Identification of myelin-associated glycoprotein as a major myelin-derived inhibitor of neurite growth. *Neuron*. (1994) 13:805–11. doi: 10.1016/0896-6273(94)90247-x

72. Mukhopadhyay G, Doherty P, Walsh FS, Crocker PR, Filbin MT. A novel role for myelin-associated glycoprotein as an inhibitor of axonal regeneration. *Neuron*. (1994) 13:757–67. doi: 10.1016/0896-62739490042-6

73. Schachner M, Bartsch U. Multiple functions of the myelin-associated glycoprotein MAG (siglec-4a) in formation and maintenance of myelin. *Glia*. (2000) 29:154–65. doi: 10.1002/sici1098-11362000011529:2154::aid-glia93.0.co;2-3

74. Collins BE, Ito H, Sawada N, Ishida H, Kiso M, Schnaar RL. Enhanced binding of the neural siglecs, myelin-associated glycoprotein and Schwann cell myelin protein, to Chol-1 (alpha-series) gangliosides and novel sulfated Chol-1 analogs. *J Biol Chem*. (1999) 274:37637–43. doi: 10.1074/jbc.274.53.37637

75. Tang S, Shen YJ, DeBellard ME, Mukhopadhyay G, Salzer JL, Crocker PR, et al. Myelin-associated glycoprotein interacts with neurons via a sialic acid binding site at ARG118 and a distinct neurite inhibition site. *J Cell Biol*. (1997) 138:1355–66. doi: 10.1083/jcb.138.6.1355

76. May AP, Robinson RC, Vinson M, Crocker PR, Jones EY. Crystal structure of the N-terminal domain of sialoadhesin in complex with 3' sialyllactose at 1.85 A resolution. *Mol Cell*. (1998) 1:719–28. doi: 10.1016/s1097-2765(00)80071-4

77. Zaccai NR, Maenaka K, Maenaka T, Crocker PR, Brossmer R, Kelm S, et al. Structure-guided design of sialic acid-based siglec inhibitors and crystallographic analysis in complex with sialoadhesin. *Structure*. (2003) 11:557–67. doi: 10.1016/s0969-2126(03)00073-x

78. Lehmann F, Gäthje H, Kelm S, Dietz F. Evolution of sialic acid–binding proteins: molecular cloning and expression of fish siglec-4. *Glycobiology*. (2004) 14:959–68. doi: 10.1093/glycob/cwh120

79. Domeniconi M, Cao Z, Spencer T, Sivasankaran R, Wang K, Nikulina E, et al. Myelin-associated glycoprotein interacts with the Nogo66 receptor to inhibit neurite outgrowth. *Neuron*. (2002) 35:283–90. doi: 10.1016/s0896-6273(02)00770-5

80. Liu BP, Fournier A, GrandPré T, Strittmatter SM. Myelin-associated glycoprotein as a functional ligand for the Nogo-66 receptor. *Science*. (2002) 297:1190–3. doi: 10.1126/science.1073031

81. Venkatesh K, Chivatakarn O, Lee H, Joshi PS, Kantor DB, Newman BA, et al. The Nogo-66 receptor homolog NgR2 is a sialic acid-dependent receptor selective for myelin-associated glycoprotein. *J Neurosci*. (2005) 25:808–22. doi: 10.1523/jneurosci.4464-04.2005

82. Atwal JK, Pinkston-Gosse J, Syken J, Stawicki S, Wu Y, Shatz C, et al. PirB is a functional receptor for myelin inhibitors of axonal regeneration. *Science*. (2008) 322:967. doi: 10.1126/science.1161151

83. Robak LA, Venkatesh K, Lee H, Raiker SJ, Duan Y, Lee-Osbourne J, et al. Molecular basis of the interactions of the Nogo-66 receptor and its homolog NgR2 with myelin-associated glycoprotein: development of NgROMNI-Fc, a novel antagonist of CNS myelin inhibition. *J Neurosci*. (2009) 29:5768–83. doi: 10.1523/JNEUROSCI.4935-08.2009

84. Cao Z, Qiu J, Domeniconi M, Hou J, Bryson JB, Mellado W, et al. The inhibition site on myelin-associated glycoprotein is within Ig-domain 5 and is distinct from the sialic acid binding site. *J Neurosci*. (2007) 27:9146–54. doi: 10.1523/jneurosci.2404-07.2007

85. Arquint M, Roder J, Chia LS, Down J, Wilkinson D, Bayley H, et al. Molecular cloning and primary structure of myelin-associated glycoprotein. *Proc Natl Acad Sci USA*. (1987) 84:600–4. doi: 10.1073/pnas.84.2.600

86. Lai C, Brow MA, Nave KA, Noronha AB, Quarles RH, Bloom FE, et al. Two forms of 1B236/myelin-associated glycoprotein, a cell adhesion molecule for postnatal neural development, are produced by alternative splicing. *Proc Natl Acad Sci USA*. (1987) 84:4337–41. doi: 10.1073/pnas.84.12.4337

SUMMARY CHAPTER 2

MULTIMODAL IMAGING OF CAR T CELLS USING BIOLUMINESCENCE TOMOGRAPHY AND LIGHT-SHEET MICROSCOPY REVEALS NEGATIVE EFFECTS OF LOCAL INTERLEUKIN-2

In this manuscript, we tracked CAR T cells in vivo and ex vivo in a subcutaneous PDAC xenograft model to gain spatial-temporal information about CAR T cell biodistribution and localization within the tumor. Recently established mutated click beetle luciferase (CBR2opt) was incorporated into two CAR constructs for direct cell labeling. One construct was redirected against epidermal growth factor receptor (EGFR) present on AsPC1 PDCA cells, while the second construct served as a functional but target unspecific control, redirected against the hematological cancer target blood dendritic cell antigen 2 (BDCA-2). Additionally, we evaluated the influence of locally injected IL-2 as a T cell support in the tumor microenvironment (TME) on in vivo and intratumoral T cell distribution.

CBR2opt facilitated 2D bioluminescence (BLI) biodistribution analysis of CAR T cells but technical drawbacks prevented the quantification of target-specific CAR T cell proliferation at the tumor. However, whole-body 3D hybrid µCT/ bioluminescence tomography (BLT) enabled for the first time 3D tracking of CAR T cells with bioluminescence. Quantification of segmented tumors displayed the antigen recognition induced proliferation of EGFR CAR T cells at the tumor. Further, segmentation of the BLT signal revealed a target unspecific proliferation of BDCA-2 CAR T cells in BDCA-2- NSG mice. Supplemented local IL-2 had no significant influence on T cell proliferation at the tumor site neither in 2D BLI nor in 3D BLT.

Ex vivo analysis was performed using light-sheet fluorescence microscopy (LSFM) and cyclic immunofluorescence (IF). Quantification and segmentation of LFSM indicated adverse side effects on CAR T cell tumor penetration depth. Combination with cyclic IF demonstrated a target-independent effect of local IL-2 on intratumoral T cell distribution but target-dependent unfavorable effect on T cell phenotype. This manuscript established 3D BLT for CAR T cell tracking but exposed a negative long-term effect of locally applied IL-2.

CHAPTER 2 – MULTIMODAL IMAGING OF CAR T CELLS USING BIOLUMINESCENCE TOMOGRAPHY AND LIGHT-SHEET MICROSCOPY REVEALS NEGATIVE EFFECTS OF LOCAL INTERLEUKIN-2

Finalized for submission: **Henze, J.**; Pfeifer, R.; Wittich, K.; Linnartz, C., Bigott, K.; Jungblut, M.; Hardt, O.; Alves, F.; and Al Rawashdeh, W. Multimodal imaging of CAR T cells using bioluminescence tomography and light-sheet microscopy reveals negative effects of local interleukin-2.

Janina Henze[1,2,‡], Rita Pfeifer[2,‡], Katharina Wittich[2], Cathrin Linnartz[2], Kevin Bigott[2], Melanie Jungblut[2], Ali Kinkhabwala[2], Olaf Hardt[2], Frauke Alves[1,3], Wa'el Al Rawashdeh[2,4,*]

Affiliations:

[1]*University Medical Center Göttingen, Translational Molecular Imaging, Institute for Diagnostic and Interventional Radiology & Clinic for Haematology and Medical Oncology, Göttingen, Lower Saxony, Germany*

[2]*Miltenyi Biotec GmbH, R&D Reagents, Bergisch Gladbach, North Rhine-Westphalia, Germany*

[3]*Max-Planck-Institute for Experimental Medicine, Translational Molecular Imaging, Göttingen, Lower Saxony, Germany*

[4] *Ossium Health, Indianapolis, Indiana, United States of America*

† Shared first authorship

[*] Corresponding author

Abstract

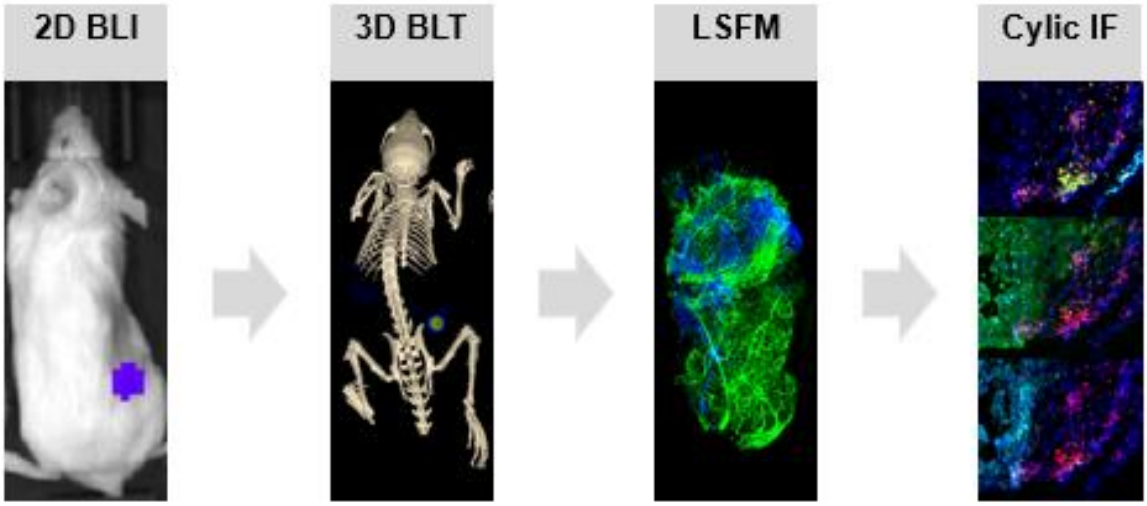

One major drawback in the field of CAR T cell therapy in solid tumors is the lack of spatiotemporal information that enables monitoring of T cell localization, distribution, and status. To address this challenge, we combined 3D µCT bioluminescence tomography (BLT), light-sheet fluorescence microscopy (LSFM) and cyclic immunofluorescence staining (MACSima™). Intratumoral CAR T cell trafficking was monitored in a subcutaneous pancreatic cancer xenograft mouse model over time. Accumulation of CAR T cell in tumor tissue based on target-dependent infiltration was significantly increased in comparison to target-independent infiltration as quantified by 3D µCT/BLT. These findings were confirmed by ex vivo LSFM 3D quantitative analysis revealing deeper T cell tumor infiltration for the target-positive cohort. MACSima™ revealed that local IL-2 application resulted in intratumoral T cell exhaustion. Overall, these results demonstrate that optical tomography-based in vivo CAR T cell whole-body tracking and ex vivo 3D- and sequential 2D-microscopy analysis are valuable tools to assess T cell infiltration and status within tumor tissue.

Keywords: CAR T Cells, Cell Tracking, Optical tomography, 3D uCT/BLT, Light-Sheet Fluorescence microscopy, Cyclic immunofluorescence

Introduction

CAR T cells failed, so far, to recapitulate their tremendous accomplishments within hematological malignancies in solid tumors [1]. Several factors have contributed to this failure, such as the availability of suitable targets. In contrast to blood cancers, there are no targets in solid tumors available with a safe expression profile, increasing the risk for on-target off-tumor toxicities due to a heterogeneous expression pattern [2]. Trafficking of CAR T cells is crucial for

clinical outcomes but diminished in solid tumors [3,4]. While CAR T cells can access most hematological malignancies easily, solid tumors are surrounded by a pronounced tumor microenvironment (TME), which needs to be overcome [5]. This major barrier for CAR T cell infiltration in solid tumors is created by suppressive immune cells, including marrow-derived suppressor cells (MDSCs), cancer-associated fibroblasts (CAFs), tumor-associated macrophages (TAMs), and regulatory T cells (Tregs), an angiogenic vasculature, and the resulting disturbance of sufficient nutrient and oxygen supply [6,7]. Majority of preclinical and clinical research addressing these and other cell therapy-associated questions are largely conducted with negligible in vivo analysis of CAR T cell behavior. The lack of these insights hinders further clinical improvements of CAR T cells. Hence, there is an urgent need for more preclinical research to overcome these drawbacks. In vivo and ex vivo 3D cell tracking strategies can provide spatial and temporal information, supporting research activities regarding the toxicology of cell-based cell therapies or TME-related strategies for combinatorial immunotherapies [8,9]. Bioluminescent imaging (BLI) combined with reporter proteins based direct cell labeling enables non-invasive whole-body and real-time mapping of CAR T cell biodistribution, tumor infiltration, expansion, and persistence [10]. The combination of 3D reconstructed BLI and µCT scan, termed bioluminescence tomography (BLT), has extensive applications for preclinical research as a comparably new modality, providing quantitative optical imaging information in 3D [11]. Pairing with other imaging modalities, such as 3D light-sheet fluorescence microscopy (LSFM) and cyclic immunofluorescence staining, enables further in-depth cellular characterization [12]. LSFM microscopy allows segmentation and quantification of immune cells in the core and periphery of the tumors down to minor differences between different CARs [13]. Cyclic immunofluorescence staining (MACSima™) has been applied to stain the same section with multiple markers to gain various information on single-cell level and evaluate individual CARs in solid tumor models [14]. In this way, the incorporation of multimodal imaging techniques into a single strategy facilitates a precise characterization of a certain CAR therapy from longitudinal 3D in vivo biodistribution to spatial resolution and phenotyping within a solid tumor.

Here, we apply this proposed multimodal imaging strategy to investigate the behavior of a CAR T cell therapy and a mock control in the in vivo and ex vivo context of a subcutaneous pancreatic adenocarcinoma (PDAC) mouse model. We further evaluate the impact of local Interleukin-2 (IL-2) as an external CAR T cell support against the hostile TME. IL-2, a T-cell growth factor with pleiotropic effects on the immune system in patients, is approved as an immunotherapeutic treatment for solid tumors [15]. Here it is subcutaneously injected under the

tumor to monitor the effect on CAR T cell tumor infiltration and biodistribution dynamics. In vivo tracking of CAR T cells is executed by the addition of recently established mutant version of click beetle red luciferase (CBR2opt) reported by Hall et al. via lentiviral T cell transduction [16]. Finally, insights from in vivo tracking are broadened with ex vivo tracking data, using LSFM and immunofluorescence, revealing long-term disadvantages of local IL-2 on spatial CAR T cell distribution, independent of the target, and on phenotype, only in target-specific CAR T cells.

Material and Methods

CAR Gene Construction

CAR genes of interest were constructed by commercial gene synthesis (ATUM). CAR expression was initiated by the EF1α promoter located upstream of the CAR gene. N-terminal addition of a human CD8α leader signaling peptide to the respective scFv sequence facilitated the trafficking of CAR receptors to the plasma membrane. The Epidermal Growth Factor Receptor (EGFR)-specific scFv was derived from the chimeric monoclonal antibody Cetuximab [17], while the blood dendritic cell antigen 2 (BDCA-2) specific scFv was derived from the humanized AC144 clone. V_L and V_H regions of the antigen-binding domains were connected via a $(G4S)_3$-linker. The hinge and transmembrane domain of human CD8α was used to link the scFvs to the intracellular signaling domains of 4-1BB, and the CD3ζ signaling domain was derived from UniProt. For in vivo tracking of CAR T cells, CAR genes were fused via a Furin-P2A sequence to a mutant version of click beetle red luciferase (CBR2opt) described by Hall et al. [16]. CBR2opt sequence was obtained from Addgene and introduced into two 2nd generation CARs redirected against epidermal growth factor receptor (EGFR) or blood dendritic cell antigen 2 (BDCA-2). EGFR is a driver of tumorigenesis in many solid tumors, including PDAC, making it an interesting target for immunotherapy [18]. In contrast to EGFR, BDCA-2, a C-type lectin, is exclusively expressed on the surface of human plasmacytoid dendritic cells (pDC) and not expressed on PDAC cell lines including AsPC1 [19,20].

Lentiviral Vector Production

Lentiviral vector productions were performed as previously described [21]. For production of third-generation self-inactivating VSV-G-pseudotyped lentiviral vectors, 1.6×10^7 HEK293T cells were seeded per T175 flask 24h before transfection, until a confluency of 70 – 90% was reached. For transfection of one T175 flask, a total amount of 50 µg DNA was combined with MACSfectin™ reagent (Miltenyi Biotec) at DNA: MACSfectin™ ratio of 1:2. The 50 µg of

DNA contained respective amounts of the transfer plasmid (encoding the CAR construct), two packaging plasmids (encoding gag/pol and rev) and the envelope plasmid (encoding VSV-G). Transfected HEK293T cells were incubated overnight before sodium butyrate was added at a final concentration of 10mM. Lentiviral vector containing supernatant was collected 48 h after transfection, centrifuged at 300 × g at 4°C for 5min and filtered through 0.45 µm-pore-size PVDF filters. Subsequently, filtered supernatant was centrifuged at 4°C and 4,000 × g for 24h to increase viral stock concentration. Air-dried pellets containing lentiviral vectors were resuspended at a 200-fold concentration with 4°C cold PBS. Aliquots of lentiviral vectors were stored at −80°C.

CAR T Cell Generation

Buffy coats from consented healthy anonymous donors were obtained from the German Red Cross Dortmund as registered and approved by the Ethics Committee of the German Red Cross. All study-related procedures have been performed according to the Declaration of Helsinki and to the relevant ethical guidelines.

CAR T cells were generated according to previously applied protocols [21]. Density gradient centrifugation was applied to isolate peripheral blood mononuclear cells (PBMCs) from buffy coats. T cells purification from PBMCs was performed using human pan T Cell Isolation Kit (Miltenyi Biotec) according to the manufacturer's instructions. Isolated T cells were then cultivated in TexMACS™ Medium (Miltenyi Biotec) supplemented with 200 IU/ml of recombinant Human IL-2 IS, research grade (Miltenyi Biotec) and activated with TransAct™, human (Miltenyi Biotec). Twenty-four hours after activation, lentiviral vectors were added to the T cell cultures for transduction. T Cell TransAct™ and excess viral vector were removed 3 days post activation and replaced with fresh TexMACS™ Medium, supplemented with 200 IU/mL IL-2, for further cultivation of T cells. Cell splitting and feeding occurred at a 2-3 days interval. After 12 days of expansion, T cells were pelleted at 300 x g for 10min and subjected to experimental studies.

Flow Cytometry

Cellular composition of purified T cells was analyzed with hCD3, hCD4 and hCD8 REAfinity recombinant antibodies (Miltenyi Biotec) as previously reported [21]. CAR expressions were detected by a sequential staining protocol. Transduction efficiency of anti-EGFR CAR T cells was determined with a recombinant EGFR protein including a His-Tag (Acrobiosystems), followed by a monoclonal anti-His antibody (Miltenyi Biotec). BDCA-2 CAR T cells were

identified by a biotin-tagged BDCA-2 CAR Detection Reagent (Miltenyi Biotec) followed by an anti-Biotin antibody (Miltenyi Biotec). For stainings, samples were incubated with the respective primary antibody at manufacturer recommended concentrations for 10min at 4°C. Samples were washed and incubated with the respective secondary antibodies at recommended concentrations for 10min at 4°C. Stained cells were acquired on a MACSQuant Analyzer 8 (Miltenyi Biotec) and analyzed using the MACSQuantify™ Software 2.13v.

In vivo analysis

Tumor model

All experiments were performed according to guidelines and regulations and were approved by the Governmental Review Committee on Animal Care in NRW, Germany (Landesamt für Natur, Umwelt and Verbraucherschutz NRW, Approval number 84-02.04.2017.A021). NOD SCID gamma (NSG; NOD.Cg-PrkdcscidIl2rgtm1Wjl/SzJ) mice (Jackson Laboratory, provided by Charles River) were injected subcutaneously with 5×10^5 AsPC1 wildtype human cells in 100 µl PBS in the right flank for tumor establishment. Tumor growth was tracked by 2D Caliper measurements of tumor volume. When tumors reached a size of >25 mm², mice were randomized based on tumor size and freshly prepared CAR T cells were injected in 100 µl PBS into the tail vein. In the cytokine-treated cohorts, IL-2 was administered under the subcutaneous tumor on day 1, 3, 5 and 7 post therapy initiation at a dose of 25,000 IU/mouse. On days 1, 3, 5 and 7 25 000 IU IL-2 in PBS were subcutaneously injected, in separate cohorts, for further CAR T cell stimulation. During the course of the experiment, well-being of mice was monitored and scored according to relevant animal use guidelines. Animals were euthanized according to guidelines upon reaching the endpoint (paralysis, stress score of >20, weight loss of >19%, or end-point of the experiment) and tumors were taken out for further ex vivo analysis.

2D and 3D bioluminescence imaging

2D and 3D CAR T cell distribution was measured on day 0, 2, 6, 9, 13, 16 and 20 after intraperitoneal injection of 100 µL (30 mg/mL) D-Luciferin Potassium Salt, LUCK-2G, (GoldBio) in with isofluorane anesthetized mice as described before [21]. 2D measurements were performed using the in vivo imaging system (IVIS) Lumina system (PerkinElmer) with open filters 10 min after substrate injection. 2D data were analyzed and quantified with living image software 4.7.3v. For comparison of the different treatment groups, total flux of dorsal, ventral and tumor region of interest (ROI) were normalized to the value at day 0.

For 3D measurements, anesthetized mice were transferred to a 3-mouse bed of the OI module connected to µCT (MILabs). 3D BLI signal was acquired according to the manufacture protocol with emission filters at 586, 615, 631 and 661 nm followed by a CT scan with 50 kV tube voltage and 0.24 mA tube current ensuring a minimal radiation exposure of 2 mGy per scan. BLT data was automatically reconstructed with MILabs BLT Recon software (MILabs) and µCT data with MILabs Rec software (MILabs). 3D BLT segmentation and quantification were performed with Imalytics Preclinical software 2.1v (Gremse-IT). Segmentation was executed based on µCT data by iteratively drawing of scribbles to delineate the tissues [22,23]. The volume of segmented spleen was dilated by a factor 40 to compensate for vertical signal shift, increasing the risk of inaccurate signal quantification by inclusion of signals resulting from other organs (Figure S1) [24]. For comparison of the treatment groups, organ bioluminescence was normalized to the amount of signal in the whole mouse on each measurement day.

Ex vivo analysis

Cyclic Immunofluorescence staining

Cyclic immunofluorescence staining was performed as it has been reported for the identification of PDAC targets [14]. Xenograft tumors were embedded in Tissue Freezing Medium (Leica) and stored at -80°C until further use. 8 µm sections were cut on a CM3050 S cryostat (Leica) and collected on SuperFrost® Plus slides (Menzel). Serial sections were either used directly or stored at -70°C not longer than 2 weeks. For immunofluorescence staining slides were thawed in -20°C acetone and staining of sections was performed with fluorochrome-labeled antibodies hCD3, (Miltenyi Biotec) together with DAPI (Sigma-Aldrich) according to manufactures instructions. Finally, stained sections were covered with Fluorescence Mounting Medium (Dako) and coverslip. Images for ROI definition were acquired with EVOS® FL Cell Imaging System (Thermo Fisher Scientific) and analyzed using ImageJ 1.49v.

After the definition of a ROI, another 8 µm section of the same frozen specimen was thawn in 4% paraformaldehyde (PFA) at room temperature. Residual PFA was removed 3 times with autoMACS™ Running Buffer (Miltenyi Biotec). Fixed sections were stained with DAPI (Sigma-Alderich) according to manufactures' instructions and stored at 4°C until further usage. For cyclic immunofluorescence staining slides were introduced into a MACSima™ system. The system facilitates sequential staining of multiple fluorochrome-labeled antibodies. One cycle consists of iterative fluorescent staining, image acquisition, and signal erasure. Cyclic section staining was performed with the following human-reactive REAfinity antibodies: CD3,

CD45RA, CD326, CD39, CD73, CD4, CD8, CD45RB, Ki-67, CD28, mCD31, and CD162 (Miltenyi Biotec). Generated and post-processed Images were analyzed using ImageJ 1.49v.

Xenograft clearing and immunostaining for 3D imaging analysis

For spatial analysis of CAR T cell distribution within the tumor, tumor tissues were stained and cleared for light-sheet fluorescence microscopy (LSFM) using the MACS® Clearing Kit (Miltenyi Biotec). Tumors for clearing were selected based on the average BLI signal and tumor size of the group. Vascular networks of tumors were stained in vivo with Rhodamine lectin (Vector Laboratories). For this, 50 µl of Rhodamine lectin (emission maximum 575 nm) were intravenously injected into the tail veins 5min before the injected mice were sacrificed. Freshly excised tumors were fixed by overnight incubation at 2-8°C in 4% PFA Buffer. Remaining PFA was removed by three times washing in PBS before tissues were permeabilized in 5 ml Permeabilization Solution (Miltenyi Biotec) per sample for 24h at room temperature and under slow continuous rotation on a MACSmix Tube Rotator (Miltenyi Biotec). Permeabilized tumors were stained with CD3-Vio667 (Miltenyi Biotec) in Antibody Staining Buffer (Miltenyi Biotec) for 7 days at 37°C under gentle shaking. Subsequently, unbound antibody was removed by washing three times in Antibody Staining Buffer (Miltenyi Biotec) for at least 4h each at room temperature under slow continuous rotation MACSmix Tube Rotator (Miltenyi Biotec). Stained tissues were dehydrated by incubation in increasing ethanol dilutions from 30% ethanol to 100% ethanol for at least 4h at room temperature under slow and continuous rotation. Dehydration was followed by tissue clearing using 5 ml Clearing Solution and incubation for at least 6h at room temperature under slow and continuous rotation.

Image acquisition and 3D LSFM data processing

Cleared tumors were transferred into the imaging chamber of a light-sheet microscope (Ultramicroscope Blaze, Miltenyi Biotec) filled with MACS® Imaging Solution. Multichannel image acquisition of z-stack was performed dependent on sample size at a magnification of 1x or 4x with a zoom of either 0.6 or 1.66 and 4 µm step size. Background signal, Rhodamine lectin and CD3-Vio667 were acquired in the following channels: 488, 561 and 640 nm, respectively. Subsequent analysis was performed with Imaris 9.5.1v (Bitplane) and ImageJ 1.49v software. Imaris software was used for 3D rendering of images and to determine the surface and volume of the tumor tissue, CD3+ areas and vessels. Tumor surrounding soft tissue was separated from the tumor by creating a mask based on manual delineation of the tumor margin. Voxels outside the mask were set to zero. Vasculature was segmented and

reconstructed based on Rhodamine lectin staining using the surface detection application. Analysis of CD3 stained areas was performed by surface segmentation or with Imaris "Spots" detection application, depending on the image resolution. Spot detection required an assignment of a cell diameter (8µm) and was used for the creation of artificial objects. This enabled the quantification of cell number and distance measurements to the tumor surface and the nearest blood vessels. Proximity of vessels to each other and different sizes of analyzed tumor determined the maximum distance. ImageJ 1.49v software was applied to investigate the gray values of the CD3+ and rhodamine lectin staining at maximum projection within the middle third of the tumors.

Statistics

Experimental results were analyzed using GraphPad Prism 9 software (Graph-Pad Software, USA). For the statistical comparison of two groups, unpaired t-tests were used. Analysis of two or more groups was conducted by One-way ANOVA with $p < 0.05$. Significance analyses of in vivo experiments were organized in a pairwise significance matrix (PSM). A comparison between two groups is represented by one box, as shown by Al Rawashdeh et al. [22]. The order of group comparison is illustrated in Figure S2. Significant differences between two comparing groups are defined by a green box, while insignificant differences are indicated by a red box.

Results

Therapeutic efficacy of EGFR CAR T cells contrasts with 2D signal of the CAR T cells within the tumor

To gain spatial-temporal information about CAR T cell behavior in a preclinical subcutaneous pancreatic xenograft mouse model, we used the recently established mutant version of click beetle red luciferase (CBR2opt), which had demonstrated a significantly higher total flux signal (photon/s) compared to standard firefly luciferase (Luc2) with D-Luciferin [16]. A strong bioluminescence signal is especially important due to the small size of T cells, resulting in a low protein amount, and can additionally enhance detection in deeper tissues, thus cell distribution mapping after i.v. injection is higher as in s.c. models [25]. For constitutive transgene expression, T cells were transduced lentivirally with bicistronic vectors co-encoding the CAR and CBR2opt genes (Figure 1A). EGFR CARs were used to target the EGFR+ AsPC1 tumors, while BDCA-2 CARs served as mock controls. In vivo cell tracking was performed as outlined in Figure 1B. Two hours after CAR T cell injection, 2D BLI imaging revealed a signal in the lung and liver as a result of the i.v. injection route (Figure S3) [26]. On the next day, half of the

two EGFR and BDCA-2 CAR T cell treated groups, respectively, animals were treated with additional subcutaneous IL-2 application to assess the cytokine's impact on local T cell distribution and phenotype [27]. Longitudinal 2D BLI imaging demonstrated an increasing bioluminescence signal at the tumor site of EGFR and EGFR + IL-2 treated mice on day 6, while BDCA-2 treated animals indicated a signal amplification in an area attributable to the spleen in dorsal and ventral view (Figure 1C). The signal at the tumor site of EGFR treated mice further amplified over time and from day 13 on background signal started to intensify and T cells started to appear in other organs during the BLI scan, such as the liver (Figure 1C). BLI scans of BDCA-2 CAR T cell groups revealed a strongly increasing signal in the lower abdominal and head area (Figure 1C). Continuously increasing bioluminescence in dorsal, ventral, and tumor regions of interest (ROI) were quantified for further analysis (Figure 1D). The comparison of dorsal signal development - without tumor area - showed no significant difference between EGFR and EGFR + IL-2 animals, just BDCA-2 + IL-2 treated animals had a significantly higher signal, which remained after the discontinuation of additional IL-2 supply. A similar pattern was visible in the ventral comparison, with the exception that there was an additional significant difference in signal intensities between BDCA-2 and BDCA-2 + IL-2 treated animals on day 6. However, we were not able to detect any differences between the tumor signals of the four treatment groups, besides a significant difference between BDCA and BDCA + IL-2 on day 6 and day 9. But these results contrasted the clear intensity peak at the tumor sites of EGFR CAR T cell treated animals visible on day 6 and day 13 and the significant tumor control of the EGFR CAR T cells at the endpoint of the analysis, in agreement with previous findings (Figure 1E) [28].

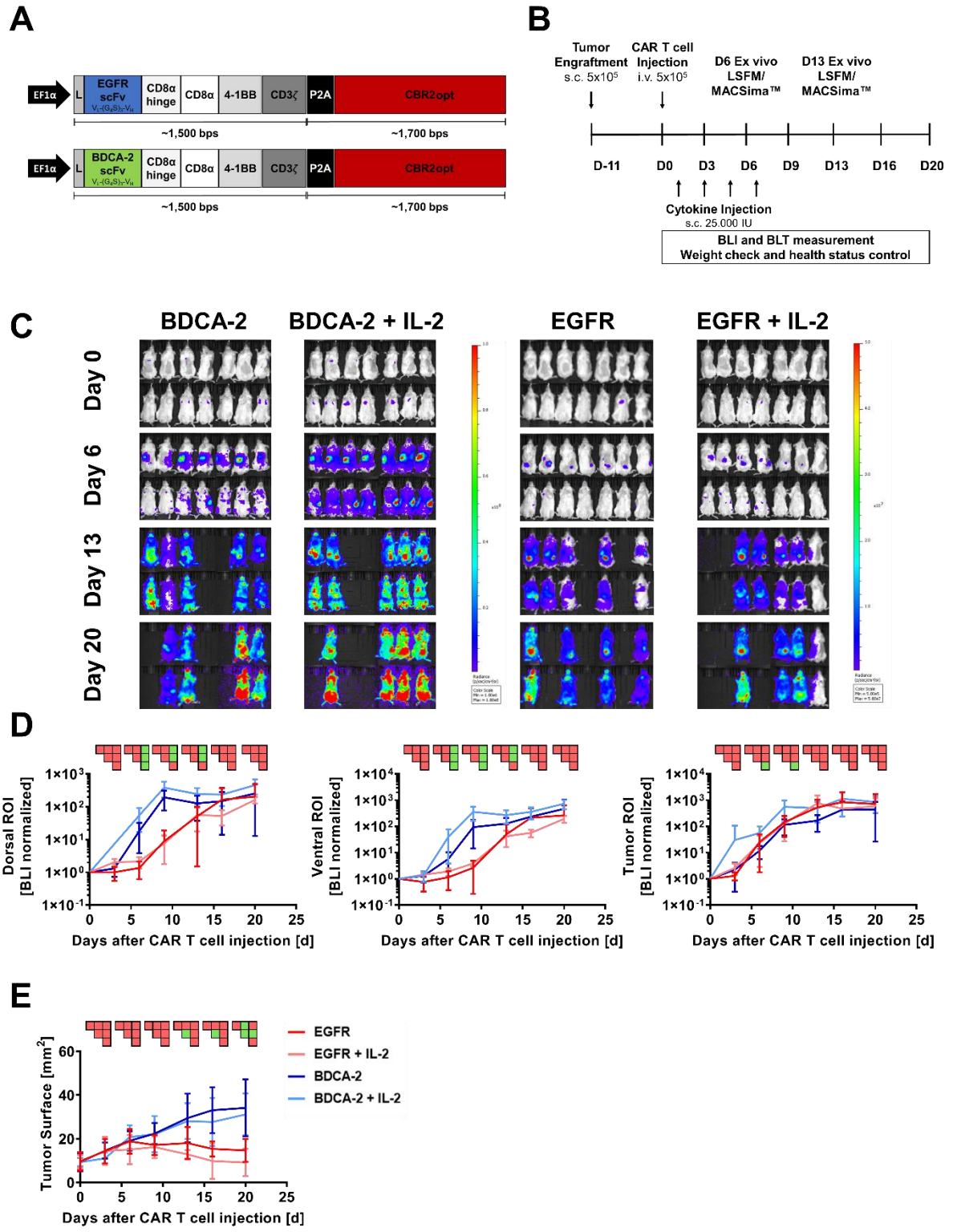

Figure 1: Therapeutic efficacy of EGFR CAR T cells does not correlate with 2D Signal of the transgenic cells within the tumor. (A) Structure of EGFR and BDCA-2 CARs. (B) Schematic representation of the in vivo study plan in the pancreatic xenograft tumor model. (C) The proliferation of CBR2opt-transduced CAR T cells in NSG mice was analyzed by 2D BLI measurements. n=7, Scale factor BDCA-2 groups: min: 1x106, max: 1x108, Scale factor EGFR groups: min: 5x105, max: 5x107 (D) Quantification of signal amplification in the dorsal, ventral and tumor ROI, PSM $p<0.05$ (green) [one-way ANOVA]. (E) Tumor burden change over time after CAR T cells infusion and repeated

subcutaneous IL-2 injections, assessed by 2D Caliper measurements, PSM $p<0.05$ (green) [one-way ANOVA].

3D hybrid µCT/BLT visualizes antigen recognition-dependent intratumoral CAR T cell trafficking and expansion over time

Subsequent to the 2D BLI measurements, 3D µCT/BLT measurements of in vivo CAR T cell distribution were performed. The baseline measurement on day 0 demonstrated a homogenous distribution of CAR T cells in all 4 groups (Figure 2A). The majority of the animals displayed a signal peak within the rib cage, originating from the lungs, even though individual mice exhibited a signal slightly below the thorax, attributed to originate from the liver. CAR T cell biodistribution on day 6 differed greatly between the EGFR and BDCA-2 groups. EGFR treated animals had a clear influx of CBR2opt expressing CAR T cells into the tumor at the right flank side of the mouse, sometimes even with a second signal intensity peak beneath the first peak. In contrast to BDCA-2 animals, for which BLT imaging revealed a signal on the left side of the spine, originating from the spleen accompanied by lack of signal in the tumor. On Day 13, BLI measurement was showing that EGFR treated animals appeared to have two distinct signal peaks matching with tumor and spleen site. However, the background signal started to increase after this time point. The same was true for BDCA-2 treated groups, which further showed a diluting spleen signal in favor of amplifying signals e.g. in the lower abdomen. Additionally, tumor influx of BDCA-2 CAR T cells in AsPC1 BDCA-2- negative tumor started to manifest. At the endpoint of the experiment, EGFR CAR T cell influx was not the dominating signal anymore due to enhanced signal in the whole mouse by arising xenogeneic graft-versus-host disease (GvHD). Visual examination of the BLT scans did not result in the detection of any differences in the CAR T cell biodistribution in the presence or absence of subcutaneous IL-2 injection. Accordingly, further analysis was required to gain further knowledge. Consequently, volume determination of the tumor size revealed a strong therapeutic effect by EGFR CAR T cells, which was slightly increased by additional IL-2 between day 6 and day 13, however without any statistical significance (Figure 2B). While the highly experimenter-sensitive 2D Caliper measurement showed significant efficacy in clearing the tumor by EGFR CAR T cells, the more objective µCT based tumor volume assessment did not confirm these results (Figure 2B). The overall CAR T cell distribution was also quantified, by organ segmentation and signal quantification. Longitudinal BLT measurements of all 4 groups demonstrated an increase of bioluminescence over time in the whole mouse, indicating CAR T cell proliferation, but the slope varied strongly dependent on the CAR and the presence of additional IL-2 (Figure 2C).

Mice treated with CAR T cells redirected against EGFR experienced a strong signal decrease between day 0 and day 3, which was prevented by local IL-2. Recovered signal of EGFR and intensity of EGFR + IL-2 treated animals reached a plateau at day 13, indicating a steady-state phase of T cell proliferation and death. Signal in BDCA-2 and BDCA-2 + IL-2 treated animals increased uniformly and continuously from day 0 without a strong signal decline at the beginning. This corresponded well to the 2D BLI data and was significantly different for BDCA-2 + IL-2 in comparison to all other groups throughout the entire experiment. An observed proliferation of BDCA-2 CAR T cell was significantly enhanced by an additional IL-2 supply (Figure 2C). In contrast to 2D BLI analysis, 3D BLT enabled a clear quantification of the antigen-specific CAR T cell proliferation at the tumor site (Figure 2D). This strong CAR T cell expansion came to an end after day 13, aligning with a plateau of the anti-tumor effect in EGFR CAR T cell treated animals between day 16 and day 20, indicating an end of the active tumor-killing phase. During the same time, BDCA-2 treated groups demonstrated only a slowly increasing signal between day 0 and day 20. Nevertheless, we could not identify an additional effect of IL-2 on CAR T cell expansion at the tumor, since an overall higher signal in the whole mouse ROI was detected. This indicated that the subcutaneous injections had a stronger systematic effect rather than a local effect. Subjective visual analysis of the signal peak in the spleen suggested a target-specific effect. However, quantification of the bioluminescence within the spleen region of interest could not corroborate the visual impression (Figure 2D). Quantification of the signal progress in the liver supported a strong BDCA-2 CAR T cell proliferation in the body, which was further elevated by IL-2, albeit lack of statistical significance.

Taken together, we demonstrated significant target-dependent trafficking of CAR T cells to the tumor correlating with indicative tumor efficacy by applying 3D BLT imaging.

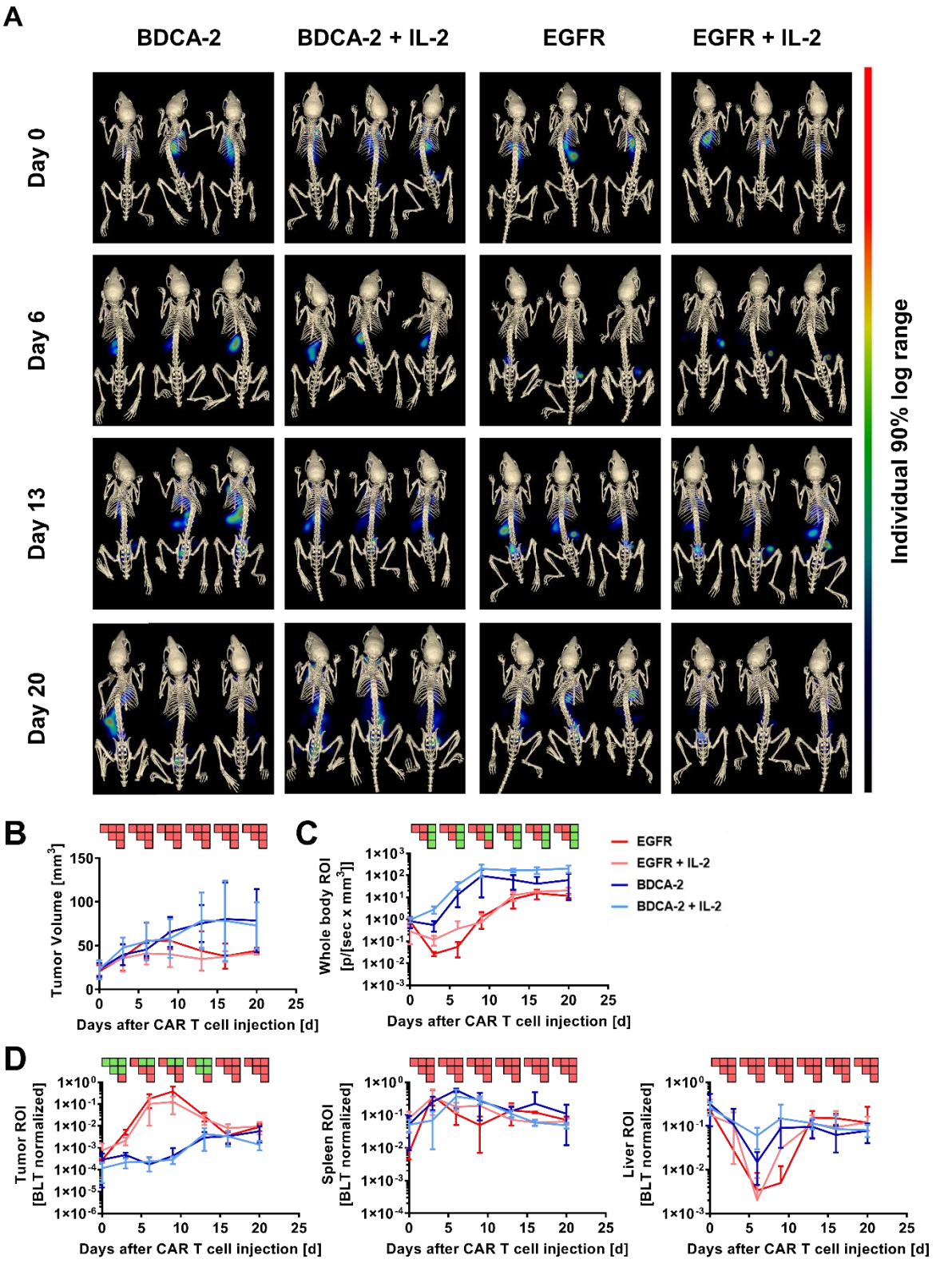

Figure 2: 3D hybrid µCT/BLT visualizes antigen recognition-dependent intratumoral CAR T cell trafficking and expansion. (A) Representative in vivo bioluminescence images of CBR2opt-transduced CAR T cell distribution in NSG mice analyzed by 3D BLT scans. n=7, Scale factor: individually adjusted to 90% of log range (B) Tumor burden change over time measured by µCT scan PSM $p<0.05$ (green) [one-way ANOVA]. (C) Quantification of bioluminescence amplification in the whole mouse, PSM $p<0.05$ (green) [one-way ANOVA]. (D) Quantification of bioluminescence amplification at the tumor and in the spleen, PSM $p<0.05$ (green) [one-way ANOVA].

Spatial analysis of tumor-infiltrating T cells using LSFM reveals increased presence of T cells in the tumor periphery

To better understand the interaction of the therapeutic cells with the solid tumor as well as the impact of additional IL-2 supply, 3D imaging at single-cell resolution was conducted using LSFM. For this, mice bearing tumors with representative bioluminescent signals and size for the respective cohorts were taken out on day 6 and 13 post therapy initiation, injected with rhodamine lectin, and 5 min later tumors were removed for further processing for light microscopy. To visualize T cells within the tumors, staining for CD3 was applied. Upon analysis, a striking observation was that the majority of the CD3+ stained areas were located in close proximity to the tumor surface or to larger feeding vessels, important sources for T cell transport and nutrient supply [29]. Reconstruction of CD3+ areas in combination with color coding of the T cells based on their location in the tumor reinforced this observation and - moreover - revealed a spatially heterogeneous, island-like distribution of the intratumoral T cells (Figure 3B). Specifically for day 6, as expected, EGFR CAR T cell treated tumors exhibited a higher T cell infiltration rate than mock treated controls (Figure 1C, 2A and 3B) and in both cohorts the addition of IL-2 was associated with an increased amount of intratumoral CD3+ cells (Figure 3B). This is in line with the results of the 3D BLT quantification of the tumor.

Intratumoral CD3+ cell distribution was quantified via the gray values of the CD3 and Rhodamine lectin staining at the maximum projection in the middle third of each tumor from both days and showed that the majority of T cells were located close to the tumor surface and vasculature (Figure 3C, 3D). Gray value comparison further verified the visual impression of increased T cell accumulation at the tumor margin and edges (Figure 3D). The BDCA 2 treated tumor revealed the lowest T cell infiltration, regardless of the time point, while the EGFR treated tumors had the highest T cell infiltration, albeit negligible difference between day 6 and day 13 (Figure 3D). IL-2 increased the overall profile intensity in the target-specific and unspecific groups, indicating a time-dependent factor for T cell accumulation in the tumor (Figure 3D).

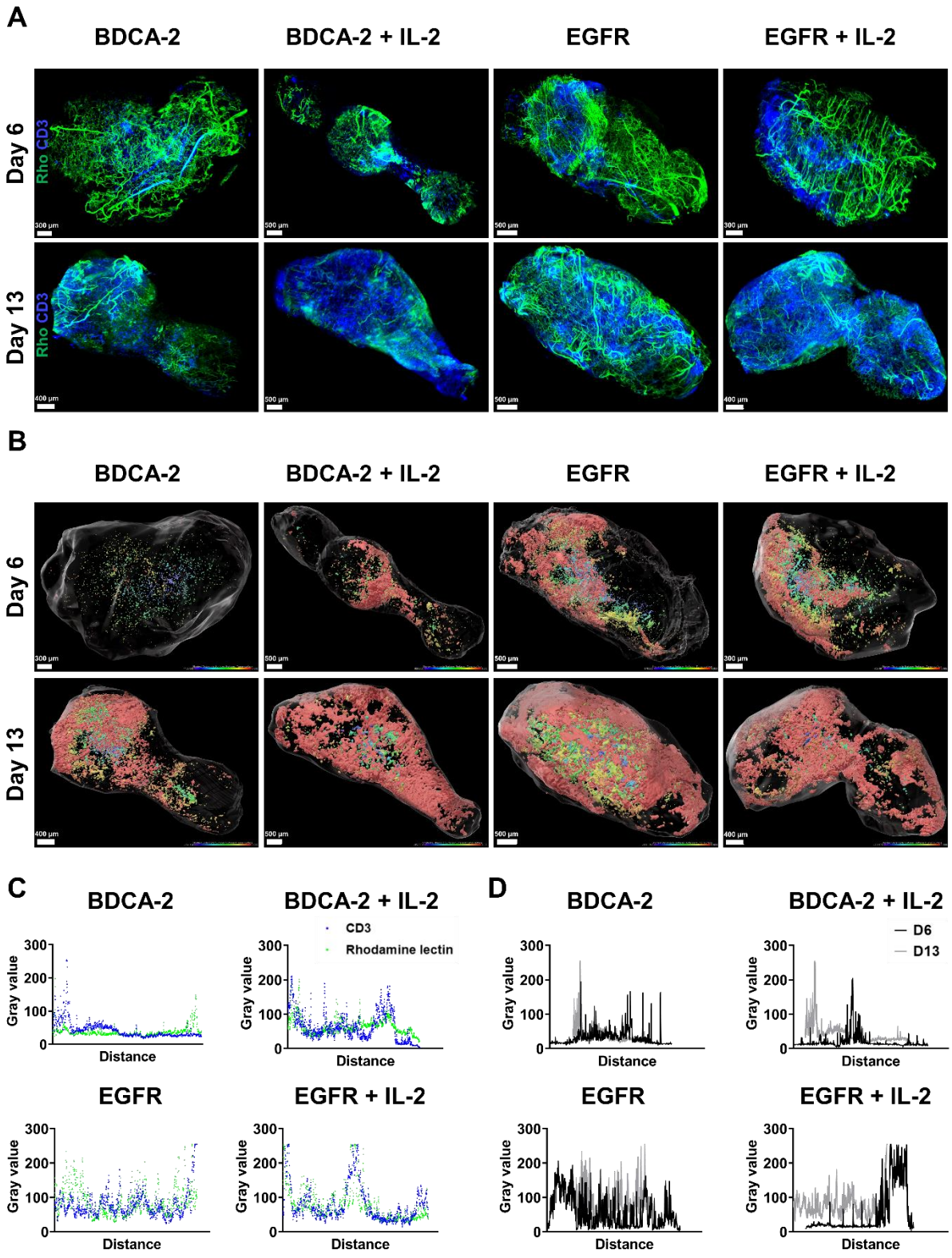

Figure 3: Light-sheet fluorescence microscopy indicates a target-dependent advance for CAR T cell distribution at an early time-point. (A) 3D rendering of tumors from day 6 and day 13 CD3-Vio667 staining (in green) merged with reconstructed 3D images of Rhodamine lectin stainings of vessels (in blue). The scale bar was adjusted to the tumor size between 300 – 500 µm. n=1, per group and day (B) Projection of reconstructed CD3-Vio667 stained surface, color gradient reflected the distance of the CD-stained surface from the tumor surface. (C) Colocalization of maximum intensity

projection gray value profiles of CD3 and Rhodamine lectin stainings on day 13. (D) Overlay of maximal intensity projected gray values of CD3 fluorescence intensities on day 7 and day 13.

Subcutaneous IL-2 induces target unspecific CAR T cell proliferation in the tumor periphery

The impact of antigen recognition and IL-2 support was further analyzed by detailed quantification of CD3+ cells within the tumor and in relation to the vasculature (Figure 4A). In addition, the tumor of the EGFR + IL-2 group of day 6 came apart into two individual tumors. Due to the highly autofluorescent structure of one of the tumor parts, the second part of the tumor was subjected to further analysis of CD3+ stained areas using the Imaris volume detection tool. As the tumor size differed depending on the applied treatment, the area occupied by CD3+ cells was set in relation to the total tumor volume (Figure 4C). As expected, a higher T cell infiltration rate was observed for EGFR CAR T cell treated tumors than for the BDCA-2 CAR T cell treated counterparts (Fig. 4C). When IL-2 was supplied additionally, this effect was further enhanced as indicated by an almost 3% increase in the BDCA-2 and ~1% increase in the EGFR CAR T cell treated tumors, respectively, on day 6. Intriguingly, however, the efficiency of IL-2 support diminished rapidly, so that the tumors extracted on day 13 displayed either equal or diminished areas of T cell infiltration when compared to their CAR T cell only treated pendants. An in-depth analysis of the intratumoral immune cells using the IMARIS spot reconstruction for CD3+ cells and segmentation of the tumor into core and periphery revealed that the majority of the T cells localized in the outer layers of the tumors and only a small fraction was able to reach the core (Figure 4D). Importantly, when IL-2 was administered, the fraction of T cells in the periphery further increased, while the fraction in the core decreased. When the T cell distribution was assessed quantitatively from the tumor surface towards the core, a greater infiltration into the peripheral tumor layers was observed for the therapeutic EGFR CAR T cells when compared to the mock control (Figure 4E). However, from a distance of 400 – 500 µm inwards, BDCA-2 and EGFR CAR T cells exhibited a comparable infiltration frequency. Additional IL-2 supply resulted in a higher frequency of CD3+ cells within the outer 300 µm of the tumor margin but then decreased steadily towards the tumor core, independent of the target specificity. To evaluate the penetration capacity of T cells from the vasculature into the tumor tissue, the distance of intratumoral CD3+ cells to the most adjacent blood vessel was measured. The relative frequency of CD3+ cells to the vessel network in a certain distance was measured (Figure 4F). Strikingly, only a minimal impact of IL-2 could be detected on the penetration capacity of T cells. Rather, the infiltration appeared to be guided by target recognition.

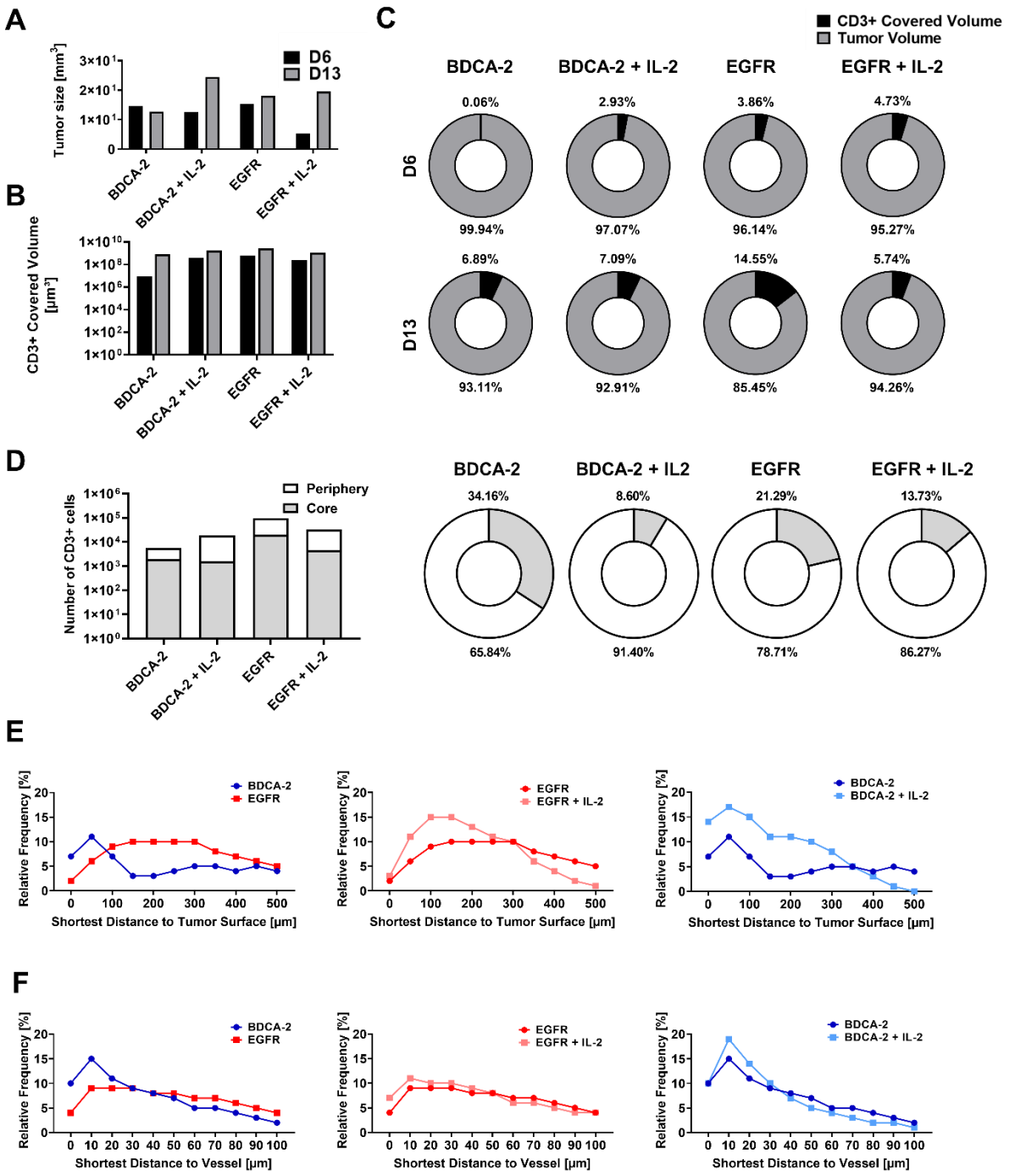

Figure 4: Subcutaneous IL-2 induces target unspecific CAR T cell proliferation in the tumor periphery. (A) Respective sizes of tumor samples were taken out for LSFM analysis on day 6 and day 13. n=1. (B) Volume of surface reconstructed CD3+ areas within tumors. n=1. (C) CD3+ covered volume percent share of the tumor volume. (D) Quantification and percentage of spot reconstructed CD3+ stained areas on day 6 concerning spatial tumor resolution. Equal amounts of spot reconstructed CD3+ spot were assigned either to core or periphery. n=1 (E) Relative frequency of tumor-infiltrating spot-reconstructed CD3+ cells in the tumor margin (500 µm). n=1. (F) Distance of spot-reconstructed CD3+ to the vessel network.

Subcutaneous IL-2 enhances proliferation and activation, resulting in increased differentiation

As shown before by LSFM analysis (Figure 3A, B), the majority of T cells were located close to the tumor surface and/or vasculature as indicated by positive stainings of structures by human CD3 and murine CD31 in cyclic immunofluorescence (Figure 5). Cytotoxic CD8+ T cells were present in samples of all 4 groups, albeit amounts varied strongly corresponding to the CD3+ amounts as quantified via LSFM before, with BDCA-2 treated having negligible T cells and EGFR + IL-2 treated having the highest amount (Figure 5). Phenotypic T cell analysis of CD45RA and CD45RB expression by infiltrating T cells revealed an equal distribution of CD3+ CD45RA+ and CD3+ CD45RA- T cells in EGFR CAR T cell treated tumors (Figure 5). This implies equal amounts of CD45RA+ naïve (TNaive), stem cell–like memory (TSCM), or effector memory T cells (TEMRA) and CD45RA- central memory T cells (TCM), effector memory T cells (TEM) within EGFR CAR T cell treated tumors [30,31]. However, in the tumor samples taken from the EGFR + IL-2 CAR T cell treated group, the majority of CD3+ cells displayed no CD45RA or CD45RB expression, indicating induction of IL-2 dependent differentiation into mature T cell phenotypes. Neither BDCA-2 nor BDCA-2 + IL-2 CAR T cell treated tumors showed any expression of CD45 related makers, also due to an overall low amount of CD3+ cells.

To further analyze the infiltrating T cells, their activation status was evaluated by investigating the upregulation of CD28 and CD162. CD28 is one of the most important costimulatory domains in antigen-recognizing T cells and is often incorporated into CARs [32]. Nevertheless, CD28 is constantly expressed on a vast majority of CD8+ and CD4+ T cells and can mediate IL-2 dependent and independent T cell proliferation [33]. Staining of CD28 and CD162 revealed no expression of these markers on T cells in BDCA-2 treated tumors. CD28 expression on CD3+ T cells was comparable in EGFR and EGFR + IL-2 CAR T cell treated tumor samples. However, CD162, known to be upregulated in activated T cells expression was highly expressed in T cells of the EGFR + IL-2 CAR T cell treated tumor. CD162 is upregulated on stimulated T cells and promotes T cell exhaustion, which slows down proliferation [34]. Ki67 proliferation marker expression profile of CD3+ in the EGFR + IL-2 CAR T cell treated sample pointed into the same direction, by a higher amount of CD3+ Ki67+ double-positive cells compared to the EGFR-treated sample. Overlays of Ki67+ with images stained with CD326, a protein expressed in epithelial-derived carcinomas, revealed a strong proliferation of tumor cells in all 4 groups. CD3+ Ki67+ CD326- signals were only observed in the 2 EGFR-treated

samples indicating active tumor cytotoxicity by T cells, unlike the 2 BDCA-2 treated samples [35]. Taking these findings in consideration, we have found a probable explanation for the lack of added value of IL-2 on long-term CAR T cell efficacy in our current model, insulated by BLT and LSFM analysis.

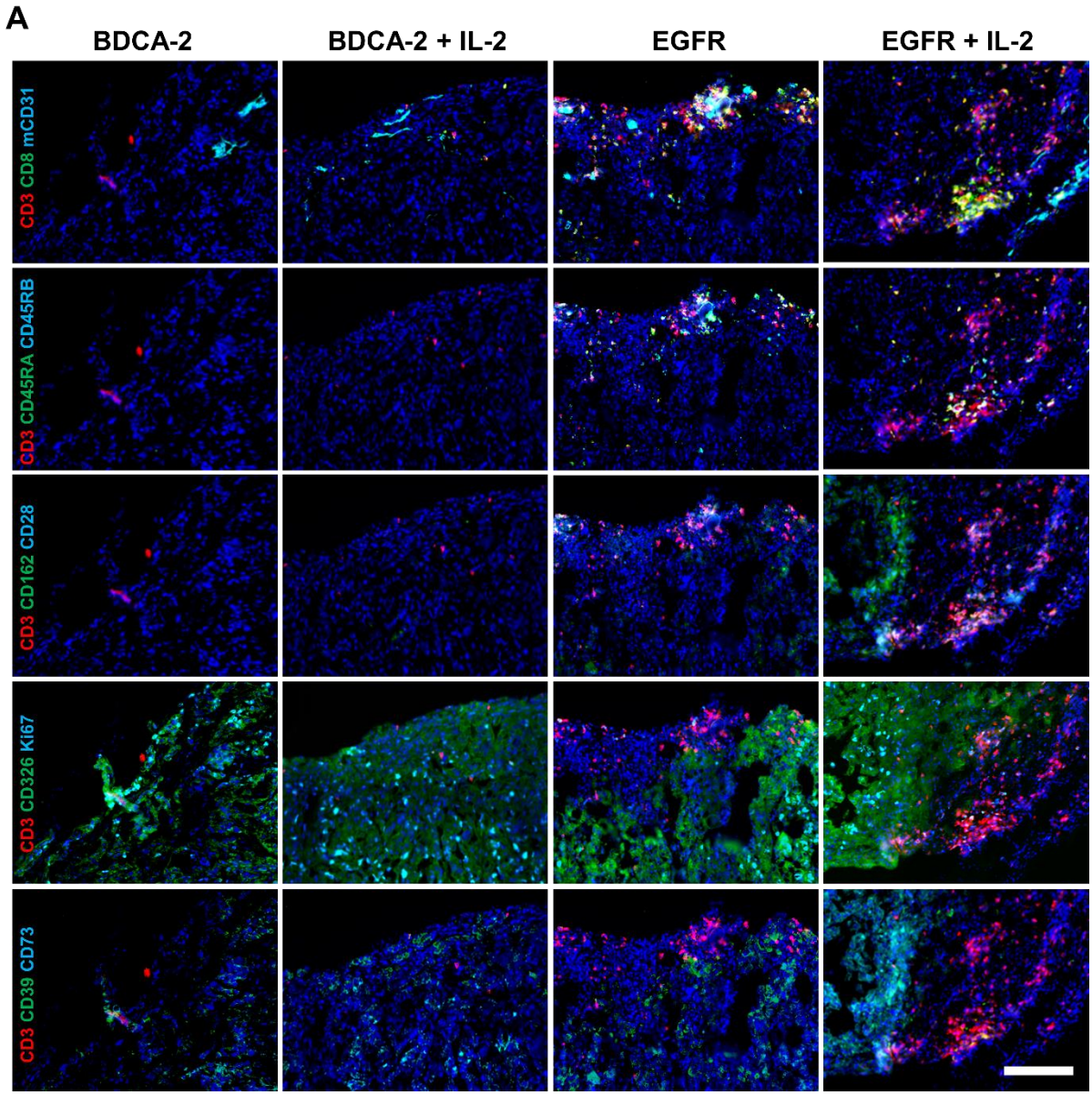

Figure 5: Subcutaneous IL-2 enhances proliferation and activation of T cells, resulting in increased T cell exhaustion. Representative immunofluorescence images of the tumor and (CAR) T cell expression profiles 6 days after CAR T cell injection. CD3, CD8, CD28, CD39, CD45RA, CD45RB, CD73, CD162, CD326 and Ki67 stainings were performed on one tumor per treatment group and each image is representative of at least three regions of interest. ROIs during cyclic IF were chosen based on manual prestaining of DAPI, CD3, and EpCAM. Scale bar = 150 µm.

Discussion

CAR T cells face several hurdles, especially in solid tumors and their TME. Here, we demonstrate a combination of in vivo and ex vivo tracking methods that enabled monitoring of T cell localization, distribution and status through the whole mouse and on a cellular level. We applied BLI, µCT/BLT, LSFM and cyclic immunofluorescence in combination with EGFR and BDCA-2 CARs to track CAR T cells in vivo and ex vivo. Proliferation and biodistribution of CBR2opt-expressing CAR T cells were successfully imaged in 2D and 3D for the first time. Even the initially low cell number of $5x10^5$ cells was visible in deeper tissues, e.g. lung or liver. This proved that the recently established mutant version of click beetle red luciferase, CBR2opt, is an interesting alternative for imaging T cells to the widely used firefly luciferase in the long term, due to substantial higher light output in combination with D-Luciferin and near-infrared emission in combination with new substrate naphthyl-luciferin [16]. A disadvantage of the standard firefly luciferase/D-Luciferin combination is the low sensitivity in deeper tissues such as the lung [36].

However, the enhanced unspecific proliferation of BDCA-2 CAR T cells in this study induced a high amount of photons emitted from intestinal tissue below the tumor, as demonstrated by ex vivo examination. This signal interfered with the 2D quantification of the tumor bioluminescence signal. Thus, 2D BLI incorrectly detected BDCA-2 CAR T cell tumor infiltration although there was a lack of tumor infiltration in the early stage and a lack of tumor reduction in this group. Therefore, the lack of the ability to distinguish depth-resolved signals in 2D BLI was highlighted [37,38].

To overcome this limitation, we performed hybrid 3D µCT/BLT measurements, enabling the creation of tomographic maps of the source intensity and location of the bioluminescence. The very initial measurement was in line with the 2D BLI results, in which lung and liver were the first organs infiltrated by the CAR T cells [39]. Starting on Day 6 post CAR t cell injection, a clear tumor-specific signal was detected only in the EGFR-treated cohorts, with a maximum normalized tumor BLT signal at Day 9 (Figure 2A and Figure 2D). This finding confirmed that hybrid µCT/BLT circumvents the limitations of standard BLI and allows 3D CAR T cell tracking in vivo and longitudinal quantification of the target-specific T cell proliferation and therapeutic effect. Therefore, we can present hybrid 3D µCT/BLT as a tomography tool for preclinical longitudinal cell therapy monitoring and as an isotope-free alternative to µCT/PET and/or µCT/SPECT. Moreover, hybrid 3D µCT/BLT could gain more impact in combination with multiple luciferase/substrate pairs and potentially with fluorescence tomography (FLT

from MiLabs or FMT from PerkinElmer) in preclinical research [24,40,41]. Apart from being isotope-free 3D tomography, hybrid 3D µCT/BLT has multiple advantages such as ease of use, lower costs, stability of the luciferase and easy access and storage, and lack of special isolation in the lab. As any other imaging modality, BLT imaging has certain limitations as demonstrated by the technical signal reconstruction issues of the spleen, which disabled an accurate quantification (Figure S1), and the signal dilution towards the end of the study. Several groups are working on the improvement of BLT acquisition and reconstruction by adjustment of experimental and computational strategies [42–44].

Although advanced multimodal imaging strategies can provide spatial, temporal, and functional information in the whole mouse, they lack resolution on a single-cell level. This information is essential to investigate the solid tumor-specific barriers for CAR T cells. Some research groups, such as Mulazzani et al. and Murty et al., have used intravital microscopy to investigate cell therapies and the role of the TME at a cellular resolution [45,46]. However, intravital microscopy requires technically challenging glass-window engraftment and it is limited to a certain depth. However, for the evaluation of complex TME redirected strategies in solid tumors, complete 3D insights might be more advantageous. We approached this by the combination of high-sensitivity whole mouse BLT imaging with high-resolution LSFM and cyclic IF microscopy on selected days. The connection of both in vivo and ex vivo methods enabled the spatial and functional analysis of CAR T cells in the solid tumor model. LFSM facilitates high-resolution profiling and mapping of single cells and revealed an approximation of CD3+ amounts between the groups, which indicated a decreased target-dependent expansion of CAR T cells in the tumor over time and low consistency of active tumor-killing, as well as target unspecific distribution of T cells over time. In this way, the multifaceted analysis characteristics of LSFM including color-coding of individual cells based on certain aspects, distance and covered area measurements as well as the creation of different layers enabled an in-depth spatial investigation of CD3+ T cells within the tumor. However, distance analysis requires a high resolution of the staining and is currently limited to a certain objective size. Additionally, distance measurements are highly influenced by the unorganized structure of the tumor itself and its vasculature [7]. So, for the comparison of distance measurements, maximum values have to be determined. Nonetheless, the numbers of channels in LSFM are limited and therefore the application of co-expression or -labeling and induction of fluorescent protein expression might circumvent this limitation [47]. Until now, protocols for LSFM and cyclic IF processes cannot be combined but we are actively working on joined protocols to gain all data from the same tumor in the future. Moreover, combining both techniques would require fewer animals and resources,

while increasing data output and complexity acquired. In the long-term, whole mouse clearing approaches might be able to fully close the gap between CAR T cells tracking in the whole mouse and on the cellular level, providing in-depth and toxicity-related insights.

Despite these problems and chances of multi-modal imaging strategies, our applied strategy enabled the dissection of target-specific and unspecific CAR T cells behavior in the presence or absence of subcutaneous IL-2 on the whole mouse and cellular level. 2D and 3D in vivo CAR T cells tracking revealed distinct biodistribution patterns of the treatment groups. While all intravenously injected CAR T cells successfully infiltrated the lungs and liver shortly after injection, the biodistribution of CAR T cells to a later time point was highly influenced by target specificity. Although quantification was technically difficult, the majority of CBR2opt-expressing BDCA-2 CAR T cells were homing to the spleen until day 6 and preferentially expanded there until day 13. At the same time, CBR2opt-expressing EGFR CAR T cells had infiltrated the tumor and started proliferating on day 6, while only a few animals showed CAR T cell infiltration in the spleen, indicating a dominating effect of target-specific T cell homing in contrast to natural spleen homing in immunodeficient NSG mice. On day 13 all EGFR CAR T cells treated animals revealed a clear spleen signal in 2D and 3D measurements that proved the successful trafficking of the applied CAR T cells to the spleen. The accumulation of CAR T cells has been often demonstrated by others in target unspecific CAR T cells and antigen-experienced specific CAR T cells [48]. Although CAR T cells could have infiltrated all spleens as early as day 3, due to the low cell number applied to the mice and the detection limit for a low number of cells, cells could not be visualized at this early time point by 2D and 3D imaging. Even though the majority of CAR T cell related research work includes mostly an endpoint analysis of the spleen, others such as Sellmyer et al. have shown a clear spleen homing on day 7 before target positive tumor infiltration of CAR T cells on day 13 in a subcutaneous colon cancer model in NSG mice [49,50]. Interestingly, they used a similar second-generation CAR and the same route of injection but performed PET CT combined with BLI imaging. Nonetheless, the small amount of CAR+ T cells, that was injected here was still enough for a temporal tumor control by target-specific EGFR CAR T cells, an antigen that has been validated in a clinical trial without severe side effects [51]. The low amount of CAR+ T cells was chosen, due to the focus of this study on in vivo and ex vivo CAR tracking [52,53]. Despite the low number of injected CAR+ T cells, the unspecific proliferation of BDCA-2 CAR T cells started early despite the lack of human BDCA-2 expression in mice [20]. The unspecific proliferation in abdominal organs and the resulting bioluminescence signal in the 2D setting disabled the clear distinction between target-specific CAR T cell proliferation as detected in the 3D setting. The beginning of GvHD

was further emphasized by the weight loss in both groups, indicating GvHD yet tonic signaling of BDCA-2 CAR T cells or a donor-dependent effect in both groups cannot be fully excluded. On-set of GvHD is often noticed after a donor- and protocol-dependent time, even in immunodeficient NSG mice, as demonstrated before by others [54].

However, BDCA-2 CAR T cells in the presence of administered IL-2 showed increased proliferation in the whole mouse and liver but not at the tumor site in comparison to BDCA-2 CAR T cells alone. This further strengthened the hypothesis of a possible negative additive effect induced by an additional IL-2 treatment on already unspecific proliferating BDCA-2 CAR T cells and confirmed a certain degree of systemic effect, which was not present in the EGFR + IL-2 treated group.

Local administration of IL-2 was well tolerated by the mice and showed no side effects as often observed by systemic intravenously applied IL-2. The latter route of administration has been reported to induce several severe side effects when it was approved as a monotherapy in metastatic renal cell carcinoma and metastatic melanoma [55]. Those side effects include fever, flu-like symptoms, nausea, low blood pressure, and cell counts and in combination with cell-based immunotherapies, systemic IL-2 treatment has been demonstrated to be unfavorable in terms of efficacy in clinical trials [56]. At the same time, IL-2 is still one of the most crucial factors for CAR T cells in the hostile TME, where T cell penetration, proliferation and differentiation are highly impaired, as by our cyclic IF stainings [57]. Local injection of subcutaneous IL-2 has been shown here to circumvent these side effects. Furthermore, this route of application is easier transferable to the clinic in contrast to other strategies, which have been applied in vivo to induce IL-2 expression [58].

IL-2 had a further effect on CAR T cells as detected by 2D and 3D in vivo imaging. Initially, we detected a loss of CBR2opt expressing cells via 3D BLT, not pronounced in 2D BLI quantification. This signal loss could potentially be caused by a combination of activation-induced cell death (AICD) and apoptosis induced by the stress due to the injection and preparation procedure [59]. However, IL-2 is known to promote AICD, here IL-2 supposedly supported the stressed cell recovery and accelerates the proliferation of CAR T cells [60]. While local IL-2 was well tolerated, we still faced some of the common disadvantages of IL-2 treatments [61]. While CAR T cells express IL-2 after antigen recognition to support proliferation, excess of IL-2 at the site of the tumor in combination with other cytokines expressed by the tumor enhanced early exhaustion of T cells. The LSFM findings suggest a short-lived IL-2 induced T cell proliferation in the tumor periphery independent of the CAR target. This

proliferation might have been further fueled by additional IL-2 expression upon antigen recognition in the target-specific group of EGFR CAR T cells [62]. Both sources of IL-2 together seem to induce initially a strong proliferation of CAR T cells as displayed in cyclic IF stainings but failed to induce an enhanced killing effect due to increased activation, which in turn favored exhaustion in tumors of the EGFR + IL-2 treated group. Cyclic IF staining revealed a clear enhanced proliferation and activation of IL-2 supported EGFR CAR T cells, which seems to have led to overstimulation. Cyclic IF also indicated a high amount of stressed cells in this treatment group, which tend to differentiate into regulatory T cells (Treg) or undergo apoptosis [63,64]. Thus, the amount of locally supplied IL-2 must be fine-tuned and should be delayed to prevent overstimulation by this cytokine e.g. by TME redirected IL-2 supply or change of IL-2 receptor kinetic as explored by other groups [65,66]. This delayed stimulation could induce a prolonged active tumor-killing phase even at lower cell numbers, in contrast to the short phase between day 6 and day 16 as indicated in this study. CAR T cell penetration depths are another factor with the TME, which could improve tumor efficacy. LSFM analysis showed that the majority of CAR T cells were located close to the vasculature and that the CAR T cells rarely penetrated deeper into the solid tumor. This emphasizes the high need for strategies to improve CAR T cells infiltration into a solid tumor, such as attraction methods or reinforcement of extracellular matrix degradation mechanisms [67,68].

Conclusion

Overall, our study revealed for the first time that non-invasive imaging and longitudinal monitoring of CAR T cell distribution in vivo is feasible using a hybrid 3DµCT/BLT imaging system. Moreover, 3D CAR T cell tracking demonstrated the correlation of increased antigen-specific CAR T cells at the tumor with the therapeutic efficacy. LSFM and cyclic IF proved to be advantageous for the analysis of CAR T cell-tumor cell interactions, assessment of CAR T intratumoral distribution at cellular resolution and analysis of IL-2 influence on CAR T cells, which induced a shift of CAR T cell proliferation, location, and phenotype within the tumor.

Acknowledgements

We would like to thank Laura Mezzanote for provision of CBR2opt sequence, Felix Gremse for help and advice regarding BLT reconstruction and Silvia Rüberg and Fabio El Yassouri for their technical support during cyclic immunofluorescence stainings. This project was funded by the LeitmarktAgentur.NRW as part of the TRACAR grant.

Contributions

J.H., R.P. and W.A.R. wrote the manuscript. J.H., R.P. and W.A.R. conceptualized and designed the study. J.H., R.P., K.W., C.L., and K.B. conducted and analyzed the experiments. M.B., O.H., F.A., and W.A.R. supervised the project. All authors discussed the data and reviewed the manuscript.

Competing interests

J.H., R.P., K.W., C.L., K.B., M.B., and O.H., are employees of Miltenyi Biotec B.V. & Co. KG. All other authors declare no competing interests. W.A.R is an employee of Ossium Health Inc.

Supplementary Materials

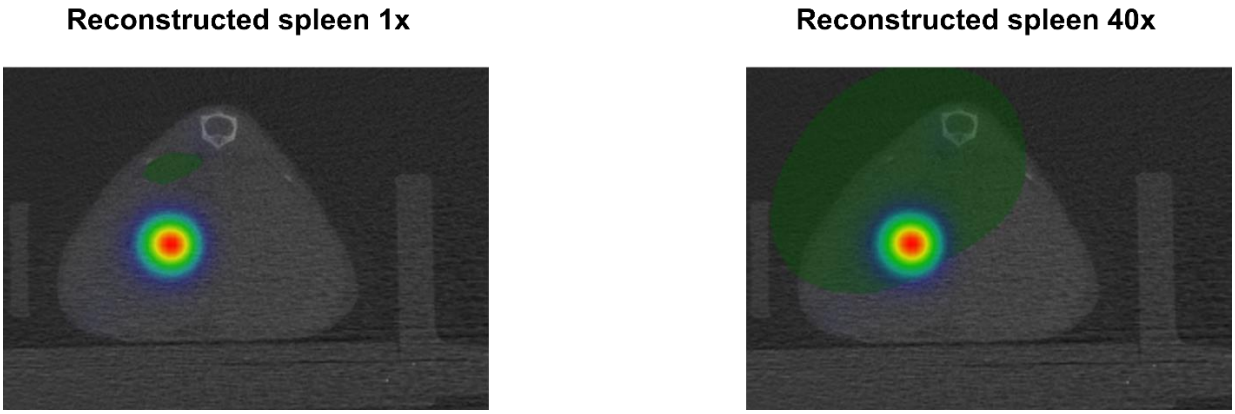

Figure S1: Compensation of vertical BLT spleen signal shift. Axial view of repesentative spleen signal on Day 6 in BDCA-2 treated mice. Spleen was manually reconstructed (green) based on CT scan. Shifted signal was included into the spleen ROI by dilatation of the ROI by factor 40 in x-, y. and dimension.

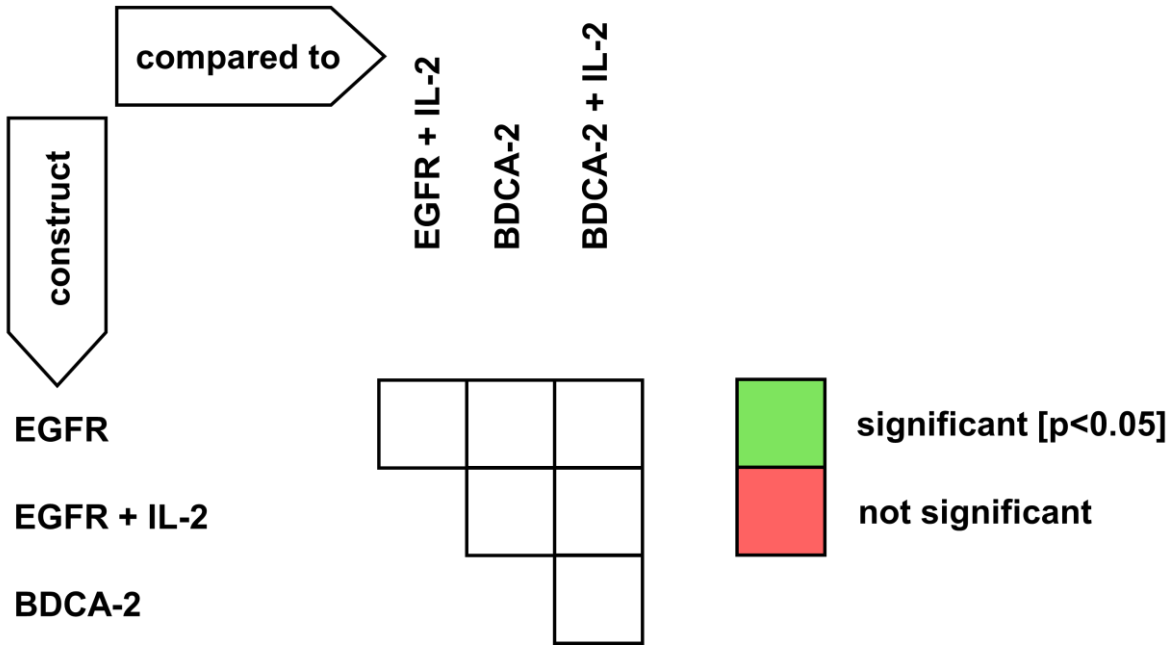

Figure S2: Organisation of the pairwise significance matrix for group comparisons. BLT and BLI of EGFR, EGFR + IL-2, BDCA-2 and BDCA-2 + IL-2 treated tumors were qnatified and compared. PSM p<0.05 (green), p>0.05 (red) [one-way ANOVA, multiple comparisons].

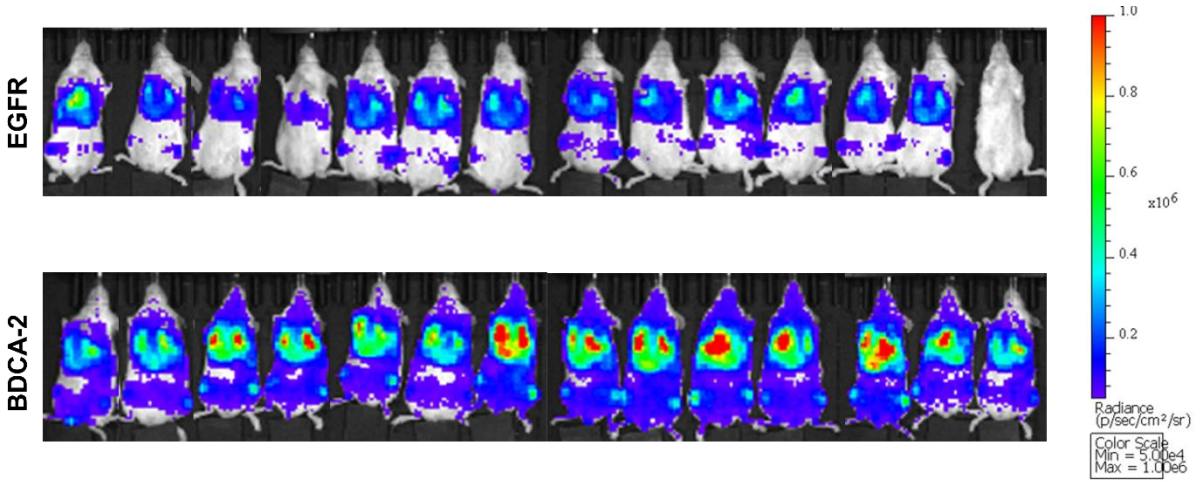

Figure S3: Homogenous distribution of CAR T cells, 2h after injection on Day 0. CAR T cells were injected intravenously via the tail vain. 2h after the injection, mice were intraperitoneally injected with 100 µl D-Luciferin and measured at the IVIS Lumina in vivo imaging system.

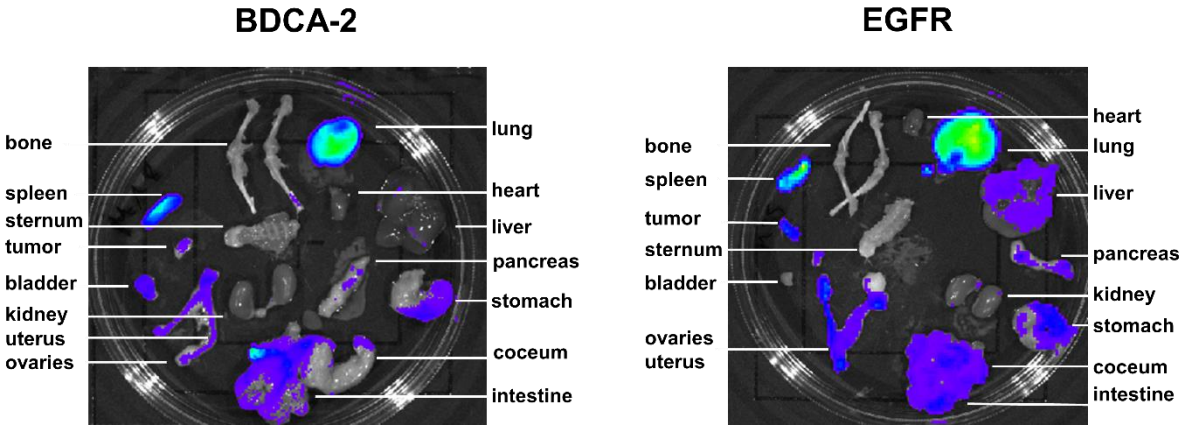

Figure S4: Ex vivo examination of organs by 2D BLI on Day 20. Directly after standard imaging procedure, including i.p. injection of 100 µl D-Luciferin, mice were sacrificed and organs were taken out quickly for 2D ex vivo imaging.

References

1. Schaft, N. The landscape of car-t cell clinical trials against solid tumors—a comprehensive overview. *Cancers* vol. 12 1–36 (2020).

2. Sun, S., Hao, H., Yang, G., Zhang, Y. & Fu, Y. Immunotherapy with CAR-modified T cells: Toxicities and overcoming strategies. *Journal of Immunology Research* vol. 2018 (2018).

3. Piersma, S. J. *et al.* High number of intraepithelial CD8+ tumor-infiltrating lymphocytes is associated with the absence of lymph node metastases in patients with large early-stage cervical cancer. *Cancer Res.* **67**, 354–361 (2007).

4. Galon, J. *et al.* Type, density, and location of immune cells within human colorectal tumors predict clinical outcome. *Science (80-.).* **313**, 1960–1964 (2006).

5. Salmon, H. *et al.* Matrix architecture defines the preferential localization and migration of T cells into the stroma of human lung tumors. *J. Clin. Invest.* **122**, 899–910 (2012).

6. Martinez, M. & Moon, E. K. CAR T Cells for Solid Tumors: New Strategies for Finding, Infiltrating, and Surviving in the Tumor Microenvironment. *Front Immunol* **10**, 128 (2019).

7. Henze, J., Tacke, F., Hardt, O., Alves, F. & Rawashdeh, W. Al. Enhancing the efficacy of car t cells in the tumor microenvironment of pancreatic cancer. *Cancers (Basel).* **12**, 1389 (2020).

8. Keu, K. V. *et al.* Reporter gene imaging of targeted T cell immunotherapy in recurrent glioma. *Sci. Transl. Med.* **9**, (2017).

9. Yaghoubi, S. S. *et al.* Noninvasive detection of therapeutic cytolytic T cells with 18 F-FHBG PET in a patient with glioma. *Nat. Clin. Pract. Oncol.* **6**, 53–58 (2009).

10. Keyaerts, M., Caveliers, V. & Lahoutte, T. Bioluminescence imaging: Looking beyond the light. *Trends in Molecular Medicine* vol. 18 164–172 (2012).

11. Darne, C., Lu, Y. & Sevick-Muraca, E. M. Small animal fluorescence and bioluminescence tomography: A review of approaches, algorithms and technology update. *Physics in Medicine and Biology* vol. 59 (2014).

12. Uhlén, P. & Tanaka, N. Improved Pathological Examination of Tumors with 3D Light-Sheet Microscopy. *Trends in Cancer* vol. 4 337–341 (2018).

13. Si, Y. *et al. Multidimensional imaging provides evidence for down-regulation of T cell effector function by MDSC in human cancer tissue*. *Sci. Immunol* vol. 4 http://immunology.sciencemag.org/ (2019).

14. Schäfer, D. *et al.* Identification of CD318, TSPAN8 and CD66c as target candidates for CAR T cell based immunotherapy of pancreatic adenocarcinoma. *Nat. Commun.* **12**, 1–18 (2021).

15. Liao, W., Lin, J. X. & Leonard, W. J. Interleukin-2 at the Crossroads of Effector Responses, Tolerance, and Immunotherapy. *Immunity* vol. 38 13–25 (2013).

16. Hall, M. P. *et al.* Click beetle luciferase mutant and near infrared naphthyl-luciferins for improved bioluminescence imaging. *Nat. Commun.* **9**, (2018).

17. Prewett, M. *et al.* The Biologic Effects of C225, A Chimeric Monoclonal Antibody to the EGFR, on Human Prostate Carcinoma. *J. Immunother.* **19**, 419–427 (1996).

18. Nedaeinia, R., Avan, A., Manian, M., Salehi, R. & Ghayour-Mobarhan, M. EGFR as a Potential Target for the Treatment of Pancreatic Cancer: Dilemma and Controversies. *Curr. Drug Targets* **15**, 1293–1301 (2014).

19. Durkin, A. J. *et al.* Defining the role of the epidermal growth factor receptor in pancreatic cancer grown in vitro. *Am. J. Surg.* **186**, 431–436 (2003).

20. Dzionek, A. *et al.* BDCA-2, BDCA-3, and BDCA-4: Three Markers for Distinct Subsets of Dendritic Cells in Human Peripheral Blood. *J. Immunol.* **165**, 6037–6046 (2000).

21. Schäfer, D. *et al.* A Novel Siglec-4 Derived Spacer Improves the Functionality of CAR T Cells Against Membrane-Proximal Epitopes. *Front. Immunol.* **11**, (2020).

22. Al Rawashdeh, W. *et al.* Noninvasive Assessment of Elimination and Retention using CT-FMT and Kinetic Whole-body Modeling. *Theranostics* **7**, 1499–1510 (2017).

23. Gremse, F. *et al.* Imalytics preclinical: Interactive analysis of biomedical volume data. *Theranostics* **6**, 328–341 (2016).

24. Rosenhain, S., Al Rawashdeh, W., Kiessling, F. & Gremse, F. Sensitivity and accuracy of hybrid fluorescence-mediated tomography in deep tissue regions. *J. Biophotonics* **10**, 1208–1216 (2017).

25. Lin, J. & Amir, A. Homeostasis of protein and mRNA concentrations in growing cells. *Nat. Commun.* **9**, 1–11 (2018).

26. Fischer, U. M. *et al.* Pulmonary passage is a major obstacle for intravenous stem cell delivery: The pulmonary first-pass effect. *Stem Cells Dev.* **18**, 683–691 (2009).

27. Malek, T. R. The biology of interleukin-2. *Annual Review of Immunology* vol. 26 453–479 (2008).

28. Li, H. *et al.* Antitumor activity of EGFR-specific CAR T cells against non-small-cell lung cancer cells in vitro and in mice. *Cell Death Dis.* **9**, 1–11 (2018).

29. Viallard, C. & Larrivée, B. Tumor angiogenesis and vascular normalization: alternative therapeutic targets. *Angiogenesis* vol. 20 409–426 (2017).

30. Caccamo, N., Joosten, S. A., Ottenhoff, T. H. M. & Dieli, F. Atypical Human Effector/Memory CD4+ T Cells With a Naive-Like Phenotype. *Front. Immunol.* **9**, 2832 (2018).

31. Krummey, S. M. *et al.* CD45RB Status of CD8+ T Cell Memory Defines T Cell Receptor Affinity and Persistence. *Cell Rep.* **30**, 1282--1291.e5 (2020).

32. Ying, Z. *et al.* Parallel Comparison of 4-1BB or CD28 Co-stimulated CD19-Targeted CAR-T Cells for B Cell Non-Hodgkin's Lymphoma. *Mol. Ther. - Oncolytics* **15**, 60–68 (2019).

33. Appleman, L. J., Berezovskaya, A., Grass, I. & Boussiotis, V. A. CD28 Costimulation Mediates T Cell Expansion Via IL-2-Independent and IL-2-Dependent Regulation of Cell Cycle Progression. *J. Immunol.* **164**, 144–151 (2000).

34. Tinoco, R. *et al.* PSGL-1 Is an Immune Checkpoint Regulator that Promotes T Cell Exhaustion. *Immunity* **44**, 1190–1203 (2016).

35. Kamada, T. *et al.* PD-1+ regulatory T cells amplified by PD-1 blockade promote hyperprogression of cancer. *Proc. Natl. Acad. Sci. U. S. A.* **116**, 9999–10008 (2019).

36. Weissleder, R. & Ntziachristos, V. Shedding light onto live molecular targets. *Nature Medicine* vol. 9 123–128 (2003).

37. Guggenheim, J. A., Basevi, H. R. A., Frampton, J., Styles, I. B. & Dehghani, H. Multi-modal molecular diffuse optical tomography system for small animal imaging. *Meas. Sci. Technol.* **24**, (2013).

38. Close, D. M., Xu, T., Sayler, G. S. & Ripp, S. In vivo bioluminescent imaging (BLI): Noninvasive visualization and interrogation of biological processes in living animals. *Sensors* vol. 11 180–206 (2011).

39. Yuzawa, S., Kano, M. R., Einama, T. & Nishihara, H. PDGFRbeta expression in tumor stroma of pancreatic adenocarcinoma as a reliable prognostic marker. *Med Oncol* **29**, 2824–2830 (2012).

40. Krebs, S., Dacek, M. M., Carter, L. M., Scheinberg, D. A. & Larson, S. M. CAR Chase: Where Do Engineered Cells Go in Humans? *Front. Oncol.* **10**, 1930 (2020).

41. Benitez, J. A., Zanca, C., Ma, J., Cavenee, W. K. & Furnari, F. B. Fluorescence molecular tomography for in vivo imaging of glioblastoma xenografts. *J. Vis. Exp.* **2018**, (2018).

42. Bentley, A., Rowe, J. E. & Dehghani, H. Simultaneous diffuse optical and bioluminescence tomography to account for signal attenuation to improve source localization. *Biomed. Opt. Express* **11**, 6428 (2020).

43. Zhang, B., Yin, W., Liu, H., Cao, X. & Wang, H. Bioluminescence tomography with structural information estimated via statistical mouse atlas registration. *Biomed. Opt. Express* **9**, 3544 (2018).

44. Feng, J. *et al.* An optimal permissible source region strategy for multispectral bioluminescence tomography. *Opt. Express* **16**, 15640 (2008).

45. Mulazzani, M. *et al.* Long-term in vivo microscopy of CAR T cell dynamics during eradication of CNS lymphoma in mice. *Proc. Natl. Acad. Sci. U. S. A.* **116**, 24275–24284 (2019).

46. Murty, S. *et al.* Intravital imaging reveals synergistic effect of CAR T-cells and radiation therapy in a preclinical immunocompetent glioblastoma model. *Oncoimmunology* **9**, 1757360 (2020).

47. Ueda, H. R. *et al.* Tissue clearing and its applications in neuroscience. *Nature Reviews Neuroscience* vol. 21 61–79 (2020).

48. Cheadle, E. J. *et al.* Natural Expression of the CD19 Antigen Impacts the Long-Term Engraftment but Not Antitumor Activity of CD19-Specific Engineered T Cells. *J. Immunol.* **184**, 1885–1896 (2010).

49. Sellmyer, M. A. *et al.* Imaging CAR T Cell Trafficking with eDFHR as a PET Reporter Gene. *Mol. Ther.* **28**, 42 (2019).

50. Xu, Y. *et al.* Closely related T-memory stem cells correlate with in vivo expansion of CAR.CD19-T cells and are preserved by IL-7 and IL-15. *Blood* **123**, 3750–3759 (2014).

51. Liu, Y. *et al.* Anti-EGFR chimeric antigen receptor-modified T cells in metastatic pancreatic carcinoma: A phase I clinical trial. *Cytotherapy* **22**, 573–580 (2020).

52. Brown, L. V, Gaffney, E. A., Ager, A., Wagg, J. & Coles, M. C. Comparative anatomical limits of CART-cell delivery to tumours in mice and men. *bioRxiv* 759167 (2019) doi:10.1101/759167.

53. Stein, A. M. *et al.* Tisagenlecleucel Model-Based Cellular Kinetic Analysis of Chimeric Antigen Receptor–T Cells. *CPT Pharmacometrics {\&} Syst. Pharmacol.* **8**, 285–295 (2019).

54. Alcantar-Orozco, E. M., Gornall, H., Baldan, V., Hawkins, R. E. & Gilham, D. E. Potential limitations of the NSG humanized mouse as a model system to optimize engineered human T cell therapy for cancer. *Hum. Gene Ther. Methods* **24**, 310–320 (2013).

55. Rosenberg, S. A. IL-2: The First Effective Immunotherapy for Human Cancer. *J. Immunol.* **192**, 5451–5458 (2014).

56. Cao, G., Lei, L. & Zhu, X. Efficiency and safety of autologous chimeric antigen receptor T-cells therapy used for patients with lymphoma: A systematic review and meta-analysis. *Medicine (Baltimore).* **98**, e17506 (2019).

57. Anderson, K. G., Stromnes, I. M. & Greenberg, P. D. Obstacles Posed by the Tumor Microenvironment to T cell Activity: A Case for Synergistic Therapies. *Cancer Cell* vol. 31 311–325 (2017).

58. Skrombolas, D. & Frelinger, J. G. Challenges and developing solutions for increasing the benefits of IL-2 treatment in tumor therapy. *Expert Review of Clinical Immunology* vol. 10 207–217 (2014).

59. Lu, P., Weaver, V. M. & Werb, Z. The extracellular matrix: a dynamic niche in cancer progression. *J Cell Biol* **196**, 395–406 (2012).

60. Richter, G. H. S., Mollweide, A., Hanewinkel, K., Zobywalski, C. & Burdach, S. CD25 blockade protects T cells from activation-induced cell death (AICD) via maintenance of TOSO expression. *Scand. J. Immunol.* **70**, 206–215 (2009).

61. Mortara, L. *et al.* Anti-cancer Therapies Employing IL-2 Cytokine Tumor Targeting: Contribution of Innate, Adaptive and Immunosuppressive Cells in the Anti-tumor Efficacy. *Frontiers in immunology* vol. 9 2905 (2018).

62. Dotti, G., Gottschalk, S., Savoldo, B. & Brenner, M. K. Design and development of therapies using chimeric antigen receptor-expressing T cells. *Immunol. Rev.* **257**, 107–126 (2014).

63. Canale, F. P. *et al.* CD39 expression defines cell exhaustion in tumor-infiltrating CD8+ T cells. *Cancer Res.* **78**, 115–128 (2018).

64. Bastid, J. *et al.* Inhibition of CD39 enzymatic function at the surface of tumor cells alleviates their immunosuppressive activity. *Cancer Immunol. Res.* **3**, 254–265 (2015).

65. Ziffels, B., Pretto, F. & Neri, D. Intratumoral administration of IL2-and TNF-based fusion proteins cures cancer without establishing protective immunity. *Immunotherapy* **10**, 177–188 (2018).

66. Parisi, G. *et al.* Persistence of adoptively transferred T cells with a kinetically engineered IL-2 receptor agonist. *Nat. Commun.* **11**, 660 (2020).

67. Caruana, I. *et al.* Heparanase promotes tumor infiltration and antitumor activity of CAR-redirected T lymphocytes. *Nat Med* **21**, 524–529 (2015).

68. D'Aloia, M. M., Zizzari, I. G., Sacchetti, B., Pierelli, L. & Alimandi, M. CAR-T cells: The long and winding road to solid tumors review-article. *Cell Death and Disease* vol. 9 (2018).

2 DISCUSSION

2.1 Assessment of the Influence of CAR Composition on In Vivo Functionality

Immunotherapy is an emerging tool for the therapy of tumors, due to the targeted cytotoxic potential of CAR T cells against cancer cells. This potential resulted in the FDA approval of to date four CAR T cell therapies for hematological malignancies after successful in vitro, in vivo, and clinical testing (Mullard 2021). CAR engineering can be facilitated in many different ways and each building block of a chimeric antigen receptor, antigen-binding, spacer, transmembrane, and signaling domains can originate from various immune or even non-immune cells (Fesnak et al. 2016). This variation may impact CAR T cell abilities. Side-by-side comparisons are missing for many CAR compositions and partially require fine-tailoring for specific tumor targets. Therefore, detailed analyses of specific building blocks are of high need to understand their full potential and enhance their efficacy against cancer cells.

2.1.1 Impact of CAR components on in vitro and in vivo performance

In order to analyze the impact of the extracellular spacer and antigen-binding domains on anti-tumor efficacy, side-by-side comparisons of differing CARs were carried out. For this purpose, we applied three CD20-redirected CAR constructs for the treatment of lymphoma, since the majority of new developments in the context of CAR T cells research is made in this tumor entity and other hematological malignancies, such as leukemia. Thus, leukemia and lymphoma are the most established models for cell therapy evaluations. We used CD20, a well-established immunotherapy target for hematological malignancies, as a CAR target by applying a CD20-specific scFv, derived from Leu16 (Polyak and Deans 2002; Shanehbandi et al. 2017). All three CD20-CARs had varying configurations of the extracellular domains, such as different V_h and V_l orientations of the scFv and IgG1- or CD8α-derived spacers, to dissect the influences of these building blocks.

The composition of CAR T cell phenotypes was similar between all three CARs and the mock control during the automated manufacturing process, showing that the varying extracellular domains had no influence on CAR T phenotype during CAR T cell production. For CAR T cell generation, $CD4^+$ and $CD8^+$ T cells were extracted from a non-mobilized leukapheresis. This initial CD4/CD8 enriched fraction contained many undifferentiated naïve T cells. A previously established protocol was applied to generate CAR T cells of the three CARs (Lock et al. 2017). This 12-day protocol is based on CD3-CD28-mediated cell activation and the IL-7/IL-15 stimulated expansion. It reduced the amount of naïve T cells and resulted in high amounts of

early differentiated T_{SCM} and T_{CM} cells in the finals cell products of all three CARs. In this way, the applied and improved protocol proved to be efficient for potent CAR T cell generation similar to other studies which have demonstrated that T cells with a memory phenotype, including $CD62^+$ $CCR7^+$ $CD45RA^+$ $CD45RO^+$ T_{SCM} and $CD62^+$ $CCR7^+$ $CD45RA^-$ $CD45RO^+$ T_{CM}, execute superior in vitro and in vivo tumor killing and induce a higher persistence and proliferation potential in comparison to differentiated $CD62^-$ $CCR7^-$ $CD45RA^+$ CD45RO- T_{EFF} cells (Liu, Sun, and Chen 2020). Additionally, the amount of $CD8^+$ T_{SCM} cells has been shown to determine the total capacity for tumor eradication more than the amount of exhausted $PD\text{-}1^+$ T cells in the finished cell product (Arcangeli et al. 2020; Jafarzadeh et al. 2020). The applied protocol, using IL-7 and IL-15 was previously validated in healthy donors and lymphoma patients, reaching sufficient amounts of memory phenotype CAR T cells in both groups (Lock et al. 2017). However, without any antigen stimulation during the manufacturing process, the composition of activation and expansion methods and cytokines had a higher impact on the phenotypes present in the final product than the introduced CAR receptor, as shown by comparisons of ex vivo CAR T cell expansion protocols (Gargett and Brown 2015). These protocols include activation with CD3 only or stimulation with IL-21 or the gold standard for T cell expansion, IL-2. Yet, a growing understanding for T cell homeostasis suggested that the applied dual stimulation with IL-7 and IL-15 rather than IL-2 mono-stimulation after CD3/CD28-mediated activation is beneficial for more robust conservation of early differentiated T_{SCM} cells during transgenic cell manufacturing and expansion (Kondo et al. 2018).

The phenotypically matching cell products of all three CARs translated into a similar cytokine expression profile and in vitro killing efficacy after antigen recognition in comparison to Mock T cells. Comparable amounts of pro-inflammatory Th1 cytokines, GM-CSF, IFN-γ, IL-2, and TNF-α were secreted by all CD20-redirected CARs. This goes in line with the main impact of the identical signaling and costimulatory domains CD3ζ and 4-1BB in all 3 CARs on cytokine secretion and killing. Only modestly delayed tumor progression caused by anergized first-generation CAR T cells, implied the addition of further costimulatory domains (Brocker and Karjalainen 1995). CD28 and the here applied 4-1BB costimulatory domains were the first in line for the creation of second-generation CAR T cells, due to their natural requirement for productive TCR activation or its maintenance, next to ICOS, OX40, or CD27 (Croft 2003; Shahinian et al. 1993). In terms of cytokine secretion after antigen stimulation, both CD28-CD3ζ and 4-1BB-CD3ζ CAR induce similar levels of Th1 cytokines, GM-CSF, IFN-γ, IL-2, and TNF-α then first-generation CAR T cells (Imai et al. 2004; Maher et al. 2002). While CD28-

CD3ζ CARs exhibit a faster release of Th1 cytokines than 4-1BB-CD3ζ CAR T cells, levels of tumor-favoring Th2 cytokines, including IL-4 and IL-10 were significantly lower in 4-1BB-CD3ζ CAR T cells (Guedan et al. 2014; Hombach and Abken 2011; Milone et al. 2009). Of note, excessive cytokine release might contribute to one of the most severe side effects of cell-based immunotherapy, the cytokine release syndrome (CRS) (Bonifant et al. 2016). Therefore, analysis of further parameters e.g. repeated killing or proliferation capacity might increase the safety profile of the evaluated CARs (Davenport et al. 2015; Garfall et al. 2019). Moreover, it has been shown, that too strong activation of CAR T cells can result in activation-induced cell death (AICD) (Green, Droin, and Pinkoski 2003). Nonetheless, short-term in vitro killing of leukemia cell lines was not strongly influenced by either CD28 or 4-1BB, as demonstrated by equal tyrosine phosphorylation patterns of CD3ζ, CD28-CD3ζ, or 4-1BB-CD3ζ CARs (Finney, Akbar, and Lawson 2004). Thus, they showed that the decision for 4-1BB and CD3ζ as costimulatory and signaling domains was advantageous for the preclinical development and influenced predominately the cytokine secretion after contact with and killing of antigen-positive $CD20^+$ JeKo-1, dependent on the target ratio despite the varying spacer and antigen-binding domains.

In vitro potential of the three CD20-redirected CARs, incorporating CD8α- and IgG1-derived spacers, for the treatment of hematological malignancies was demonstrated by efficient in vitro killing and cytokine expression. Subsequently, we compared the anti-tumor efficacy of the three CD20 CARs in a $CD20^+$ Raji lymphoma model in immunodeficient NSG mice. The established lymphoma was only efficiently eradicated by CD20_lh_CD8 and CD20_hl_CD8 CAR T cells, while the construct CD20_hl_IgG1 failed to demonstrate any impact on Raji lymphoma cell proliferation similar to Mock T cells. This is in agreement with past studies, which reported a trend, that CD8α-based spacer, as incorporated here, and CD28-based spacer execute a stronger anti-tumor efficacy than IgG1-based spacer (Jensen et al. 2010; Savoldo et al. 2011; Till et al. 2012).

Our results can be explained by the observation that interactions between Fcγ Receptor- (FcγR) expressing innate immune cells and the CH2 domain of IgG1 can prevent CAR T cell efficacy (Almåsbak et al. 2015). Mice, including NSGs, express one inhibitory FcγRIIb and three activating FcγRs (mFcγRI, mFcγRIII, and mFcγRIV) (Bruhns and Jönsson 2015). The majority of NSG immune cells are either absent or defective, but innate immune cells, such as monocytes, neutrophils, macrophages, and DC cells are still present and can interact with human IgGs (Clémenceau et al. 2015). Despite the functional impairment of NSG immune cells,

binding of human IgG1 by all murine FcγRs is still possible and might even lead to off-target activation of the CAR T cell or the respective FcγR$^+$ immune cell, eventually leading to AICD (Overdijk et al. 2012). We aimed to prevent this unspecific binding by modifications of the IgG1 spacer and replaced selected amino acids in the CH2 domain with the corresponding amino acids from the IgG2, which has a lower affinity to FcγRs than IgG1 (Hombach et al. 2010). Here, the modified IgG1 spacer successfully abrogated FcγR-mediated off-target activation of the CAR T cells by NSG macrophages derived from a peritoneal lavage. This was demonstrated by killing assays, where CD20_hl_IgG1 CAR T cells were able to efficiently eradicate Raji lymphoma cells in the absence or presence of NSG macrophages. But in this study, the abrogated interaction between the modified IgG1 spacer and the murine FcγR$^+$ immune cells did not translate into successful in vivo tumor eradication. Interactions of the here incorporated low-affinity residues derived from IgG2 with FcγRs might have been still strong enough to prevent further trafficking of CAR T cells to the tumor sites. Initial interactions with FcγR$^+$ tissue-resident innate immune cells, e.g. macrophages in the gatekeeper organs, lung, and liver, shortly after injection might have trapped the CAR T cells (Gordon and Plüddemann 2017; Li et al. 2016). This would explain the absence of CAR$^+$ T cells but the presence of CAR$^-$ T cells in our ex vivo flow cytometry analysis on day 20 of spleen, bone marrow, and blood of CD20_hl_IgG1 CAR T cell treated animals. In contrast, CAR$^+$ T cells were still present in spleen, bone marrow, and blood of CD20_lh_CD8 and CD20_hl_CD8 CAR T cell treated animals. However, others reported that similar modifications, introduced into IgG4-derived spacers, resulted in efficient tumor eradication and persistence (Hudecek et al. 2015; Jonnalagadda et al. 2015). This points in the direction of IgG1-specific or further underlying mechanisms, which prevent in vivo efficacy of CARs with IgG-based spacers. One example of these hindering mechanisms is the potential generation of immunogenic peptides by the human T cell itself, due to the introduction of murine scFvs, such as Leu16, or other non-self gene-products, which might elicit HLA-restricted and TCR-triggered fratricide of CAR-expressing T cells (Berger et al. 2006; Riddell et al. 1996). Therefore, further research would be necessary to increase the in vivo functionality of IgG1-based spacers and reveal the underlying mechanisms e.g. by evaluating the influence of different NSG immune cells from various tissues, the immunogenic capacity of CAR molecules, or the in-depth vivo behavior of CAR T cells.

Despite, the observed drawbacks of CD20_hl_IgG1-expressing CAR T cells, both CD20_lh_CD8 and CD20_hl_CD8 CARs exhibited a strong cytotoxic potential towards the lymphoma in the mouse model. Unfortunately, one of the mice in the CD20_lh_CD8 treated

group of the first in vivo comparative study developed a lymphoma localized in the jaw, which is hardly accessible for CAR T cells and in this way difficult to treat. Accordingly, the first and second in vivo analysis of CD20_lh_CD8 and CD20_hl_CD8 CAR T cells demonstrated the minor influence of the scFv orientation, in contrast to the strong influence of the spacer domain on CAR T cell in vivo efficacy. Here, both CARs, including a CD8α spacer, showed a robust and durable anti-tumor activity. This is in line with previous studies using 4-1BB-CD3ζ CARs, in which this combination was proven to be superior to other first- but similar to other second-generation CAR T cells in terms of tumor eradication (Brentjens et al. 2007). Thus, taken together the application of 4-1BB-CD3ζ CARs in the well-established lymphoma model has proven its strong potential for hematological CAR T cell therapy by the efficient in vivo tumor eradication. However, some reports have also shown a higher risk for constitutive T cell activation or tonic signaling of 4-1BB-CD3ζ CARs, leading to accelerated T cell differentiation and exhaustion, compared to other second-generation CARs, depending on the scFv or applied vector system (Song et al. 2011). The CAR composition requires the integration of 4-1BB in a rather unnatural dimeric structure, which enables easier activation of downstream TCR signaling by the already partially altered conformation, depending on scFv orientation or spacer domain (Chattopadhyay et al. 2009; Van Der Stegen, Hamieh, and Sadelain 2015). Certain viral vectors might also contribute to tonic signaling of T cells (Gomes-Silva et al. 2017). Nonetheless, the here evaluated scFv orientations in combination with the spacer domains of CD8α and IgG1 were not prone to induce tonic signaling. In contrast, we found long-lasting persistence of CD20_lh_CD8 and CD20_hl_CD8 CAR T cells, demonstrated by their presence in blood, bone marrow, and spleen of treated animals on day 20. The persistence is a decisive and special characteristic of 4-1BB-CD3ζ CAR T cells in comparison to other second-generation CARs (Carpenito et al. 2009). Multiple mechanisms are in discussion as a reason for this favorable feature of 4-1BB-CD3ζ CARs, including lower expression of pro-apoptotic factors, a persistent increase of telomerase activity, or reduced exhaustion and apoptosis upon repeated antigen stimulation (Fan et al. 2021; Van Der Stegen et al. 2015). This question has not yet been answered, albeit growing preclinical and clinical knowledge of third-generation CAR T cells further supports an underlying benefit for incorporation of 4-1BB to enhance persistent CAR T cells circulation and efficacy (Guedan et al. 2018). In-depth side-by-side comparisons might resolve the reason.

All in all, CD20_lh_CD8 and CD20_hl_CD8 were confirmed as potential candidates for further clinical transfer. Nonetheless, the displayed results illustrated the influence of the various CAR building blocks on in vitro and in vivo characteristics, although in vitro analysis alone is not yet

able to fully predict in vivo performance. This became clear early on, when the failed in vivo activity of first-generation CAR T cells encouraged the establishment of second, third, and further generations of CARs (Brocker and Karjalainen 1995). The lack of in vitro to in vivo transferability requires the further improvement and fine-tailoring of preclinical CAR T cell validation methods, to ensure a higher safety level before translation into first-in-human trials.

2.1.2 Development of a Novel Spacer Class Derived from the Siglec family

Since comparison of CD20-redirected CARs in the lymphoma mouse model demonstrated the crucial influence of the spacer domain on in vivo efficacy, we choose a comparatively long spacer derived from IgG1. In contrast to our expectations, this did not translate to a superior in vitro or sufficient in vivo functionality. This decision was supported by previous studies, which demonstrated that membrane-proximal targets, such as CD20 expressed on blood cancer cells, require a longer spacer in contrast to membrane-distal targets, to ensure the optimal distance between target and effector cell surface (Guest et al. 2005; Haso et al. 2013; Hudecek et al. 2013; James et al. 2008). The importance of an optimal distance between CAR T cell and target cell can be explained by the fact, that the spacer domain has to mimic the optimal inter-membrane distance between effector:target to form a functional immunological synapse, as naturally occurring between TCR and MHC (Hudecek et al. 2015). Targeting of CD20 should have benefited from the usage of a long spacer, such as IgG1, compared to our second spacer the short but highly flexible CD8α spacer, which allows the binding of inaccessible epitopes (Wilkie et al. 2008). However, none of the approved cell therapies uses a disadvantageous IgG-based spacer, contributing to a shortage of unimpaired spacers for membrane-proximal targets. Therefore, we aimed to develop a functional spacer class for these targets.

We performed a literature screening of various receptors, expressed on immune and non-immune cells to identify possible candidates for the novel spacer class. Our screening determined the sialic acid-binding immunoglobulin-type lectin (Siglec) family as a suitable option for CAR spacers due to Ig-like receptor modularity and expression profiles on various immune cells (MacAuley, Crocker, and Paulson 2014). The receptors of the Siglec family consist of a V-set Ig-like domain at the N-terminal end and a varying numbers of C2-set domains, as adaptive spacers, at the C-terminus (Bornhöfft et al. 2018). Following the principle of the adaptation of the spacer length to the location of the epitope, depending on the respective target, we selected one, two, or three C2-sets derived from Siglec-3, -4, -7, or -8 for evaluation of the new spacer class. Similar amounts of C2-set were also previously tested in IgG-derived spacers for transgenic cell therapy (Clemenceau et al. 2015; Watanabe et al. 2016). Yet,

exaggerated spacer shortening might eventually lead to signaling abrogation (McComb et al. 2020). The designed Siglec spacer length ranged between 280 aa (Siglec-4) to 119 aa (Siglec-3), similar to 230 aa of full-length IgG spacers in comparison to the 45 aa of the short but highly flexible and versatile CD8α spacer.

In this way, we replaced the CD8α domain of the previously analyzed anti-CD20_hl_CD8α_4-1BB-CD3ζ CAR with the novel Siglec-derived spacers. Subsequently, we performed CAR expression in HEK and T cells in comparison to the original CAR. While expression in HEK cells was only modestly influenced by the respective Siglec spacers, some CARs were not expressible in T cells. Thus, testing more than one Siglec-derived spacer was convenient due to the possible impact of the "inert" depicted hinge and transmembrane domains on CAR expression levels. However impact of the transmembrane domain was shown to be more influential than the spacer domain, especially for dimerization and subsequent signal transduction (Muller et al. 2021). The spacer domain might control the modality of CAR expression by membrane transport efficacy of the CAR, while the transmembrane domain is thought to regulate the amount of CAR signaling by controlling the CAR surface expression level (Fujiwara et al. 2020). Nonetheless, this was only evaluated by comparisons of the established spacer and transmembrane domains, including CD3, CD4, CD28, or CD8α, and might vary in so far untested combinations. We further investigated the in vitro functionality of Siglec spacers with beneficial expression patterns in T cells, such as Siglec-4, Siglec-7.2, and Siglec-8. By evaluating degranulation, cytokine, and exhaustion marker expression after coculture with Raji cells, we revealed the comparable in vitro functionality of the longest Siglec-4 spacer, with a total of three C2-sets, to the established CD8α spacer. Neither the Siglec-7.2 nor the Siglec-8 spacer were too short to induce activation of transduced T cells. On one hand, we proved in vitro the principle for membrane-proximal targets, but on the other hand, the experimental setup was not fully appropriate for further evaluation of the feasibility of Siglec-7.2 and Siglec-8 to be used as possible short spacers for membrane-distal epitopes. Further experiments with membrane-distal targets would be necessary to evaluate the full potential of both spacers for efficient CAR T cell therapy.

This distance-dependent spacer principle was further challenged by the translation to a PDAC model. Thus, we compared the Siglec-4 spacer to the CD8α spacer and a modified version of the IgG4 spacer in a 4-1BB-CD3ζ CAR setting. However, the applied IgG4 spacer needs adjustments to abrogate interactions with $Fc\gamma R^+$ murine immune cells. Hudecek et al. described mutations, which successfully blocked interactions of IgG4-based CAR spacers with $Fc\gamma R^+$ -

expressing immune cells (Hudecek et al. 2015). CARs were redirected against CD66c and TSPAN8, two newly discovered targets for the immunotherapy of PDAC (Schäfer et al. 2021). While the here applied scFv for TSPAN8 is redirected to a membrane-proximal epitope, like CD20, the scFv redirected to CD66 binds a membrane-distal epitope. In vitro cytotoxicity assays showed a pronounced cytotoxic potential against AsPC1 PDAC cells of all tested CARs, besides CD66c_lh_Sig4 CAR T cells. Endpoint analysis of cytokine and exhaustion marker expression confirmed the infunctionality of CD66c_lh_Sig4 CAR T cells, by low expression of Th1 cytokines, IL-2, TNF-α, GM-CSF and IFN-γ and exhaustion markers, LAG3, PD1, and 4-1BB. We showed with this examination of killing capacity, Th1 cytokine expression, and exhaustion markers the selectivity of the long Siglec-4 spacer towards membrane-proximal targets. The inferiority of IgG-based spacers was confirmed by in vitro evaluation in the PDAC model. Interestingly, cytokine and exhaustion marker expression profile was tremendously lower in TSPAN8_hl_Sig4 transduced T cells compared to TSPAN8_hl_CD8 CAR T cells at similar levels of cytotoxicity against $TSPAN^{+}$ AsPC1 cells. Thus, an extension of in vitro analysis by the inclusion of exhaustion markers LAG3, PD1, and 4-1BB proved to be practical to increase the safety and well-balanced analysis of the CARs for potential clinical transfer (Garfall et al. 2019). By examining the vivo efficacy of Siglec-4, CD8α, and IgG4 spacers incorporated into TSPAN8-redirected CAR T cells in a xenograft PDAC mouse model, we found that all three CARs showed an anti-tumor efficacy of varying strengths. Both TSPAN8_hl_CD8 and TSPAN8_hl_Sig4 CAR T cells were able to eradicate the pancreatic tumor completely within a short time frame. TSPAN8_hl_IgG4 transduced T cells were efficient to control tumor growth of AsPC1 cells but did not induce full tumor clearance. Ex vivo analysis further reinforced the beneficial exhaustion marker and cytokine expression profile of TSPAN8_hl_Sig4 CAR T cells. Our in vivo and ex vivo results showed reduced pro-inflammatory Th1 cytokine secretion and low expression levels of exhaustion markers in TSPAN8_hl_Sig4 CAR T cells. These CAR T cell characteristics are associated with a better clinical prognosis due to the reduced risk for severe CRS (Bonifant et al. 2016; Gust et al. 2020). Nevertheless, the overall amount of ex vivo retrieved TSPAN8_hl_Sig4 transduced CAR T cells was decreased compared to TSPAN8_hl_CD8 CAR T cells, indicating a lower in vivo proliferation due to comparative injected cell numbers at the start of the experiment. But the T cells of TSPAN8_hl_Sig4 CAR T cell treated animals displayed a more favorable early differentiated T_{CM} phenotype, which has been found by others in lymphoma models to be associated with a higher proliferative capacity (Liu et al. 2020). Differences of TSPAN8_hl_Sig4 and TSPAN8_hl_CD8 CAR T cell expression profiles demonstrate the

importance of the knowledge of exhaustion marker profiles in response to CAR generation or target cell contact for further preclinical in vivo studies. However, many reasons for the observed differences between TSPAN8_hl_Sig4 and TSPAN8_hl_CD8 CAR T cells are possible and should be addressed before a potential clinical transfer of TSPAN8_hl_Sig4 CAR T cells. One possible explanation is the previously discussed influence of the spacer domain on the membrane transport efficacy of the CAR (Fujiwara et al. 2020). Preclinical and clinical studies have evaluated the steering influence of CAR surface density on in vivo efficacy and activation (Ho et al. 2021; Walker et al. 2017). In the future, comparisons of CAR densities on TSPAN8_hl_Sig4 and TSPAN8_hl_CD8 CAR T cells as well as other examinations, e.g. to analyze Siglec-4 spacer interactions with cell surface ligands, have to be performed to validate this hypothesis. Whereas further research is mandatory for clinical transfer, Siglec-derived spacers were successfully established in hematological and solid tumor settings.

2.2 Imaging of CAR T cell therapy

One contributing factor for the limited success of cell therapy in PDAC (Akce et al. 2018) is the reduced accessibility for CAR T cells in solid tumors, due to the TME, which is most pronounced in PDAC (M M D'Aloia et al. 2018; Ho, Jaffee, and Zheng 2020). Here, imaging methods are versatile and useful tools to detect, quantify and visualize transgenic cells and enable the tracking of cells in vivo, thereby promoting translational research. However, established preclinical research methods, such as flow cytometry, do not facilitate longitudinal or spatial analysis, which is indispensable for examining CAR T cells within the structure of solid tumors or inside an animal model. Thus, this study aimed to establish and apply imaging tools that, provide longitudinal and spatial information, for the in vivo and ex vivo tracking of CAR T cells in a subcutaneous tumor PDAC mouse model to support clinical translation of CAR T cells for pancreatic cancer.

2.2.1 In Vivo Tracking of CAR T cells by 2D BLI and 3D BLT Imaging

We generated new CARs, suitable for lentiviral transduction of transgenic cells, to perform spatiotemporal in vivo tracking of CAR T cells. Two scFvs were chosen for the application in a PDAC model. One of the selected scFvs, derived from the chimeric monoclonal antibody C225, was redirected to the epidermal growth factor receptor (EGFR) (Prewett et al. 1996). EGFR is a crucial driver of tumorigenesis in many solid tumors, including PDAC (Durkin et al. 2003; Nedaeinia et al. 2014). A second scFv was selected as target unspecific but functional control, in contrast to an unspecific mock control. The chosen scFv was created based on an internal humanized antibody clone MB101, specific for blood dendritic cell antigen 2 (BDCA-

2). In contrast to EGFR, BDCA-2 is not expressed on established PDAC cell lines, including AsPC1, but is exclusively expressed on the surface of human plasmacytoid dendritic cells (pDC) (Dzionek et al. 2000). Generated scFvs were fused to the previously applied combination of flexible CD8α spacer and transmembrane domains, as well as to the 4-1BB costimulatory and CD3ζ signaling domains. This second-generation CAR sequence serves currently as the standard for clinical trials in PDAC (DeSelm et al. 2017). The second-generation CARs were further connected via a furin-P2A self-cleaving site with the click beetle red luciferase gene (CBR2opt) for cell tracking.

Subsequently, we evaluated the in vivo biodistribution of the newly generated CARs in 2D and 3D in a subcutaneous PDAC xenograft model, using the previously described AsPC1 pancreatic cancer cell line. 2D tracking of CAR T cells enabled the visualization and quantification of the bioluminescent signal from dorsal, ventral and tumor ROIs. Two hours after CAR T cell intravenously injection via the tail vein, CAR T cells of both treatment groups had mainly accumulated in the lung and partially in the liver. These organs are the first to pass, when cells are injected via the tail vein (Fischer et al. 2009). A clear visible 2D BLI signal was detected in injected mice, depicting CAR T cell localization in these organs. Here, CBR2opt luciferase proved its enhanced potential. One of the disadvantages of standard firefly luciferase combined with D-Luciferin is the low emission for cell tracking in deeper tissues, such as the lung (Weissleder and Ntziachristos 2003). Even at the comparatively low cell number of $5x10^5$ CAR^+ T cells, imaging of lung-infiltrating CAR T cells was facilitated by CBR2opt plus D-Luciferin. This validated the rational selection of the recently established CBR2 mutant, from the range of available luciferase (Hall et al. 2018). When paired with D-Luciferin, this mutant version emitted significantly more photons per second when paired with D-Luciferin in comparison to standard firefly luciferase in a C57BL/6 black mouse model. The size and protein content of natural and modified T cells highlight the need for a bright and strong luciferase/substrate combination (Lin and Amir 2018). Furthermore, CBR2opt offers an extended emission spectrum in the near-infrared area when paired with the novel substrate naphthyl-luciferin (Hall et al. 2018). Thus, CBR2opt was shown to facilitate deep tissue imaging or dual imaging with other luciferase/substrate combinations (Zambito et al. 2021).

Applying this 2D and 3D BLI imaging approach, we showed after therapy induction, a different biodistribution pattern of BDCA-2 and EGFR CAR T cells in vivo. While BDCA-2 transgenic cells infiltrate the spleen first, target-specific EGFR CAR T cells home directly to the tumor within the first week. During the second and third weeks of the experiment, BDCA-2 CAR T

cells proliferated in the treated mice. At the same time, EGFR CAR T cells proliferated primarily at the tumor site and only to a limited extent in the spleen and in the third week in the abdomen. 2D ventral and dorsal ROI quantifications confirmed the observed increased proliferation of target unspecific BDCA-2 CAR T cells.

Besides the well-established 2D BLI measurement, we performed, to our knowledge, the first longitudinal 3D BLT study to assess CAR T cell treatment in mice. The visualization of 3D measurements recapitulated the 2D visualization in a more detailed and accurate manner, due to the 3D perspective. On day 0, two hours after injection, all treated mice showed a clear signal cloud inside the thorax. Some mice even displayed a slight branching of the signal in the center, indicating accumulation of T cells in both parts of the lung or exhibited a second signal peak in the upper abdominal area, presumably arising from the presence of T cells within the liver. Furthermore, 3D BLT imaging enabled the clear presentation of the tumor-infiltrating EGFR-redirected CAR T cells on day 6, whereas, BDCA-2 specific CAR T cells were mainly found in the spleen. Spleen homing and proliferation of EGFR CAR T cells in the spleen, was only detected after day 13. However, towards the end of the study, the acquired and reconstructed bioluminescence signals declined inaccuracy due to the strong proliferation of CAR T cells in the whole mouse induced by the onset of GvHD, as proven by 2D ex vivo examination of the organs. Both, 2D BLI and 3D BLT enabled a coherent in vivo biodistribution analysis of EGFR and BDAC-2 redirected CAR T cells, albeit 3D BLT provided additional spatiotemporal information. Only a few other cell tracking studies of solid tumor redirected CAR T cells in mice have been reported so far, since the majority of CAR T cell research work includes only endpoint analysis of CAR T cell localization and BLI is mainly applied for tumor control examination. These few studies use different imaging modalities or culture protocols and reported a slightly divergent biodistribution pattern of solid tumor redirected CAR T cells to our results (Lee et al. 2020; Sellmyer et al. 2019; Torres Chavez et al. 2019). Sellmyer et al. performed CAR T cell tracking in NSG mice with PET reporter genes and the applied GD2 4-1BB-CD3ζ CAR T cells homed within the first 7 days to the spleen before redistributing to the $GD2^+$ subcutaneous tumors in the upper back area at day 13 (Sellmyer et al. 2019). Torres Chaves et al. detected primarily trafficking of PSCA-redirected CD28-CD3ζ CAR T cells to the subcutaneous Capan-1 tumor at day 7 in NSG mice, using 2D BLI, but did not analyze the spleen or further cell biodistribution (Torres Chavez et al. 2019). Lee et al. performed PET CT-based cell tracking in a solid Raji lymphoma mouse model and confirmed a strong accumulation in lung and liver two hours after injection and a shift to the spleen from day 1, but could not detect any CAR T cells in the tumor until the endpoint of the experiment at day 7 (Lee et al.

2020). Importantly, PET-CT imaging enables a more precise quantification of in vivo signal distribution, whereas BLT imaging enables more frequent measurements. Furthermore, different CAR T cell generation or culturing conditions, as well as co-transduction with PET reporter genes, may have resulted in these differing biodistribution patterns in vivo, e.g. due to altered CAR T cell phenotypes. Further extensive research is needed to reveal the underlying mechanisms of the differing biodistribution patterns of the CAR T cells.

2D BLI and 3D BLT measurements of the tumor ROI or the segmented tumor enabled the quantification of the antigen-dependent proliferation of EGFR CAR T cells. This proved again the sufficient anti-tumor efficacy of 4-1BB-CD3ζ second-generation CARs as described in 2.1. and in the literature (DeSelm et al. 2017). Despite the clearly visible signal peak in EGFR CAR T cell treated mice, 2D BLI quantification displayed a similar increase of bioluminescence in BDAC-2 CAR T cell treated animals. The unspecific proliferation of BDCA-2 CAR T cells in the intestine may have interfered with the technical signal detection of the 2D tumor ROI. In contrast to 2D BLI, reconstruction and tumor segmentation of 3D BLT signals enabled the efficient detection of proportional CAR T cell tumor homing and antigen-recognition induced proliferation of EGFR CAR T cells at the tumor site. Thus, 3D BLT imaging could potentially facilitate a more distinct dissection of tumor homing and anti-tumor efficacy mechanisms or toxicities of various CARs, as described in 2.1., to support the understanding of underlying processes and to assist the clinical translation of cell therapy research. Furthermore, CT-supported tumor size assessment is more accurate than 2D caliper measurements as demonstrated here. Nonetheless, the application of CT measurements for the replacement of 2D assessment without any further 3D imaging does not justify the effort and expenses.

Further quantification of the 3D BLT signal increase over time in the whole mouse and other organs confirmed the strong proliferation of target-unspecific BDCA-2 CAR T cells, which was also strengthened by the 2D BLI dorsal and ventral ROI quantification. Unfortunately, technical signal reconstruction problems prevented a successful evaluation of the spleen signal, but improvements of technical reconstruction methods are still ongoing. Nonetheless, both 2D and 3D signal quantification showed a differently pronounced initial signal reduction of EGFR CAR T cells, which was not observed in BDCA-2 CAR T cell treated animals. The initial signal loss detected between day 3 and day 10 in EGFR CAR treated animals contrasted the strong proliferation at the tumor site during the same period. EGFR CAR T cell death may have resulted from stress induced by the preparation and injection procedure combined with activation-induced cell death (AICD) (Künkele et al. 2015). The proportional contribution of

each factor needs to be further evaluated. The previously discussed research studies in the context of the in vivo biodistribution of CAR T cells did not include any comparable longitudinal measurements between day 0 and day 7 (Lee et al. 2020; Sellmyer et al. 2019; Torres Chavez et al. 2019). The missing BLI signal decrease of BDCA-2 CAR T cells points to a scFv dependent influence, these cells started early on to proliferate, although injected CAR T cells number was comparatively low and human BDCA-2 is not expressed in mice (Dzionek et al. 2000). Multiple factors could have contributed to the unspecific proliferation. As previously discussed, tonic signaling is a risk factor of 4-1BB-CD3ζ CARs in contrast to other second-generation CARs, which can also induce early exhaustion (Chattopadhyay et al. 2009; Gomes-Silva et al. 2017; Song et al. 2011; Van Der Stegen et al. 2015). However, over the course of this experiment weight loss in both groups started as early as two weeks after the start of the experiment and endpoint ex vivo organ imaging in both groups confirmed strong bioluminescence signals in similar organs, including intestine, lung and ovaries. These organs, together with the liver, are some of the most prevalent organs associated with xenogeneic GvHD (Shrestha et al. 2020). Although a scFv specific effect cannot be fully excluded, a donor-dependent influence might have further contributed to the strong unspecific proliferation and early on-set of GvHD. Another contributing factor to GvHD could be a low transduction efficiency caused by the extended construct size, resulting in the injection of high numbers of untransduced T cells (Kumar et al. 2001). However, all virus-based CAR T cell generation techniques depend on high viral titers and transduction efficiencies decrease with the increasing size of the construct. Other CAR generation methods, such as transposons or electroporation-based systems do not have the same size restraints and can facilitate the gene transfer of advanced CARs, without the requirement of double transduction or the risk of low transduction efficiencies (Almåsbak et al. 2011; Huang et al. 2008).

These gene transfer techniques could also be beneficial for the evaluation of reasons for the unspecific proliferation of BDCA-2 CAR T cells or the life cycle and localization of CD20_IgG1_4-1BB-CD3ζ CAR, described previously, due to the expanded construct options. Nonetheless, tracking of CD20_IgG1_4-1BB-CD3ζ CAR T cells with CBR2opt, could already reveal the possible interaction location of FcR^+ expressing cells and CAR T cell interaction. Moreover, luciferase genes of choice could be expressed under the control of an inducible promotor, activated by the CAR signaling after target recognition. While other promotors are under investigation, the nuclear factor of activated T cells (NFAT) promotor is the most established inducible promotor for T cells (Uchibori et al. 2019). During activation of CD3ζ and CD28 containing CARs, downstream signaling promotes the transcription of NFAT

regulated genes, after activation by phosphatase calcineurin (Serfling et al. 2006). Luciferase expression regulated by the NFAT promotor combined with BLT imaging could indicate unspecific cell activation by tonic signaling, in case of BDCA-2 CAR T cells, or activation in specific organs, such as lung or liver, in case of CD20_hl_IgG1_4-1BB-CD3ζ CARs. This would pave the way for further selection of proteomic, transcriptomic or genomic examinations to obtain insights into the underlying mechanisms.

NFAT regulated activation analysis would also be advantageous for PET CT imaging, a technique that has been widely applied for CAR T cell tracking. Multiple reporter genes and probes have been validated in preclinical studies and later applied in clinical trials e.g. analyzing herpes simplex virus type 1 thymidine kinase with 9-[4-[18F]fluoro-3-(hydroxymethyl)butyl]guanine (NCT00730613 and NCT01082926) (Krebs et al. 2020). So far, NFAT regulated activation has mainly been applied in the context of TCR dependent mechanisms and in vivo CAR T cell activation was evaluated with ICOS-redirected antibody-based PET (Ponomarev et al. 2001; Simonetta et al. 2021). These studies showed the high accuracy of PET CT imaging in detection of CAR T cell activation. By contrast, 3D BLT is not as advanced and established as clinical transferable PET imaging and still needs some improvements, as demonstrated by the problematic signal reconstruction of the spleen or the decreasing specificity at the end of our study caused by the on-set of GvHD. Other groups are actively working on improvements to overcome the current drawbacks (Bentley, Rowe, and Dehghani 2020; Feng et al. 2008; Zhang et al. 2018). Despite these challenges, we demonstrated that, hybrid 3D µCT/BLT is an alternative isotope-free tomography tool for preclinical CAR T cell tracking. Additionally, some BLT devices already enable an easy dual optical imaging of sequential BLT and fluorescence molecular tomography (FMT), encouraging combinatorial preclinical research. Further advantages of BLT imaging as compared to PET-CT are the cost-efficiency, an easy usage, the stability of the luciferase and the luciferin storage conditions.

Further technical and biochemical improvements of devices, filters, reconstruction patterns and luciferase/substrate combinations might be able to further compensate the current drawbacks, and the more frequent longitudinal measurements, as well as the benefits of non-radioactive methods, justify the continued development of BLT imaging.

2.2.2 Ex Vivo Tracking of CAR T cells by LSFM and Cyclic Immunofluorescence

While in vivo bioluminescence enabled a whole-body spatiotemporal imaging of CAR T cells, resolution on a cellular level is missing but essential for solid tumor and TME redirected

research. Thus, in vivo tracking was subsequently followed by ex vivo tracking using light-sheet fluorescence microscopy (LFSM) and cyclic immunofluorescence stainings. We performed LFSM using a fluorescent anti-CD3 antibody and rhodamine lectin for vessel visualization with tumors taken out on day 6 and day 13. An additional channel detected the autofluorescence of the tumor tissue for tumor segmentation. Information combined from all three channels enables the spatial resolution and proportion of $CD3^+$ T cells inside the tumor as well as distance measurements between T cells, vessels, and tumor surface. Intratumoral T cell distribution differed depending on treatment with either target-specific EGFR or target-unspecific BDCA-2 CAR T cells. In alignment with 2D BLI and 3D BLT visualizations, on day 6 only a few $CD3^+$ T cells infiltrated the tumor in BDCA-2 CAR T cell treated animals. At the same time, $CD3^+$ T cells of EGFR CAR T cell treated animals had infiltrated one-half of the tumor, potentially originating from larger feeding vessels at the bottom half of the tumor, which was close to murine back muscles. During the next week, the antigen-recognition-induced proliferation of $CD3^+$ T cells in the EGFR group resulted in the full infiltration of the tumor. At the same time, the amount of $CD3^+$ T cell in the BDCA-2 treated tumor increased, potentially fueled by the discussed unspecific proliferation, and ongoing in vivo biodistribution of CAR T cells. Further staining profile analysis of CD3 and rhodamine lectin staining patterns confirmed that the majority of T cells was either present at the tumor margin or in close proximity to the larger feeding vessels.

Besides the visualization, we quantified and compared signals of each channel. $CD3^+$ covered volume analysis demonstrated the low proportion of tumor-infiltrating T cells in the target unspecific group, whereas $CD3^+$ T cells of the EGFR CAR T cell treated group which had homed to the tumor, proliferated and further penetrated the tumor alongside the larger feeding vessel. Over time, almost 15% of the EGFR treated tumor was infiltrated with $CD3^+$ T cells. Of note, at that time point, antigen-dependent proliferation and active killing were already decreasing and some $CD3^+$ T cell may have died due to AICD or could have been exhausted, contributing to the problematic in vivo persistence of CAR T cells, especially in the TME of solid tumors (Borghans and Ribeiro 2017; Nakajima et al. 2019). Nonetheless, the amount of $CD3^+$ T cells in the tumors of the EGFR group was still two times higher than the amount measured in the BDCA-2 group, which also increased over time. It has long been known that some mechanisms, MHC-dependent and -independent, support tumor cell recognition, activation, and proliferation, without an additional CAR or specific TCR (Golby, Chinyama, and Spencer 2002; Katz and Rabinovich 2020; Tietze et al. 2012). These could have contributed to a target-independent proliferation of BDCA-2 at the tumor.

Higher resolution on day 6, caused by the larger tumor size on day 13 and the subsequent requirement of a larger objective, enabled another evaluation method for $CD3^+$ T cell with the Imaris "Spot Detection" tool and more examination options. We segmented the detected $CD3^+$ spots and thereby facilitated the estimation of $CD3^+$ T cells in the tumor core and periphery. In both treatment groups, the majority of T cells were located in the tumor periphery and did not efficiently enter the tumor core. However, the low total number of $CD3^+$ T cells in BDCA-2 may be falsely interpreted into a better tumor infiltration capacity. Distance measurements of each $CD3^+$ spot to the tumor surface proved that $CD3^+$ T cells of the EGFR treated group managed to infiltrate deeper into the tumor, while target specificity did not induce increased infiltration from the vasculature. This emphasized a central problem for CAR T cells in solid tumors but also introduced a tool to analyze CAR-related improvements to overcome these barriers e.g. as presented in the context of heparan sulfate degrading CAR T cells (Caruana et al. 2015).

As demonstrated here, LFSM offers various analysis options, such as color-rendering of single cells based on distinctive characteristics, covered area and distance measurements and generation of diverse layers. This enabled an in-depth spatial investigation of CD3+ T cells within the tumor. However, the unorganized architecture of the tumor and its vasculature can impede the resolution of the stainings and the distance measurements between the reconstructed cell surface and vessel network (Jain 2013). Unregulated tumor growth in different dimensions inhibits the direct comparison of tumor surface distances to a certain structure, unless the tumors have comparable volumes. Evaluation of vasculature-related reconstructions and measurements are also complex, since tumor vasculature networks grow highly unregulated and vessels close to each other are difficult to distinguish for data interpretation. Moreover, LSFM has a limited number of channels. Cyclic immunofluorescence confirmed and extended the here gained data from LSFM, in terms of $CD3^+$ and vessel distance. This emphasized the relevancy of this combination, which is required to increase the amount of accessible data, especially in the context of the complex TME of solid tumors. Furthermore, co-expression or -labeling, as well as induction of fluorescent protein expression, could extend LSFM options (Ueda et al. 2020). Whole mouse clearing approaches might be able to provide a full bridging between whole mouse and cellular level cell tracking for in-depth and toxicity-related insight in preclinical research (Cai et al. 2019). Another solution to connect whole-body and cellular CAR T cell tracking is intravital two-photon microscopy. This technique has a deep tissue penetration due to the absorption of near-infrared photons and low scattering but often requires the technically challenging engraftment of an intravital window (Ishii and Ishii 2011). Some groups provided

interesting insights into CAR T cell persistence and functionality in hematologic tumor models by the application of this technique for single-cell tracking with multiple colors (Cazaux et al. 2019; Mulazzani et al. 2019; Murty et al. 2020). Nevertheless, solid tumor and TME aimed research may benefit from a spatial whole tumor analysis, which is not fully possible with two-photon microscopy depending on tumor size or stage. Thus, a combination of LSFM and cyclic immunofluorescence was used in this study. Each method requires currently an individual tumor and therefore results in a lower sample size, while a workflow combination of both methods is still under development. Tissue clearing and dehydration are necessary steps for LSFM which use reagents that potentially interfere with antigen retrieval in cyclic immunofluorescence staining, the latter enabling in-depth ex vivo phenotyping of CAR T cells and the TME. Still, microscopy-based ex vivo CAR tracking by 2-photon microscopy or LSFM/cyclic immunofluorescence is inevitable and necessary for CAR engineering research in solid tumors.

2.3 Supporting CAR T cells in TME of PDAC

Essential T cell functions, such as penetration, proliferation and differentiation are highly impaired in the TME (Anderson, Stromnes, and Greenberg 2017). Therefore, CAR T cell therapy faces various barriers especially in solid tumors e.g. PDAC with its dense and immunosuppressive TME (Chu et al. 2007). We combined in vivo and ex vivo CAR T cell tracking strategies to facilitate the analysis of local and systemic IL-2 effects as well as on the cellular level as a possible and exemplary support strategy for CAR T cells in the TME. In vivo tracking of CAR T cells revealed a systemic effect of subcutaneous IL-2 injections at the tumor site on the whole-body level. 2D and 3D bioluminescence imaging revealed significantly higher signals in BDCA-2 + IL-2 CAR T treated animals, as displayed by 2D ventral and dorsal ROI or segmented whole mouse signal quantification. During the initial treatment phase, IL-2 co-treated EGFR or BDCA-2 CAR T cell treated animals displayed increased bioluminescent signals compared to the groups without additional IL-2 support, indicating higher live cell numbers in these treatment groups. Comparison of signals in the segmented whole-body, tumor, and liver ROIs showed that IL-2 prevented the cell loss due to the injection procedure in both groups and further increased target unspecific expansion of BDCA-2 CAR T cells. This effect reduced the likelihood of AICD as a strong contributor to early signal loss in EGFR treated groups, since AICD is enhanced by excess IL-2 (Richter et al. 2009). Despite the systemic effect of local IL-2, treated mice did not experience any side effects. Nevertheless, local IL-2 was not

able to increase the amount of CAR T cells at the tumor significantly, neither in EGFR nor in BDCA-2 CAR T cell treated animals on a whole-body level or to enhance anti-tumor efficacy of EGFR CAR T cells.

But, visual examination of LSFM data exhibited an influence of IL-2 on CAR T cell infiltration into the tumor on the cellular level in both CAR T cell treatment groups. However, the majority of $CD3^+$ cells was still located at the tumor margin or in proximity to the large feeding vessels. Quantification of LFSM-based ex vivo tracking pointed to first disadvantages of local administration of IL-2 support. At an early time point, day 6, the EGFR + IL-2 treated animal showed more $CD3^+$ covered volume within the tumor than the EGFR CAR T cell treated animal without any IL-2 support. Analysis of the later time point 6 days after the last IL-2 injection revealed fewer $CD3^+$ T cells in the target-specific and IL-2 supported group compared to the target-specific group without IL-2. Proportional covered volume was also analyzed in BDCA-2 treated animals, but the initial target-specific effect of the EGFR CAR T cells was not sustained until day 13. Spot detection-based measurements indicated the IL-2 dependent expansion of $CD3^+$ T cells in the tumor margin in both groups as validated by higher cell numbers in the defined periphery and closer proximity to the tumor surface and a reduced T cell infiltration rate in deep tissue. However, limited channels of LFSM hampered the detailed identification of the underlying mechanism, e.g. by costaining of activation markers.

Cyclic immunofluorescence stainings provided more insight into the impact of IL-2 on tumor-infiltrating CAR T cells. An enhanced number of co-localizations of $CD3^+$ with activation (e.g. CD28), and proliferation (Ki67) markers was detected on cells in tumor tissue of the EGFR + IL-2 group in comparison to the EGFR group at day 6. Thus, the applied local IL-2 potentially induced in our study a short-term expansion of $CD3^+$ T cells in the tumor periphery, but at the cost of a reduced T cell penetration depth and long-term T cell exhaustion. This would explain the lack of added value of IL-2 on CAR T cell efficacy.

IL-2 is expressed by $CD4^+$ T cells after antigen recognition and plays a decisive role in $CD4^+$ and $CD8^+$ T cell proliferation. However, in patients, systemic monotherapy induced not only high efficacies but also resulted in severe toxicities (Rosenberg 2014). Fever, flu-like symptoms, nausea, low blood pressure, and cell counts were the critical side effects, which occurred in treated patients with solid tumors ultimately leading to the loss of the FDA approval as a monotherapy in metastatic renal cell carcinoma and metastatic melanoma (Klapper et al. 2008; Rosenberg 2014; Schwartzentruber 2001). Systemic IL-2 support was evaluated for cell-based immunotherapies in clinical trials but did not improve anti-tumor efficacy (Cao, Lei, and Zhu

2019). Clinical trials demonstrated a higher efficacy of a low amount of intraperitoneal and intratumoral injections of IL-2 in comparison to systemic treatment, albeit not all tumors are sensitive to IL-2 treatment (Den Otter et al. 2008). Thus, local IL-2, dose-adjusted based on clinical trials could enhance CAR T cell infiltration in the immunosuppressive TME. However, excess IL-2 might induce differentiation of $CD4^+$ into multiple phenotypes, including $CD3^+$ $CD4^+$ $Foxp3^+$ T_{regs} (Zorn et al. 2006). However, cyclic immunofluorescence results, such as low CD45RA or CD28 expressions in BDCA-2 and BDCA-2 + IL-2 treated groups indicate that the applied dose of IL-2 was not too high for an overactivation of T cells, without additional IL-2 expression after target recognition by specific CAR T cells. Combined sources of endogenous and exogenous IL-2 resulted in an initial stronger proliferation in the EGFR + IL-2 treated group, which did not result in an enhanced anti-tumor efficacy due to the early exhaustion of those T cells. Therefore, IL-2 supplementation requires a careful dosing and fine-tailored application scheme, e.g. by longer injection intervals or TME-redirected antibody-based supply (Catania et al. 2015; Parisi et al. 2020; Ziffels, Pretto, and Neri 2018). Other or improved cytokines and chemokines might reduce the risk of overstimulation (Danielli et al. 2015). Further studies could evaluate a more specific local IL-2 treatment scheme after the initial killing phase, as in this case after day 16. However, the optimal time point might vary for different CARs and TME support techniques, e.g. other cytokines and application methods and depend on the various in vivo biodistribution patterns found by in vivo imaging of the used CAR and TME-treatment options.

2.4 Conclusion and Outlook

The first objective of this project focused on the evaluation of the influence of the CAR composition on in vitro and in vivo functionality, which encouraged the development of a new spacer class. Three CD20-redirected CARs with variable scFvs and spacer domains demonstrated a similar in vitro killing potential and cytokine expression profile, whereas one CAR showed no tumor reduction. The remaining two CARs displayed a safe in vivo profile for clinical transfer. Since the critical CAR contained a problematic IgG1-based but modified spacer domain, this non anti-tumor efficiency can be explained by non-activating interaction with $Fc\gamma R^+$ cells of the introduced modification. These modifications were not able to fully abrogate interactions with FcR^+ murine immune cells during in vivo testing. However, in vitro target-dependent cytotoxicity of the modified CAR was not prevented by these murine immune cells. This highlights the missing in vitro to in vivo transferability and further emphasizes the

high need for further research to clarify the in vivo distribution patterns of cell-based immunotherapies, to enhance CAR T cell efficacy in solid tumor and to avoid potential unfavorable side effects. IgG-based spacers are not suitable for preclinical transfer and this resulted in a shortage of suitable spacers for membrane-proximal targets to mimic the natural immunological synapse. Siglec-4 of the Siglec protein family displayed a beneficial profile, in terms of the cytotoxic potential and potent marker and cytokine expression profile and was able to successfully recapitulate this anti-tumor potential in a PDAC xenograft model. In vivo testing revealed a similar cytotoxic potential but superior cytokine and marker expression profile of Siglec-4 CARs compared to established CD8α CARs in response to the PDAC xenograft. Multiple factors could contribute to this preferential anti-tumor pattern, such as CAR surface densities. Further research would be required to validate the clinical reduced risk for CRS in response to Siglec-4 CARs. Nevertheless, the novel spacer class was successfully tested and established in PDAC xenograft models.

Although we verified the general functionality of cell-based immunotherapies, in solid tumors such as PDAC, in the clinical setting however, CAR T cells do not only need to find the way to the tumor but also through the pronounced TME and survive there. Hence, preclinical in vivo and ex vivo cell tracking strategies are necessary to identify the best CARs and TME-addressing support mechanisms with only marginal side effects. For the first time, 3D µCT/BLT imaging was successfully established and applied for CAR T cell tracking. Therefore, 3D µCT/BLT imaging represents a valuable and isotope-free tool to assess longitudinal and spatiotemporal in vivo biodistribution of cell-based therapies and the antigen-recognition-induced target-specific proliferation of CAR T cells within tumors. Expression of the luciferase gene under the NFAT promotor would even allow the localization and kinetic examination of in vivo CAR T cell activation for preclinical and toxicity-related research. Nonetheless, technical improvements are mandatory for the signal reconstruction of some organs, e.g. the spleen, which is essential for immunotherapy research. Ex vivo tracking, using LSFM and cyclic immunofluorescence, extends the whole-body analysis at a cellular level, enabling proportional, distance, and phenotypical evaluation of the target-specific T cell reaction. A combination of both, LSFM and cyclic immunofluorescence, techniques for one tumor, would reduce the costs, save animals, and extend the available data. The presented stringent in vivo and ex vivo strategy facilitated the evaluation of local IL-2 as possible support for CAR T cells in the TME. The subcutaneous under the tumor applied treatment had a short-term stimulatory effect on the CAR T cells, but induced overstimulation that resulted in decreased tumor infiltration and early exhaustion. In this way, local IL-2 did not increase the anti-tumor efficacy of CAR T cells, subsequently

disqualifying the local IL-2 supply method. TME-redirected supply of IL-2 or other cytokines and chemokines without the overstimulation risk as well as adjusted application schemes could be a strategy for the future to support CAR T cell accumulation and efficacy in the immunosuppressive TME of PDCA.

Overall, this study evaluated the preclinical eligibility of multiple CARs, for hematological and solid tumor treatment, including constructs with the new Siglec-4 derived spacer. The new spacer revealed a high preferential cytokine and activation profile for clinical transfer. In addition, 3D BLT CAR T cell tracking was established and facilitated together with ex vivo LSFM and cyclic immunofluorescence tracking, ultimately excluding local IL-2 for enhanced CAR T cell efficacy in solid tumors, such as PDAC. But to make CAR T cell therapy a valid option for PDAC patients, major adjustments are required. One central point is the modification of the TME to bring CAR T cells to the tumor and to sustain their anti-tumor potential in the immunosuppressive environment. These modifications may include adjustments of the CAR itself e.g. to ensure an early differentiation state for a sufficient cytotoxic potential. TME-modifying options, such as supporting cytokines, enhanced metabolic capacities or ECM-degrading enzymes, can be applied additionally to the CAR T cell therapy or as part of the CAR itself. In vivo and ex vivo imaging strategies, as demonstrated here, are decisive tools to evaluate the efficacy, safety, and feasibility of the adjusted CARs and combined TME-targeting options on whole-body and single-cell level.

3 REFERENCES

Abate-Daga, Daniel, and Marco L. Davila. 2016. “CAR Models: Next-Generation CAR Modifications for Enhanced T-Cell Function.” *Official Journal of the American Society of Gene {\&} Cell Therapy* 3:16014. doi: 10.1038/mto.2016.14.

Abramson, Jeremy S., and Andrew D. Zelenetz. 2013. “Recent Advances in the Treatment of Non-Hodgkin’s Lymphomas.” Pp. 671–75 in *JNCCN Journal of the National Comprehensive Cancer Network*. Vol. 11. Harborside Press.

Agarwal, Shiwani, Tatjana Weidner, Frederic B. Thalheimer, and Christian J. Buchholz. 2019. “In Vivo Generated Human CAR T Cells Eradicate Tumor Cells.” *OncoImmunology* 8(12). doi: 10.1080/2162402X.2019.1671761.

Ahmad, Farida B., and Robert N. Anderson. 2021. “The Leading Causes of Death in the US for 2020.” *JAMA*. doi: 10.1001/jama.2021.5469.

Akce, M., M. Y. Zaidi, E. K. Waller, B. F. El-Rayes, and G. B. Lesinski. 2018. “The Potential of CAR T Cell Therapy in Pancreatic Cancer.” *Front Immunol* 9:2166. doi: 10.3389/fimmu.2018.02166.

Alhmoud, Jehad F., John F. Woolley, Ala Eddin Al Moustafa, and Mohammed Imad Malki. 2020. “DNA Damage/Repair Management in Cancers.” *Cancers* 12(4).

Alizadeh, Ash A., Michael B. Elsen, R. Eric Davis, Ch L. Ma, Izidore S. Lossos, Andreas Rosenwald, Jennifer C. Boldrick, Hajeer Sabet, True Tran, Xin Yu, John I. Powell, Liming Yang, Gerald E. Marü, Troy Moore, James Hudson, Lisheng Lu, David B. Lewis, Robert Tibshirani, Gavin Sherlock, Wing C. Chan, Timothy C. Greiner, Dennis D. Weisenburger, James O. Armitage, Roger Warnke, Ronald Levy, Wyndham Wilson, Michael R. Grever, John C. Byrd, David Botstein, Patrick O. Brown, and Louis M. Staudt. 2000. “Distinct Types of Diffuse Large B-Cell Lymphoma Identified by Gene Expression Profiling.” *Nature* 403(6769):503–11. doi: 10.1038/35000501.

Allen, M., and J. Louise Jones. 2011. “Jekyll and Hyde: The Role of the Microenvironment on the Progression of Cancer.” *J Pathol* 223(2):162–76. doi: 10.1002/path.2803.

Almåsbak, H., E. Walseng, A. Kristian, M. R. Myhre, E. M. Suso, L. A. Munthe, J. T. Andersen, M. Y. Wang, G. Kvalheim, G. Gaudernack, and J. A. Kyte. 2015. “Inclusion of an IgG1-Fc Spacer Abrogates Efficacy of CD19 CAR T Cells in a Xenograft Mouse Model.” *Gene Therapy* 22(5):391–403. doi: 10.1038/gt.2015.4.

Almåsbak, Hilde, Edith Rian, Hanna Julie Hoel, Martin Pulè, Séébastien Wälchli, Gunnar Kvalheim, Gustav Gaudernack, and Anne Marie Rasmussen. 2011. “Transiently Redirected T Cells for Adoptive Transfer.” *Cytotherapy* 13(5):629–40. doi: 10.3109/14653249.2010.542461.

Alsawaftah, Nour, Afifa Farooq, Salam Dhou, and Amin F. Majdalawieh. 2021. “Bioluminescence Imaging Applications in Cancer: A Comprehensive Review.” *IEEE Reviews in Biomedical Engineering* 14:307–26.

Anderson, Kristin G., Ingunn M. Stromnes, and Philip D. Greenberg. 2017. "Obstacles Posed by the Tumor Microenvironment to T Cell Activity: A Case for Synergistic Therapies." *Cancer Cell* 31(3):311–25.

Andtbacka, Robert H. I., Howard L. Kaufman, Frances Collichio, Thomas Amatruda, Neil Senzer, Jason Chesney, Keith A. Delman, Lynn E. Spitler, Igor Puzanov, Sanjiv S. Agarwala, Mohammed Milhem, Lee Cranmer, Brendan Curti, Karl Lewis, Merrick Ross, Troy Guthrie, Gerald P. Linette, Gregory A. Daniels, Kevin Harrington, Mark R. Middleton, Wilson H. Miller, Jonathan S. Zager, Yining Ye, Bin Yao, Ai Li, Susan Doleman, Ari Van Der Walde, Jennifer Gansert, and Robert S. Coffin. 2015. "Talimogene Laherparepvec Improves Durable Response Rate in Patients with Advanced Melanoma." *Journal of Clinical Oncology* 33(25):2780–88. doi: 10.1200/JCO.2014.58.3377.

Arcangeli, Silvia, Laura Falcone, Barbara Camisa, Federica De Girardi, Marta Biondi, Fabio Giglio, Fabio Ciceri, Chiara Bonini, Attilio Bondanza, and Monica Casucci. 2020. "Next-Generation Manufacturing Protocols Enriching TSCM CAR T Cells Can Overcome Disease-Specific T Cell Defects in Cancer Patients." *Frontiers in Immunology* 11:1217. doi: 10.3389/fimmu.2020.01217.

Armenian, Saro H., Lanfang Xu, Kimberly L. Cannavale, F. Lennie Wong, Smita Bhatia, and Chun Chao. 2020. "Cause-Specific Mortality in Survivors of Adolescent and Young Adult Cancer." *Cancer* 126(10):2305–16. doi: 10.1002/cncr.32775.

Athanasiou, A., S. Bowden, M. Paraskevaidi, C. Fotopoulou, P. Martin-Hirsch, E. Paraskevaidis, and M. Kyrgiou. 2020. "HPV Vaccination and Cancer Prevention." *Best Practice and Research: Clinical Obstetrics and Gynaecology* 65:109–24.

Bailey, Peter, David K. Chang, Katia Nones, Amber L. Johns, Ann-Marie Patch, Marie-Claude Gingras, David K. Miller, Angelika N. Christ, Tim J. C. Bruxner, Michael C. Quinn, Craig Nourse, L. Charles Murtaugh, Ivon Harliwong, Senel Idrisoglu, Suzanne Manning, Ehsan Nourbakhsh, Shivangi Wani, Lynn Fink, Oliver Holmes, Venessa Chin, Matthew J. Anderson, Stephen Kazakoff, Conrad Leonard, Felicity Newell, Nick Waddell, Scott Wood, Qinying Xu, Peter J. Wilson, Nicole Cloonan, Karin S. Kassahn, Darrin Taylor, Kelly Quek, Alan Robertson, Lorena Pantano, Laura Mincarelli, Luis N. Sanchez, Lisa Evers, Jianmin Wu, Mark Pinese, Mark J. Cowley, Marc D. Jones, Emily K. Colvin, Adnan M. Nagrial, Emily S. Humphrey, Lorraine A. Chantrill, Amanda Mawson, Jeremy Humphris, Angela Chou, Marina Pajic, Christopher J. Scarlett, Andreia V Pinho, Marc Giry-Laterriere, Ilse Rooman, Jaswinder S. Samra, James G. Kench, Jessica A. Lovell, Neil D. Merrett, Christopher W. Toon, Krishna Epari, Nam Q. Nguyen, Andrew Barbour, Nikolajs Zeps, Kim Moran-Jones, Nigel B. Jamieson, Janet S. Graham, Fraser Duthie, Karin Oien, Jane Hair, Robert Grützmann, Anirban Maitra, Christine A. Iacobuzio-Donahue, Christopher L. Wolfgang, Richard A. Morgan, Rita T. Lawlor, Vincenzo Corbo, Claudio Bassi, Borislav Rusev, Paola Capelli, Roberto Salvia, Giampaolo Tortora, Debabrata Mukhopadhyay, Gloria M. Petersen, Initiative Australian Pancreatic Cancer Genome, Donna M. Munzy, William E. Fisher, Saadia A. Karim, James R. Eshleman, Ralph H. Hruban, Christian Pilarsky, Jennifer P. Morton, Owen J. Sansom, Aldo Scarpa, Elizabeth A. Musgrove, Ulla-Maja Hagbo Bailey, Oliver Hofmann, Robert L. Sutherland,

David A. Wheeler, Anthony J. Gill, Richard A. Gibbs, John V Pearson, Nicola Waddell, Andrew V Biankin, and Sean M. Grimmond. 2016. “Genomic Analyses Identify Molecular Subtypes of Pancreatic Cancer.” *Nature* 531(7592):47–52. doi: 10.1038/nature16965.

Barber, Amorette, Tong Zhang, Christina J. Megli, Jillian Wu, Kenneth R. Meehan, and Charles L. Sentman. 2008. “Chimeric NKG2D Receptor-Expressing T Cells as an Immunotherapy for Multiple Myeloma.” *Experimental Hematology* 36(10):1318–28. doi: 10.1016/j.exphem.2008.04.010.

Beatty, Gregory L., and Whitney L. Gladney. 2015. “Immune Escape Mechanisms as a Guide for Cancer Immunotherapy.” *Clinical Cancer Research* 21(4):687–92.

Bentley, Alexander, Jonathan E. Rowe, and Hamid Dehghani. 2020. “Simultaneous Diffuse Optical and Bioluminescence Tomography to Account for Signal Attenuation to Improve Source Localization.” *Biomedical Optics Express* 11(11):6428. doi: 10.1364/boe.401671.

De Berardinis, Ralph J., and Navdeep S. Chandel. 2016. “Fundamentals of Cancer Metabolism.” *Science Advances* 2(5).

Berger, Carolina, Mary E. Flowers, Edus H. Warren, and Stanley R. Riddell. 2006. “Analysis of Transgene-Specific Immune Responses That Limit the in Vivo Persistence of Adoptively Transferred HSV-TK-Modified Donor T Cells after Allogeneic Hematopoietic Cell Transplantation.” *Blood* 107(6):2294–2302. doi: 10.1182/blood-2005-08-3503.

Berraondo, Pedro, Miguel F. Sanmamed, María C. Ochoa, Iñaki Etxeberria, Maria A. Aznar, José Luis Pérez-Gracia, María E. Rodríguez-Ruiz, Mariano Ponz-Sarvise, Eduardo Castañón, and Ignacio Melero. 2019. “Cytokines in Clinical Cancer Immunotherapy.” *British Journal of Cancer* 120(1):6–15.

Bian, Jessica, and Khaldoun Almhanna. 2021. “Pancreatic Cancer and Immune Checkpoint Inhibitors—Still a Long Way to Go.” *Translational Gastroenterology and Hepatology* 6.

Bibby, M. C. 2004. “Orthotopic Models of Cancer for Preclinical Drug Evaluation: Advantages and Disadvantages.” *European Journal of Cancer* 40(6):852–57. doi: 10.1016/j.ejca.2003.11.021.

Bonifant, Challice L., Hollie J. Jackson, Renier J. Brentjens, and Kevin J. Curran. 2016. “Toxicity and Management in CAR T-Cell Therapy.” *Molecular Therapy - Oncolytics* 3:16011.

Borghans, Jose, and Ruy M. Ribeiro. 2017. “The Maths of Memory: Mathematical Modeling Reveals That Long-Term Immunological Memory Is Maintained in a Manner That Is Even More Dynamic than Previously Thought.” *ELife* 6.

Bornhöfft, Kim F., Tom Goldammer, Alexander Rebl, and Sebastian P. Galuska. 2018. “Siglecs: A Journey through the Evolution of Sialic Acid-Binding Immunoglobulin-Type Lectins.” *Developmental and Comparative Immunology* 86:219–31.

Le Bourgeois, Thibault, Laura Strauss, Halil-Ibrahim Aksoylar, Saeed Daneshmandi, Pankaj

Seth, Nikolaos Patsoukis, and Vassiliki A. Boussiotis. 2018. “Targeting T Cell Metabolism for Improvement of Cancer Immunotherapy.” *Front Oncol* 8:237. doi: 10.3389/fonc.2018.00237.

Branchini, Bruce R., Danielle M. Ablamsky, Martha H. Murtiashaw, Lerna Uzasci, Hugo Fraga, and Tara L. Southworth. 2007. “Thermostable Red and Green Light-Producing Firefly Luciferase Mutants for Bioluminescent Reporter Applications.” *Analytical Biochemistry* 361(2):253–62. doi: 10.1016/j.ab.2006.10.043.

Brenner, David J., and Eric J. Hall. 2007. “Computed Tomography — An Increasing Source of Radiation Exposure.” *New England Journal of Medicine* 357(22):2277–84. doi: 10.1056/nejmra072149.

Brentjens, R. J., E. Santos, Y. Nikhamin, R. Yeh, M. Matsushita, K. La Perle, A. Quintas-Cardama, S. M. Larson, and M. Sadelain. 2007. “Genetically Targeted T Cells Eradicate Systemic Acute Lymphoblastic Leukemia Xenografts.” *Clin Cancer Res* 13(18 Pt 1):5426–35. doi: 10.1158/1078-0432.ccr-07-0674.

Bridgeman, John S., Robert E. Hawkins, Steve Bagley, Morgan Blaylock, Mark Holland, and David E. Gilham. 2010. “The Optimal Antigen Response of Chimeric Antigen Receptors Harboring the CD3ζ Transmembrane Domain Is Dependent upon Incorporation of the Receptor into the Endogenous TCR/CD3 Complex.” *The Journal of Immunology* 184(12):6938–49. doi: 10.4049/jimmunol.0901766.

Brocker, Thomas, and Klaus Karjalainen. 1995. “Signals through T Cell Receptor-ζ Chain Alone Are Insufficient to Prime Resting T Lymphocytes.” *Journal of Experimental Medicine* 181(5):1653–59. doi: 10.1084/jem.181.5.1653.

Brosseau, Jean Philippe, and Lu Q. Le. 2019. “Heterozygous Tumor Suppressor Microenvironment in Cancer Development.” *Trends in Cancer* 5(9):541–46.

Bruhns, Pierre, and Friederike Jönsson. 2015. “Mouse and Human FcR Effector Functions.” *Immunological Reviews* 268(1):25–51.

Bukowski, Karol, Mateusz Kciuk, and Renata Kontek. 2020. “Mechanisms of Multidrug Resistance in Cancer Chemotherapy.” *International Journal of Molecular Sciences* 21(9).

Cai, Ruiyao, Chenchen Pan, Alireza Ghasemigharagoz, Mihail Ivilinov Todorov, Benjamin Förstera, Shan Zhao, Harsharan S. Bhatia, Arnaldo Parra-Damas, Leander Mrowka, Delphine Theodorou, Markus Rempfler, Anna L. R. Xavier, Benjamin T. Kress, Corinne Benakis, Hanno Steinke, Sabine Liebscher, Ingo Bechmann, Arthur Liesz, Bjoern Menze, Martin Kerschensteiner, Maiken Nedergaard, and Ali Ertürk. 2019. “Panoptic Imaging of Transparent Mice Reveals Whole-Body Neuronal Projections and Skull–Meninges Connections.” *Nature Neuroscience* 22(2):317–27. doi: 10.1038/s41593-018-0301-3.

Campo, Elias, Steven H. Swerdlow, Nancy L. Harris, Stefano Pileri, Harald Stein, and Elaine S. Jaffe. 2011. “The 2008 WHO Classification of Lymphoid Neoplasms and beyond: Evolving Concepts and Practical Applications.” *Blood* 117(19):5019–32.

Cao, Genmao, Lijian Lei, and Xiaolin Zhu. 2019. “Efficiency and Safety of Autologous

Chimeric Antigen Receptor T-Cells Therapy Used for Patients with Lymphoma: A Systematic Review and Meta-Analysis." *Medicine* 98(42):e17506. doi: 10.1097/MD.0000000000017506.

Carpenito, Carmine, Michael C. Milone, Raffit Hassan, Jacqueline C. Simonet, Mehdi Lakhal, Megan M. Suhoski, Angel Varela-Rohena, Kathleen M. Haines, Daniel F. Heitjan, Steven M. Albelda, Richard G. Carroll, James L. Riley, Ira Pastan, and Carl H. June. 2009. "Control of Large, Established Tumor Xenografts with Genetically Retargeted Human T Cells Containing CD28 and CD137 Domains." *Proceedings of the National Academy of Sciences of the United States of America* 106(9):3360–65. doi: 10.1073/pnas.0813101106.

Carstens, Julienne L., Pedro Correa De Sampaio, Dalu Yang, Souptik Barua, Huamin Wang, Arvind Rao, James P. Allison, Valerie S. Le Bleu, and Raghu Kalluri. 2017. "Spatial Computation of Intratumoral T Cells Correlates with Survival of Patients with Pancreatic Cancer." *Nature Communications* 8(1):1–13. doi: 10.1038/ncomms15095.

Caruana, I., B. Savoldo, V. Hoyos, G. Weber, H. Liu, E. S. Kim, M. M. Ittmann, D. Marchetti, and G. Dotti. 2015. "Heparanase Promotes Tumor Infiltration and Antitumor Activity of CAR-Redirected T Lymphocytes." *Nat Med* 21(5):524–29. doi: 10.1038/nm.3833.

Catania, Chiara, Michela Maur, Rossana Berardi, Andrea Rocca, Anna Maria Di Giacomo, Gianluca Spitaleri, Cristina Masini, Chiara Pierantoni, Reinerio González-Iglesias, Giulia Zigon, Annaelisa Tasciotti, Leonardo Giovannoni, Valeria Lovato, Giuliano Elia, Hans D. Menssen, Dario Neri, Stefano Cascinu, Pier Franco Conte, and Filippo de Braud. 2015. "The Tumor-Targeting Immunocytokine F16-IL2 in Combination with Doxorubicin: Dose Escalation in Patients with Advanced Solid Tumors and Expansion into Patients with Metastatic Breast Cancer." *Cell Adh Migr* 9(1–2):14–21. doi: 10.4161/19336918.2014.983785.

Cazaux, Marine, Capucine L. Grandjean, Fabrice Lemaître, Zacarias Garcia, Richard J. Beck, Idan Milo, Jérémy Postat, Joost B. Beltman, Eleanor J. Cheadle, and Philippe Bousso. 2019. "Single-Cell Imaging of CAR T Cell Activity in Vivo Reveals Extensive Functional and Anatomical Heterogeneity." *Journal of Experimental Medicine* 216(5):1038–49. doi: 10.1084/jem.20182375.

Chattopadhyay, Kausik, Eszter Lazar-Molnar, Qingrong Yan, Rotem Rubinstein, Chenyang Zhan, Vladimir Vigdorovich, Udupi A. Ramagopal, Jeffrey Bonanno, Stanley G. Nathenson, and Steven C. Almo. 2009. "Sequence, Structure, Function, Immunity: Structural Genomics of Costimulation." *Immunological Reviews* 229(1):356–86.

Chehade, Moussa, Amit K. Srivastava, and Jeff W. M. Bulte. 2016. "Co-Registration of Bioluminescence Tomography, Computed Tomography, and Magnetic Resonance Imaging for Multimodal In Vivo Stem Cell Tracking." *Tomography* 2(2):158–65. doi: 10.18383/j.tom.2016.00160.

Cheng, Zhi, Runhong Wei, Qiuling Ma, Lin Shi, Feng He, Zixiao Shi, Tao Jin, Ronglin Xie, Baofeng Wei, Jing Chen, Hongliang Fang, Xiaolu Han, Jennifer A. Rohrs, Paul Bryson, Yarong Liu, Qi Jing Li, Bo Zhu, and Pin Wang. 2018. "In Vivo Expansion and Antitumor

Activity of Coinfused CD28- and 4-1BB-Engineered CAR-T Cells in Patients with B Cell Leukemia." *Molecular Therapy* 26(4):976–85. doi: 10.1016/j.ymthe.2018.01.022.

Chmielewski, Markus, Andreas A. Hombach, and Hinrich Abken. 2014. "Of CARs and TRUCKs: Chimeric Antigen Receptor (CAR) T Cells Engineered with an Inducible Cytokine to Modulate the Tumor Stroma." *Immunological Reviews* 257(1):83–90. doi: 10.1111/imr.12125.

Chmielewski, Markus, Caroline Kopecky, Andreas A. Hombach, and Hinrich Abken. 2011. "IL-12 Release by Engineered T Cells Expressing Chimeric Antigen Receptors Can Effectively Muster an Antigen-Independent Macrophage Response on Tumor Cells That Have Shut down Tumor Antigen Expression." *Cancer Research* 71(17):5697–5706. doi: 10.1158/0008-5472.CAN-11-0103.

Chu, G. C., A. C. Kimmelman, A. F. Hezel, and R. A. DePinho. 2007. "Stromal Biology of Pancreatic Cancer." *J Cell Biochem* 101(4):887–907. doi: 10.1002/jcb.21209.

Chu, Yaya, Jessica Hochberg, Ashlin Yahr, Janet Ayello, Carmella Van De Ven, Matthew Barth, Myron Czuczman, and Mitchell S. Cairo. 2015. "Targeting CD20+ Aggressive B-Cell Non-Hodgkin Lymphoma by Anti-CD20 CAR MRNA-Modified Expanded Natural Killer Cells in Vitro and in NSG Mice." *Cancer Immunology Research* 3(4):333–44. doi: 10.1158/2326-6066.CIR-14-0114.

Clemenceau, B., S. Valsesia-Wittmann, A. C. Jallas, R. Vivien, R. Rousseau, A. Marabelle, C. Caux, and H. Vie. 2015. "In Vitro and In Vivo Comparison of Lymphocytes Transduced with a Human CD16 or with a Chimeric Antigen Receptor Reveals Potential Off-Target Interactions Due to the IgG2 CH2-CH3 CAR-Spacer." *J Immunol Res* 2015:482089. doi: 10.1155/2015/482089.

Clémenceau, Béatrice, Sandrine Valsesia-Wittmann, Anne Catherine Jallas, Régine Vivien, Raphaël Rousseau, Aurélien Marabelle, Christophe Caux, and Henri Vié. 2015. "In Vitro and In Vivo Comparison of Lymphocytes Transduced with a Human CD16 or with a Chimeric Antigen Receptor Reveals Potential Off-Target Interactions Due to the IgG2 CH2-CH3 CAR-Spacer." *Journal of Immunology Research* 2015. doi: 10.1155/2015/482089.

Conroy, Thierry, Pascal Hammel, Mohamed Hebbar, Meher Ben Abdelghani, Alice C. Wei, Jean-Luc Raoul, Laurence Choné, Eric Francois, Pascal Artru, James J. Biagi, Thierry Lecomte, Eric Assenat, Roger Faroux, Marc Ychou, Julien Volet, Alain Sauvanet, Gilles Breysacher, Frédéric Di Fiore, Christine Cripps, Petr Kavan, Patrick Texereau, Karine Bouhier-Leporrier, Faiza Khemissa-Akouz, Jean-Louis Legoux, Béata Juzyna, Sophie Gourgou, Christopher J. O'Callaghan, Claire Jouffroy-Zeller, Patrick Rat, David Malka, Florence Castan, and Jean-Baptiste Bachet. 2018. "FOLFIRINOX or Gemcitabine as Adjuvant Therapy for Pancreatic Cancer." *New England Journal of Medicine* 379(25):2395–2406. doi: 10.1056/nejmoa1809775.

Corrales, Leticia, Vyara Matson, Blake Flood, Stefani Spranger, and Thomas F. Gajewski. 2017. "Innate Immune Signaling and Regulation in Cancer Immunotherapy." *Cell Research*

27(1):96–108.

Croft, Michael. 2003. “Costimulation of T Cells by OX40, 4-1BB, and CD27.” *Cytokine and Growth Factor Reviews* 14(3–4):265–73.

D’Aloia, M M, I. G. Zizzari, B. Sacchetti, L. Pierelli, and M. Alimandi. 2018. “CAR-T Cells: The Long and Winding Road to Solid Tumors.” *Cell Death Dis* 9(3):282. doi: 10.1038/s41419-018-0278-6.

D’Aloia, Maria Michela, Ilaria Grazia Zizzari, Benedetto Sacchetti, Luca Pierelli, and Maurizio Alimandi. 2018. “CAR-T Cells: The Long and Winding Road to Solid Tumors Review-Article.” *Cell Death and Disease* 9(3).

Daniel, Catherine, Sabine Poiret, Véronique Dennin, Denise Boutillier, Delphine Armelle Lacorre, Benoit Foligné, and Bruno Pot. 2015. “Dual-Color Bioluminescence Imaging for Simultaneous Monitoring of the Intestinal Persistence of Lactobacillus Plantarum and Lactococcus Lactis in Living Mice.” *Applied and Environmental Microbiology* 81(16):5344–49. doi: 10.1128/AEM.01042-15.

Danielli, R., R. Patuzzo, A. M. Di Giacomo, G. Gallino, A. Maurichi, A. Di Florio, O. Cutaia, A. Lazzeri, C. Fazio, C. Miracco, L. Giovannoni, G. Elia, D. Neri, M. Maio, and M. Santinami. 2015. “Intralesional Administration of L19-IL2/L19-TNF in Stage III or Stage IVM1a Melanoma Patients: Results of a Phase II Study.” *Cancer Immunol Immunother* 64(8):999–1009. doi: 10.1007/s00262-015-1704-6.

Davenport, Alexander J., Misty R. Jenkins, Ryan S. Cross, Carmen S. Yong, H. Miles Prince, David S. Ritchie, Joseph A. Trapani, Michael H. Kershaw, Phillip K. Darcy, and Paul J. Neeson. 2015. “CAR-T Cells Inflict Sequential Killing of Multiple Tumor Target Cells.” *Cancer Immunology Research* 3(5):483–94. doi: 10.1158/2326-6066.CIR-15-0048.

Day, Chi Ping, Glenn Merlino, and Terry Van Dyke. 2015. “Preclinical Mouse Cancer Models: A Maze of Opportunities and Challenges.” *Cell* 163(1):39–53.

Demaria, Olivier, Stéphanie Cornen, Marc Daëron, Yannis Morel, Ruslan Medzhitov, and Eric Vivier. 2019. “Harnessing Innate Immunity in Cancer Therapy.” *Nature* 574(7776):45–56.

DeSelm, Carl J., Zachary E. Tano, Anna M. Varghese, and Prasad S. Adusumilli. 2017. “CAR T-Cell Therapy for Pancreatic Cancer.” *Journal of Surgical Oncology* 116(1):63–74.

Dilek, Nahzli, Nicolas Poirier, Philippe Hulin, Flora Coulon, Caroline Mary, Simon Ville, Henri Vie, Béatrice Clémenceau, Gilles Blancho, and Bernard Vanhove. 2013. “Targeting CD28, CTLA-4 and PD-L1 Costimulation Differentially Controls Immune Synapses and Function of Human Regulatory and Conventional t-Cells.” *PLoS ONE* 8(12). doi: 10.1371/journal.pone.0083139.

Durkin, Alan J., P. Mark Bloomston, Alexander S. Rosemurgy, Natalie Giarelli, Diane Cojita, Timothy J. Yeatman, and Emmanuel E. Zervos. 2003. “Defining the Role of the Epidermal Growth Factor Receptor in Pancreatic Cancer Grown in Vitro.” *American Journal of Surgery* 186(5):431–36. doi: 10.1016/j.amjsurg.2003.07.008.

Dzionek, Andrzej, Anja Fuchs, Petra Schmidt, Sabine Cremer, Monika Zysk, Stefan Miltenyi, David W. Buck, and Jürgen Schmitz. 2000. "BDCA-2, BDCA-3, and BDCA-4: Three Markers for Distinct Subsets of Dendritic Cells in Human Peripheral Blood." *The Journal of Immunology* 165(11):6037–46. doi: 10.4049/jimmunol.165.11.6037.

Eales, K. L., K. E. R. Hollinshead, and D. A. Tennant. 2016. "Hypoxia and Metabolic Adaptation of Cancer Cells." *Oncogenesis* 5(1):e190--e190. doi: 10.1038/oncsis.2015.50.

Elenitoba-Johnson, Kojo S. J., and Megan S. Lim. 2018. "New Insights into Lymphoma Pathogenesis." *Annual Review of Pathology: Mechanisms of Disease* 13:193–217. doi: 10.1146/annurev-pathol-020117-043803.

Eric Davis, R., Keith D. Brown, Ulrich Siebenlist, and Louis M. Staudt. 2001. "Constitutive Nuclear Factor KB Activity Is Required for Survival of Activated B Cell-like Diffuse Large B Cell Lymphoma Cells." *Journal of Experimental Medicine* 194(12):1861–74. doi: 10.1084/jem.194.12.1861.

Erkan, Mert, Simone Hausmann, Christoph W. Michalski, Alexander A. Fingerle, Martin Dobritz, Jãrg Kleeff, and Helmut Friess. 2012. "The Role of Stroma in Pancreatic Cancer: Diagnostic and Therapeutic Implications." *Nature Reviews Gastroenterology and Hepatology* 9(8):454–67.

Erstad, Derek J., Mozhdeh Sojoodi, Martin S. Taylor, Sarani Ghoshal, Allen A. Razavi, Katherine A. Graham-O'Regan, Nabeel Bardeesy, Cristina R. Ferrone, Michael Lanuti, Peter Caravan, Kenneth K. Tanabe, and Bryan C. Fuchs. 2018. "Orthotopic and Heterotopic Murine Models of Pancreatic Cancer and Their Different Responses to FOLFIRINOX Chemotherapy." *Disease Models & Mechanisms* 11(7). doi: 10.1242/dmm.034793.

Esensten, Jonathan H., Ynes A. Helou, Gaurav Chopra, Arthur Weiss, and Jeffrey A. Bluestone. 2016. "CD28 Costimulation: From Mechanism to Therapy." *Immunity* 44(5):973–88.

Eshhar, Z., T. Waks, G. Gross, and D. G. Schindler. 1993. "Specific Activation and Targeting of Cytotoxic Lymphocytes through Chimeric Single Chains Consisting of Antibody-Binding Domains and the Gamma or Zeta Subunits of the Immunoglobulin and T-Cell Receptors." *Proc Natl Acad Sci U S A* 90(2):720–24. doi: 10.1073/pnas.90.2.720.

Fan, Jiaqiao, Jugal Kishore Das, Xiaofang Xiong, Hailong Chen, and Jianxun Song. 2021. "Development of CAR-T Cell Persistence in Adoptive Immunotherapy of Solid Tumors." *Frontiers in Oncology* 10:2920. doi: 10.3389/fonc.2020.574860.

Feng, Jinchao, Kebin Jia, Guorui Yan, Shouping Zhu, Chenghu Qin, Yujie Lv, and Jie Tian. 2008. "An Optimal Permissible Source Region Strategy for Multispectral Bioluminescence Tomography." *Optics Express* 16(20):15640. doi: 10.1364/oe.16.015640.

Fesnak, A. D., C. H. June, and B. L. Levine. 2016. "Engineered T Cells: The Promise and Challenges of Cancer Immunotherapy." *Nat Rev Cancer* 16(9):566–81. doi: 10.1038/nrc.2016.97.

Finney, Helene M., Arne N. Akbar, and Alastair D. G. Lawson. 2004. "Activation of Resting Human Primary T Cells with Chimeric Receptors: Costimulation from CD28, Inducible Costimulator, CD134, and CD137 in Series with Signals from the TCR$ζ$ Chain." *The Journal of Immunology* 172(1):104–13. doi: 10.4049/jimmunol.172.1.104.

Fischer, Uwe M., Matthew T. Harting, Fernando Jimenez, Werner O. Monzon-Posadas, Hasen Xue, Sean I. Savitz, Glen A. Laine, and Charles S. Cox. 2009. "Pulmonary Passage Is a Major Obstacle for Intravenous Stem Cell Delivery: The Pulmonary First-Pass Effect." *Stem Cells and Development* 18(5):683–91. doi: 10.1089/scd.2008.0253.

Fraga, Hugo, Diogo Fernandes, Jiri Novotny, Rui Fontes, and Joaquim C. G. Esteves da Silva. 2006. "Firefly Luciferase Produces Hydrogen Peroxide as a Coproduct in Dehydroluciferyl Adenylate Formation." *ChemBioChem* 7(6):929–35. doi: 10.1002/cbic.200500443.

Fujiwara, Kento, Ayaka Tsunei, Hotaka Kusabuka, Erika Ogaki, Masashi Tachibana, and Naoki Okada. 2020. "Hinge and Transmembrane Domains of Chimeric Antigen Receptor Regulate Receptor Expression and Signaling Threshold." *Cells* 9(5). doi: 10.3390/cells9051182.

Fukuhara, Hiroshi, Yasushi Ino, and Tomoki Todo. 2016. "Oncolytic Virus Therapy: A New Era of Cancer Treatment at Dawn." *Cancer Science* 107(10):1373–79.

Garfall, Alfred L., Ehren K. Dancy, Adam D. Cohen, Wei Ting Hwang, Joseph A. Fraietta, Megan M. Davis, Bruce L. Levine, Don L. Siegel, Edward A. Stadtmauer, Dan T. Vogl, Adam Waxman, Aaron P. Rapoport, Michael C. Milone, Carl H. June, and J. Joseph Melenhorst. 2019. "T-Cell Phenotypes Associated with Effective CAR T-Cell Therapy in Postinduction vs Relapsed Multiple Myeloma." *Blood Advances* 3(19):2812–15. doi: 10.1182/bloodadvances.2019000600.

Gargett, Tessa, and Michael P. Brown. 2015. "Different Cytokine and Stimulation Conditions Influence the Expansion and Immune Phenotype of Third-Generation Chimeric Antigen Receptor Tcells Specific for Tumor Antigen GD2." *Cytotherapy* 17(4):487–95. doi: 10.1016/j.jcyt.2014.12.002.

Gillison, Maura L., Anil K. Chaturvedi, and Douglas R. Lowy. 2008. "HPV Prophylactic Vaccines and the Potential Prevention of Noncervical Cancers in Both Men and Women." *Cancer* 113(S10):3036–46. doi: 10.1002/cncr.23764.

Golby, S. J. C., C. Chinyama, and J. Spencer. 2002. "Proliferation of T-Cell Subsets That Contact Tumour Cells in Colorectal Cancer." *Clinical and Experimental Immunology* 127(1):85–91. doi: 10.1046/j.1365-2249.2002.01730.x.

Gomes-Silva, Diogo, Malini Mukherjee, Madhuwanti Srinivasan, Giedre Krenciute, Olga Dakhova, Yueting Zheng, Joaquim M. S. Cabral, Cliona M. Rooney, Jordan S. Orange, Malcolm K. Brenner, and Maksim Mamonkin. 2017. "Tonic 4-1BB Costimulation in Chimeric Antigen Receptors Impedes T Cell Survival and Is Vector-Dependent." *Cell Reports* 21(1):17–26. doi: 10.1016/j.celrep.2017.09.015.

Gonzalez, Hugo, Catharina Hagerling, and Zena Werb. 2018. “Roles of the Immune System in Cancer: From Tumor Initiation to Metastatic Progression.” *Genes and Development* 32(19–20):1267–84.

Gordon, Siamon, and Annette Plüddemann. 2017. “Tissue Macrophages: Heterogeneity and Functions.” *BMC Biology* 15(1):1–18.

Green, Douglas R., Nathalie Droin, and Michael Pinkoski. 2003. “Activation-Induced Cell Death in T Cells.” *Immunological Reviews* 193:70–81.

Grimm, E. A., A. Mazumder, H. Z. Zhang, and S. A. Rosenberg. 1982. “Lymphokine-Activated Killer Cell Phenomenon. Lysis of Natural Killer-Resistant Fresh Solid Tumor Cells by Interleukin 2-Activated Autologous Human Peripheral Blood Lymphocytes.” *Journal of Experimental Medicine* 155(6):1823–41. doi: 10.1084/jem.155.6.1823.

Gross, G., T. Waks, and Z. Eshhar. 1989. “Expression of Immunoglobulin-T-Cell Receptor Chimeric Molecules as Functional Receptors with Antibody-Type Specificity.” *Proceedings of the National Academy of Sciences of the United States of America* 86(24):10024–28. doi: 10.1073/pnas.86.24.10024.

Gu, Xuejun, Qizhi Zhang, Lyndon Larcom, and Huabei Jiang. 2004. “Three-Dimensional Bioluminescence Tomography with Model-Based Reconstruction.” *Optics Express* 12(17):3996. doi: 10.1364/opex.12.003996.

Guedan, Sonia, Hugo Calderon, Avery D. Posey, and Marcela V. Maus. 2019. “Engineering and Design of Chimeric Antigen Receptors.” *Molecular Therapy - Methods and Clinical Development* 12:145–56.

Guedan, Sonia, Xi Chen, Aviv Madar, Carmine Carpenito, Shannon E. McGettigan, Matthew J. Frigault, Jihyun Lee, Avery D. Posey, John Scholler, Nathalie Scholler, Richard Bonneau, and Carl H. June. 2014. “ICOS-Based Chimeric Antigen Receptors Program Bipolar TH17/ TH1 Cells.” *Blood* 124(7):1070–80. doi: 10.1182/blood-2013-10-535245.

Guedan, Sonia, Aviv Madar, Victoria Casado-Medrano, Carolyn Shaw, Anna Wing, Fang Liu, Regina M. Young, Carl H. June, and Avery D. Posey. 2020. “Single Residue in CD28-Costimulated CAR-T Cells Limits Long-Term Persistence and Antitumor Durability.” *Journal of Clinical Investigation* 130(6):3087–97. doi: 10.1172/JCI133215.

Guedan, Sonia, Avery D. Posey, Carolyn Shaw, Anna Wing, Tong Da, Prachi R. Patel, Shannon E. McGettigan, Victoria Casado-Medrano, Omkar U. Kawalekar, Mireia Uribe-Herranz, Decheng Song, J. Joseph Melenhorst, Simon F. Lacey, John Scholler, Brian Keith, Regina M. Young, and Carl H. June. 2018. “Enhancing CAR T Cell Persistence through ICOS and 4-1BB Costimulation.” *JCI Insight* 3(1). doi: 10.1172/jci.insight.96976.

Guest, Ryan D., Robert E. Hawkins, Natalia Kirillova, Eleanor J. Cheadle, Jennifer Arnold, Allison O’Neill, Joely Irlam, Kerry A. Chester, John T. Kemshead, David M. Shaw, M. J. Embleton, Peter L. Stern, and David E. Gilham. 2005. “The Role of Extracellular Spacer Regions in the Optimal Design of Chimeric Immune Receptors: Evaluation of Four Different ScFvs and Antigens.” *Journal of Immunotherapy* 28(3):203–11. doi:

10.1097/01.cji.0000161397.96582.59.

Guo, Zong Sheng. 2018. “The 2018 Nobel Prize in Medicine Goes to Cancer Immunotherapy (Editorial for BMC Cancer).” *BMC Cancer* 18(1):1086.

Gust, Juliane, Rafael Ponce, W. Conrad Liles, Gwenn A. Garden, and Cameron J. Turtle. 2020. “Cytokines in CAR T Cell–Associated Neurotoxicity.” *Frontiers in Immunology* 11:1.

Hall, MacLean, Hao Liu, Mokenge Malafa, Barbara Centeno, Pamela J. Hodul, José Pimiento, Shari Pilon-Thomas, and Amod A. Sarnaik. 2016. “Expansion of Tumor-Infiltrating Lymphocytes (TIL) from Human Pancreatic Tumors.” *Journal for ImmunoTherapy of Cancer* 4(1):61. doi: 10.1186/s40425-016-0164-7.

Hall, Mary P., Carolyn C. Woodroofe, Monika G. Wood, Ivo Que, Moniek Van’T Root, Yanto Ridwan, Ce Shi, Thomas A. Kirkland, Lance P. Encell, Keith V Wood, Clemens Löwik, and Laura Mezzanotte. 2018. “Click Beetle Luciferase Mutant and near Infrared Naphthyl-Luciferins for Improved Bioluminescence Imaging.” *Nature Communications* 9(1). doi: 10.1038/s41467-017-02542-9.

Han, Weimin, and Ge Wang. 2008. “Bioluminescence Tomography: Biomedical Background, Mathematical Theory, and Numerical Approximation.” *Journal of Computational Mathematics* 26(3):324–35.

Hanahan, Douglas, and Robert A. Weinberg. 2011. “Hallmarks of Cancer: The next Generation.” *Cell* 144(5):646–74.

Haso, Waleed, Daniel W. Lee, Nirali N. Shah, Maryalice Stetler-Stevenson, Constance M. Yuan, Ira H. Pastan, Dimiter S. Dimitrov, Richard A. Morgan, David J. FitzGerald, David M. Barrett, Alan S. Wayne, Crystal L. MacKall, and Rimas J. Orentas. 2013. “Anti-CD22-Chimeric Antigen Receptors Targeting B-Cell Precursor Acute Lymphoblastic Leukemia.” *Blood* 121(7):1165–71. doi: 10.1182/blood-2012-06-438002.

Heinhuis, K. M., W. Ros, M. Kok, N. Steeghs, J. H. Beijnen, and J. H. M. Schellens. 2019. “Enhancing Antitumor Response by Combining Immune Checkpoint Inhibitors with Chemotherapy in Solid Tumors.” *Annals of Oncology* 30(2):219–35.

Heinrich, Stefan, Bernhard Pestalozzi, Mickael Lesurtel, Frederik Berrevoet, Stéphanie Laurent, Jean Robert Delpero, Jean Luc Raoul, Phillippe Bachellier, Patrick Dufour, Markus Moehler, Achim Weber, Hauke Lang, Xavier Rogiers, and Pierre Alain Clavien. 2011. “Adjuvant Gemcitabine versus NEOadjuvant Gemcitabine/Oxaliplatin plus Adjuvant Gemcitabine in Resectable Pancreatic Cancer: A Randomized Multicenter Phase III Study (NEOPAC Study).” *BMC Cancer* 11. doi: 10.1186/1471-2407-11-346.

Heiser, Patrick W., David A. Cano, Limor Landsman, Grace E. Kim, James G. Kench, David S. Klimstra, Maketo M. Taketo, Andrew V. Biankin, and Matthias Hebrok. 2008. “Stabilization of β-Catenin Induces Pancreas Tumor Formation.” *Gastroenterology* 135(4):1288–1300. doi: 10.1053/j.gastro.2008.06.089.

Henze, Janina, Frank Tacke, Olaf Hardt, Frauke Alves, and Wa’El Al Rawashdeh. 2020. “Enhancing the Efficacy of Car t Cells in the Tumor Microenvironment of Pancreatic

Cancer." *Cancers* 12(6):1389. doi: 10.3390/cancers12061389.

Hezel, Aram F., Alec C. Kimmelman, Ben Z. Stanger, Nabeel Bardeesy, and Ronald A. DePinho. 2006. "Genetics and Biology of Pancreatic Ductal Adenocarcinoma." *Genes and Development* 20(10):1218–49.

Ho, Jin Yuan, Lin Wang, Ying Liu, Min Ba, Junfang Yang, Xian Zhang, Dandan Chen, Peihua Lu, and Jianqiang Li. 2021. "Promoter Usage Regulating the Surface Density of CAR Molecules May Modulate the Kinetics of CAR-T Cells in Vivo." *Molecular Therapy - Methods and Clinical Development* 21:237–46. doi: 10.1016/j.omtm.2021.03.007.

Ho, Won Jin, Elizabeth M. Jaffee, and Lei Zheng. 2020. "The Tumour Microenvironment in Pancreatic Cancer — Clinical Challenges and Opportunities." *Nature Reviews Clinical Oncology* 1–14. doi: 10.1038/s41571-020-0363-5.

Hodi, F. Stephen, Steven J. O'Day, David F. McDermott, Robert W. Weber, Jeffrey A. Sosman, John B. Haanen, Rene Gonzalez, Caroline Robert, Dirk Schadendorf, Jessica C. Hassel, Wallace Akerley, Alfons J. M. van den Eertwegh, Jose Lutzky, Paul Lorigan, Julia M. Vaubel, Gerald P. Linette, David Hogg, Christian H. Ottensmeier, Celeste Lebbé, Christian Peschel, Ian Quirt, Joseph I. Clark, Jedd D. Wolchok, Jeffrey S. Weber, Jason Tian, Michael J. Yellin, Geoffrey M. Nichol, Axel Hoos, and Walter J. Urba. 2010. "Improved Survival with Ipilimumab in Patients with Metastatic Melanoma." *New England Journal of Medicine* 363(8):711–23. doi: 10.1056/NEJMoa1003466.

Hollingsworth, Robert E., and Kathrin Jansen. 2019. "Turning the Corner on Therapeutic Cancer Vaccines." *Npj Vaccines* 4(1):1–10.

Hombach, A., A. A. Hombach, and H. Abken. 2010. "Adoptive Immunotherapy with Genetically Engineered T Cells: Modification of the IgG1 Fc Spacer Domain in the Extracellular Moiety of Chimeric Antigen Receptors Avoids off-Target Activation and Unintended Initiation of an Innate Immune Response." *Gene Therapy* 17(10):1206–13. doi: 10.1038/gt.2010.91.

Hombach, Andreas A., and Hinrich Abken. 2011. "Costimulation by Chimeric Antigen Receptors Revisited the T Cell Antitumor Response Benefits from Combined CD28-OX40 Signalling." *International Journal of Cancer* 129(12):2935–44. doi: 10.1002/ijc.25960.

Huang, Lei, Lina Jansen, Yesilda Balavarca, Masoud Babaei, Lydia van der Geest, Valery Lemmens, Liesbet Van Eycken, Harlinde De Schutter, Tom B. Johannesen, Maja Primic-Žakelj, Vesna Zadnik, Marc G. Besselink, Petra Schrotz-King, and Hermann Brenner. 2018. "Stratified Survival of Resected and Overall Pancreatic Cancer Patients in Europe and the USA in the Early Twenty-First Century: A Large, International Population-Based Study." *BMC Medicine* 16(1):125. doi: 10.1186/s12916-018-1120-9.

Huang, Xin, Hongfeng Guo, Johnthomas Kang, Suet Choi, Tom C. Zhou, Syam Tammana, Christopher J. Lees, Zhong Ze Li, Michael Milone, Bruce L. Levine, Jakub Tolar, Carl H. June, R. Scott McIvor, John E. Wagner, Bruce R. Blazar, and Xianzheng Zhou. 2008. "Sleeping Beauty Transposon-Mediated Engineering of Human Primary T Cells for Therapy of CD19+ Lymphoid Malignancies." *Molecular Therapy* 16(3):580–89. doi:

10.1038/sj.mt.6300404.

Hudecek, Michael, Maria Teresa Lupo-Stanghellini, Paula L. Kosasih, Daniel Sommermeyer, Michael C. Jensen, Christoph Rader, and Stanley R. Riddell. 2013. "Receptor Affinity and Extracellular Domain Modifications Affect Tumor Recognition by ROR1-Specific Chimeric Antigen Receptor T Cells." *Clinical Cancer Research* 19(12):3153–64. doi: 10.1158/1078-0432.CCR-13-0330.

Hudecek, Michael, Daniel Sommermeyer, Paula L. Kosasih, Anne Silva-Benedict, Lingfeng Liu, Christoph Rader, Michael C. Jensen, and Stanley R. Riddell. 2015. "The Nonsignaling Extracellular Spacer Domain of Chimeric Antigen Receptors Is Decisive for in Vivo Antitumor Activity." *Cancer Immunology Research* 3(2):125–35. doi: 10.1158/2326-6066.CIR-14-0127.

Imai, C., K. Mihara, M. Andreansky, I. C. Nicholson, C. H. Pui, T. L. Geiger, and Dario Campana. 2004. "Chimeric Receptors with 4-1BB Signaling Capacity Provoke Potent Cytotoxicity against Acute Lymphoblastic Leukemia." *Leukemia* 18(4):676–84. doi: 10.1038/sj.leu.2403302.

Inoue, Yusuke, Shigeru Kiryu, Kiyoko Izawa, Makoto Watanabe, Arinobu Tojo, and Kuni Ohtomo. 2009. "Comparison of Subcutaneous and Intraperitoneal Injection of D-Luciferin for in Vivo Bioluminescence Imaging." *European Journal of Nuclear Medicine and Molecular Imaging* 36(5):771–79. doi: 10.1007/s00259-008-1022-8.

Irving, Bryan A., and Arthur Weiss. 1991. "The Cytoplasmic Domain of the T Cell Receptor ζ Chain Is Sufficient to Couple to Receptor-Associated Signal Transduction Pathways." *Cell* 64(5):891–901. doi: 10.1016/0092-8674(91)90314-O.

Ishii, Taeko, and Masaru Ishii. 2011. "Intravital Two-Photon Imaging: A Versatile Tool for Dissecting the Immune System." in *Annals of the Rheumatic Diseases*. Vol. 70. Ann Rheum Dis.

Jafarzadeh, Leila, Elham Masoumi, Keyvan Fallah-Mehrjardi, Hamid Reza Mirzaei, and Jamshid Hadjati. 2020. "Prolonged Persistence of Chimeric Antigen Receptor (CAR) T Cell in Adoptive Cancer Immunotherapy: Challenges and Ways Forward." *Frontiers in Immunology* 11:702.

Jain, R. K. 2013. "Normalizing Tumor Microenvironment to Treat Cancer: Bench to Bedside to Biomarkers." *J Clin Oncol* 31(17):2205–18. doi: 10.1200/jco.2012.46.3653.

James, Scott E., Philip D. Greenberg, Michael C. Jensen, Yukang Lin, Jinjuan Wang, Brian G. Till, Andrew A. Raubitschek, Stephen J. Forman, and Oliver W. Press. 2008. "Antigen Sensitivity of CD22-Specific Chimeric TCR Is Modulated by Target Epitope Distance from the Cell Membrane." *The Journal of Immunology* 180(10):7028–38. doi: 10.4049/jimmunol.180.10.7028.

Jensen, Michael C., Leslie Popplewell, Laurence J. Cooper, David DiGiusto, Michael Kalos, Julie R. Ostberg, and Stephen J. Forman. 2010. "Antitransgene Rejection Responses Contribute to Attenuated Persistence of Adoptively Transferred CD20/CD19-Specific

Chimeric Antigen Receptor Redirected T Cells in Humans." *Biology of Blood and Marrow Transplantation* 16(9):1245–56. doi: 10.1016/j.bbmt.2010.03.014.

Jinesh, G. G., V. Sambandam, S. Vijayaraghavan, K. Balaji, and S. Mukherjee. 2018. "Molecular Genetics and Cellular Events of K-Ras-Driven Tumorigenesis." *Oncogene* 37(7):839–46.

De Jong, Marion, Jeroen Essers, and Wytske M. Van Weerden. 2014. "Imaging Preclinical Tumour Models: Improving Translational Power." *Nature Reviews Cancer* 14(7):481–93.

Jonnalagadda, M., A. Mardiros, R. Urak, X. Wang, L. J. Hoffman, A. Bernanke, W. C. Chang, W. Bretzlaff, R. Starr, S. Priceman, J. R. Ostberg, S. J. Forman, and C. E. Brown. 2015. "Chimeric Antigen Receptors with Mutated IgG4 Fc Spacer Avoid Fc Receptor Binding and Improve T Cell Persistence and Antitumor Efficacy." *Mol Ther* 23(4):757–68. doi: 10.1038/mt.2014.208.

Kagoya, Yuki, Shinya Tanaka, Tingxi Guo, Mark Anczurowski, Chung Hsi Wang, Kayoko Saso, Marcus O. Butler, Mark D. Minden, and Naoto Hirano. 2018. "A Novel Chimeric Antigen Receptor Containing a JAK-STAT Signaling Domain Mediates Superior Antitumor Effects." *Nature Medicine* 24(3):352–59. doi: 10.1038/nm.4478.

Kaijzel, Eric L., Gabri Van Der Pluijm, and Clemens W. G. M. Löwik. 2007. "Whole-Body Optical Imaging in Animal Models to Assess Cancer Development and Progression." *Clinical Cancer Research* 13(12):3490–97.

Kandoth, Cyriac, Michael D. McLellan, Fabio Vandin, Kai Ye, Beifang Niu, Charles Lu, Mingchao Xie, Qunyuan Zhang, Joshua F. McMichael, Matthew A. Wyczalkowski, Mark D. M. Leiserson, Christopher A. Miller, John S. Welch, Matthew J. Walter, Michael C. Wendl, Timothy J. Ley, Richard K. Wilson, Benjamin J. Raphael, and Li Ding. 2013. "Mutational Landscape and Significance across 12 Major Cancer Types." *Nature* 502(7471):333–39. doi: 10.1038/nature12634.

Katz, Samuel G., and Peter M. Rabinovich. 2020. "T Cell Reprogramming against Cancer." Pp. 3–44 in *Methods in Molecular Biology*. Vol. 2097. Humana Press Inc.

Kershaw, Michael H., Jennifer A. Westwood, Linda L. Parker, Gang Wang, Zelig Eshhar, Sharon A. Mavroukakis, Donald E. White, John R. Wunderlich, Silvana Canevari, Linda Rogers-Freezer, Clara C. Chen, James C. Yang, Steven A. Rosenberg, and Patrick Hwu. 2006. "A Phase I Study on Adoptive Immunotherapy Using Gene-Modified T Cells for Ovarian Cancer." *Clinical Cancer Research* 12(20 PART 1):6106–15. doi: 10.1158/1078-0432.CCR-06-1183.

Klapper, Jacob A., Stephanie G. Downey, Franz O. Smith, James C. Yang, Marybeth S. Hughes, Udai S. Kammula, Richard M. Sherry, Richard E. Royal, Seth M. Steinberg, and Steven Rosenberg. 2008. "High-Dose Interleukin-2 for the Treatment of Metastatic Renal Cell Carcinoma: A Retrospective Analysis of Response and Survival in Patients Treated in the Surgery Branch at the National Cancer Institute between 1986 and 2006." *Cancer* 113(2):293–301. doi: 10.1002/cncr.23552.

Kondo, Taisuke, Yuki Imura, Shunsuke Chikuma, Sana Hibino, Setsuko Omata-Mise, Makoto Ando, Takashi Akanuma, Mana Iizuka, Ryota Sakai, Rimpei Morita, and Akihiko Yoshimura. 2018. "Generation and Application of Human Induced-Stem Cell Memory T Cells for Adoptive Immunotherapy." *Cancer Science* 109(7):2130–40. doi: 10.1111/cas.13648.

Kowolik, Claudia M., Max S. Topp, Sergio Gonzalez, Timothy Pfeiffer, Simon Olivares, Nancy Gonzalez, David D. Smith, Stephen J. Forman, Michael C. Jensen, and Laurence J. N. Cooper. 2006. "CD28 Costimulation Provided through a CD19-Specific Chimeric Antigen Receptor Enhances in Vivo Persistence and Antitumor Efficacy of Adoptively Transferred T Cells." *Cancer Research* 66(22):10995–4. doi: 10.1158/0008-5472.CAN-06-0160.

Krebs, Simone, Megan M. Dacek, Lukas M. Carter, David A. Scheinberg, and Steven M. Larson. 2020. "CAR Chase: Where Do Engineered Cells Go in Humans?" *Frontiers in Oncology* 10:1930. doi: 10.3389/fonc.2020.577773.

Krenciute, Giedre, Simone Krebs, David Torres, Meng Fen Wu, Hao Liu, Gianpietro Dotti, Xiao Nan Li, Maciej S. Lesniak, Irina V. Balyasnikova, and Stephen Gottschalk. 2016. "Characterization and Functional Analysis of ScFv-Based Chimeric Antigen Receptors to Redirect T Cells to IL13Rα2-Positive Glioma." *Molecular Therapy* 24(2):354–63. doi: 10.1038/mt.2015.199.

Kucerova, Petra, and Monika Cervinkova. 2016. "Spontaneous Regression of Tumour and the Role of Microbial Infection - Possibilities for Cancer Treatment." *Anti-Cancer Drugs* 27(4):269–77.

Kumar, Mukesh, Brian Keller, Ndeye Makalou, and Richard E. Sutton. 2001. "Systematic Determination of the Packaging Limit of Lentiviral Vectors." *Human Gene Therapy* 12(15):1893–1905. doi: 10.1089/104303401753153947.

Kuünkele, Annette, Adam J. Johnson, Lisa S. Rolczynski, Cindy A. Chang, Virginia Hoglund, Karen S. Kelly-Spratt, and Michael C. Jensen. 2015. "Functional Tuning of CARs Reveals Signaling Threshold above Which CD8+ CTL Antitumor Potency Is Attenuated Due to Cell Fas-FasL-Dependent AICD." *Cancer Immunology Research* 3(4):368–79. doi: 10.1158/2326-6066.CIR-14-0200.

Kuwana, Yoshihisa, Yoshihiro Asakura, Naoko Utsunomiya, Mamoru Nakanishi, Yohji Arata, Seiga Itoh, Fumihiko Nagase, and Yoshikazu Kurosawa. 1987. "Expression of Chimeric Receptor Composed of Immunoglobulin-Derived V Resions and T-Cell Receptor-Derived C Regions." *Biochemical and Biophysical Research Communications* 149(3):960–68. doi: 10.1016/0006-291X(87)90502-X.

Lafferty, K. J., and A. J. Cunningham. 1975. "A New Analysis of Allogeneic Interactions." *Australian Journal of Experimental Biology and Medical Science* 53(1):27–42. doi: 10.1038/icb.1975.3.

Lecanda, Jon, Vidya Ganapathy, Christine D'Aquino-Ardalan, Brad Evans, Caprice Cadacio, Aidee Ayala, and Leslie I. Gold. 2009. "TGFβ Prevents Proteasomal Degradation of the Cyclin-Dependent Kinase Inhibitor P27kip1 for Cell Cycle Arrest." *Cell Cycle* 8(5):742–

56. doi: 10.4161/cc.8.5.7871.

Lee, Daniel W., Bianca D. Santomasso, Frederick L. Locke, Armin Ghobadi, Cameron J. Turtle, Jennifer N. Brudno, Marcela V. Maus, Jae H. Park, Elena Mead, Steven Pavletic, William Y. Go, Lamis Eldjerou, Rebecca A. Gardner, Noelle Frey, Kevin J. Curran, Karl Peggs, Marcelo Pasquini, John F. DiPersio, Marcel R. M. van den Brink, Krishna V. Komanduri, Stephan A. Grupp, and Sattva S. Neelapu. 2019. "ASTCT Consensus Grading for Cytokine Release Syndrome and Neurologic Toxicity Associated with Immune Effector Cells." *Biology of Blood and Marrow Transplantation* 25(4):625–38.

Lee, Ji Eun, Yeo Wool Kang, Kyung Hee Jung, Mi Kwon Son, Seung-Min Shin, Ji-Sun Kim, Soo Jung Kim, Zhenghuan Fang, Hong Hua Yan, Jung Hee Park, Young-Chan Yoon, Boreum Han, Min Ji Cheon, Min Gyu Woo, Myung Sung Seo, Joo Han Lim, Yong-Sung Kim, and Soon-Sun Hong. 2021. "Intracellular KRAS-Specific Antibody Enhances the Anti-Tumor Efficacy of Gemcitabine in Pancreatic Cancer by Inducing Endosomal Escape." *Cancer Letters* 507. doi: 10.1016/j.canlet.2021.03.015.

Lee, Suk Hyun, Hyunsu Soh, Jin Hwa Chung, Eun Hye Cho, Sang Ju Lee, Ji Min Ju, Joong Hyuk Sheen, Hyori Kim, Seung Jun Oh, Sang Jin Lee, Junho Chung, Kyungho Choi, Seog Young Kim, and Jin Sook Ryu. 2020. "Feasibility of Real-Time in Vivo 89Zr-DFO-Labeled CAR T-Cell Trafficking Using PET Imaging." *PLoS ONE* 15(1). doi: 10.1371/journal.pone.0223814.

Lekka, Kyriaki, Evanthia Tzitzi, Alexander Giakoustidis, Vassilios Papadopoulos, and Dimitrios Giakoustidis. 2019. "Contemporary Management of Borderline Resectable Pancreatic Ductal Adenocarcinoma." *Annals of Hepato-Biliary-Pancreatic Surgery* 23(2):97. doi: 10.14701/ahbps.2019.23.2.97.

Li, Tinglu, Guangbo Kang, Tingyue Wang, and He Huang. 2018. "Tumor Angiogenesis and Anti-Angiogenic Gene Therapy for Cancer (Review)." *Oncology Letters* 16(1):687–702.

Li, Xiu Yun, Lun Wu, Sheng Wei Li, Wen Bo Zhou, Meng Yuan Wang, Guo Qing Zuo, Chang An Liu, and Xiong Ding. 2016. "Effect of CD16a, the Surface Receptor of Kupffer Cells, on the Growth of Hepatocellular Carcinoma Cells." *International Journal of Molecular Medicine* 37(6):1465–74. doi: 10.3892/ijmm.2016.2561.

Lim, Wendell A., and Carl H. June. 2017. "The Principles of Engineering Immune Cells to Treat Cancer." *Cell* 168(4):724–40.

Lin, Jie, and Ariel Amir. 2018. "Homeostasis of Protein and MRNA Concentrations in Growing Cells." *Nature Communications* 9(1):1–11. doi: 10.1038/s41467-018-06714-z.

Liu, Qingjun, Zhongjie Sun, and Ligong Chen. 2020. "Memory T Cells: Strategies for Optimizing Tumor Immunotherapy." *Protein and Cell* 11(8):549–64.

Liu, Yang, and Stefan Klaus Barta. 2019. "Diffuse Large B-Cell Lymphoma: 2019 Update on Diagnosis, Risk Stratification, and Treatment." *American Journal of Hematology* 94(5):604–16.

Lo, A., L. S. Wang, J. Scholler, J. Monslow, D. Avery, K. Newick, S. O'Brien, R. A. Evans, D.

J. Bajor, C. Clendenin, A. C. Durham, E. L. Buza, R. H. Vonderheide, C. H. June, S. M. Albelda, and E. Pure. 2015. “Tumor-Promoting Desmoplasia Is Disrupted by Depleting FAP-Expressing Stromal Cells.” *Cancer Res* 75(14):2800–2810. doi: 10.1158/0008-5472.can-14-3041.

Lock, D., N. Mockel-Tenbrinck, K. Drechsel, C. Barth, D. Mauer, T. Schaser, C. Kolbe, W. Al Rawashdeh, J. Brauner, O. Hardt, N. Pflug, U. Holtick, P. Borchmann, M. Assenmacher, and A. Kaiser. 2017. “Automated Manufacturing of Potent CD20-Directed Chimeric Antigen Receptor T Cells for Clinical Use.” *Hum Gene Ther* 28(10):914–25. doi: 10.1089/hum.2017.111.

Lotze, M. T., and S. A. Rosenberg. 1986. “Results of Clinical Trials with the Administration of Interleukin 2 and Adoptive Immunotherapy with Activated Cells in Patients with Cancer.” *Immunobiology* 172(3–5):420–37. doi: 10.1016/S0171-2985(86)80122-X.

MacAuley, Matthew S., Paul R. Crocker, and James C. Paulson. 2014. “Siglec-Mediated Regulation of Immune Cell Function in Disease.” *Nature Reviews Immunology* 14(10):653–66.

Maher, J., R. J. Brentjens, G. Gunset, I. Riviere, and M. Sadelain. 2002. “Human T-Lymphocyte Cytotoxicity and Proliferation Directed by a Single Chimeric TCRzeta /CD28 Receptor.” *Nat Biotechnol* 20(1):70–75. doi: 10.1038/nbt0102-70.

McComb, Scott, Tina Nguyen, Kevin A. Henry, Darin Bloemberg, Susanne Maclean, Rénald Gilbert, Christine Gadoury, Rob Pon, Traian Sulea, Qin Zhu, and Risini D. Weeratna. 2020. “Fine Molecular Tuning of Chimeric Antigen Receptors through Hinge Length Optimization.” *BioRxiv* 2020.10.30.360925.

Mezzanotte, Laura, Moniek van ‘t Root, Hacer Karatas, Elena A. Goun, and Clemens W. G. M. Löwik. 2017. “In Vivo Molecular Bioluminescence Imaging: New Tools and Applications.” *Trends in Biotechnology* 35(7):640–52.

Milone, Michael C., Jonathan D. Fish, Carmine Carpenito, Richard G. Carroll, Gwendolyn K. Binder, David Teachey, Minu Samanta, Mehdi Lakhal, Brian Gloss, Gwenn Danet-Desnoyers, Dario Campana, James L. Riley, Stephan A. Grupp, and Carl H. June. 2009. “Chimeric Receptors Containing CD137 Signal Transduction Domains Mediate Enhanced Survival of T Cells and Increased Antileukemic Efficacy in Vivo.” *Molecular Therapy* 17(8):1453–64. doi: 10.1038/mt.2009.83.

Morris, John P., Sam C. Wang, and Matthias Hebrok. 2010. “KRAS, Hedgehog, Wnt and the Twisted Developmental Biology of Pancreatic Ductal Adenocarcinoma.” *Nature Reviews Cancer* 10(10):683–95.

Motoi, Fuyuhiko, and Michiaki Unno. 2021. “Adjuvant and Neoadjuvant Treatment for Pancreatic Adenocarcinoma.” *Japanese Journal of Clinical Oncology* 50(5):483–89.

Moustakas, Aristidis, and Carl Henrik Heldin. 2005. “Non-Smad TGF-β Signals.” *Journal of Cell Science* 118(16):3573–84.

Mulazzani, Matthias, Simon P. Fräßle, Iven von Mücke-Heim, Sigrid Langer, Xiaolan Zhou,

Hellen Ishikawa-Ankerhold, Justin Leube, Wenlong Zhang, Sarah Dötsch, Mortimer Svec, Martina Rudelius, Martin Dreyling, Michael von Bergwelt-Baildon, Andreas Straube, Veit R. Buchholz, Dirk H. Busch, and Louisa von Baumgarten. 2019. "Long-Term in Vivo Microscopy of CAR T Cell Dynamics during Eradication of CNS Lymphoma in Mice." *Proceedings of the National Academy of Sciences of the United States of America* 116(48):24275–84. doi: 10.1073/pnas.1903854116.

Mullard, Asher. 2021. "FDA Approves Fourth CAR-T Cell Therapy." *Nature Reviews. Drug Discovery* 20(3):166.

Muller, Yannick D., Duy P. Nguyen, Leonardo M. R. Ferreira, Patrick Ho, Caroline Raffin, Roxxana Valeria Beltran Valencia, Zion Congrave-Wilson, Theodore L. Roth, Justin Eyquem, Frederic Van Gool, Alexander Marson, Laurent Perez, James A. Wells, Jeffrey A. Bluestone, and Qizhi Tang. 2021. "The CD28-Transmembrane Domain Mediates Chimeric Antigen Receptor Heterodimerization With CD28." *Frontiers in Immunology* 12. doi: 10.3389/fimmu.2021.639818.

Murty, Surya, Samuel T. Haile, Corinne Beinat, Amin Aalipour, Israt S. Alam, Tara Murty, Travis M. Shaffer, Chirag B. Patel, Edward E. Graves, Crystal L. Mackall, and Sanjiv S. Gambhir. 2020. "Intravital Imaging Reveals Synergistic Effect of CAR T-Cells and Radiation Therapy in a Preclinical Immunocompetent Glioblastoma Model." *OncoImmunology* 9(1):1757360. doi: 10.1080/2162402X.2020.1757360.

Nakajima, Masao, Yukimi Sakoda, Keishi Adachi, Hiroaki Nagano, and Koji Tamada. 2019. "Improved Survival of Chimeric Antigen Receptor-engineered T (<scp>CAR</Scp> -T) and Tumor-specific T Cells Caused by Anti-programmed Cell Death Protein 1 Single-chain Variable Fragment-producing <scp>CAR</Scp> -T Cells." *Cancer Science* 110(10):3079–88. doi: 10.1111/cas.14169.

Narayanan, Jayanth S. Shankar., Partha Ray, Ibtehaj Naqvi, and Rebekah White. 2018. "A Syngeneic Pancreatic Cancer Mouse Model to Study the Effects of Irreversible Electroporation." *Journal of Visualized Experiments* 2018(136). doi: 10.3791/57265.

Nedaeinia, Reza, Amir Avan, Mostafa Manian, Rasoul Salehi, and Majid Ghayour-Mobarhan. 2014. "EGFR as a Potential Target for the Treatment of Pancreatic Cancer: Dilemma and Controversies." *Current Drug Targets* 15(14):1293–1301. doi: 10.2174/1389450115666141125123003.

Neoptolemos, John P., Jörg Kleeff, Patrick Michl, Eithne Costello, William Greenhalf, and Daniel H. Palmer. 2018. "Therapeutic Developments in Pancreatic Cancer: Current and Future Perspectives." *Nature Reviews Gastroenterology and Hepatology* 15(6):333–48.

O'Neill, Karen, Scott K. Lyons, William M. Gallagher, Kathleen M. Curran, and Annette T. Byrne. 2010. "Bioluminescent Imaging: A Critical Tool in Pre-Clinical Oncology Research." *Journal of Pathology* 220(3):317–27.

Onaciu, Anca, Raluca Munteanu, Vlad Cristian Munteanu, Diana Gulei, Lajos Raduly, Richard Ionut Feder, Radu Pirlog, Atanas G. Atanasov, Schuyler S. Korban, Alexandru Irimie, and Ioana Berindan-Neagoe. 2020. "Spontaneous and Induced Animal Models for Cancer

Research." *Diagnostics* 10(9):660.

Orhan, Adile, Rasmus P. Vogelsang, Malene B. Andersen, Michael T. Madsen, Emma R. Hölmich, Hans Raskov, and Ismail Gögenur. 2020. "The Prognostic Value of Tumour-Infiltrating Lymphocytes in Pancreatic Cancer: A Systematic Review and Meta-Analysis." *European Journal of Cancer* 132:71–84.

Oshima, Minoru, Keiichi Okano, Shinobu Muraki, Reiji Haba, Takashi Maeba, Yasuyuki Suzuki, and Shinichi Yachida. 2013. "Immunohistochemically Detected Expression of 3 Major Genes (CDKN2A/P16, TP53, and SMAD4/DPC4) Strongly Predicts Survival in Patients with Resectable Pancreatic Cancer." *Annals of Surgery* 258(2):336–46. doi: 10.1097/SLA.0b013e3182827a65.

Den Otter, Willem, John J. L. Jacobs, Jan J. Battermann, Gerrit Jan Hordijk, Zachary Krastev, Ekaterina V. Moiseeva, Rachel J. E. Stewart, Paul G. P. M. Ziekman, and Jan Willem Koten. 2008. "Local Therapy of Cancer with Free IL-2." *Cancer Immunology, Immunotherapy* 57(7):931–50.

Overdijk, Marije B., Sandra Verploegen, Antonio Ortiz Buijsse, Tom Vink, Jeanette H. W. Leusen, Wim K. Bleeker, and Paul W. H. I. Parren. 2012. "Crosstalk between Human IgG Isotypes and Murine Effector Cells." *The Journal of Immunology* 189(7):3430–38. doi: 10.4049/jimmunol.1200356.

Parisi, Giulia, Justin D. Saco, Felix B. Salazar, Jennifer Tsoi, Paige Krystofinski, Cristina Puig-Saus, Ruixue Zhang, Jing Zhou, Gardenia C. Cheung-Lau, Alejandro J. Garcia, Catherine S. Grasso, Richard Tavaré, Siwen Hu-Lieskovan, Sean Mackay, Jonathan Zalevsky, Chantale Bernatchez, Adi Diab, Anna M. Wu, Begoña Comin-Anduix, Deborah Charych, and Antoni Ribas. 2020. "Persistence of Adoptively Transferred T Cells with a Kinetically Engineered IL-2 Receptor Agonist." *Nature Communications* 11(1):660. doi: 10.1038/s41467-019-12901-3.

Pawałowski, Bartosz, Hubert Szweda, Alina Dudkowiak, and Tomasz Piotrowski. 2019. "Quality Evaluation of Monoenergetic Images Generated by Dual-Energy Computed Tomography for Radiotherapy: A Phantom Study." *Physica Medica* 63:48–55. doi: 10.1016/j.ejmp.2019.05.019.

Pérez-Herrero, Edgar, and Alberto Fernández-Medarde. 2015. "Advanced Targeted Therapies in Cancer: Drug Nanocarriers, the Future of Chemotherapy." *European Journal of Pharmaceutics and Biopharmaceutics* 93:52–79.

Pirovano, Giacomo, Sheryl Roberts, Susanne Kossatz, and Thomas Reiner. 2020. "Optical Imaging Modalities: Principles and Applications in Preclinical Research and Clinical Settings." *Journal of Nuclear Medicine* 61(10):1419–27. doi: 10.2967/jnumed.119.238279.

Polyak, Maria J., and Julie P. Deans. 2002. "Alanine-170 and Proline-172 Are Critical Determinants for Extracellular CD20 Epitopes; Heterogeneity in the Fine Specificity of CD20 Monoclonal Antibodies Is Defined by Additional Requirements Imposed by Both Amino Acid Sequence and Quaternary Structure." *Blood* 99(9):3256–62. doi:

10.1182/blood.V99.9.3256.

Pompella, Luca, Giuseppe Tirino, Annalisa Pappalardo, Marianna Caterino, Anna Ventriglia, Valeria Nacca, Michele Orditura, Fortunato Ciardiello, and Ferdinando De Vita. 2020. "Pancreatic Cancer Molecular Classifications: From Bulk Genomics to Single Cell Analysis." *International Journal of Molecular Sciences* 21(8).

Ponomarev, Vladimir, Michael Doubrovin, Clay Lyddane, Tatiana Beresten, Julius Balatoni, William Bornman, Ronald Finn, Timothy Akhurst, Steven Larson, Ronald Blasberg, Michel Sadelain, and Juri Gelovani Tjuvajev. 2001. "Imaging TCR-Dependent NFAT-Mediated T-Cell Activation with Positron Emission Tomography in Vivo." *Neoplasia* 3(6):480–88. doi: 10.1038/sj.neo.7900204.

Prewett, Marie, Patricia Rockwell, R. F. Rockwell, Nicholas A. Giorgio, John Mendelsohn, Howard I. Scher, and Neil I. Goldstein. 1996. "The Biologic Effects of C225, A Chimeric Monoclonal Antibody to the EGFR, on Human Prostate Carcinoma." *Journal of Immunotherapy* 19(6):419–27. doi: 10.1097/00002371-199611000-00006.

Qin, Le, Yunxin Lai, Ruocong Zhao, Xinru Wei, Jianyu Weng, Peilong Lai, Baiheng Li, Simiao Lin, Suna Wang, Qiting Wu, Qiubin Liang, Yangqiu Li, Xuchao Zhang, Yilong Wu, Pentao Liu, Yao Yao, Duanqing Pei, Xin Du, and Peng Li. 2017. "Incorporation of a Hinge Domain Improves the Expansion of Chimeric Antigen Receptor T Cells." *Journal of Hematology and Oncology* 10(1). doi: 10.1186/s13045-017-0437-8.

Rafei-Shamsabadi, David, Saskia Lehr, Dagmar von Bubnoff, and Frank Meiss. 2019. "Successful Combination Therapy of Systemic Checkpoint Inhibitors and Intralesional Interleukin-2 in Patients with Metastatic Melanoma with Primary Therapeutic Resistance to Checkpoint Inhibitors Alone." *Cancer Immunology, Immunotherapy* 68(9):1417–28. doi: 10.1007/s00262-019-02377-x.

Rafiq, Sarwish, Christopher S. Hackett, and Renier J. Brentjens. 2020. "Engineering Strategies to Overcome the Current Roadblocks in CAR T Cell Therapy." *Nature Reviews Clinical Oncology* 17(3):147–67.

Ramos, Carlos A., Rayne Rouce, Catherine S. Robertson, Amy Reyna, Neeharika Narala, Gayatri Vyas, Birju Mehta, Huimin Zhang, Olga Dakhova, George Carrum, Rammurti T. Kamble, Adrian P. Gee, Zhuyong Mei, Meng Fen Wu, Hao Liu, Bambi Grilley, Cliona M. Rooney, Helen E. Heslop, Malcolm K. Brenner, Barbara Savoldo, and Gianpietro Dotti. 2018. "In Vivo Fate and Activity of Second- versus Third-Generation CD19-Specific CAR-T Cells in B Cell Non-Hodgkin's Lymphomas." *Molecular Therapy* 26(12):2727–37. doi: 10.1016/j.ymthe.2018.09.009.

Raphael, Benjamin J., Ralph H. Hruban, Andrew J. Aguirre, Richard A. Moffitt, Jen Jen Yeh, Chip Stewart, A. Gordon Robertson, Andrew D. Cherniack, Manaswi Gupta, Gad Getz, Stacey B. Gabriel, Matthew Meyerson, Carrie Cibulskis, Suzanne S. Fei, Toshinori Hinoue, Hui Shen, Peter W. Laird, Shiyun Ling, Yiling Lu, Gordon B. Mills, Rehan Akbani, Phillipe Loher, Eric R. Londin, Isidore Rigoutsos, Aristeidis G. Telonis, Ewan A. Gibb, Anna Goldenberg, Aziz M. Mezlini, Katherine A. Hoadley, Eric Collisson, Eric Lander,

Bradley A. Murray, Julian Hess, Mara Rosenberg, Louis Bergelson, Hailei Zhang, Juok Cho, Grace Tiao, Jaegil Kim, Dimitri Livitz, Ignaty Leshchiner, Brendan Reardon, Eliezer Van Allen, Atanas Kamburov, Rameen Beroukhim, Gordon Saksena, Steven E. Schumacher, Michael S. Noble, David I. Heiman, Nils Gehlenborg, Jaegil Kim, Michael S. Lawrence, Volkan Adsay, Gloria Petersen, David Klimstra, Nabeel Bardeesy, Mark D. M. Leiserson, Reanne Bowlby, Katayoon Kasaian, Inanc Birol, Karen L. Mungall, Sara Sadeghi, John N. Weinstein, Paul T. Spellman, Yuexin Liu, Laufey T. Amundadottir, Joel Tepper, Aatur D. Singhi, Rajiv Dhir, Drwiega Paul, Thomas Smyrk, Lizhi Zhang, Paula Kim, Jay Bowen, Jessica Frick, Julie M. Gastier-Foster, Mark Gerken, Kevin Lau, Kristen M. Leraas, Tara M. Lichtenberg, Nilsa C. Ramirez, Jeremy Renkel, Mark Sherman, Lisa Wise, Peggy Yena, Erik Zmuda, Juliann Shih, Adrian Ally, Miruna Balasundaram, Rebecca Carlsen, Andy Chu, Eric Chuah, Amanda Clarke, Noreen Dhalla, Robert A. Holt, Steven J. M. Jones, Darlene Lee, Yussanne Ma, Marco A. Marra, Michael Mayo, Richard A. Moore, Andrew J. Mungall, Jacqueline E. Schein, Payal Sipahimalani, Angela Tam, Nina Thiessen, Kane Tse, Tina Wong, Denise Brooks, J. Todd Auman, Saianand Balu, Tom Bodenheimer, D. Neil Hayes, Alan P. Hoyle, Stuart R. Jefferys, Corbin D. Jones, Shaowu Meng, Piotr A. Mieczkowski, Lisle E. Mose, Charles M. Perou, Amy H. Perou, Jeffrey Roach, Yan Shi, Janae V. Simons, Tara Skelly, Matthew G. Soloway, Donghui Tan, Umadevi Veluvolu, Joel S. Parker, Matthew D. Wilkerson, Anil Korkut, Yasin Senbabaoglu, Patrick Burch, Robert McWilliams, Kari Chaffee, Ann Oberg, Wei Zhang, Marie Claude Gingras, David A. Wheeler, Liu Xi, Monique Albert, John Bartlett, Harman Sekhon, Yeager Stephen, Zaren Howard, Miller Judy, Anne Breggia, Rachna T. Shroff, Sudha Chudamani, Jia Liu, Laxmi Lolla, Rashi Naresh, Todd Pihl, Qiang Sun, Yunhu Wan, Ye Wu, Smith Jennifer, Kevin Roggin, Karl Friedrich Becker, Madhusmita Behera, Joseph Bennett, Lori Boice, Eric Burks, Carlos Gilberto Carlotti Junior, John Chabot, Daniela Pretti da Cunha Tirapelli, Jose Sebastião dos Santos, Michael Dubina, Jennifer Eschbacher, Mei Huang, Lori Huelsenbeck-Dill, Roger Jenkins, Alexey Karpov, Rafael Kemp, Vladimir Lyadov, Shishir Maithel, Georgy Manikhas, Eric Montgomery, Houtan Noushmehr, Adeboye Osunkoya, Taofeek Owonikoko, Oxana Paklina, Olga Potapova, Suresh Ramalingam, W. Kimryn Rathmell, Kimberly Rieger-Christ, Charles Saller, Galiya Setdikova, Alexey Shabunin, Gabriel Sica, Tao Su, Travis Sullivan, Pat Swanson, Katherine Tarvin, Michael Tavobilov, Leigh B. Thorne, Stefan Urbanski, Olga Voronina, Timothy Wang, Daniel Crain, Erin Curley, Johanna Gardner, David Mallery, Scott Morris, Joseph Paulauskis, Robert Penny, Candace Shelton, Troy Shelton, Klaus Peter Janssen, Oliver Bathe, Nathan Bahary, Julia Slotta-Huspenina, Amber Johns, Hanina Hibshoosh, Rosa F. Hwang, Antonia Sepulveda, Amie Radenbaugh, Stephen B. Baylin, Mario Berrios, Moiz S. Bootwalla, Andrea Holbrook, Phillip H. Lai, Dennis T. Maglinte, Swapna Mahurkar, Timothy J. Triche, David J. Van Den Berg, Daniel J. Weisenberger, Lynda Chin, Raju Kucherlapati, Melanie Kucherlapati, Angeliki Pantazi, Peter Park, Gordon Saksena, Doug Voet, Pei Lin, Scott Frazer, Timothy Defreitas, Sam Meier, Lynda Chin, Sun Young Kwon, Yong Hoon Kim, Sang Jae Park, Sung Sik Han, Seong Hoon Kim, Hark Kim, Emma Furth, Margaret Tempero, Chris Sander, Andrew Biankin, David Chang, Peter Bailey, Anthony Gill, James Kench, Sean Grimmond, Amber Johns, Australian Pancreatic Cancer Genome Initiative (APGI, Russell Postier, Rosemary Zuna, Hugues

Sicotte, John A. Demchok, Martin L. Ferguson, Carolyn M. Hutter, Kenna R. Mills Shaw, Margi Sheth, Heidi J. Sofia, Roy Tarnuzzer, Zhining Wang, Liming Yang, Jiashan (Julia) Zhang, Ina Felau, and Jean C. Zenklusen. 2017. "Integrated Genomic Characterization of Pancreatic Ductal Adenocarcinoma." *Cancer Cell* 32(2):185-203.e13. doi: 10.1016/j.ccell.2017.07.007.

Rawson, Shelley D., Jekaterina Maksimcuka, Philip J. Withers, and Sarah H. Cartmell. 2020. "X-Ray Computed Tomography in Life Sciences." *BMC Biology* 18(1).

Rehemtulla, Alnawaz, Lauren D. Stegman, Shaun J. Cardozo, Sheila Gupta, Daniel E. Hall, Christopher H. Contag, and Brian D. Ross. 2000. "Rapid and Quantitative Assessment of Cancer Treatment Response Using in Vivo Bioluminescence Imaging." *Neoplasia* 2(6):491–95. doi: 10.1038/sj.neo.7900121.

Rice, B. W., M. D. Cable, and M. B. Nelson. 2001. "In Vivo Imaging of Light-Emitting Probes." *Journal of Biomedical Optics* 6(4):432. doi: 10.1117/1.1413210.

Richter, G. H. S., A. Mollweide, K. Hanewinkel, C. Zobywalski, and S. Burdach. 2009. "CD25 Blockade Protects T Cells from Activation-Induced Cell Death (AICD) via Maintenance of TOSO Expression." *Scandinavian Journal of Immunology* 70(3):206–15. doi: 10.1111/j.1365-3083.2009.02281.x.

Riddell, Stanley R., Mark Elliott, Deborah A. Lewinsohn, Mark J. Gilbert, Linda Wilson, Sara A. Manley, Stephen D. Lupton, Robert W. Overell, Thomas C. Reynolds, Lawrence Corey, and Philip D. Greenberg. 1996. "T-Cell Mediated Rejection of Gene-Modified HIV-Specific Cytotoxic T Lymphocytes in HIV-Infected Patients." *Nature Medicine* 2(2):216–23. doi: 10.1038/nm0296-216.

Romeo, Charles, Martine Amiot, and Brian Seed. 1992. "Sequence Requirements for Induction of Cytolysis by the T Cell Antigen Fc Receptor ζ Chain." *Cell* 68(5):889–97. doi: 10.1016/0092-8674(92)90032-8.

Rosenberg, Steven A. 2014. "IL-2: The First Effective Immunotherapy for Human Cancer." *The Journal of Immunology* 192(12):5451–58. doi: 10.4049/jimmunol.1490019.

Rosenwald, Andreas, George Wright, Karen Leroy, Xin Yu, Philippe Gaulard, Randy D. Gascoyne, Wing C. Chan, Tong Zhao, Corinne Haioun, Timothy C. Greiner, Dennis D. Weisenburger, James C. Lynch, Julie Vose, James O. Armitage, Erlend B. Smeland, Stein Kvaloy, Harald Holte, Jan Delabie, Elias Campo, Emili Montserrat, Armando Lopez-Guillermo, German Ott, H. Konrad Muller-Hermelink, Joseph M. Connors, Rita Braziel, Thomas M. Grogan, Richard I. Fisher, Thomas P. Miller, Michael LeBlanc, Michael Chiorazzi, Hong Zhao, Liming Yang, John Powell, Wyndham H. Wilson, Elaine S. Jaffe, Richard Simon, Richard D. Klausner, and Louis M. Staudt. 2003. "Molecular Diagnosis of Primary Mediastinal B Cell Lymphoma Identifies a Clinically Favorable Subgroup of Diffuse Large B Cell Lymphoma Related to Hodgkin Lymphoma." *Journal of Experimental Medicine* 198(6):851–62. doi: 10.1084/jem.20031074.

Sadelain, Michel, Renier Brentjens, and Isabelle Rivière. 2013. "The Basic Principles of Chimeric Antigen Receptor Design." *Cancer Discovery* 3(4):388–98.

Sadelain, Michel, Isabelle Rivière, and Renier Brentjens. 2003. “Targeting Tumours with Genetically Enhanced T Lymphocytes.” *Nature Reviews Cancer* 3(1):35–45.

Sakudo, Akikazu. 2016. “Near-Infrared Spectroscopy for Medical Applications: Current Status and Future Perspectives.” *Clinica Chimica Acta* 455:181–88.

Salles, Gilles, Martin Barrett, Robin Foà, Joerg Maurer, Susan O’Brien, Nancy Valente, Michael Wenger, and David G. Maloney. 2017. “Rituximab in B-Cell Hematologic Malignancies: A Review of 20 Years of Clinical Experience.” *Advances in Therapy* 34(10):2232–73.

Sano, Makoto, David R. Driscoll, Wilfredo E. DeJesus-Monge, Brian Quattrochi, Victoria A. Appleman, Jianhong Ou, Lihua Julie Zhu, Nao Yoshida, Shintaro Yamazaki, Tadatoshi Takayama, Masahiko Sugitani, Norimichi Nemoto, David S. Klimstra, and Brian C. Lewis. 2016. “Activation of WNT/β-Catenin Signaling Enhances Pancreatic Cancer Development and the Malignant Potential Via Up-Regulation of Cyr61.” *Neoplasia (United States)* 18(12):785–94. doi: 10.1016/j.neo.2016.11.004.

Sarantis, Panagiotis, Evangelos Koustas, Adriana Papadimitropoulou, Athanasios G. Papavassiliou, and Michalis V. Karamouzis. 2020. “Pancreatic Ductal Adenocarcinoma: Treatment Hurdles, Tumor Microenvironment and Immunotherapy.” *World Journal of Gastrointestinal Oncology* 12(2):173–81.

Savoldo, Barbara, Carlos Almeida Ramos, Enli Liu, Martha P. Mims, Michael J. Keating, George Carrum, Rammurti T. Kamble, Catherine M. Bollard, Adrian P. Gee, Zhuyong Mei, Hao Liu, Bambi Grilley, Cliona M. Rooney, Helen E. Heslop, Malcolm K. Brenner, and Gianpietro Dotti. 2011. “CD28 Costimulation Improves Expansion and Persistence of Chimeric Antigen Receptor-Modified T Cells in Lymphoma Patients.” *Journal of Clinical Investigation* 121(5):1822–26. doi: 10.1172/JCI46110.

Schäfer, Daniel, Stefan Tomiuk, Laura N. Küster, Wa’el Al Rawashdeh, Janina Henze, German Tischler-Höhle, David J. Agorku, Janina Brauner, Cathrin Linnartz, Dominik Lock, Andrew Kaiser, Christoph Herbel, Dominik Eckardt, Melina Lamorte, Dorothee Lenhard, Julia Schüler, Philipp Ströbel, Jeannine Missbach-Guentner, Diana Pinkert-Leetsch, Frauke Alves, Andreas Bosio, and Olaf Hardt. 2021. “Identification of CD318, TSPAN8 and CD66c as Target Candidates for CAR T Cell Based Immunotherapy of Pancreatic Adenocarcinoma.” *Nature Communications* 12(1):1–18. doi: 10.1038/s41467-021-21774-4.

Schmid, Roland M. 2002. “Acinar-to-Ductal Metaplasia in Pancreatic Cancer Development.” *Journal of Clinical Investigation* 109(11):1403–4. doi: 10.1172/jci15889.

Schmidt-Wolf, Ingo G. H., Robert S. Negrin, Hans Peter Kiem, Karl G. Blume, and Irving L. Weissman. 1991. “Use of a SCID Mouse/Human Lymphoma Model to Evaluate Cytokine-Induced Killer Cells with Potent Antitumor Cell Activity.” *Journal of Experimental Medicine* 174(1):139–49. doi: 10.1084/jem.174.1.139.

Schmitz, Norbert, Beate Pfistner, Michael Sextro, Markus Sieber, Angelo M. Carella, Matthias Haenel, Friederike Boissevain, Reinhart Zschaber, Peter Müller, Hartmut Kirchner,

Andreas Lohri, Susanne Decker, Bettina Koch, Dirk Hasenclever, Anthony H. Goldstone, and Volker Diehl. 2002. “Aggressive Conventional Chemotherapy Compared with High-Dose Chemotherapy with Autologous Haemopoietic Stem-Cell Transplantation for Relapsed Chemosensitive Hodgkin’s Disease: A Randomised Trial.” *Lancet* 359(9323):2065–71. doi: 10.1016/S0140-6736(02)08938-9.

Schwartzentruber, Douglas J. 2001. “Guidelines for the Safe Administration of High-Dose Interleukin-2.” *Journal of Immunotherapy* 24(4):287–93.

Sellmyer, Mark A., Sarah A. Richman, Katheryn Lohith, Catherine Hou, Chi Chang Weng, Robert H. Mach, Roddy S. O’Connor, Michael C. Milone, and Michael D. Farwell. 2019. “Imaging CAR T Cell Trafficking with EDFHR as a PET Reporter Gene.” *Molecular Therapy* 28(1):42. doi: 10.1016/j.ymthe.2019.10.007.

Serfling, Edgar, Stefan Klein-Hessling, Alois Palmetshofer, Tobias Bopp, Michael Stassen, and Edgar Schmitt. 2006. “NFAT Transcription Factors in Control of Peripheral T Cell Tolerance.” *European Journal of Immunology* 36(11):2837–43.

Shahinian, Arda, Klaus Pfefer, Kelvin P. Lee, Thomas M. Kündig, Kenji Kishihara, Andrew Wakeham, Kazuhiro Kawai, Pamela S. Ohashi, Craig B. Thompson, and Tak W. Mak. 1993. “Differential T Cell Costimulatory Requirements in CD28-Deficient Mice.” *Science* 261(5121):609–12. doi: 10.1126/science.7688139.

Shanehbandi, Dariush, Jafar Majidi, Tohid Kazemi, Behzad Baradaran, and Leili Aghebati-Maleki. 2017. “CD20-Based Immunotherapy of B-Cell Derived Hematologic Malignancies.” *Current Cancer Drug Targets* 17(5):423–44. doi: 10.2174/1568009617666170109151128.

Shankland, Kate R., James O. Armitage, and Barry W. Hancock. 2012. “Non-Hodgkin Lymphoma.” *The Lancet* 380(9844):848–57.

Sharifzadeh, Zahra, Fatemeh Rahbarizadeh, Mohammad A. Shokrgozar, Davoud Ahmadvand, Fereidoun Mahboudi, Fatemeh Rahimi Jamnani, and S. Moein Moghimi. 2013. “Genetically Engineered T Cells Bearing Chimeric Nanoconstructed Receptors Harboring TAG-72-Specific Camelid Single Domain Antibodies as Targeting Agents.” *Cancer Letters* 334(2):237–44. doi: 10.1016/j.canlet.2012.08.010.

Sharma, Aditi, Lawrence H. Boise, and Mala Shanmugam. 2019. “Cancer Metabolism and the Evasion of Apoptotic Cell Death.” *Cancers* 11(8).

Shrestha, Bishwas, Kelly Walton, Jordan Reff, Elizabeth M. Sagatys, Nhan Tu, Justin Boucher, Gongbo Li, Tayyebb Ghafoor, Martin Felices, Jeffrey S. Miller, Joseph Pidala, Bruce R. Blazar, Claudio Anasetti, Brian C. Betts, and Marco L. Davila. 2020. “Human CD83-Targeted Chimeric Antigen Receptor T Cells Prevent and Treat Graft-versus-Host Disease.” *Journal of Clinical Investigation* 130(9):4652–62. doi: 10.1172/JCI135754.

Siamof, Cerise M., Shreya Goel, and Weibo Cai. 2020. “Moving Beyond the Pillars of Cancer Treatment: Perspectives From Nanotechnology.” *Frontiers in Chemistry* 8:598100.

Siegel, R. L., and K. D. Miller. 2019. “Cancer Statistics, 2019.” 69(1):7–34. doi:

10.3322/caac.21551.

Simonetta, Federico, Israt S. Alam, Juliane K. Lohmeyer, Bita Sahaf, Zinaida Good, Weiyu Chen, Zunyu Xiao, Toshihito Hirai, Lukas Scheller, Pujan Engels, Ophir Vermesh, Elise Robinson, Tom Haywood, Ataya Sathirachinda, Jeanette Baker, Meena B. Malipatlolla, Liora M. Schultz, Jay Y. Spiegel, Jason T. Lee, David B. Miklos, Crystal L. Mackall, Sanjiv S. Gambhir, and Robert S. Negrin. 2021. "Molecular Imaging of Chimeric Antigen Receptor T Cells by ICOS-ImmunoPET." *Clinical Cancer Research* 27(4):1058–68. doi: 10.1158/1078-0432.CCR-20-2770.

Soloff, Erik V, Atif Zaheer, Jeffrey Meier, Marc Zins, and Eric P. Tamm. 2018. "Staging of Pancreatic Cancer: Resectable, Borderline Resectable, and Unresectable Disease." *Abdominal Radiology* 43(2):301–13. doi: 10.1007/s00261-017-1410-2.

Song, De Gang, Qunrui Ye, Carmine Carpenito, Mathilde Poussin, Li Ping Wang, Chunyan Ji, Mariangela Figini, Carl H. June, George Coukos, and Daniel J. Powell. 2011. "In Vivo Persistence, Tumor Localization, and Antitumor Activity of CAR-Engineered T Cells Is Enhanced by Costimulatory Signaling through CD137 (4-1BB)." *Cancer Research* 71(13):4617–27. doi: 10.1158/0008-5472.CAN-11-0422.

Sperb, Nadine, Miltiadis Tsesmelis, and Thomas Wirth. 2020. "Crosstalk between Tumor and Stromal Cells in Pancreatic Ductal Adenocarcinoma." *International Journal of Molecular Sciences* 21(15):1–23.

Van Der Stegen, Sjoukje J. C., Mohamad Hamieh, and Michel Sadelain. 2015. "The Pharmacology of Second-Generation Chimeric Antigen Receptors." *Nature Reviews Drug Discovery* 14(7):499–509.

Stone, Jennifer D., and David M. Kranz. 2013. "Role of T Cell Receptor Affinity in the Efficacy and Specificity of Adoptive T Cell Therapies." *Frontiers in Immunology* 4(AUG).

Sung, Hyuna, Jacques Ferlay, Rebecca L. Siegel, Mathieu Laversanne, Isabelle Soerjomataram, Ahmedin Jemal, and Freddie Bray. 2021. "Global Cancer Statistics 2020: GLOBOCAN Estimates of Incidence and Mortality Worldwide for 36 Cancers in 185 Countries." *CA: A Cancer Journal for Clinicians* caac.21660. doi: 10.3322/caac.21660.

Tang, Bo, Yang Li, Guangying Qi, Shengguang Yuan, Zhenran Wang, Shuiping Yu, Bo Li, and Songqing He. 2015. "Clinicopathological Significance of CDKN2A Promoter Hypermethylation Frequency with Pancreatic Cancer." *Scientific Reports* 5(1):13563. doi: 10.1038/srep13563.

Taylor, Arthur, Jack Sharkey, Antonius Plagge, Bettina Wilm, and Patricia Murray. 2018. "Multicolour in Vivo Bioluminescence Imaging Using a NanoLuc-Based BRET Reporter in Combination with Firefly Luciferase." *Contrast Media and Molecular Imaging* 2018. doi: 10.1155/2018/2514796.

Tietze, Julia K., Danice E. C. Wilkins, Gail D. Sckisel, Myriam N. Bouchlaka, Kory L. Alderson, Jonathan M. Weiss, Erik Ames, Kevin W. Bruhn, Noah Craft, Robert H. Wiltrout, Dan L. Longo, Lewis L. Lanier, Bruce R. Blazar, Doug Redelman, and William

J. Murphy. 2012. “Delineation of Antigen-Specific and Antigen-Nonspecific CD8+ Memory T-Cell Responses after Cytokine-Based Cancer Immunotherapy.” *Blood* 119(13):3073–83. doi: 10.1182/blood-2011-07-369736.

Till, B. G., M. C. Jensen, J. Wang, X. Qian, A. K. Gopal, D. G. Maloney, C. G. Lindgren, Y. Lin, J. M. Pagel, L. E. Budde, A. Raubitschek, S. J. Forman, P. D. Greenberg, S. R. Riddell, and O. W. Press. 2012. “CD20-Specific Adoptive Immunotherapy for Lymphoma Using a Chimeric Antigen Receptor with Both CD28 and 4-1BB Domains: Pilot Clinical Trial Results.” *Blood* 119(17):3940–50. doi: 10.1182/blood-2011-10-387969.

Tokarew, Nicholas, Justyna Ogonek, Stefan Endres, Michael von Bergwelt-Baildon, and Sebastian Kobold. 2019. “Teaching an Old Dog New Tricks: Next-Generation CAR T Cells.” *British Journal of Cancer* 120(1):26–37.

Torres Chavez, Alejandro, Mary Kathryn McKenna, Emanuele Canestrari, Christina T. Dann, Carlos A. Ramos, Premal Lulla, Ann M. Leen, Juan F. Vera, and Norihiro Watanabe. 2019. “Expanding CAR T Cells in Human Platelet Lysate Renders T Cells with in Vivo Longevity.” *Journal for ImmunoTherapy of Cancer* 7(1). doi: 10.1186/s40425-019-0804-9.

Uchibori, Ryosuke, Takeshi Teruya, Hiroyuki Ido, Ken Ohmine, Yoshihide Sehara, Masashi Urabe, Hiroaki Mizukami, Junichi Mineno, and Keiya Ozawa. 2019. “Functional Analysis of an Inducible Promoter Driven by Activation Signals from a Chimeric Antigen Receptor.” *Molecular Therapy - Oncolytics* 12:16–25. doi: 10.1016/j.omto.2018.11.003.

Ueda, Hiroki R., Ali Ertürk, Kwanghun Chung, Viviana Gradinaru, Alain Chédotal, Pavel Tomancak, and Philipp J. Keller. 2020. “Tissue Clearing and Its Applications in Neuroscience.” *Nature Reviews Neuroscience* 21(2):61–79.

Versteijne, Eva, Casper H. J. van Eijck, Cornelis J. A. Punt, Mustafa Suker, Aeilko H. Zwinderman, Miriam A. C. Dohmen, Karin B. C. Groothuis, Oliver R. C. Busch, Marc G. H. Besselink, Ignace H. J. T. de Hingh, Albert J. ten Tije, Gijs A. Patijn, Bert A. Bonsing, Judith de Vos-Geelen, Joost M. Klaase, Sebastiaan Festen, Djamila Boerma, Joris I. Erdmann, I. Quintus Molenaar, Erwin van der Harst, Marion B. van der Kolk, Coen R. N. Rasch, and Geertjan van Tienhoven. 2016. “Preoperative Radiochemotherapy versus Immediate Surgery for Resectable and Borderline Resectable Pancreatic Cancer (PREOPANC Trial): Study Protocol for a Multicentre Randomized Controlled Trial.” *Trials* 17(1):127. doi: 10.1186/s13063-016-1262-z.

Walewski, J., E. Kraszewska, O. Mioduszewska, J. Romejko-Jarosińska, A. Hellmann, J. Czyz, J. Holowiecki, M. Kopera, S. Grosicki, M. Komarnicki, L. Rumianowski, K. Kuliczkowski, T. Wróbel, J. Dwilewicz-Trojaczek, T. Robak, K. Warzocha, J. Zaluski, E. Wójcik, A. Dmoszyńska, and A. Walter-Croneck. 2001. “Rituximab (Mabthera™, Rituxan™) in Patients with Recurrent Indolent Lymphoma: Evaluation of Safety and Efficacy in a Multicenter Study.” *Medical Oncology* 18(2):141–48. doi: 10.1385/MO:18:2:141.

Walker, Alec J., Robbie G. Majzner, Ling Zhang, Kelsey Wanhainen, Adrienne H. Long, Sang

M. Nguyen, Paola Lopomo, Marc Vigny, Terry J. Fry, Rimas J. Orentas, and Crystal L. Mackall. 2017. “Tumor Antigen and Receptor Densities Regulate Efficacy of a Chimeric Antigen Receptor Targeting Anaplastic Lymphoma Kinase.” *Molecular Therapy* 25(9):2189–2201. doi: 10.1016/j.ymthe.2017.06.008.

Wang, Y., M. Chen, Z. Wu, C. Tong, H. Dai, Y. Guo, Y. Liu, J. Huang, H. Lv, C. Luo, K. C. Feng, Q. M. Yang, X. L. Li, and W. Han. 2018. “CD133-Directed CAR T Cells for Advanced Metastasis Malignancies: A Phase I Trial.” *OncoImmunology* 7(7):e1440169. doi: 10.1080/2162402x.2018.1440169.

Watanabe, N., P. Bajgain, S. Sukumaran, S. Ansari, H. E. Heslop, C. M. Rooney, M. K. Brenner, A. M. Leen, and J. F. Vera. 2016. “Fine-Tuning the CAR Spacer Improves T-Cell Potency.” *OncoImmunology* 5(12):e1253656. doi: 10.1080/2162402x.2016.1253656.

Weijtens, M. E. M., E. H. Hart, and R. L. H. Bolhuis. 2000. “Functional Balance between T Cell Chimeric Receptor Density and Tumor Associated Antigen Density: CTL Mediated Cytolysis and Lymphokine Production.” *Gene Therapy* 7(1):35–42. doi: 10.1038/sj.gt.3301051.

Weinkove, Robert, Philip George, Nathaniel Dasyam, and Alexander D. McLellan. 2019. “Selecting Costimulatory Domains for Chimeric Antigen Receptors: Functional and Clinical Considerations.” *Clinical {\&} Translational Immunology* 8(5):e1049--e1049. doi: 10.1002/cti2.1049.

Weissleder, Ralph, and Vasilis Ntziachristos. 2003. “Shedding Light onto Live Molecular Targets.” *Nature Medicine* 9(1):123–28.

Wen, Hairuo, Zhe Qu, Yujing Yan, Chengfei Pu, Chao Wang, Hua Jiang, Tiantian Hou, and Yan Huo. 2019. “Preclinical Safety Evaluation of Chimeric Antigen Receptor-Modified T Cells against CD19 in NSG Mice.” *Annals of Translational Medicine* 7(23):735–735. doi: 10.21037/atm.2019.12.03.

Wilkie, Scott, Gianfranco Picco, Julie Foster, David M. Davies, Sylvain Julien, Lucienne Cooper, Sefina Arif, Stephen J. Mather, Joyce Taylor-Papadimitriou, Joy M. Burchell, and John Maher. 2008. “Retargeting of Human T Cells to Tumor-Associated MUC1: The Evolution of a Chimeric Antigen Receptor.” *The Journal of Immunology* 180(7):4901–9. doi: 10.4049/jimmunol.180.7.4901.

Wood, Laura D., and Ralph H. Hruban. 2012. “Pathology and Molecular Genetics of Pancreatic Neoplasms.” *Cancer Journal (United States)* 18(6):492–501.

Wrangle, John M., Alicia Patterson, C. Bryce Johnson, Daniel J. Neitzke, Shikhar Mehrotra, Chadrick E. Denlinger, Chrystal M. Paulos, Zihai Li, David J. Cole, and Mark P. Rubinstein. 2018. “IL-2 and beyond in Cancer Immunotherapy.” *Journal of Interferon and Cytokine Research* 38(2):45–68.

Wu, Annie A., Katherine M. Bever, Won Jin Ho, Elana J. Fertig, Nan Niu, Lei Zheng, Rose M. Parkinson, Jennifer N. Durham, Beth Onners, Anna K. Ferguson, Cara Wilt, Andrew H. Ko, Andrea Wang-Gillam, Daniel A. Laheru, Robert A. Anders, Elizabeth D. Thompson,

Elizabeth A. Sugar, Elizabeth M. Jaffee, and Dung T. Le. 2020. “A Phase II Study of Allogeneic GM-CSF–Transfected Pancreatic Tumor Vaccine (GVAX) with Ipilimumab as Maintenance Treatment for Metastatic Pancreatic Cancer.” *Clinical Cancer Research* 26(19):5129–39. doi: 10.1158/1078-0432.ccr-20-1025.

Wu, Yongxia, and Xue-Zhong Yu. 2019. “Modelling CAR-T Therapy in Humanized Mice.” *EBioMedicine* 40:25–26. doi: 10.1016/j.ebiom.2018.12.013.

Xu, Tingting, Dan Close, Winode Handagama, Enolia Marr, Gary Sayler, and Steven Ripp. 2016. “The Expanding Toolbox of in Vivo Bioluminescent Imaging.” *Frontiers in Oncology* 6(JUN):150.

Yao, Wantong, Anirban Maitra, and Haoqiang Ying. 2020. “Recent Insights into the Biology of Pancreatic Cancer.” *EBioMedicine* 53.

Yeh, Hsien Wei, Omran Karmach, Ao Ji, David Carter, Manuela M. Martins-Green, and Hui Wang Ai. 2017. “Red-Shifted Luciferase-Luciferin Pairs for Enhanced Bioluminescence Imaging.” *Nature Methods* 14(10):971–74. doi: 10.1038/nmeth.4400.

You, Wenpeng, and Maciej Henneberg. 2018. “Cancer Incidence Increasing Globally: The Role of Relaxed Natural Selection.” *Evolutionary Applications* 11(2):140–52. doi: 10.1111/eva.12523.

Zambito, Giorgia, Chintan Chawda, and Laura Mezzanotte. 2021. “Emerging Tools for Bioluminescence Imaging.” *Current Opinion in Chemical Biology* 63:86–94. doi: 10.1016/j.cbpa.2021.02.005.

Zeng, Siyuan, Marina Pöttler, Bin Lan, Robert Grützmann, Christian Pilarsky, and Hai Yang. 2019. “Chemoresistance in Pancreatic Cancer.” *International Journal of Molecular Sciences* 20(18).

Zhang, Bin, Wanzhou Yin, Hao Liu, Xu Cao, and Hongkai Wang. 2018. “Bioluminescence Tomography with Structural Information Estimated via Statistical Mouse Atlas Registration.” *Biomedical Optics Express* 9(8):3544. doi: 10.1364/boe.9.003544.

Zhang, Yuanyuan, and Zemin Zhang. 2020. “The History and Advances in Cancer Immunotherapy: Understanding the Characteristics of Tumor-Infiltrating Immune Cells and Their Therapeutic Implications.” *Cellular and Molecular Immunology* 17(8):807–21.

Zhao, Hui, Timothy C. Doyle, Olivier Coquoz, Flora Kalish, Bradley W. Rice, and Christopher H. Contag. 2005. “Emission Spectra of Bioluminescent Reporters and Interaction with Mammalian Tissue Determine the Sensitivity of Detection in Vivo.” *Spiedigitallibrary.Org*. doi: 10.1117/1.2032388.

Zhao, Zeguo, Maud Condomines, Sjoukje J. C. van der Stegen, Fabiana Perna, Christopher C. Kloss, Gertrude Gunset, Jason Plotkin, and Michel Sadelain. 2015. “Structural Design of Engineered Costimulation Determines Tumor Rejection Kinetics and Persistence of CAR T Cells.” *Cancer Cell* 28(4):415–28. doi: 10.1016/j.ccell.2015.09.004.

Ziffels, Barbara, Francesca Pretto, and Dario Neri. 2018. “Intratumoral Administration of IL2-

and TNF-Based Fusion Proteins Cures Cancer without Establishing Protective Immunity." *Immunotherapy* 10(3):177–88. doi: 10.2217/imt-2017-0119.

Zorn, Emmanuel, Erik A. Nelson, Mehrdad Mohseni, Fabrice Porcheray, Haesook Kim, Despina Litsa, Roberto Bellucci, Elke Raderschall, Christine Canning, Robert J. Soiffer, David A. Frank, and Jerome Ritz. 2006. "IL-2 Regulates FOXP3 Expression in Human CD4+CD25+ Regulatory T Cells through a STAT-Dependent Mechanism and Induces the Expansion of These Cells in Vivo." *Blood* 108(5):1571–79. doi: 10.1182/blood-2006-02-004747.

ACKNOWLEDGEMENTS

First, I have to thank Dr. Wa'el Al Rawashdeh for the possibility of this research project and the continuous support, motivation and supervision. I am grateful for his introduction into the world of imaging and the opportunities to present my work and myself on various occasions to the imaging world.

Moreover, I would like to thank Dr. Rita Pfeifer for the profound collaboration during many different projects, including the shared first-authored publications and her constant support.

I would like to thank Prof. Dr. Frauke Alves for her supervision during this project and to give me the chance to join the GAUSS graduate program. I am grateful for her constructive input while writing the thesis, helping me to focus and improve my research work.

In addition, I would like to express my gratitude to the members of my thesis committee, Prof. Dr. Ralf Dressel and Prof. Dr. Luis Pardo for participating in my Ph.D. thesis committee meetings and the encouraging and fruitful discussions during the last three years.

Furthermore, I would like to acknowledge the members of the examination board, Prof. Dr. Hubertus Jarry, Prof. Dr. Dieter Kube and Prof. Dr. Lutz Walter for taking the time and for their interest in this project.

Nevertheless, this work, would not have been possible without an amazing team. First and foremost, I would like to thank Cathrin Linnartz and Katharina Wittich for their outstanding practical, technical and personal support, especially down in the basement and during hard times. Second, Janina Brauner for the technical introduction into the in vivo procedures and her tremendous efforts in the experimental work. Finally, Natascha D'Apolito, Evelyn Halupka, and Mira Ebbinghaus thank you for your assistance.

Furthermore, I want to thank Laura Nadine Preiß and David Agorku for their technical support and many insightful and sometimes personal exchanges.

I owe many thanks to all other coauthors of the publications. Their hard work, longstanding experience, and essential input made these publications possible.

I would like to thank my good friend and shared first-author Daniel Schäfer, for his constant support from the first to the last day of this project.

A big thank you goes to my fellow Ph.D. students and good friends, Aparajita Singh, Jona Drushku, Jonathan Druge, Joana Nowacka, Alba-Maria Albert I Robledo, Gene Swinerd and Julie Daigre. Thank you for supporting and motivating me every day.

Finally, I am most grateful to my parents, brother, not yet sister-in-law and my beloved husband. You were always there for me, even when we were hundreds of kilometers apart. Thank you for your understanding, patience, encouragement, and inspiration during the last 3 years. You enabled me to finish my doctoral thesis, during these times, which were difficult in many ways.